NIST GCR 94-640-1

ADVANCED SURFACE ENGINEERING

U.S. Department of Commerce
Technology Administration • National Institute of Standards and Technology

---

National Institute of Standards and Technology

Arati Prabhakar, *Director*

Technology Services

Peter L. M. Heydemann, *Director*

Jaromir J. Ulbrecht, *Director*

Technical Programs

Series Editor

NIST GCR 94-640-1

Opportunities for Innovation: Advanced Surface Engineering

Edited by

William D. Sproul and Keith O. Legg
BIRL Industrial Research Laboratory
Northwestern University
Evanston, IL 60201

Prepared for

U.S. Department of Commerce
National Institute of Standards and Technology
Gaithersburg, MD 20899

Grant 60NANB32D1223

May 1994

FOREWORD

At the National Institute of Standards and Technology (NIST), our primary mission is to promote U.S. economic growth by working with industry to develop and apply technology, measurements, and standards.

We carry out this mission through a portfolio of four major programs:

- a rigorously competitive Advanced Technology Program providing cost-shared grants to industry for development of high-risk technologies with significant commercial potential;
- a grassroots Manufacturing Extension Partnership helping small to medium-sized companies adopt new technologies;
- a strong laboratory effort planned and implemented in cooperation with industry and focused on measurements, standards, evaluated data, and test methods; and
- a highly visible quality outreach program associated with the Malcolm Baldridge National Quality Award.

There are common threads running through each of these programs: they are designed to spur innovation and they all foster industrial partnerships.

Strategic partnerships, the new paradigm of the nineties, have proved to be, in most cases, a "win-win" structural arrangement for all partners. Strategic partnerships and other corporate alliances have resulted in the formation of "virtual enterprises" in a broad spectrum of functions, including research and development of new products, that is gradually replacing rigid hierarchical structures of vertically integrated companies.

The majority of small companies, however, do not participate in this process to the full extent of their capabilities because of their limited human and material resources. Therefore, small firms that are engaged in developing and marketing a single product or a limited line of products are often not aware of the many opportunities that exist outside their main line of business. And yet, because small companies are frequently endowed with a great deal of enthusiasm, entrepreneurial spirit, motivation, and intellectual capital, they could increase their spectrum of new products given the opportunity. At the same time, small entrepreneurial companies often represent a resource of "niche" technologies that large corporations could help commercialize and market worldwide.

By promoting strategic partnerships between small to medium-sized technology-based companies and large manufacturing corporations, the NIST "Opportunities for Innovation" Program aims at facilitating and accelerating the commercialization of technology. Through regional workshops and monographs like this one, the Program stimulates the intercorporate transfer of technological information.

This monograph, "Opportunities for Innovation in Advanced Surface Engineering", was conceived with the needs of a small company in mind. It provides the technical staff of a small firm with a "multi-company" report on the best opportunities for new business endeavors in a technology-driven market.

Each chapter of the monograph, written by an expert in the field, focuses on one specific issue of surface engineering where new technical advances hold promise of early commercialization and entry into a new market. The authors point out the barriers and shortcomings in current, state-of-the-art practice that prevent the commercialization of the current technological knowledge and that represent an opportunity for a small firm.

Using the technological information in this monograph as a basis, we plan to hold a series of regional workshops that will include both small companies and large manufacturers. The workshops also will provide discussions on business opportunities and the availability of financial and material resources.

The Program has already produced monographs and workshops dealing with polymer composites, a fast evolving technology, finding wide applications in the automobile, aerospace, and consumer goods markets; chemical and biological sensors for the chemical and processing, automotive and power-generating, and health care industries; advanced manufacturing technology that addresses the needs of small to medium-sized firms engaged in the manufacturing of discrete parts; and biotechnology spanning the whole field from health care to agriculture.

It is by improving the flow of technological information and encouraging the formation of strategic industrial partnerships that we hope to help U.S. companies accelerate commercialization of technological advances.

Arati Prabhakar
Director, NIST

PREFACE

Every manufactured component interacts with the environment via its surface. The surface is therefore generally the source of its ultimate deterioration through wear, corrosion, fatigue, oxidation or other failure mechanism. To combat these attacks, surface treatments have been used for many years—indeed, for millennia. We are all familiar with some established surface treatments, such as glazing, painting, or electroplating. Many people are also familiar with less common surface treatments, such as case hardening, carburizing, and salt bath nitriding. Over the last 20 years more advanced surface treatments have been developed. While some have been widely deployed (PVD, CVD, thermal spray, and plasma nitriding, for example), others are less commonly used, or are just beginning to appear commercially (including ion implantation, diamond coating, and laser coating).

The need for advanced surface engineering is growing with the increasing demands being placed on engineering materials. At the same time, increasing emphasis on quality and environmental impact is forcing reductions in the use of many of the older processes. Consequently, there is an expanding market for advanced surface treatments to provide the properties that will be required of 21st century materials used in machinery, consumer products, optics, and biomedical implants.

Most of the advanced surface treatments are presently provided by small companies specializing in particular processes. Successful suppliers know that it is not enough to master a single process and apply it indiscriminately to all components. The successful provider of these treatments must have the knowledge base to match the materials and the required use conditions of the components being processed with his coating materials and processing options. This materials and process knowledge is combined with good quality control to provide the customer with a well-engineered product.

The purpose of this volume is to provide information on the basics of advanced surface engineering processes to small businesses, especially to those not currently directly involved with the technology, in order to make them aware of the current state of the art. Each chapter has been written by an industrial expert in the particular area, and following the basic description of the technology are sections outlining the needs of the surface treatment (such as better controls, improved materials, or better knowledge of fundamental processes) and the future markets that can be expected to open. Meeting these needs and exploiting these new markets is likely to be best done by the combined efforts of present providers with companies whose experience lies in entirely different areas, and it is this type of cross-fertilization that this volume seeks to promote.

We are indebted to the authors of the individual chapters, who put in long hours of effort, and to Dr. Jarda Ulbrecht of NIST, who guided the overall effort and assured that the manuscripts and figures met the proper standards of quality and readability.

William D. Sproul and Keith O. Legg
BIRL Industrial Research Laboratory
Northwestern University

TABLE OF CONTENTS

Introduction to Advanced Surface Treatments

William D. Sproul and Keith O. Legg

BIRL Industrial Research Laboratory
Northwestern University
Evanston, IL 60201

Tel: (708) 491-4108
Fax: (708) 467-1022

Advanced surface treatments are being used increasingly for industrial production. This chapter introduces the general area of advanced treatments and discusses their common requirements and the considerations that must be taken into account when applying them.

Key words: coating; heat treatment; production; process control; quality control; surface engineering; surface treatment; testing.

1. Overview

Surface treatments are critical to the engineering of modern machine components and tools, where the underlying material is chosen for its bulk properties (elastic modulus, hot hardness, etc.) while the surface is treated to provide the necessary surface properties (corrosion or wear resistance, for example). Treatments historically range from glazing and painting to gas carburizing and electroplating. In recent years, a host of new surface treatments have come into existence, partly in response to the shortcomings and environmental problems of older methods, and partly as a result of advances in materials, (such as ceramics and composites) and technologies (such as vacuum processing and high power lasers).

This monograph covers a range of modern surface treatments that provide mechanical components with improved tribological (friction and wear) or corrosion properties. Broadly, these treatments can be broken down into those that work by depositing a protective layer—

- sputtering
- ion plating
- arc deposition
- chemical vapor deposition
- thermal spray
- laser coating
- and diamond coating

and those that work by modifying the existing surface by chemical addition or heat treatment—

- ion implantation
- laser hardening
- plasma nitriding.

The specific technologies covered in the monograph are representative of modern surface treatments and cover the basic treatment methods, but they are by no means comprehensive. Many variations of these methods exist, and new technologies are constantly being developed. Processes are increasingly being combined for better effectiveness—e.g., plasma nitriding or ion implantation with ceramic coating.

The market for surface treatments is growing as increasing demands are placed on modern high performance materials. As engineers recognize that the surface properties of a component can be just as

critical as those of its base material, they are increasingly turning to modern surface engineering to provide those properties. At the same time, many of the older methods of surface treatment, which were the mainstays of industrial engineers, are becoming environmentally unacceptable, and will become prohibitively costly over the next few years - for example, salt bath nitriding, cadmium plating, and chrome plating. Alternatives to these treatments will have to be found and adopted on a wide scale within a very few years. This will open up new high-volume markets for advanced surface treatments.

Engineers who are accustomed to the relatively high prices of applying advanced surface treatments to rather small numbers of tools such as cutters and molds, are finding that the costs can be brought down to acceptable levels for volume production of components. As a result, treatments that used to be considered almost exclusively for costly tools or high value electronics are now being exploited for cheaper items, such as shaver foils, gears, and computer discs. As volume production systems and controls become more widely available, we expect the market for these treatments to grow.

Treatment of many components, such as gears and consumer items used to be impossible because of the high temperatures required. Some of the advanced surface treatments are now available at temperatures low enough to make it possible for them even to be used on plastics. This too will open up new markets for these technologies.

All of the surface treatment technologies described here are already in use industrially on varying scales. Their evolution into large scale processes has created a need for improvements in equipment, processes, and controls. These needs are discussed in each chapter. However, although the different treatments vary markedly in their particulars, they have many points of commonality (which we address below), so that improvements addressing one technology are often applicable across a broad range of technologies. This means that the markets for improved equipment or process control techniques are often broader than one might at first imagine.

2. Features and Considerations Common to Advanced Surface Treatments

Energy

All the surface treatments described here employ some means of depositing energy into the surface in order to effect some metallurgical change or to ensure formation of high quality surface layers. Whereas older methods of treatment frequently involved the application of heat to the entire part (as in gas carburizing, for example), the newer methods usually add energy and material into the surface, keeping the bulk of the object relatively cool and unchanged. This allows surface properties to be modified with minimal effect on the structure and properties of the underlying material.

For example, plasma nitriding uses plasma (ion and electron) bombardment of the surface to clean it and inject nitrogen. Sputtering, ion plating, and arc deposition all bombard the surface with ions from a plasma during coating to provide the energy needed for the formation of dense, well-bonded films. In ion implantation, the ion beam deposits energy in the outermost few tenths of a micron, disrupting atomic bonds, allowing rapid diffusion, and permitting the creation of metastable materials. Laser cladding uses the fact that light is strongly absorbed in the surface to create intense local heating that forces metallurgical alloying at the surface to provide a strong bond. Similarly, laser glazing modifies only the outermost layer of the material, leaving the inside untouched.

Therefore, improved methods of monitoring and controlling surface temperature and energy deposition would be of use to almost all the advanced surface treatments.

Plasmas

Almost all the surface treatments covered here use plasmas (i.e., clouds of ions and electrons from which particles can be extracted), primarily to lower process temperatures by adding energy to the surface in the form of kinetic energy of ions rather than thermal energy:

- Plasma nitriding uses a plasma to provide heat and surface cleaning.
- The arc used in arc deposition is an intense plasma that provides large numbers of metal ions.
- Ion beams are always formed from plasma sources of various types.
- Plasma spraying uses a plasma to melt the spray powder.
- All of the physical hard coating methods (sputtering, ion plating, and diamond deposition) bathe the surface in a plasma to provide the energy for proper film formation.

To meet production requirements of uniformity and reproducibility, there is a growing market for simple methods of generating, controlling, and monitoring large-volume plasmas—power supplies capable of excellent arc suppression, simple probes and plasma analysis software, for example.

Vacuum

Almost all of the advanced surface treatments (except most thermal spray and laser methods) require the use of vacuum chambers to ensure proper cleanliness and control. In fact, it is the advent of simple, relatively inexpensive vacuum equipment that has made many of them cost-effective.

If vacuum processing is used properly the payback in reliability and product quality is worth the added cost and complexity. Vacuum processes are generally more expensive and difficult to use than liquid or air processes, and the correct design of vacuum processing equipment is important. At the outset, one must decide whether to employ batch, load lock, or continuous processing. Batch processing is easier and cheaper to set up, but it consumes a great deal of time in vacuum cycling. It is also difficult to remove residual water vapor from the chamber and fixturing surfaces, and this water vapor may contaminate the process. Load lock and continuous flow processing have higher capital costs and complexity, but are cheaper and faster for processing large numbers of similar items. Once these chambers are pumped down initially, they do not have to contend with water vapor problems, and the cycle time of components to and from vacuum is minimal.

The choice of the pumping system depends on the demands of the process (ultimate vacuum, gas flow rates, etc.) and on the cycle time required. Diffusion, cryo-, and turbo-pumps all have different advantages and disadvantages, and any competent vacuum professional or equipment company should be able to match the equipment to the needs of the process.

While basic vacuum equipment (even of very large size) is now readily available, there is still a lot of room for simplification. For example, most processes still require two different types of pumps, two types of gauges, and a variety of valves, plumbing, and controls. Simple, industrially accepted methods for measuring vacuum cleanliness, checking for leaks, etc., are readily available, but are relatively expensive and little used in industry, although solid advances have been made in recent years. The growth of advanced treatments is driving a developing market for simpler pumps, gauges, mass spectrometers, and other hardware and instrumentation.

Difficult Geometries and Large Areas

When choosing a process for a particular application, the process must be matched to the end use, the geometry of the component to be treated, and the material of which the component is made.

For example, while most of the technologies covered here can be used for large scale industrial production, the directed beam techniques, such as ion beam implantation, thermal spray, and laser methods, are generally more suitable for treating small components, or small areas on large components, since the treatment time for these processes is proportional to the area to be treated.

Methods for treating the insides of holes and tubes are limited. High temperature methods such as thermal chemical vapor deposition (CVD) are very effective, but are limited to those materials capable of withstanding high temperatures. Lower temperature treatments, such as plasma nitriding and plasma spraying can be used, but only if the dimensions are adequate.

Quality Control of Advanced Surface Treatments

In adopting advanced surface treatment technologies, one must also adopt adequate quality assurance tests. Satisfactory QC and QA tests are available, but one must be circumspect in choosing tests that properly reflect the requirements placed on the treated component. One must be especially careful in applying older test methods to advanced treatments. Engineers frequently attempt to apply older standards, and find them wholly inadequate for testing the new treatments. In contrast to older coatings, such as electroplates, paints, and glazes, whose thickness is usually measured in thousandths of an inch, advanced surface treatments are usually thin—i.e., they apply or modify a layer only up to about 5 μm (0.0002") thick. Thicker coatings are often unnecessary, or even counterproductive, because of the extreme hardness of the advanced coatings. Thinner treatments are usually less expensive, and depositing energy only into the surface keeps the component relatively cool. The thinness of these advanced surface treatment layers often makes it difficult to carry out quality control checks using traditional methods.

Methods such as Rockwell hardness testing, that work well on gas carburized material or hard chrome, cannot be used on ion implanted materials or most physical and chemical vapor deposited materials, since the surface layers are far thinner than the depth of a typical indent. Microhardness methods, such as Vickers and Knoop hardness, can be used, but their numbers must be treated with some caution, since they vary with the thickness of the treated layer. Very low load indentation hardness equipment is currently too expensive and sensitive for shop floor use.

Similarly, the older methods of measuring coating thickness, such as eddy current testing, are not usable for measuring thin layers. Other methods must be used, such as x-ray fluorescence, ball cratering, or cross-sectional microscopy.

Because most advanced coatings adhere extremely strongly to the underlying material, the older methods of measuring adhesion—the Scotch Tape test, adhesive pull testing, etc.,—cannot reach the high ranges required. Methods that can do so, such as scratch testing, do not give absolute numbers, but for the same coating on the same substrate, the scratch test is an excellent relative test for adhesion. In general, one must find or define a test that works for a particular application, and consequently, one must be careful in applying that test to other materials, components, or surface finishes.

Similarly, the chemistry of advanced surface layers can be difficult to measure, partly because of the limited amount of material, and partly because the differences between a good coating and a bad one, for example, are often subtle. Diamond coating is a good example of this.

With the growth of advanced surface treatments there has therefore developed a market for improved industrial methods of measuring hardness, adhesion, chemistry, and other properties of surface layers.

In consonance with improved measurement equipment and methods, there is a definite need for new accepted engineering standards for hardness, adhesion and other surface properties that the industrial engineer can apply to modern thin coatings.

Testing of Performance

The choice of valid tribological tests has always been a matter of considerable debate, and truly universal methods have never been devised, either for the old treatments or for the new. One common approach is to use a simple screening test (pin-on-disk, for example) that gives a rough feel for the relative performance, but no measure of actual expected performance in use. Alternatively the test can be made to duplicate the real life situation as closely as possible, but usually at higher loads or speeds to achieve measurable results in a reasonable time.

Neither approach is wholly satisfactory, although careful attention to detail can yield very useful tribological data. Screening tests must be chosen carefully to engender the correct failure mechanisms, otherwise they may correlate poorly with actual performance. In accelerated testing, loads and speeds must be chosen with care to ensure that they do not move the test into a totally different failure regime, where the results are meaningless.

In measuring the performance of surface engineered materials, simple tribological tests would be very useful that could easily be used by industrial engineers and could accurately predict performance. Combined with this, simple methods for measuring very low wear rates in actual field use would be invaluable.

Substrate Cleaning and Coating Removal

Until recently, the universal practice in preparing surfaces for coating or other surface treatments involved cleaning with organic solvents, freon, etc. Because of environmental concerns and costs, these methods are no longer viable. New aqueous cleaning methods and solutions have been developed and are now used by most surface treatment providers, but they are still not widely known or well characterized. There is a growing market for more-or-less universal cleaners and cleaning systems that will ensure a high level of cleanliness—even for heavily soiled or oily surfaces—with no contamination or rusting, and with easy separation of potentially harmful materials, so that residues can be disposed of safely and cheaply.

Most advanced coatings concentrate on providing excellent adhesion between the substrate and the coating. This is of course essential for high performance, but it causes difficulty in stripping them for refurbishing or for correcting errors in processing. Many of the advanced coatings are ceramics that are virtually impervious to all solvents and most acids, and are certainly less reactive than the components on which they are placed. Most advanced coating companies have developed proprietary stripping techniques. Most of these stripping solutions pose environmental or health problems,

or risk damage to the underlying material. There is therefore a growing market for "universal" methods of coating removal, whether chemical or physical. New methods under study and development include lasers, high velocity water jets, and high velocity particle suspensions.

Process Control and Sensing

Proper process control is critical to the performance of any surface treatment. Advanced processes are capable of producing outstanding properties, provided the process is properly controlled. In common with many of the older processes, quite subtle variations in process conditions can be catastrophic. All of the advanced treatments incorporate a level of control capable of allowing them to work well on a day-to-day production basis.

For more complex production requirements, improved computer process analysis and control (such as intelligent processing) is increasingly available, but it still generally requires sophisticated programming or system set-up and is often very difficult to add onto existing industrial equipment. To gain the most from these sophisticated process controls, it is necessary to use simple, robust sensors capable of monitoring process conditions, such as temperatures, plasma parameters, gas constituents, etc. The market is therefore growing for robust process sensors and simplified software and hardware that will put this modern control technology into the hands of the process engineer in industry.

Linking Treatment Conditions with Properties and Performance

In general, the development of surface treatments is largely empirical and based on experience. There is a general lack of basic information on the links between process conditions, material structure, material properties, and performance. Analytical or computer models capable of linking processing conditions with materials structure, and ultimately materials structure with properties and resultant performance, would be invaluable and would ultimately lower development costs and reduce time-to-market.

3. Adopting Advanced Surface Treatments for Production

At the present time almost any advanced surface treatment requires some development and modification to match it to any particular item. This matching can be very simple, involving nothing more than checking that standard process conditions are adequate. On the other hand, it can be very expensive and time consuming, involving the development of new processes and detailed field testing. Usually one should check both the surface treated layer and the underlying component to ensure compatibility, and getting the most out of an advanced treatment may require the choice of new materials or production processes.

Unfortunately, many companies whose products could benefit from advanced treatments are unable or unwilling to underwrite this development and reject any process whose standard conditions do not immediately produce good results. Given the empirical nature of the technology at present, this frequently results in long-term losses in productivity or market performance. It often also costs more in personnel time and testing to try out many different processes than to choose a process carefully at the outset and then bring it to production.

Therefore, if an advanced surface treatment is being considered either as a replacement for an older process or as a means to gain acceptable performance for a new component, the process should be carefully investigated and costed for development and production. The development cost should include a sufficient sum for adequate development to ensure a proper match to manufacturing conditions and end use, but the evaluation of long term cost should take into account the probable improvements in performance, reliability, and product life.

About the authors: *William Sproul received his Ph.D. in Materials Engineering from Brown University. While working at Borg Warner's R&D laboratories, he developed the high rate reactive sputtering technology used for depositing high density thin PVD coatings, and authored several patents in the area. He is the Group Leader for Vapor Deposited Coatings at BIRL, the Industrial Research Laboratory of Northwestern University.*

Keith Legg received his Ph.D. in Surface Physics from the University of York, England, in 1973. He was one of the founders and Vice President for R&D of Ionic Atlanta, a company specializing in advanced coatings and ion implantation. He is now a Research Scientist at BIRL, developing various types of coatings for industrial applications.

Sputter Deposition

Stephen Rossnagel

IBM Research Laboratories
Yorktown Heights, NY 10598

Tel: (914) 945-1503
Fax: (914) 945-2141

Sputter deposition is widely used in the electronics industry, for producing integrating circuits, and in the glass industry, for coating architectural glass. It is becoming more and more widely used for the production of hard, wear resistant coatings on tools and machine components. At the same time it is being incorporated into a new generation of integrated production tools in the semiconductor industry.

The expansion of its use and widening of its market bring new problems and new opportunities in the development of improved equipment, power supplies, and processes.

Key words: magnetron; plasma; reactive sputtering; sputtering; TiN; unbalanced magnetron.

1. Introduction

Sputtering and sputter deposition are commonly used techniques to alter surfaces. Sputtering, or more exactly, sputter etching, is a process by which energetic particles (for example, ions) bombard a surface and erode it. A macroscopic analogy would be sandblasting. The sputter etching process results in the removal of the surface layers, exposing the underlying material. In the case of a compound, the process may also selectively remove certain components, resulting in an altered surface composition over time.

Sputter deposition is simply the process by which the sputtered atoms land on a nearby surface and form a layer or film. The film is typically the same composition as the surface being sputtered, if the sputtering is done in an inert atmosphere. In a reactive background gas, gas atoms may combine with the depositing film atoms on the substrate surface in the form of a compound. This latter case, known as reactive sputter deposition, is commonly used for the deposition of oxide or nitride films.

Sputter deposited films are used routinely in the microelectronics industry to form the metal and compound circuitry on integrated circuits. They are also commonly used to form coatings on other surfaces for the purposes of protection (hard coatings), decoration, corrosion resistance, conduction, the reflection of light, and many other applications. This chapter will examine some of these sputter deposition processes and applications in a variety of industries.

2. Sputtering

Sputtering is the result of the impact of a very fast particle with a solid surface. In effect, the incident particle can dislodge atoms from the surface or near-surface region of the solid simply by momentum transfer from the fast, incident particle to the atoms near the surface of the solid. The type and kinetic energy of incident particle used helps determine the magnitude of the effect, as well as

other related features such as the emission direction or energy. Sputtering has been observed for bombardment by ions, atoms, electrons and even photons. For all practical purposes, ions are used, and the remainder of this chapter will deal almost exclusively with ion bombardment induced sputtering.

A schematic of a sputtering event is shown in figure 1. Sputtering is usually characterized by the ratio of the number of the ejected particles per incident particle: the ratio is known as the sputter yield, Y.

Y = (number of ejected atoms / each incident particle)

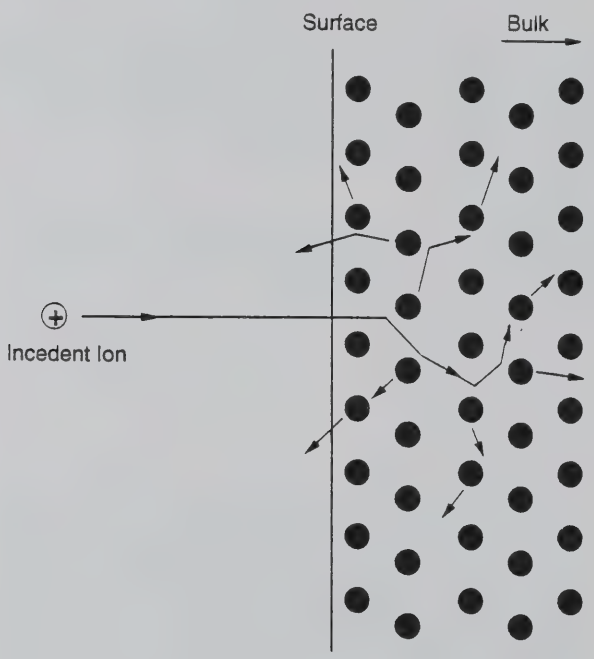

Figure 1. A schematic of physical sputtering. This process would be characteristic of the knock-on energy regime, at energies of 20 to 1000 eV.

Depending on the kinetic energy of the incident ion, different physical effects will be seen in the solid. At the very lowest ion energies (below 15 eV or so), the incident ion has only enough energy to dislodge atoms near the surface. Surface binding energies are typically 4-8 eV, and there is simply not enough energy to overcome this bond except in very unique geometries. This energy region is known as threshold sputtering, and the typical sputter yields are almost immeasurably small (10^{-5} or smaller). In most plasma devices, threshold sputtering is an insignificant effect. In the past several years, however, several new high density plasma tools have been developed in which this very low energy sputtering can be important. These devices include the electron cyclotron resonance (ECR) plasma, the radio-frequency inductive (RFI) plasma, the helicon and the helical resonator plasmas. In each of these cases, the plasmas have a much higher density than the conventional rf-diode and magnetron devices, and the ion currents can be very high. For example, in a small ECR tool, the net ion current at 1 kW can exceed 10 A. For a sputter yield of 10^{-5}, this means on the order of 10^{15} atoms are sputtered per second. For a typical 2-3 liter source, this is an erosion rate of 10-20 Å per hour, an almost immeasurably low rate. However, it is a sufficiently large amount to contaminate microelectronic junctions.

In the energy range of about 20 eV up to perhaps 700-800 eV, a more complicated, multi-atom process occurs. In this case, the incident particle collides with one or more near-surface atoms and transfers sufficient energy to dislodge the target atom from its binding site. The dislodged atoms then may have sufficient energy to dislodge additional atoms. Eventually, this chain of dislodged atoms may reach the surface with the result that some of them may leave the surface. This energy regime is known as "knock-on" sputtering, and is the region most commonly used for thin film processing. Figure 1 shows a series of collision events that is characteristic of knock-on sputtering. Figure 2 shows the sputter yield as a function of ion energy for several materials in the knock-on sputtering regime.

Theoretically, this process is difficult to handle. The yield depends critically on the exact point of impact, the local crystallinity as well the topography of the surface. The most successful models have used a technique known as molecular dynamics. This technique uses a very large computer to keep track of the status of several hundreds to thousands of atoms in the near surface region. The incident trajectory of the ion is plotted, the collisions are simulated, and the status of each atom is calculated every femtosecond or so. Eventually, atoms may or may not be emitted from the surface, and the region cools prior to the next ion impact. After a few hundred thousand bombardment events, an estimate of the average sputter yield can be made. This process is, in effect, a theoretical experiment.

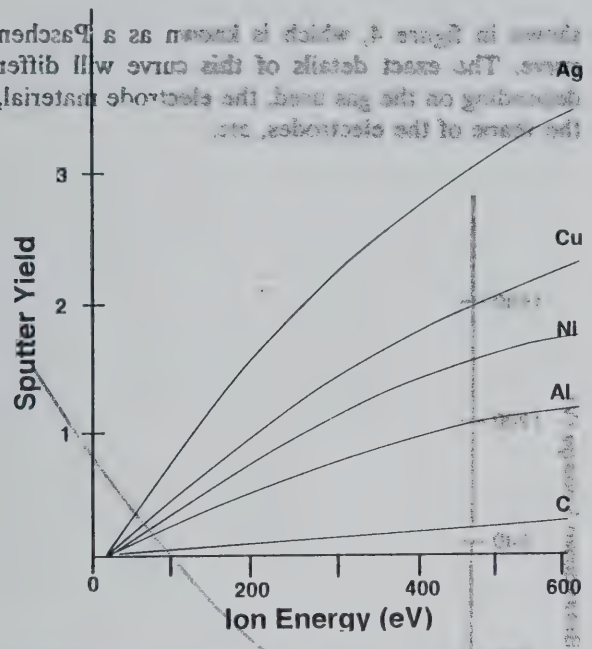

Figure 2. The sputter yield for common materials as a function of incident Ar ion energy.

At higher ion energies, typically from about 1000 eV to 50 keV, the kinetic energy of the incident ion is sufficient to break all the bonds near the point of impact in the form of a collision cascade. This cascade is on the order of tens of atoms in radius and may encompass hundreds of atoms. Atoms in the first or second layer of this cascade from the surface may have sufficient energy to overcome the local average binding energy and be emitted. The cascade freezes out very rapidly (10^{-13} s) as the energy is carried away from the cascade in the form of phonons. Collision-cascade sputtering has been successfully modelled, first by Sigmund in the late 1960s [1].

At even higher energies (50 keV to MeV) the sputtering process tends to be less effective. At these high energies the incident ion travels many atomic layers below the surface before depositing its kinetic energy through collisions. The result, however, is that most of the energy is deposited far from the surface of the target, and relatively little sputtering takes place. In this energy range, the incident ion is generally "implanted" and may significantly alter the physical or electrical characteristics on the near surface region. This technique is commonly used to treat surfaces and is described much more fully in Chapter 8.

For the purpose of many thin film deposition technologies, the knock-on sputtering region is the most energy efficient region. It is also technically more convenient to sputter surfaces at energies in the < 1000 eV range. This lessens the complexity in the power supplies, feedthroughs and insulation, and reduces the safety risk of high voltages.

The physical sputtering process differs from evaporation in that the emitted, sputtered atoms have much higher kinetic energy than evaporated atoms. As an example, a sputtered Cu atom may have an average of 8 eV of kinetic energy, whereas an evaporated atom has typically less than 1 eV. This energy difference will result in differences in the resultant film properties, particularly density, microstructure, and adhesion.

In the presence of reactive gas species, it is also possible to augment the physical sputtering rate by additional chemical reactions. If the products of these reactions are volatile, the net removal rate may exceed the physical sputtering rate by a factor of ten or more. This technique is known as Reactive Ion Etching (RIE) and is commonly used to etch patterns in deposited films for integrated circuit applications.

As a last note about sputtering: because physical sputtering is effectively a momentum and energy transfer process, the electrical state (charge) on the incident particle is mostly irrelevant. In reality, ions are typically neutralized as they approach a surface (within a few Angstroms) and strike the surface as neutrals. Therefore, the sputter yield of an ion and a neutral are indistinguishable. However, experiments used to measure the sputter yield have no reliable way to measure an incident neutral flux. Therefore, the topic is virtually ignored, although under some circumstances it can lead to a significant underestimate of the rate of sputtering or deposition.

3. Plasma Technology

The most convenient technique for creating the fast moving particles needed for sputtering is to accelerate ions by means of an applied electric field. The ions are typically generated in a plasma, and then accelerated either across a sheath to a surface near the plasma, or else through a set of grids or other ion optics in the form of an ion beam to a more remote sample. The former case is typically implemented in the form of a diode plasma, where the surface to be sputtered is the cathode in the circuit.

3.1 Diode Plasmas

The most basic form of a 2-electrode or diode plasma is shown in figure 3. The device consists of a cathode, an anode, a DC power supply, and an enclosure. The power supply sets up an electric field between the electrodes. A plasma may be formed under suitable conditions of applied voltage and gas density. Electrons are accelerated towards the anode, and can cause ionization by colliding with gas atoms. Ions, which are accelerated towards the cathode, cause the emission of secondary electrons from the cathode surface. These electrons are accelerated into the plasma, and cause subsequent ionization of background gas atoms. The number of secondaries emitted for each ion bombardment event is known as the secondary electron yield, y_i, and is typically a number on the order of 3-10%. To make up for the loss rate of the ions, each secondary electron must ionize a number of gas atoms equal to at least the inverse of the secondary electron yield. In many cases, depending on the geometry of the cathode and the operating conditions, this required ionization rate must be a factor of 2-3 times higher. A rough estimate of the minimum discharge voltage can be made by dividing the ionization energy for the background gas by the secondary electron yield, and then multiplying by a factor of about two. This last factor is due to the geometrical relation that at best, about 1/2 of the ions might strike the cathode. The interrelation between gas density, electrode spacing and applied voltage needed for the breakdown of the gas and the formation of a plasma is shown in figure 4, which is known as a Paschen curve. The exact details of this curve will differ depending on the gas used, the electrode material, the shape of the electrodes, etc.

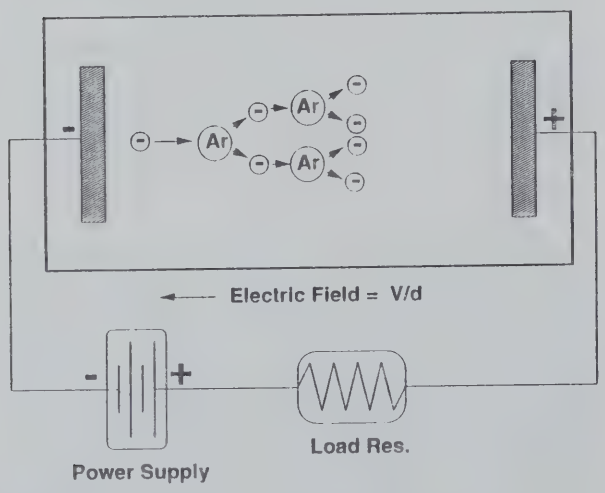

Figure 3. A diode plasma device. The enclosure is in reality a vacuum system with the ability to vary pressure in the mTorr or Torr pressure range.

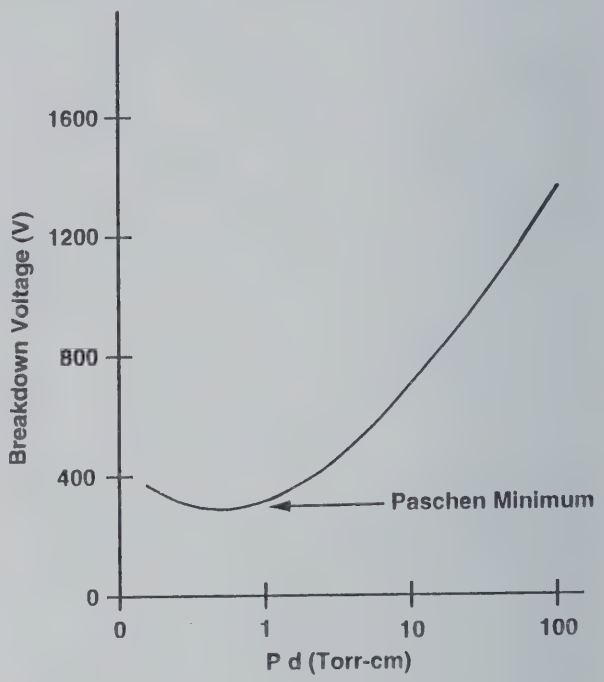

Figure 4. A representative Paschen curve for the breakdown voltage of a gas as a function of the proudct of the chamber pressure (in Torr) and the electrode spacing, d, in cm.

The plasma formed between these two electrodes has several characteristics. First, it is a conductor with roughly equal numbers of ions and electrons. Second, only a tiny fraction (perhaps 0.01%) of the gas atoms are ionized: the majority are neutral. Third, the electrons in the plasma are relatively hot, with a Maxwellian energy distribution and an equivalent thermal temperature of 10,000-50,000 K. The electron temperature is usually described with energy units (eV), where 1 eV is about 11,000 K.

The properties of the plasma lead to several other characteristics. Because the plasma is conductive, there is virtually no potential gradient within the plasma itself. All of the electric fields occur at the edge of the plasma in a region known as a sheath. Due to the large proportion of neutral gas atoms to ions, the ions are in thermal equilibrium with the gas atoms (through collisions) and are only at a temperature on the 100-1000 °C range. Due to the much higher electron temperature and

lower mass, the electrons move very rapidly around the plasma. This last effect results in the appearance of several different potentials within the system.

The first of these potentials is known as the plasma potential. Due to the higher mobility of the electrons in the plasma, the plasma becomes slightly depleted of electrons. This results in a slightly positive potential for the plasma, typically a few volts more positive than the anode. This positive potential tends to retard the loss rate of electrons, such that it equals the ion loss rate. The plasma potential scales roughly with the electron temperature, but may also be related to the relative sizes of the electrodes.

The second potential is known as the floating potential, and is the potential that an electrically floating object immersed in the plasma reaches. This potential is again related to the significantly higher electron mobility. The object receives a higher flux of electrons, compared to ions, and charges negatively. The resulting negative potential reduces the electron flux, such that it again equals the ion flux. The floating potential is always negative of the plasma potential, typically by a factor of three times the electron temperature (in eV).

The energy with which an ion strikes a surface is then the difference between the plasma potential and the potential of that surface. For most plasmas, all the ions have a charge of +1. The energy they reach, in eV, is then just equal to the voltage across which they are accelerated, in V. For objects floating electrically in the plasma, the energy is less than 20 eV, and causes little sputtering. For a surface such as the cathode, the ion energy is equal to the difference between the plasma potential (a few more volts positive than the anode) and the cathode voltage. These energies can be several hundreds of eV and will cause significant sputtering of the cathode surface.

In diode plasmas, generally the cathode surface is sputter etched, and all other surfaces receive a net deposition of the atoms sputtered from the cathode. Therefore, a sample to be coated with a thin film of sputtered atoms could be located on the anode surface, or else virtually anywhere within the chamber. Several practical issues, such as coating uniformity and rate, will be discussed later, and will help define appropriate experimental conditions.

DC-diode plasmas are not used in any practical manufacturing devices due to relatively low etching and deposition rates. The reason for the low rates is a low plasma density because the cross section for electron-impact ionization is fairly small. Therefore, to get a high plasma density, and hence a high ion bombardment rate, the gas pressure must be increased to pressures near 1 Torr. In addition, the voltages needed for moderate currents are fairly high, several keV. The resultant sputtered atoms are rapidly scattered by the relatively high pressure background gas, and the net deposition rate on a sample surface is fairly low.

An additional constraint on DC-diode sputtering is that the electrodes must be metallic conductors. If one of the electrodes is insulating, it charges rapidly, and additional current is suppressed. This effect can also occur if a reactive gas, such as oxygen or nitrogen, is introduced into the plasma, resulting in the oxidation of the metal surfaces on the electrodes. Therefore, DC diode sputtering is not an appropriate technology for depositing most compounds and dielectrics.

3.2 RF Diodes

Many of these problems can be overcome by powering the diode electrodes with an AC rather than DC voltage. At the most commonly used frequency of 13.6 MHz, there is little voltage drop across an insulating electrode or layer. The electrodes will not charge up, and therefore it is possible to sputter dielectrics or reactively sputter metals. There is an additional degree of ionization with an rf-powered plasma due to additional energy transmitted to the plasma electrons at the oscillating sheath [2]. The net result is a higher plasma density, compared to DC-powered plasmas, and the ability to operate at lower system pressures (5-200 mTorr).

RF-diode systems are typically configured as in figure 5. In this case, the cathode is powered through an impedance-matching device known as a matchbox or matching network. The function of the matchbox is to maximize the power flow from the rf generator, which has an output impedance of 50 Ohms, to the plasma, which has a complex impedance usually in the 1000 Ohm range. A series capacitor is included in the matchbox to allow the formation of a DC bias on the cathode. This occurs due to the higher electron mobility, and results in a negative DC potential on the powered electrode of up to half the applied rf peak-to-peak voltage. The ions in the plasma which are accelerated to the cathode are too massive to respond to the 13.6 MHz fields, and respond only to the DC-bias.

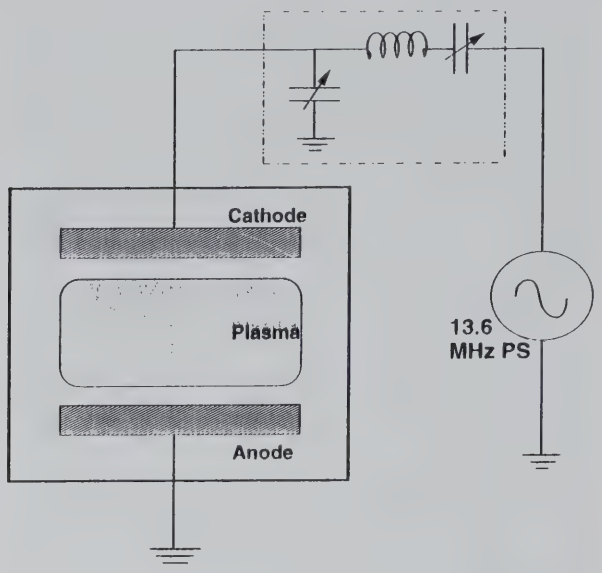

Figure 5. An rf-powered plasma system. The matching network (matchbox) is shown within the dotted rectangle. This device is shown with the anode grounded. It may be the case, however, that the anode is connected to the lower part of the power supply for some applications.

Matchboxes used to be configured with manually operated, adjustable air-gap capacitors. These have been replaced with motor-driven adjustable capacitors, which are feedback-controlled to minimize the reflected power to the supply. The inductor coil in the matchbox is less-easily adjusted. Some manufacturers provide clamps for the coil which either selectively short out a section, or simply make contact at the desired point on the coil. Very early matchboxes were configured with inductors with sliding contacts, allowing for continuous, real time control. These coils are limited to powers of a few hundred watts and are not compatible with industrial applications.

Currently, coils are usually silver-plated Cu, and are water-cooled at powers greater than 1 kW. In the late 1980's, commercial matchboxes were re-engineered to be physically smaller and more contained. There was no real functional change inside, but the smaller units are lighter and more compatible with cleanroom and integrated-processing technology (discussed below).

RF-diode sputtering devices are used routinely in the microelectronics industry for the deposition of dielectric films, generally as insulating layers between conductive layers on an IC chip. Often the sample surface is biased slightly during the deposition to provide some level of ion bombardment, which results in changes to the density and microstructure of the films, and some degree of resputtering which leads to increased planarization. This technique is known as bias-sputtering. Magnetron devices can also be operated using rf power (next section).

RF-sputter deposition is also routinely used for the deposition of hard coatings, such as alumina, on such surfaces as magnetic pick-up heads for disk drives. The deposition rate is fairly slow, though, and this technique tends to be used only for small-scale parts.

RF-sputter deposition is complicated by the presence of the high voltage, rf signal within the chamber. Any lead or feedthrough into the chamber must be shielded carefully, or it will pick up potentially dangerous potentials. Many companies and locations have strict limitations on the amount of rf emissions that can be leaked from these systems. The health issues for this leakage are not explicit, but it is generally always better to contain the emission.

Measurements in rf plasmas can be complicated by the rf noise. For deposition systems, quartz crystal microbalances (rate-monitors) are routinely used to measure the rate of film build-up. In an rf environment, it is necessary to shield the microbalance sensing unit from the highly energetic electrons which are moving in response to the rf potential. The most common fix is to impose a strong magnetic field on the microbalance to shield it from the electrons. Langmuir probe measurements of the plasma are also complicated, and a number of experimenters have begun to examine the problem [3,4].

The most recent work with rf-plasmas has been in the area of inductively coupled plasmas. The diode plasmas discussed so far are effectively capacitively coupled. The sheaths between the electrodes and the plasma function like the gap in a large capacitor. The result of capacitive coupling is that a lot of voltage is dropped across the sheath. Most of this energy turns up as either the kinetic energy of the ions, or in kinetic energy for the secondary electrons coming back into the plasma. This is very adequate for sputtering applications. For reactive applications, though, too much energy is wasted at the sheath.

Reactive applications are based on chemical reactions, which typically might require a few eV to 20 eV for each reaction. For conventional sputtering, an ion might typically have 500 to 2000 eV of kinetic energy; more than enough for the reaction. The extra energy is used for sputtering and to heat the substrate and does not lead to faster reactive

etching. Inductively coupled plasmas operate by attempting to drive macroscopic currents in the plasma. Typically, an inductor (a coil or a spiral) is placed adjacent to the plasma chamber. When driven at 13.6 MHz, an oscillating electric and magnetic field is set up near the inductor. The electrons in the plasma are sensitive to this applied field and can move in response. These energetic electrons then cause additional ionization and a much denser plasma than the capacitively coupled plasma. The resultant plasma density is much higher than with the diode, with proportionately higher currents and lower ion energies. This does not lead to any increases in sputtering, but the higher flux results in higher rates of chemical reactions, and as a result, higher etching rates. Inductively coupled plasma are just becoming used for etching applications, and should also be appropriate for reactive deposition using plasma enhanced chemical vapor deposition (PECVD).

3.3 Magnetically Enhanced Plasmas

The second approach to solving the difficulties present with DC-diode sputtering is to use magnetic fields to enhance the plasma. Electrons in a magnetic field are subject to a force,

$$\boldsymbol{F} = q\,\boldsymbol{v} \times \boldsymbol{B},$$

where q is the electronic charge, $\boldsymbol{v}$ the electron velocity, and $\boldsymbol{B}$ the magnetic field strength. A simple magnetic field perpendicular to the electron motion would cause the electron to move in a circular path with radius, r = mv/qB (where m is the electron mass), known as the Larmour radius. In the direction of the magnetic field, there is no net magnetic force, so the electrons are unconfined. The net result is that electrons tend to spiral along magnetic field lines in a helical path. By constraining the electron to this motion, the effective path length of the electron is increased significantly, and hence the probability of an ionizing electron-atom collision is increased.

This effect has been successfully applied to plasmas for many years, with the result that the ionization rate is increased, the plasma density is increased, and as a result, the plasma impedance is reduced. For a given applied power, then, the effect of the magnetic field is to cause a low current, high voltage plasma to change into a high current, lower voltage plasma. The increased density also allows significant reductions in the background pressure, such that the magnetically enhanced plasmas can operate at pressures as low as the 0.1 mTorr range.

The most prevalent application of magnetic fields to sputter deposition is with a device known as a magnetron. In this device, a magnetic field is configured to be parallel to the surface of the cathode. There is a resulting electron drift, caused by the cross-product of the electric and magnetic fields (known as an E-cross-B drift) which tends to trap electrons close to the cathode surface. The drift motion is directional, and in a magnetron is configured to close on itself. A common example of this is shown in figure 6, for a circular geometry, and is called a circular planar magnetron. In this case, the magnetic field is configured to be radial, and is set up between a central magnetic pole and a perimeter, or ring magnetic pole.

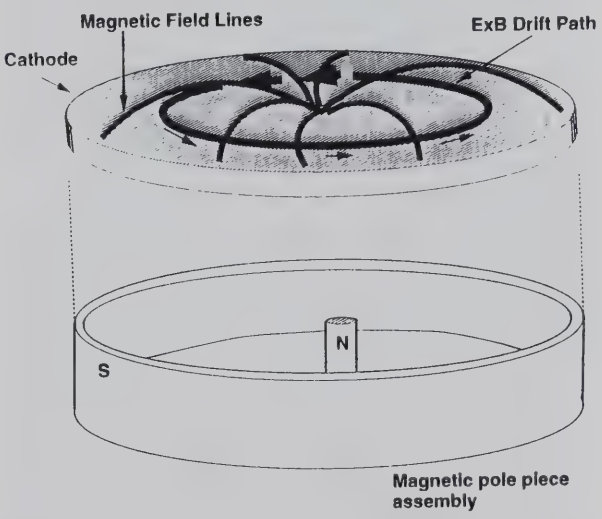

Figure 6. A perspective drawing of a circular planar magnetron, showing an expanded view of the pole piece configuration. The water cooling is not shown, but typically occupies the volume between the cathode and the back of the pole piece assembly.

The closed-loop, E-cross-B drift configuration is not limited to a circular geometry, however. Perhaps the most common alternative is to use a rectangular configuration, known as a "racetrack" magnetron (fig. 7). This geometry has some intrinsic advantages for the automated handling of parts, as will be discussed below.

The intrinsic advantage of the magnetron modification to the DC-diode is that the secondary electrons are strongly constrained to a region near to the cathode surface. This causes a dense plasma to form near the cathode in the region of the drift-loop. The dense plasma results in very high levels of

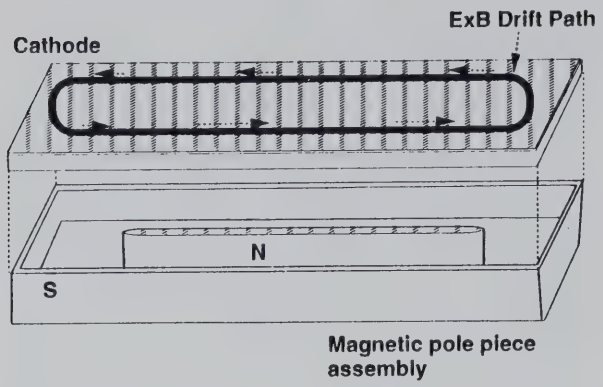

Figure 7. A rectangular, or racetrack magnetron.

ion bombardment of the cathode surface, and hence, high rates of sputtering. The high rate ion bombardment is localized on the cathode directly under the $\boldsymbol{E} \times \boldsymbol{B}$ path. The resultant sputter emission of atoms is also localized, which means that deposition uniformity is usually not good. Therefore, for most deposition systems, it will be necessary to either move the sample, or alter the magnetron location to attain good deposition uniformity. In addition, the erosion of the cathode is also localized, which results in poor utilization of the cathode material as deep grooves are eroded into the cathode surface in the vicinity of the $\boldsymbol{E} \times \boldsymbol{B}$ drift path. The wide groves are called the "etch track" and are very characteristic of magnetron sputtering. Typically, only 10-15% of the cathode material can be used before the grooves start to etch through the back of the cathode.

Magnetrons can also be operated at 13.6 MHz. The plasma impedance is lower than with a conventional rf-diode, so the matchbox may need to be altered. The motor-driven adjustable air-gap capacitors in matchboxes are fairly expensive and relatively difficult to change. The easier solution is to change the inductor, usually by eliminating a turn or two either with a clamp device or by making a new coil from Cu tubing.

RF magnetrons are less efficient than dc magnetrons, generally by a factor of two [5]. The exact reasons for this remain an open issue. RF magnetrons are typically used for sputtering dielectrics and for reactive sputtering (discussed below). Arcing becomes a significant issue when sputtering dielectrics. An arc, when formed in the etch track, moves rapidly around the track etching a deep groove into the material in a mostly uncontrolled manner. This effect is usually undesired, because the arcing process strongly dominates any physical sputtering (the voltage becomes very low in an arc) and the arc tends to lead to the emission of particulates. Power supplies are usually inadequate in controlling arcs, and arcs remain an operational problem in sputter deposition technology. However, due to increases in the understanding and applications of arc-based deposition, this effect does have a positive side. Several manufacturers have configured combination magnetron-arc deposition systems which use the same cathode for both applications, and can be changed from magnetron to arc and vice-versa at will. This is attractive for the deposition of hard coatings, such as TiN, particularly for applications where the microstructure of the deposited film is not critical.

4. Deposition Systems

4.1 Conventional Systems

Magnetrons are used for the high rate deposition of metal, compound and dielectric films. The deposition rate for magnetron sputtering is only limited by the ability to cool the cathode. Physical sputtering is relatively inefficient from a power point-of-view. An Ar ion incident at 500 eV onto a Cu cathode will sputter roughly two Cu atoms, each with an average energy of 8-10 eV. Most of the remaining energy is deposited in the cathode in the form of heat. The maximum power that can be deposited on a cathode is limited by the allowable surface temperature and the ability to remove heat from the backside of the cathode, typically by cooling water. If the output water temperature is below 100 °C, then for a given maximum surface temperature, the maximum discharge power, and hence the deposition rate, is limited by the water flow rate. A simple approximation leads to:

$$P_{max} = 2.5\ f$$

where P_{max} is the maximum discharge power in kWatts, and f is the water flow (gal/min). This relation is independent of the size of the cathode, because it is simply limited by the boiling point of the cooling water. For practical purposes, this limits a 15 cm diameter magnetron to about 5 kW, a 30 cm diameter magnetron to about 25 kW, and a 60 cm rectangular magnetron to about 40 kW. It is always possible, depending on the quality (or lack thereof) of the cooling design to alter these numbers by a factor of two. The deposition rate is also strongly related to the geometry of the system. The closest practical spacing between a sample and a cathode is about 5 cm. The maximum practical deposition rate, then, for Cu deposition is on the order of 2 μm/min.

The emission from a magnetron is localized to the high plasma density, etch-track region. At cathode-to-sample, or "throw" distances on the order of the cathode radius, the distribution of the deposited atoms on the sample mimics the cathode erosion profile (fig. 8). At intermediate throw distances, the deposition profile is approximately uniform, and at large distances, the deposition is more consistent with a point source. The middle distribution is acceptable for some deposition systems, particularly if the sample is small. However, the uniformity is inadequate for most other applications.

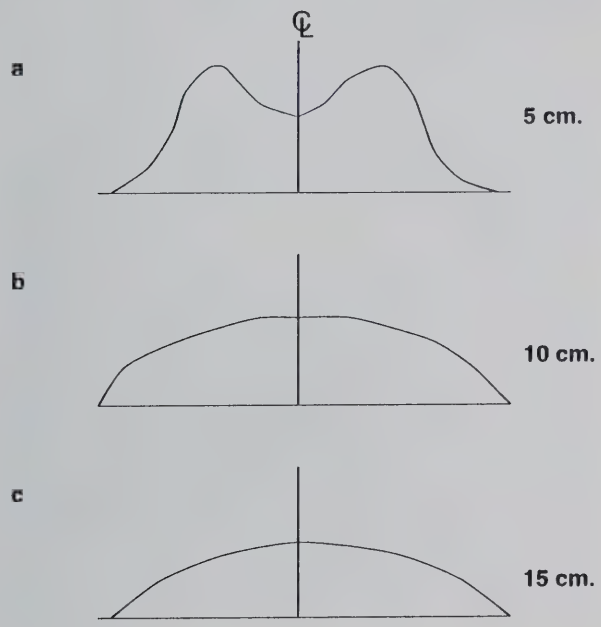

Figure 8. The deposition profile onto a sample plane opposite a circular planar magnetron as a function of distance from the cathode. In (a) the humps in the distribution correspond to the etch-track region on the magnetron. This structure is lost at farther throw distances (b, c).

Utilization of the cathode is limited by the time it takes to sputter through the back of the cathode in the etch track region. While cathodes can be as thick as several centimeters, most systems operate with thicknesses on the order of 1 cm. At a current density of 200 mA/cm2, this leads to a practical lifetime of about 50 hrs for a 1 cm Cu cathode, and proportionately longer times for lower sputter yield materials. The fraction of the total cathode material used by the time it sputtered through the back is on the order of 15%. This is a rather low number for high purity, expensive cathodes, and also requires a system shutdown to change the cathode. Some manufacturers have developed cathodes which are in the form of thick bars located in the etch tracks. This leads to better utilization and potentially longer runs. The topic of cathode utilization is still of major interest in the field of magnetron design.

The sample, in many cases, must be moved to provide better uniformity. A common example is in the form shown in figure 9, where a substrate tray rotates under 3 magnetron cathodes arranged symmetrically around the same central axis as the rotation. This, by itself, does not lead to good uniformity, because the center of the large sample tray

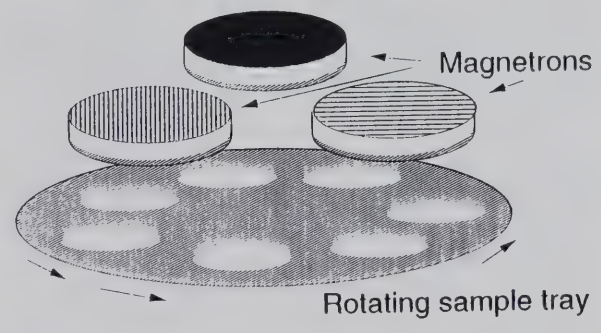

Figure 9. A typical experimental configuration for the depositidiGn from a circular magnetron onto multiple samples. The magnetrons are sputtering down onto a rotating substrate tray. One or more of the magnetrons can be operated at the same time. Not shown are the various shutters, deposition shields, and other fixtures, as well as the vacuum system.

moves effectively slower than the outer perimeter. Deposition shields must be added to reduce the deposition and shape the resulting uniformity of the profile. This type of geometry is commercially available in systems such as the Leybold 650, or the Perkin Elmer 4400[1]-series tools. An example of a deposition shield is shown in Figure 10.

For some industrial applications, in particular those where large semiconductor wafers are the samples and particulate contamination is a critical concern, it may not be desirable to move the samples during deposition. In this case, magnetrons have been developed which have a moving etch track. The track is in the form of a heart-shape, and this rotates around the centerline of the cathode

[1] Certain commercial equipment, instruments, or materials are identified in this paper to specify adequately the experimental procedure. Such identification does not imply recommendation or endorsement by the National Institute of Standards and Technology, nor does it imply that the materials or equipment identified are necessarily the best available for the purpose.

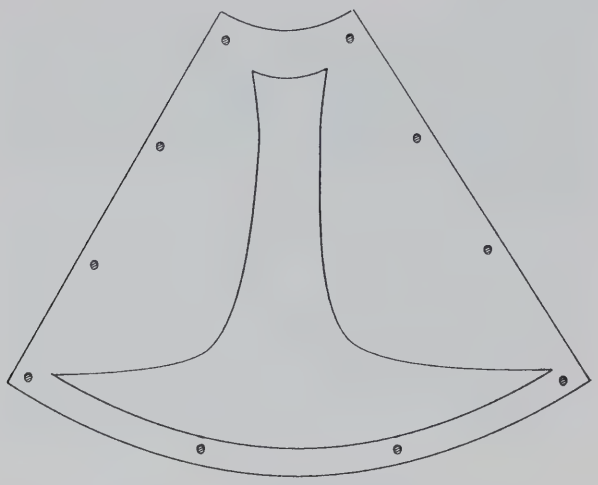

Figure 10. A typical deposition shield for one of the magnetrons in figure 9. The relative size of the magnetron is such that it is fully covered by this shield.

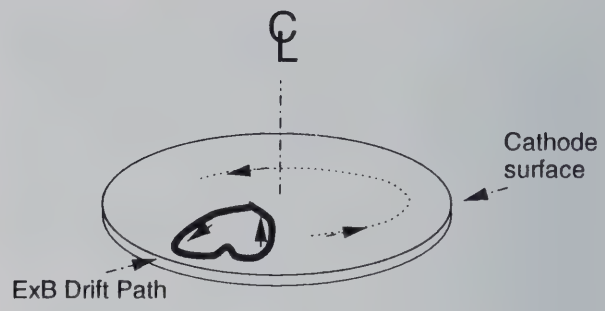

Figure 11. A sketch of the heart-shaped, rotating magnetron cathode. The etch track is in the shape of a heart, rather than a circle or a rectangle. The track is rotated about the centerline of the cathode by moving the entire magnet assembly behind the cathode (typically in the water coolant bath).

(fig. 11). Over time, the eroded area is fairly uniform and a high degree of uniformity can be obtained when depositing films on large, stationary substrates. The moving etch track is set up by rotating the magnet assembly in the cooling water behind the cathode face. An industrial cathode of this design might have a diameter of 25 cm (to deposit on a 200 mm, or 8 in, Si wafer) and be rated at a power of 25 kW. The second important advantage of these magnetrons is that the utilization of the cathode is very efficient: up to 80% of the cathode material can be used for sputtering, compared to 15% for a nonrotating magnetron. This results in much better efficiency and longer time periods between cathode changes. Because of this intrinsic efficiency, this type of magnetron is becoming more common and is being used in such varied applications as hard coatings and roll or web-coating.

For the rectangular-shaped magnetrons, good deposition uniformity can be obtained by translating samples across the short dimension of the etch track. In this way, assuming the sample is still shorter than the long dimension of the magnetron, the magnetron etch tracks appear as two line sources to the sample. Again, if the sample were fixed, the deposition would be localized under the etch tracks. However, with the simple linear motion, a high degree of uniformity is obtained. This geometry is characteristic of a number of sputtering systems, and is shown in figure 12.

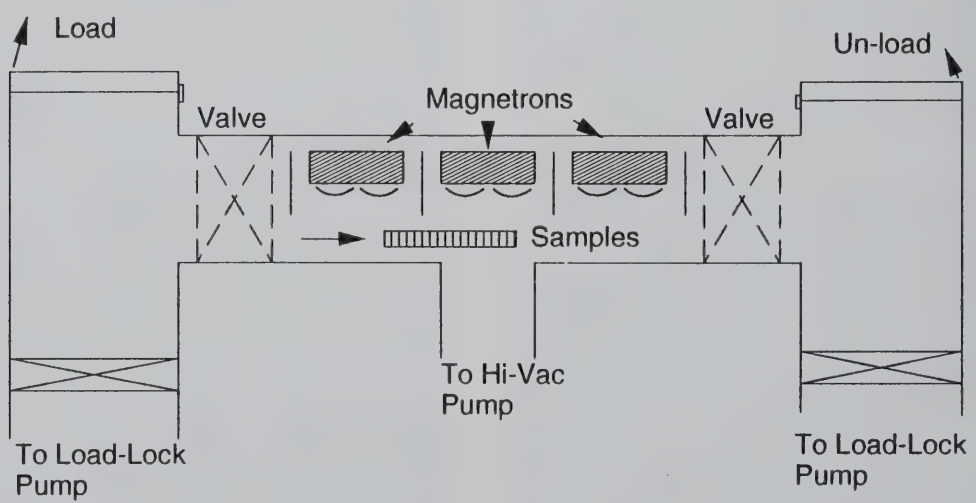

Figure 12. A typical in-line sputter deposition system for rectangular magnetrons. The magnetrons are shown end-on (short dimension).

Systems of this type are the workhorses of many commercial sputter deposition systems, with cathode dimensions up to 2 m in length at a power level of 100 kW or more. A system of this size might be 20 m in length.

Magnetic materials sputter in the same way as nonmagnetic materials. However, in a magnetron, the presence of a plate of some ferromagnetic material as the cathode has a major impact on the magnetic field in the plasma. In effect, the cathode shorts-out the magnetic field, and the plasma region is almost field-free. The magnetron effect (closed $E \times B$ drift path) requires a magnetic field of at least 150 Gauss to operate. To attain this with a magnetic cathode has generally required brute force. For sputtering magnetic materials it is necessary to saturate the cathode magnetically, such that additional field is available in the plasma region above the cathode. This is done either by dramatically increasing the magnetic field strength of the magnetron or by making the cathode very thin. Normally, both of these are done. The result is a cathode that has an even more limited lifetime. There are other geometrical changes that have been made to change the cathode size and configuration. For example, using specially shaped pole pieces and cathode inserts. These, however, do not really solve the problem, and it remains a fundamental problem in magnetron sputtering. The widespread application to sputtering of magnetic media has made this an important area in sputtering. Magnetic disks were formerly electrodeposited in large baths. Sputtered media have proved much superior, and are widely used.

4.2 Multiple Magnetron Systems

Magnetrons can be routinely operated in groups within the same chamber. The plasmas from each interact only slightly. Chambers configured with 2-4 magnetrons of the same cathode material can be used to coat large or complex parts more uniformly than a single source. Systems are also configured with multiple sources with different cathodes for the purpose of producing multiple layers in-situ, perhaps for adhesion or diffusion-barrier applications. Depending on the geometry, it may be necessary to shield the magnetrons in this latter case so that one does not contaminate the other by depositing a film onto the cathode.

Large commercial systems are usually configured with individual power supplies for each cathode, which are then combined into a system control unit. Smaller systems are usually run independently—no multiple source power supplies are commercially available. This can be an issue for aspects of running the system, such as safety interlocks, rack space, pressure trips, etc.

One of the most challenging topics with magnetron sputtering in the past decades has been the deposition of the high temperature superconductors, the copper-oxide, 1-2-3 materials. These materials are difficult to deposit because of the complicated chemical and structural requirements of the films, as well as difficulties in target fabrication for some of the components. A third major problem which has been recognized is the formation of negative ions during sputtering [6]. Negative ions, typically of oxygen, are formed during the sputtering process and accelerated to the sample. This can result at low levels in a selective resputtering of the film, removing its elements at different rates, leading to poor control of composition. At high negative ion levels, the result is that the film can be entirely sputtered off during the deposition process. Several fixes have been developed. The most common uses multiple cathodes configured either facing each other, or with the sample off-axis from the cathodes. This reduces the negative ion effect, but results in a lower net deposition rate than expected for a magnetron deposition.

An alternative to multiple magnetrons within a single system is to modify the cathode composition. Because of cathode heating limitations, most cathodes are machined as plates which are then either clamped or soldered to a water cooled backing plate. The production of the cathode plate can be very expensive, particularly for unusual compositions. It may also not be possible, based on the instability of certain combinations of materials. A solution on a laboratory scale is to sputter upward (i.e., cathode horizontal, sample mounted over the cathode) from a target consisting of a powder or small chunks or wires of material. For short sputtering runs, this allows the freedom to adjust film composition by adjusting the powder. For long runs, however, heating effects and changes in composition will make this method more difficult. This method was routinely used in the early search for thin film, high temperature superconductors.

4.3 Integrated Processing Systems

Over the past 10 years, sputter deposition systems have become grouped into two fundamental classes. The first is the dedicated, single-purpose tool, which typically runs a single process in a single chamber. These tools are often engineered for

the production of large numbers of parts, either in a batch mode, or in an automated, load-locked process. This type of tool is the workhorse of most industrial applications of sputter deposition.

A second class of tools has developed over the past several years which are more intrinsically flexible, known as integrated processing tools. These tools, which are used almost exclusively in the semiconductor industry, have multiple, independent process chambers which are serviced by a central sample handler (fig. 13). The central handler takes samples from the load-lock and delivers them to the appropriate process chamber. The process in each chamber may be different: one may be for sputter deposition, a second for Chemical Vapor Deposition (CVD), and so on. The central handler may be programmed such that samples are moved to multiple process chambers before being sent back to the load-lock for removal.

There are several advantages to this type of system. First, samples can undergo multiple, varied steps without leaving the vacuum system, resulting in less contamination and handling. Second, the process can be changed at will, simply by changing the program. Third, process chambers can be removed without disrupting operation of the tool, either for maintenance or repair. Additional backup modules can be kept in waiting for rapid repair. The total space for these tools is almost always less than stand-alone units, because of the sharing of the central handler and sample introduction region. This results in significantly less expense for multiple process steps. Finally, this sort of tool allows the development of new processes or steps

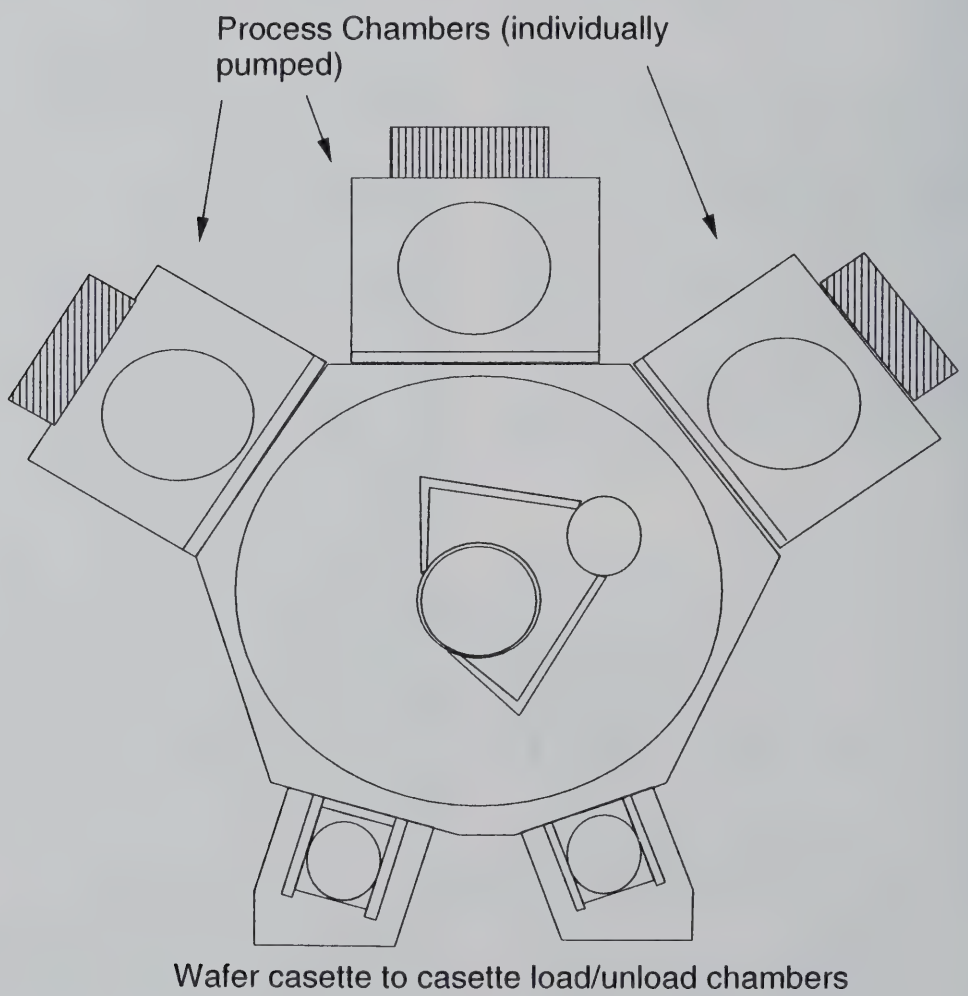

Figure 13. An integrated processing tool. The central handler has extendable arms to pick and place samples in the various chambers or in the load-lock.

at the module level, without requiring the dedication of the entire tool. This allows for more flexibility in research. More recently, tools of this type have been developed with multiple levels of integration.

The programming of these tools can be fairly complicated. Each chamber may be operating concurrently with the other, and therefore must be configured with programmable flow and vacuum control, controls and sensors for the various powered cathodes and cooling systems and detectors for aspects of the process such as film thickness or resistivity. Most current generation integrated process tools are not capable of full utilization of all chambers concurrently. This will become an important feature in the future because of the extraordinary cost of semiconductor manufacturing facilities. Current generation manufacturing facilities for 16 and 64 Mbit memory chips cost on the order of $500 Million, with the next generation estimated at $1 Billion, so any potential savings in process systems can indeed be significant.

4.4 Pressure Effects

The pressure of the background gas, as discussed above, is typically lowest for the magnetron deposition systems. While most magnetrons operate well in the 5-30 mTorr range, some well-designed cathodes can operate well down into the 0.1 mTorr range. This differs from RF-diode devices, operating in the 10s-100s of mTorr, and DC-diodes in the hundreds of mTorr to Torr range. The desirability of low pressure operation stems from the effects of gas scattering on the sputtered atoms. Some magnetrons have been configured with hollow cathode electron sources to allow low pressure operation [7]. In this case, the electrons from the hollow cathode make up for the inefficiency of the secondary electrons at low pressure, and can sustain a higher plasma density.

The mean free path for sputtered atoms scales inversely with pressure, and can be shown in figure 14. While only a statistical estimate of the distance a sputtered particle moves between collisions, the mean free path is still valuable in estimating deposition efficiency. Experiments measuring deposition probability have shown that for typical sputtering conditions (sputtering Cu with Ar at 5 mTorr), there is only a 63% chance of a sputtered atom landing on a substrate plane only 5 cm away [8]. This work shows clearly that heavy gas atoms, while often thought to lead to higher rates of sputtering due to a higher sputter yield, often result in lower net deposition rates, particularly for light mass cathode species (e.g., Al, Ti). The effect of the heavy gas atoms is to simply scatter the sputtered atoms. Once scattered, the sputtered atoms diffuse around the system in the gas phase, and no longer are directed towards the substrate plane (Table 1).

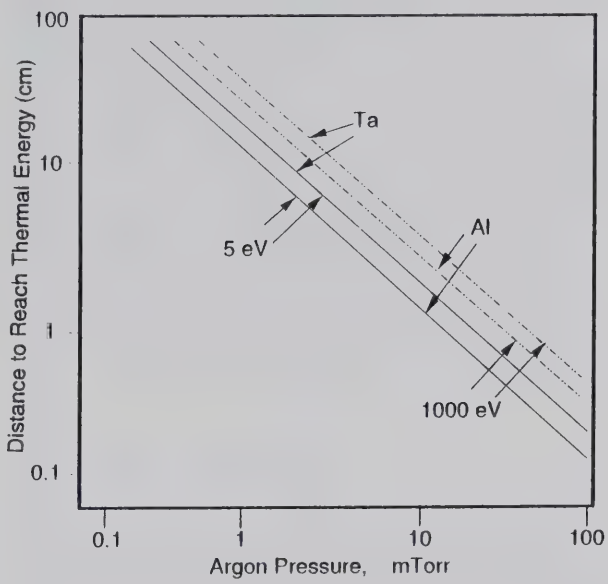

Figure 14. The approximate distance for sputtered atoms to reach thermal, or background, temperature as a function of chamber pressure. Two sets of lines are shown, for 5 and 1000 eV atoms, showing that the cross section is slightly smaller at high energy. This plot is indicative of the mean free path for the sputtered atoms.

The conclusion from this work is that it's best to sputter with as light a mass gas atom as possible, preferably near the mass of the cathode species. The effect of gas scattering, unfortunately, can also lead to easily measurable composition changes in sputtered films when sputtering from alloy cathodes. In that case, the lighter atom species is preferentially scattered and the net deposition rate from the cathode is lessened.

As mentioned earlier in Section 2 above, sputtered atoms typically have 5-10 eV of kinetic energy when they leave the cathode. This energy can be shared with gas atoms if there are any gas-phase collisions. In that case, the sputtered atom effectively cools, and its kinetic energy drops. After five or so collisions, the sputtered atom has effectively been stopped by the gas and is now at the same temperature as the gas. This concept is known as thermalization. A thermalized, sputtered atom

Table 1. The probability of deposition of a sputtered atom from a magnetron cathode onto the sample plane, the plane of the magnetron (including the magnetron cathode), and side areas, as a function of cathode material, gas presure and cathode-to-sample, or throw distance. The experiment utilized a 20 cm diameter circular plane cathode [3].

Throw	P (Pa)	Sample plane	Magnetron plane	Side areas
Cu (200W)				
5 cm	4.0	0.53	0.23	0.13
Cu (1000W)				
5 cm	0.7	0.63	0.031	0.16
	2.6	0.49	0.11	0.20
	4.0	0.53	0.14	0.22
9.5 cm	0.7	0.48	0.031	0.24
	2.6	0.47	0.13	0.24
	4.0	0.45	0.18	0.18
14.5 cm	0.7	0.39	0.045	0.25
	2.6	0.335	0.16	0.30
	4.0	0.31	0.18	0.35
Cu (3000W)				
5 cm	4.0	0.48	0.09	0.24
Al (1000W)				
5 cm	0.7	0.60	0.12	0.10
	2.6	0.46	0.26	0.12
	4.0	0.42	0.32	0.09
9.5 cm	0.7	0.44	0.13	0.10
	2.6	0.45	0.35	0.10
	4.0	0.36	0.40	0.17

arrives at the sample surface "cold" and therefore condenses only weakly onto the film. This will alter the microstructure of the deposited films as a function of pressure. A pictorial drawing of film structures, known as the "Thornton Zone Diagram" is shown in figure 15 [9]. This figure plots the structures of deposited films as a function of substrate temperature (on one axis) and gas pressure on another. The highest pressure films (30 mTorr) look quite similar to evaporated films deposited at low pressure. Evaporation is a very low energy deposition process and leads to columnar films, usually in tensile stress. These are usually not desirable film properties.

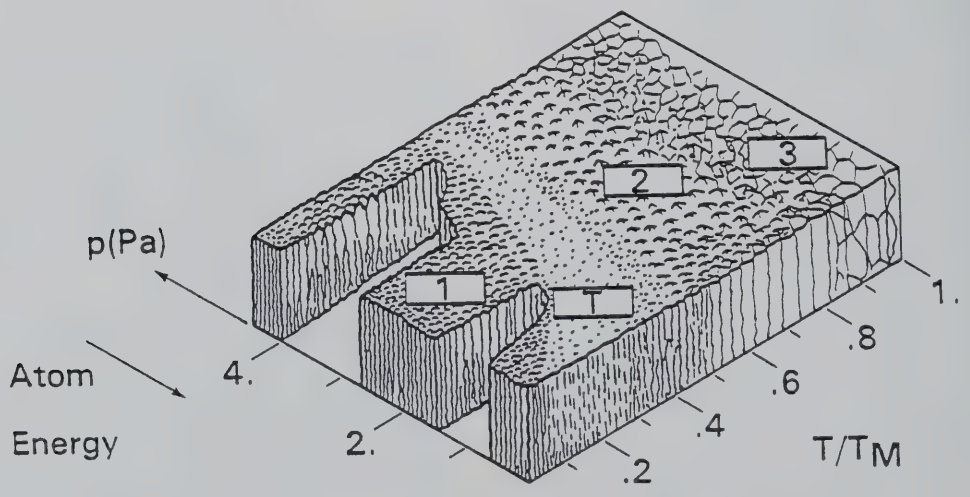

Figure 15. The Thornton Zone Diagram, showing the structure of films deposited as a function of magnetron pressure (1 Pa = 7.5 mTorr) and also sample temperature (as a fraction of the melting point).

As a corollary to the thermalization or cooling of the sputtered atoms, there can be a significant heating of the background gas atoms by the energy in the sputtered atoms. Since the sputtering process is taking place typically in an open vacuum container, this local heating can result in a local reduction in the gas particle density in the vicinity of the cathode. This effect was measured by local gas density probes in the plasma region, which showed significant reductions in gas density as the discharge power was increased (fig. 16). This effect scales directly with the sputtering process, as well as the thermal conductivity of the background gas. The gas density in the near cathode region can be given by [10]:

$$N_g = (6nT\pi K/(EY\sigma)^{1/2})\, I^{-1/2}$$

where K is the thermal conductivity of the gas, Y the sputter yield, E the average sputtered energy, n the original density, σ the gas collision cross section and I the discharge current.

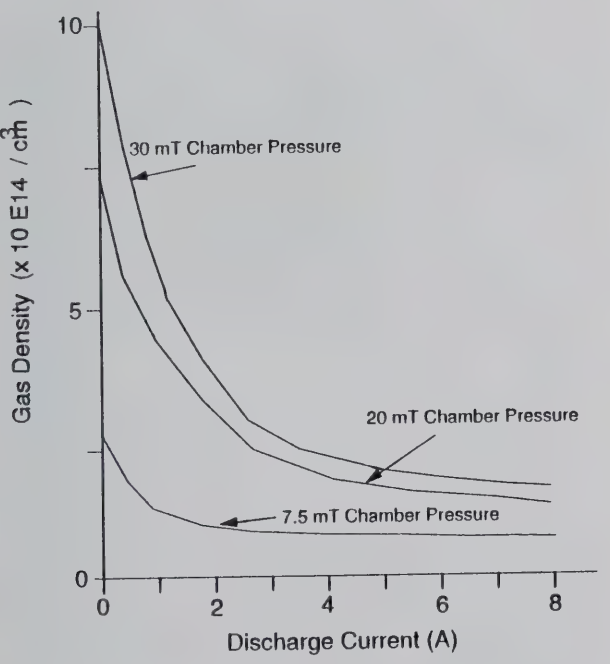

Figure 16. The local gas density near a magnetron cathode as a function of discharge current for the sputtering of Cu with Kr.

The effect of gas density reduction, or "rarefaction" at high discharge powers can be linked to a variety of effects during sputtering. The general trend is that high discharge powers behave in a similar way to lowered chamber pressures. Therefore the discharge impedance (hence voltage) is susceptible to this effect, as is the ability to transport atoms to the sample. In addition, the composition of alloy films can also become power sensitive, and at high powers the composition can more closely approach the target composition than at low powers.

One of the recent developments in low pressure sputtering has been the use of filters between the cathode and the sample region [11]. These filters take the form of collimators, or long tubes whose axis is perpendicular to the cathode and the sample planes. The collimators collect non-perpendicular depositing atoms, such that whatever is deposited at the sample has arrived within a few degrees of normal incidence. This allows sputtering to be used for filling deep structures, such as vias or trenches on semiconductors. It also is useful for lining deep features for the purpose of a diffusion boundary or selective adsorption site for another process.

5. Reactive Sputtering

If a metal cathode is sputtered in the presence of certain reactive gases, the gas atoms can react with the depositing film atoms at the sample surface to form a compound film. For example, if an Al cathode is sputtered in the presence of oxygen, the films will be partially oxidized; the degree of oxidation depending on the relative arrival rates of Al and O atoms at the sample.

Reactive sputter deposition can be described by figure 17. A metal cathode is sputtered in an inert

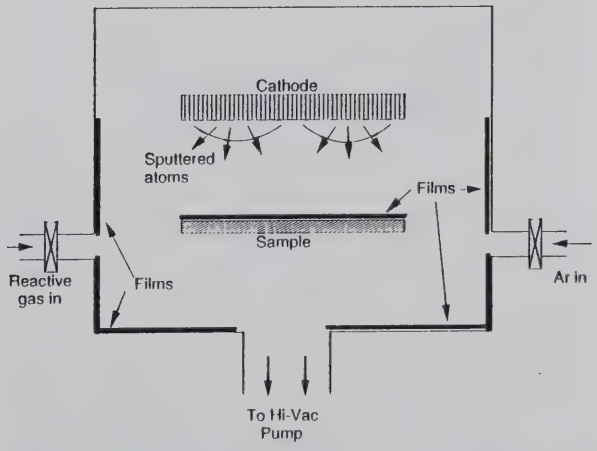

Figure 17. A schematic of a reactive deposition chamber. The gases are introduced through leak valves or flow controllers. There may also be a baffle on the high-vacuum pump, which is not shown.

gas background, resulting in the deposition of metal films on the sample and the chamber walls. As a reactive gas is added to this process, the gas atoms combine with depositing film atoms to form compound films or varying stoichiometry. At this point, even though additional gas is being added to the chamber, there is no rise in chamber pressure because all of the gas atoms are absorbed by the films. With increasing flow of the reactive gas, the films become more and more reacted, and eventually at a sufficiently high reactive gas flow, the films reach their "final" reacted state. This is typically a stable, or "terminal" compound, such as Al_2O_3, where additional oxygen cannot be absorbed by the film. Once this point is reached, additional reactive gas atoms cannot be absorbed by the depositing film. Now, any additional flow of reactive gas results in the formation of a reacted, compound film on the cathode surface. This compound almost invariably has a lower sputter yield than the pure metal cathode, which results in a reduction of the rate of metal atoms sputtered from the cathode. Reducing the rate of metal deposition reduces the rate at which the film can absorb the reactive gas, further increasing the residual background of the reactive species. This, in turn, causes additional reaction at the cathode surface, which reduces the metal sputtering rate even further. In effect, the cathode undergoes a transition from a metallic to a compound state, and the deposition process slows dramatically, as shown in figure 18. The deposition rate is plotted in figure 18a, and the chamber pressure in figure 18b, as a function of increasing reactive gas flow.

If the reactive gas flow is now lowered, the reverse transition does not occur at the same flow rate. This is due to the reduced metal emission rate from the compound surface. It is not simply due to the need to sputter through the reacted layer. A significantly lower reactive gas flow rate is needed to make up for the low level of metal emission. At a much lower flow, the cathode switches back to the metallic mode, and all of the reactive gas is again absorbed in the films. This shows up in figure 18 in the form of a hysteresis loop.

The behavior is different for the two main cases of sputter deposition in reactive atmospheres of either oxygen or nitrogen. With oxygen, most oxides are formed spontaneously and the reactions are exothermic, requiring no additional energy. The hysteresis curves in this case tend to have fairly sharp transitions. For the case of reactive sputter deposition with nitrogen, the nitride reaction often requires additional energy to form. In

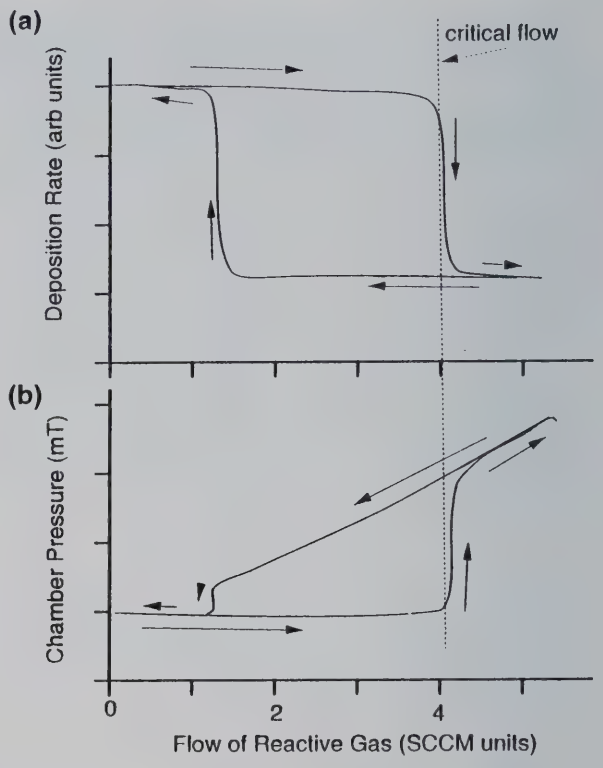

Figure 18. Hysteresis curves of the deposition rate and the chamber pressure for the case of reactive sputtering. The deposition rate and chamber pressure are shown as a function of increasing flow of reactive gas. There is a working background of inert gas, typically Ar.

addition, the sticking probability of the nitrogen, even under the best of circumstances, is considerably less than 1.0. The result is that the transitions are less abrupt from the metallic to the compound state.

Unfortunately, it is difficult to operate the sputtering system at the critical flow rate at which the films are just reaching their terminal oxide state. The transition is almost irreversible and extremely rapid feedback methods need to be employed. The most common techniques are to try to control the power supply or else the flow of reactive gas. The sensor often used is a gas sensor of some sort—a mass spectrometer, a pressure gauge, or an optical gas analyzer. The placement of the sensor is critical due to local gas density reductions that may occur in the near cathode region [12]. The nitride transition is less difficult to control, partially due to the broadness of the transition, the non-unity sticking coefficient, as well as the smaller differences between the metallic and compound sputtering rates. It is generally easier to operate near the critical flow transition with reactive nitride deposition, because the surface reaction requires addition

energy, which is often supplied from the plasma. This makes feedback control, based on the power supply, more straightforward.

Control of the oxide transition has proven to be very difficult on an industrial scale. The metal-to-oxide transition is fairly rapid. Industrial systems also tend to have a high cathode area-to-sample area ratio. They are designed so that a large fraction of the deposited atoms are actually used in the form of films on the sample. Smaller, laboratory-scale systems tend to have much lower ratios—the magnetrons are smaller and the chambers are proportionately larger. This lessens the effect of the transition. Similarly, if one is able to attain very high pumping speeds in the deposition chamber, the transitions become less abrupt. This, again, is more practical on a laboratory scale than on an industrial scale. The control of the metal-to-oxide transition is one of the remaining significant problems in sputter deposition technology.

Titanium nitride (TiN) is one of the most commonly deposited films using reactive sputtering. Good TiN is gold in color and has a high hardness, making it ideal not only for decorative coatings, but also for protective coatings on tool bits, cutting surfaces, punches, etc. The formation of good TiN requires the addition of energy to the film during deposition. One means to do this is to use substrate heating, typically at 600-700 °C. This is undesirable for quite a number of applications: interdiffusion is enhanced at these high temperatures, and more importantly, hard steel becomes annealed and much rofter at high temperature.

There are two other practical methods for attaining good TiN. The first is to operate at very low pressure. At pressures below 0.5 mTorr, there is very little gas scattering, and the depositing Ti atoms may have as much as 10-13 eV of kinetic energy. This energy may help in the formation of reasonably high quality TiN. Unfortunately, most common magnetron systems operate relatively poorly at these low pressures, which makes it difficult for production environments. It is, however, well within the operating range of broad beam ion sources.

The second method for enhancing the formation of TiN is to bias the sample to a negative voltage during deposition. The bias causes ions from the plasma to be accelerated to the sample, depositing additional energy in the near surface region. The required level of ion bombardment scales with the deposition rate. For high-rate depositions (up to a micrometer/minute or so), the required bias current density approaches 2 mA/cm^2.

High levels of bias current are, unfortunately, difficult to achieve with conventional magnetron deposition systems. The plasma is confined close to the cathode, which is desirable for high rate sputtering of the cathode, but results in an inability to draw ions to the sample region many centimeters away. A solution has been the development of magnetically unbalanced magnetrons by B. Windows [13]. In this device a conventional magnetron is intentionally configured with an array of magnetic pole pieces or coils which add an additional vertical component to the magnetic field at the cathode. Three common configurations are shown in figure 19. The first two configurations (fig. 19 a, b) are based on additional permanent magnets in the pole-piece configuration behind the magnetron cathode. In the first case, the central pole piece has been made much stronger than the perimeter pole piece, resulting in an additional axial field. In the second case, the perimeter pole has been made stronger, resulting in an additional cylindrical component to the field. In the third case (fig. 19c), an electromagnet has been added external to the magnetron to provide a simple axial field.

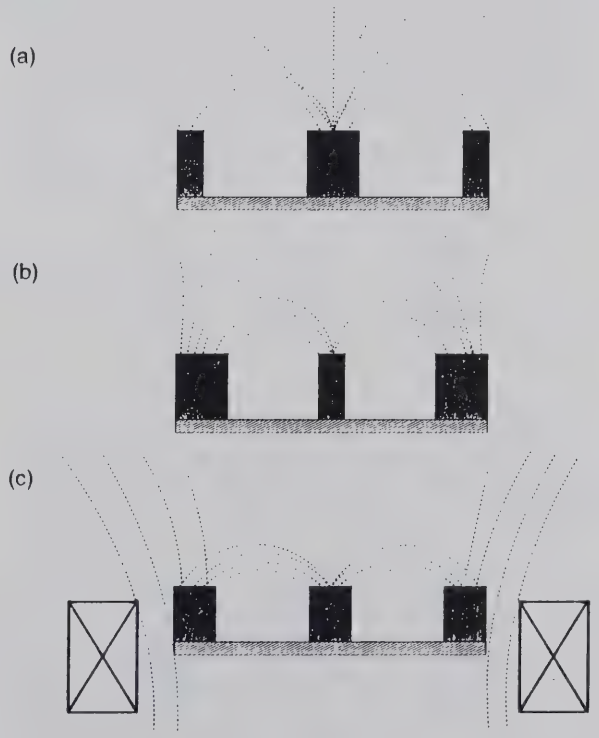

Figure 19. Unbalanced magnetrons: (a) has a strong axial pole, (b) has a strong perimeter pole, and (c) has an additional electromagnet around the magnetron to provide additional magnetic field.

The result of each of these unbalanced configurations is that the magnetic field lines are no longer constrained between the central and perimeter pole pieces of the magnetron. Additional field lines leave the region of the magnetron and intersect the sample region. Electron motion along these field lines is unconstrained by the $\boldsymbol{E} \times \boldsymbol{B}$ trapping effect near the cathode, and is actually enhanced due to the grad-$\boldsymbol{B}$ drift of electrons from high B field regions to lower strength regions. As a result, electrons can leak away from the near-cathode region. This sets up a very weak potential which tends to draw ions from the cathode region out to the near-sample region. It is these ions which can then be used to form the basis of a sample bias current necessary for the enhancement of the TiN reaction.

The unbalanced magnetron approach has been used successfully on a manufacturing scale for the production of TiN and related compounds. To cover large numbers of parts, or else to cover large parts with unusual shapes, systems are often configured with multiple magnetrons within a single chamber [14]. A simple example of this is shown in figure 20, where two unbalanced magnetrons have been configured opposite each other, with the sample placed between them. The magnetrons can be configured to be coupled or repelling, which results in a significant difference in the observed bias current densities at the sample (fig. 21). An additional example of this is in figure 22, where four large

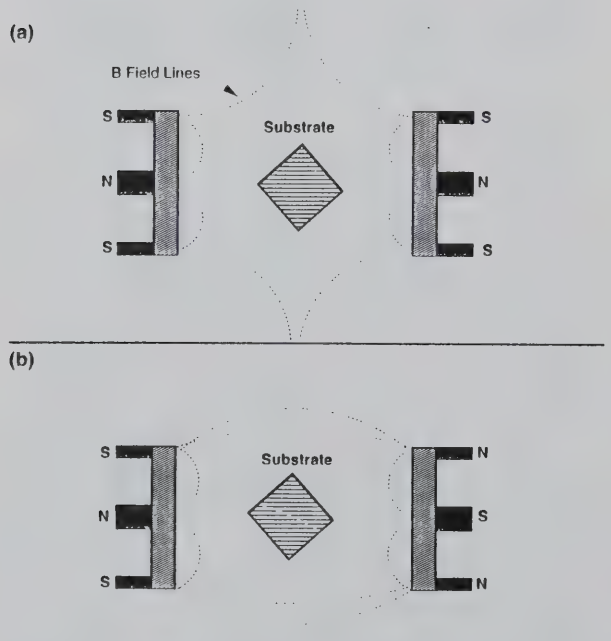

Figure 20. Two configurations of coupled, unbalanced magnetrons: (a) mirrored fields, and (b) closed field (adapted from ref. [8]).

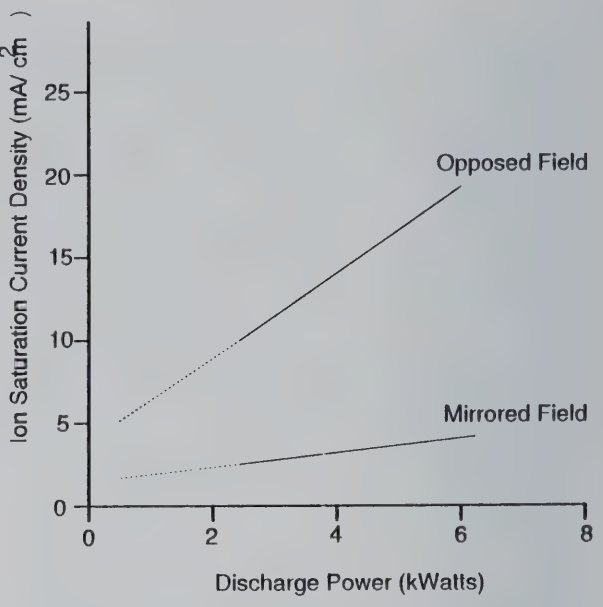

Figure 21. The sample bias current density (at −100 V bias) as a function of discharge power for the two unbalanced configurations of figure 20 (adapted from ref. [8]).

(24 in long) unbalanced magnetrons are configured at 90 degree intervals around a large chamber [15]. In this commercial system, electromagnets are placed around conventional magnetrons to provide the additional unbalanced magnetic field necessary for high levels of sample bias. A system of this type would be used for coating fairly large parts (0.4 m) or else large numbers of smaller parts, such as drill bits or watch casings, for example.

Unbalanced magnetron sputtering is a fairly recent development in deposition technology (developed in the late 1980s). As such, several problems remain in the implementation of the process. The leakage of the plasma from the cathode region to the sample is dependent on the operating pressure, the gas used, and even the power level of the discharge. The bombardment of the sample can be measured in the form of current to the sample and the voltage applied. Sample temperature is also an important parameter in depositing high quality films. The interplay between bias current, energy and sample temperature is not well known for all types of applications. The reduction in sample temperature, for example, can be extremely important for depositing on certain types of substrates, such as plastics or tool steels. In-situ process control of the deposition process remains an open area for development. Since nitride films are hard and inert the problem of removing substandard films from samples can be significant.

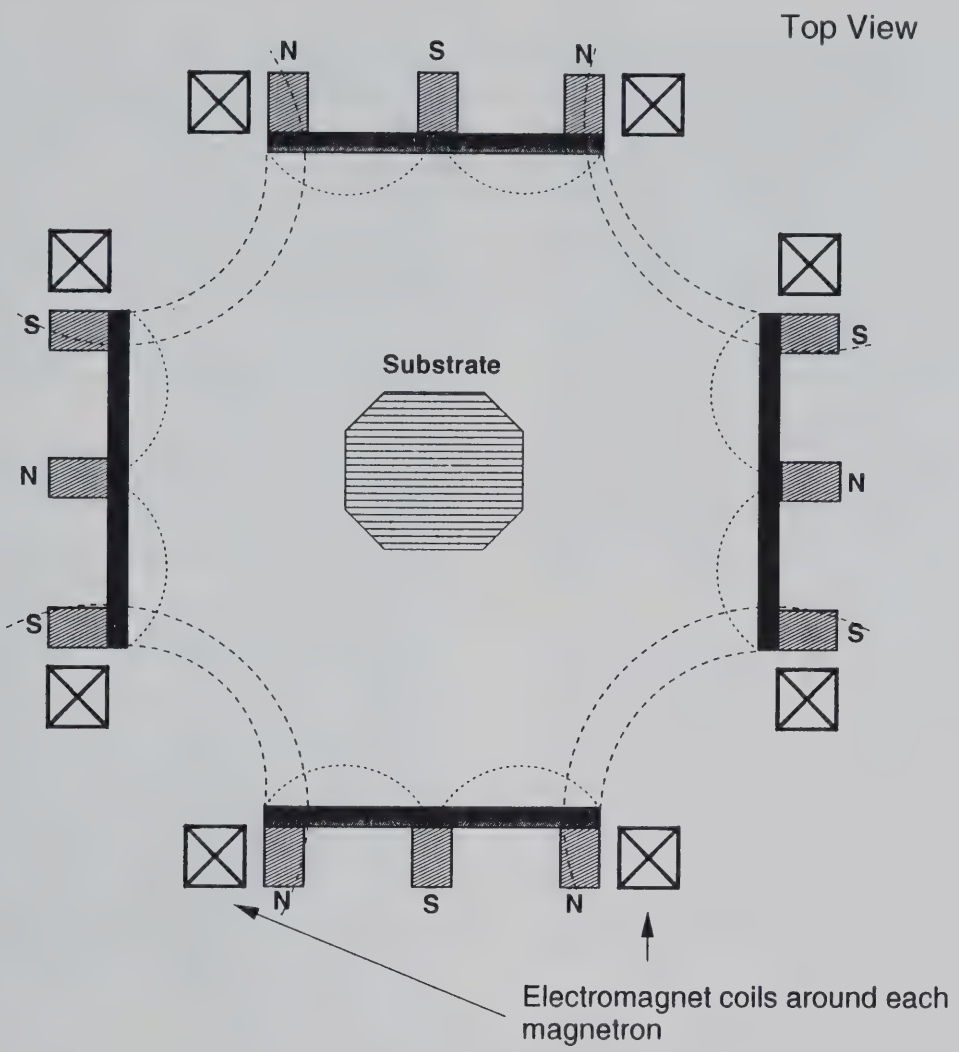

Figure 22. A four-magnetron sputter deposition system. Additional electromagnets have been added to each magnetron to unbalance the devices for additional ion bombardment to the sample.

6. Summary

Sputter deposition is a versatile process used for depositing coatings of metals, alloys, compounds and dielectrics on surfaces. Sputter deposited films have found broad applications in industrial hard and protective coatings. Primarily TiN, as well as other nitrides and carbides, these sputter deposited films have high hardness, low porosity, good chemical inertness, good conductivity and also an attractive appearance. Sputter deposited films are routinely used simply as decorative coatings on such surfaces as watchbands, eyeglasses and jewelry. The films can have all of the attractive aspects of gold, silver or platinum, with usually greater resiliency, at a fraction of the cost of the expensive materials used in the past.

The deposition process for nitrides continues to provide challenges in terms of temperature reduction, high rates, uniform coverage over unusual objects, process control and cost on an industrial scale.

The electronics industry is totally reliant on sputtered coatings and films. Sputtered metal films make up a large fraction of the thin film wiring on chips as well as recording heads. Sputtered films are the material of choice for magnetic and magneto-optic recording media due to high density, ease of fabrication, resiliency and adhesion. Hard sputtered films are also used in this industry to function as wear-resistant surfaces, corrosion resistant layers, diffusion barriers and even adhesion

layers. In this industry, the chip-level production has almost totally moved to single-wafer processing, in which a single sample is handled at a time. This puts enormous stress on the deposition process to be fast and reliable. In the packaging area of microelectronics, sputtering is used to deposit thick conducting films in a batch environment with cathodes several meters in length.

Other industries have become dependent on sputtering and new applications are developing rapidly. The sputter deposition of reflective films on large pieces of architectural glass has become commonplace. The downtown areas of many large cities have perhaps square miles of sputter deposited films in use on the sides of buildings. This field is moving from simply reflective films towards hard and protective coatings. This opens up significant opportunity, as large-scale reactive sputtering is still not well understood.

The automotive industry has used sputtering for at least 15 years for the coating of decorative films on plastic. Originally developed to allow the weight-saving advantages of plastic parts, as opposed to metal, sputtered films have potential opportunities in terms of hard coatings as well as optical coatings to reduce glare on windshields. The food packaging industry has also become dependent on sputtering for the coating of thin plastic films. The metal layer provides a clean, nonporous surface for packaging pretzels, potato chips and a variety or other foods.

Sputter deposition is a rapid, fairly inexpensive process which produces dense films, often with near-bulk qualities. It is anticipated that sputtering and sputter deposition will grow as a field as new and innovative applications and techniques are developed.

7. Future Markets and Industry Needs

The future markets for sputtering technology will both further develop its use in present industrial markets (primarily semiconductor fabrication and glass coating) and extend its use to markets from which it has previously been largely excluded, such as the hard-coating of cutting tools.

In semiconductor fabrication, the trend is toward integrated processing systems, in which several processes, including sputter deposition, are carried out in a single system with various appendage-like chambers. These manufacturing tools are expected to be less capital intensive, to be more flexible, and to produce fewer defects than stand-alone or batch systems. The computer control and monitoring of such tools will also become an important growth area.

Until recently, sputtering was seldom used commercially for the coating of metal-cutting and forming tools. With the advent of unbalanced magnetrons, there are now several manufacturers offering deposition systems for these applications, and systems are going into production use in various locations world-wide.

Several areas which have been introduced in this section present a number of opportunities and problems in the sputter coating field:

- Vacuum instruments are needed that operate better in RF fields.
- New magnetron designs are needed to increase target utilization and to make targets simpler to fabricate.
- There is a need for better arc-suppressing power supplies, and for power supplies able to run more than one magnetron at a time.
- Better methods are needed to sputter deposit magnetic materials at high rates using magnetrons, and to allow the sputtering of materials which cannot be easily formed into targets.
- For sputtering materials such as the high temperature superconductors, there is a need to control the problem of negative ion bombardment of the sample.
- Improved methods are needed for the reactive sputtering of oxides and other difficult materials
- Methods that permit sputtering at very low pressures would be advantageous.
- Integrated processing systems are in need of better hardware and software for optimum efficiency.
- Better methods are needed for in-situ process control.
- There is a great need for methods of removing deposited TiN and other hard, ceramic-like coatings from poorly coated or worn components, without damage to the components themselves.
- An understanding is needed of the interplay between temperature, energy, bias and bias voltage, and the resulting effect on film properties.

8. References

[1] P. Sigmund, Phys Rev, 184, 383 (1969).

[2] B. Chapman, "Glow Discharge Processes," John Wiley and Sons, New York (1980), 150.

[3] M. J. Kushner, "A kinetic study of the plasma etching process, II. Probe measurements of electron properties in an rf-etching reactor," J. Appl. Phys., 53(4), 2939-2946 (1982).

[4] E. Y. Wang, N. Hershkowitz, T. Intrator and C. Forest, "Techniques for using emitting probes for potential measurement in rf plasmas," Rev. Sci. Instrum., 57(10) 2425-2431 (1986).

[5] G. E. Este and W. D. Westwood, "A quasi direct current sputtering technique for the deposition of dielectrics at enhanced rates," J. Vac. Sci. Technol., A6, 1845-1848 (1986).

[6] S. M. Rossnagel and J. J. Cuomo, "Negative ion effects during magnetron and ion beam sputtering of Yt-Ba-Cu-Ox," AIP Conf. Proc., 165 (106-113) 1988.

[7] J. J. Cuomo and S. M. Rossnagel, "Hollow cathode enhanced magnetron sputtering," J. Vac. Sci. Technol., A4, 393-396 (1986).

[8] S. M. Rossnagel, "Deposition and redeposition in magnetrons," J. Vac. Sci. Technol., A6, 3049-3054 (1988).

[9] J. L. Thornton, J. Vac. Sci. Technol., 11, 666 (1974).

[10] S. M. Rossnagel, "Gas density reduction effects in magnetrons," J. Vac. Sci. Technol., A6, 19-24 (1988).

[11] S. M. Rossnagel, D. J. Mikalsen, H. Kinoshita and J. J. Cuomo, "Collimated magnetron sputter deposition," J. Vac. Sci. Technol., A9, 216-265 (1991).

[12] W. D. Sproul, P. J. Rudnik, C. A. Gogol and R. A. Mueller, "Advances in partial-pressure control applied to reactive sputtering," Surf. & Coat. Technol., 39/40 (1989) 499.

[13] B. Windows and N. Savvides, "Charged particle fluxes from planar magnetron sputtering sources," J. Vac. Sci. Technol., A4, 196-202 (1986).

[14] W. D. Sproul, P. J. Rudnick, M. E. Graham and S. L. Rohde, "High rate reactive sputtering in an opposed cathode closed-field unbalanced magnetron sputtering system," Surface and Coatings Technology, 43/44, 270-278 (1990).

[15] W. D. Sproul, private communication, 6-92.

About the author: *Dr. Stephen Rossnagel is a Research Staff Member at IBM Research in Yorktown Heights. He has specialized in the fields of sputter deposition and plasma processing, has published about a hundred articles and two books in these fields, holds six patents on related technology, and regularly teaches courses on Sputter Deposition. He received the Peter Mark award from the AVS in 1990 for work on magnetron and ion beam sputtering. He has held previous positions at Princeton University and the Max Planck Institute in Munich.*

ION PLATING

Donald M. Mattox

IP Industries
440 Live Oak Loop
Albuquerque, NM 87122

Tel: (505) 292-7763
Fax: (505) 298-7942

"Ion plating" is a term applied to Physical Vapor Deposition (PVD) processes in which the substrate surface and the growing film are subjected to continuous or periodic bombardment by massive energetic particles. This bombardment causes changes in the film formation process and the properties of the deposited film such as adhesion, residual film stress, density, or chemical composition. The beneficial effects of ion plating arise from the input of momentum and energy directly into the first few monolayers of the growing surface. This leads to densification of the surface layer and enhancement of chemical reactions on the surface. Bombardment may be performed using ions accelerated from a plasma using an applied or self-bias on the film, ions from an "ion gun" in a vacuum, "film-ions" accelerated from an arc discharge in a vacuum or reflected high-energy neutrals in low-pressure sputter deposition. Ion plating is particularly useful in applications where other deposition techniques do not provide adequate film properties such as adhesion, surface coverage, film density, residual film stress or composition, or where the bulk substrate temperature must be kept low.

Key words: IBAD; Ion Beam Assisted Deposition (IBAD); Ion plating – plasma-based; Ion plating, Ion plating – vacuum-based; Physical Vapor Deposition (PVD) processes, PVD.

1. Introduction

"Ion plating" is a term applied to *P*hysical *V*apor *D*eposition (PVD) processes in which the substrate surface and the growing film are subjected to continuous or periodic bombardment by massive (atomic not electron size) energetic particles. This bombardment causes changes in the film formation process and the properties of the deposited film such as adhesion, stress, density, residual stress and chemical composition [1-4]. The beneficial effects of ion plating arise from the input of momentum and energy directly into the first few monolayers of the growing surface. This leads to densification of the surface layer and enhancement of chemical reactions on the surface. Bombardment may be performed using ions accelerated from a plasma using an applied bias or self-bias on the film, ions from an "ion gun" in a vacuum, "film-ions" accelerated from an arc discharge in a vacuum or reflected high-energy neutrals in low-pressure sputter deposition. This broad definition does not specify the source of the depositing film atoms, the source of bombarding particles nor the environment in which the deposition takes place. The principal criterion is that energetic particle bombardment is used to modify the film properties.

The two basic versions of the ion plating process are shown in figure 23. In plasma-based ion plating (fig. 23a), which is the most common form, the substrate is in proximity to a plasma and ions are accelerated from the plasma by a negative bias on the substrate. The accelerated ions and high-energy neutrals from charge exchange processes in the plasma arrive at the surface with a spectrum of energies. In addition, the surface is exposed to

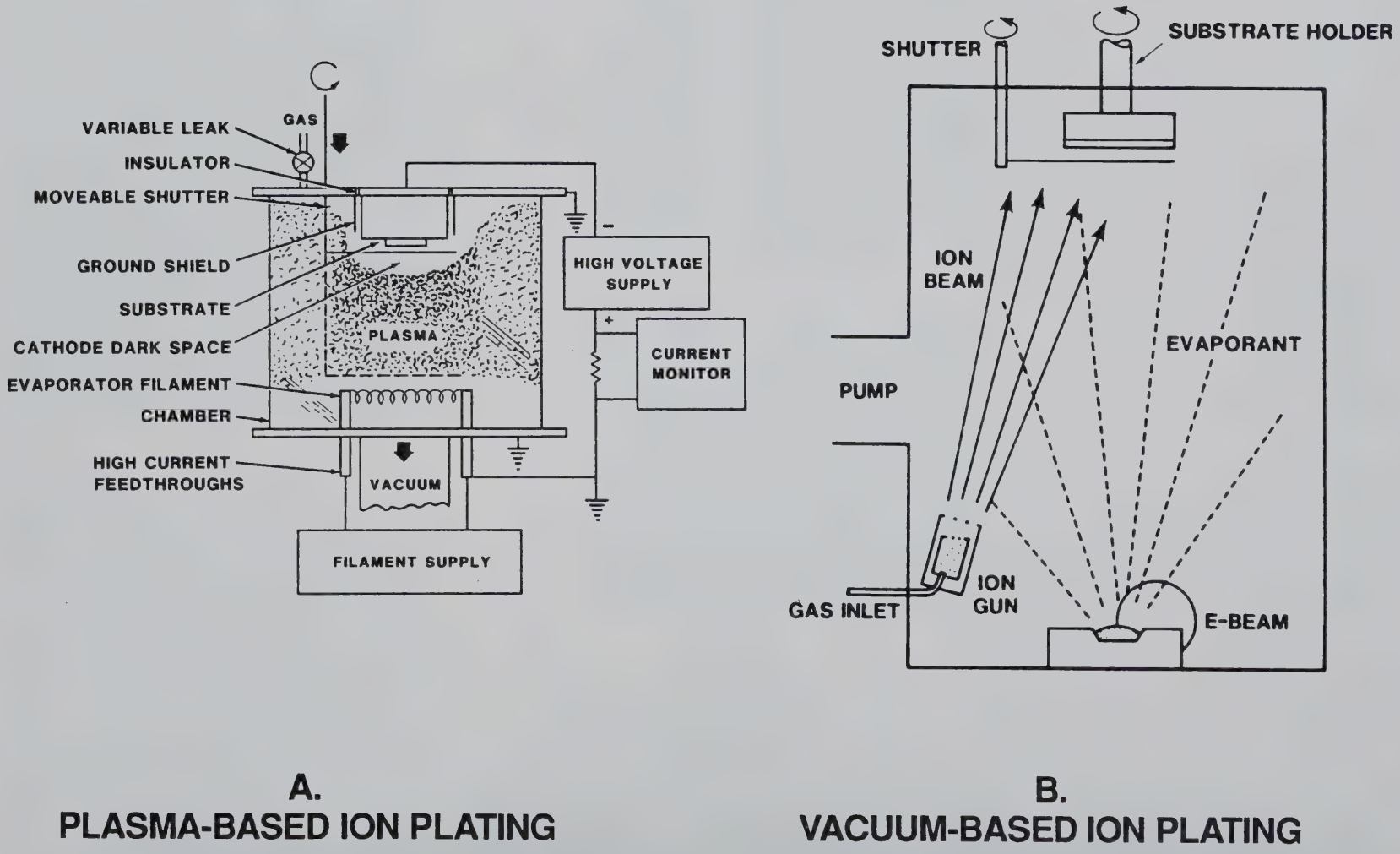

Figure 23. The basic versions of the ion plating process: (a) plasma-based ion plating where the energetic particles used for bombardment are from a plasma in the vicinity of the substrate and, (b) vacuum-based ion plating where the bombardment is from a separate ion source.

chemically "activated" species, both desirable and contaminant from the plasma, and adsorption of gaseous species from the plasma environment. In vacuum-based ion plating (fig. 1b), the deposition and bombardment occur in a vacuum where the gas density is low and the contamination level can be easily controlled and monitored. In this case, the bombarding species are either ions from an "ion gun" or high-energy reflected neutrals from the sputtering target when low-pressure or ion beam sputter deposition is being performed. Many of the film growth effects of the two versions of ion plating are the same but there are also important differences, particularly with respect to surface coverage, where gas scattering is an important factor [5], and reactive deposition where plasma "activation," generation of chemical species in the plasma, and gas adsorption on the surface are important [6,7].

Often in plasma-based ion plating the term ion plating is accompanied by modifying terms such as "sputter ion plating" [8], "reactive ion plating" [89,10], "chemical ion plating" [11], "alternating ion plating" [12,13], or "pulsed ion plating," which indicate the source of the depositing material or other particular condition of the deposition. Chemical ion plating is similar to "*P*lasma *E*nhanced *C*hemical *V*apor *D*eposition" (PECVD), and "bias PECVD" [14], where chemical vapor precursor gases are used as the source of the depositing material. In addition, other terms are applied to deposition processes where ion plating conditions exist. Examples are "bias sputtering" [15], "asymmetrical AC sputtering" [16], "pulsed implantation" [17], *I*on *V*apor *D*eposition (IVD) [18,19] and *B*iased *A*ctivated *R*eactive *E*vaporation (BARE) [20].

Vacuum-based ion plating has been called "vacuum ion plating" [21], "*I*on *A*ssisted *D*eposition" (IAD) [22,23], "*I*on *B*eam *A*ssisted *D*eposition" (IBAD) [24,25] and "*I*on *B*eam *E*nhanced *D*eposition" (IBED) [26]. In these cases, the periodic or concurrent bombardment is from a source of inert or reactive ions formed in an ion gun and accelerated to the surface with a specific and controllable energy distribution. When low pressure plasma-based sputtering or ion beam sputtering is used as the source of depositing material, the deposition is often accompanied by an undefined bombardment by high-energy reflected neutrals [27-30]. In this work, the term "IBAD" will be used to refer to vacuum-based ion plating and "ion plating" will be used to refer to the plasma-based version of the process.

Some advantages of ion plating include:

- ability to have thermal vaporization, sputtering, arc vaporization, laser ablation or chemical vapor precursor gases as the source of depositing material
- ability to have in-situ cleaning ("ion scrubbing," plasma etching or sputtering) of the substrate surface prior to film deposition
- excellent surface covering ability ("throwing power") due to gas scattering and sputtering/redeposition
- ability to introduce heat and lattice defects into the first few atomic layers of the surface to enhance nucleation, reaction and diffusion while the bulk of the substrate can be maintained at a low temperature
- ability to obtain good adhesion in many otherwise difficult systems
- enhancement of the reactive deposition process by "activation" of reactive gases, bombardment-enhanced chemical reaction [31,32], adsorption of reactive species [33,34], preferential sputtering of unreacted species, and use of ions of the reactive material
- ability to use reactive gas bombardment to pretreat the substrate surface (e.g., plasma nitriding of steel surface [35] and oxidation of polymers [36])
- flexibility in tailoring film properties such as morphology, density and residual film stress by controlling the bombardment conditions [37]
- equipment requirements and costs equivalent to those of sputter deposition.

Many of the same advantages are found in IBAD as in ion plating, with the exception that covering ability is not as good because there is no gas scattering, decreased sputtering-redeposition and the more line-of-sight nature of the ion beam. These factors may require the use of more substrate fixturing in IBAD when processing large areas or complex surface configurations than when using ion plating. Major advantages for the IBAD process are that the contamination level in the deposition environment (vacuum) can be controlled more easily than when a plasma is used, gaseous contaminant species are not "activated," and the bombardment conditions are more easily defined and controlled.

Some possible disadvantages of ion plating include:

- There are many processing parameters that must be controlled.
- To bombard insulating films the surface must attain a high "self-bias" or must be biased with an rf potential.
- Contamination may be released from surfaces and be "activated" in the plasma.
- Processing and "position equivalency" may be very dependent on substrate geometry and fixturing, since obtaining uniform bombardment and the availability of reactive species over a complex surface can be difficult.
- Bombarding gas species may be incorporated in the substrate surface and deposited film.
- Substrate heating may be excessive [38,39].
- High compressive stresses may be developed in the bombarded film [37].

IBAD has many of the same disadvantages as plasma-based ion plating. In addition, the diameter of the ion beam is usually small which limits the area that can be bombarded. The IBAD process does not activate reactive gases and thus must rely solely on the use of reactive ions from the ion source and surface chemical processes to attain bombardment-enhanced reactive deposition effects [6,31,32]. In IBAD, where physical sputtering is the source of depositing atoms, bombardment by a flux of high-energy-reflected neutrals, the nature of which is generally unknown, is superimposed on the deliberate bombardment [27-30].

2. Bombardment Effects on Film Formation

The properties of films formed by any PVD process depend on:

- substrate surface condition – e.g., morphology (roughness, inclusions, particulate contamination), outgassing, chemistry (substrate composition, contaminant layers), surface flaws
- details of the deposition process and system geometry – e.g., angle-of-incidence of the depositing adatom flux, substrate temperature, nature of concurrent or periodic energetic particle bombardment, deposition rate, gaseous contamination, outgassing from vaporization source, pinhole formation mechanisms
- details of film growth on the substrate surface [40] – e.g., nucleation, interface formation, interfacial flaw generation, film growth, energy input to growing film, surface mobility of the depositing adatoms, growth of columnar morphology in the film due to geometrical factors, residual film stress, generation of lattice defects, gas entrapment, reaction with deposition ambient (including reactive deposition processes)
- postdeposition processes and reactions – e.g., heating, encapsulation, reaction or adsorption on columnar surfaces with the ambient, thermal or mechanical cycling, corrosion, interfacial degradation, burnishing of soft surfaces, shot peening.

In order to have a reproducible film properties each of these factors must be controlled.

Figure 24 shows the effect of energetic particle bombardment on a surface [41]. On collision with the surface the energetic particle loses energy and may be reflected as a high-energy neutral whose energy is dependent on the relative masses of the incident and surface atom [27-30]. The energy and momentum imparted to the surface atoms cause a "collision cascade" in the vicinity of the impact. If enough energy is imparted to a surface atom, it is physically ejected in a process known as "physical sputtering" or just "sputtering." The number of surface atoms ejected from the surface per incident energetic particle is called the "sputtering yield." The sputtering yield depends primarily on the energy and mass of the bombarding particle, the mass and bonding energy of the surface atom, and the angle-of-incidence of the bombarding particle. The sputtered atoms leave a point on the surface with a cosine distribution. Since sputtered surfaces are usually extensive, this gives rise to a multidirectional flux of atoms from the sputtering target.

The deposition of atoms whose origin is the sputtering process is called "sputter deposition," or often just "sputtering" as in "sputtered gold films." In sputtering, the sputtered particle leaves the surface ("target") with greater than thermal energy. If the surface is in vacuum so that there are no gas phase collisions, the sputtered atoms arrive at the substrate with high kinetic energies [30]. If the gas density is such that there are gas phase collisions, the ejected particles are "thermalized" to the ambient gas energy. Figure 25 shows the distance required for thermalization for various particle masses, energies and gas pressures [42]. If there is a high particle density above the source either due to the gas pressure or to a high vaporization rate, the ejected particles can nucleate in the gas phase ("vapor phase nucleation") [43,44] and/or may be scattered back ("backscattered") to the

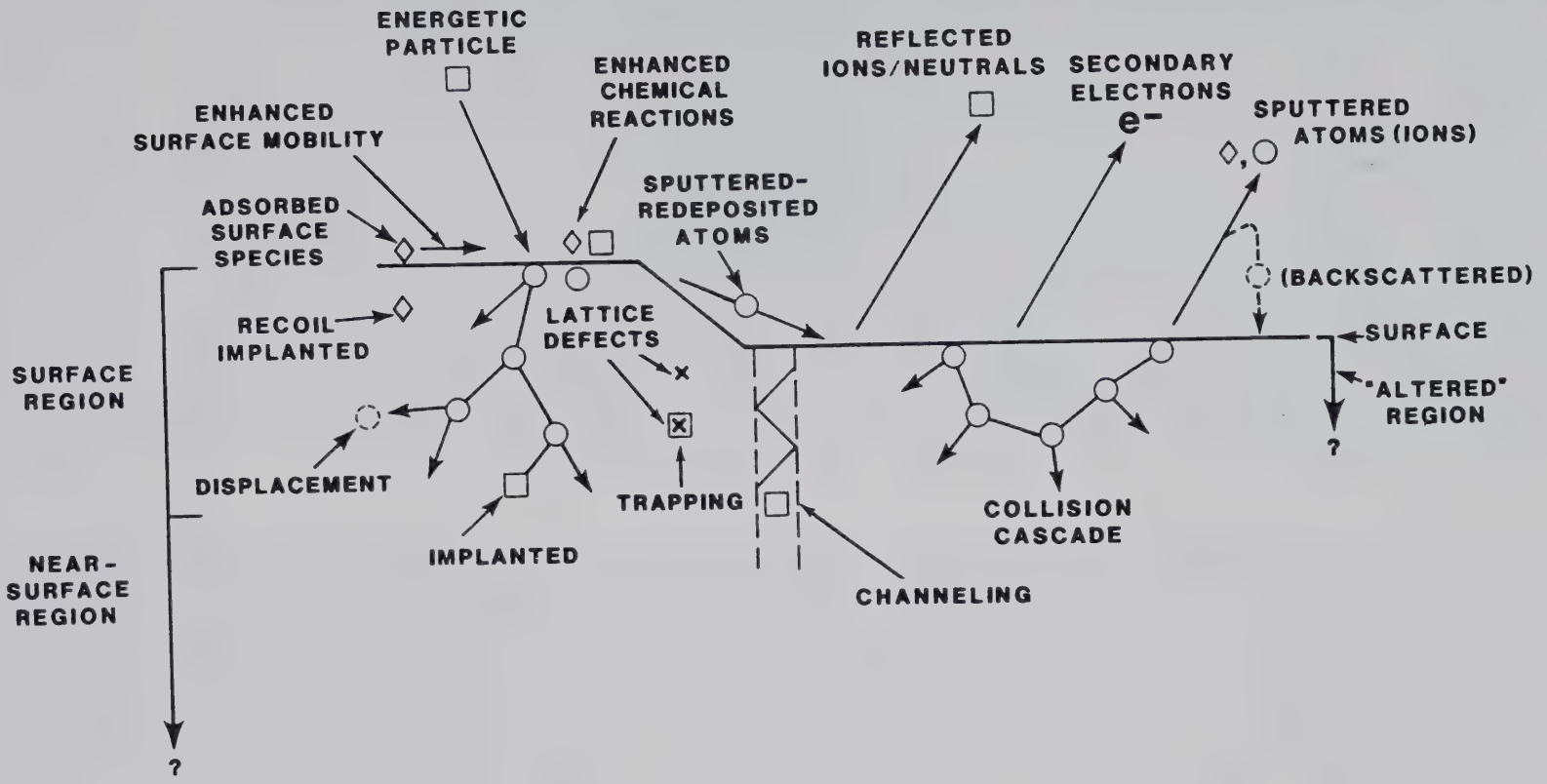

INTERACTION OF ENERGETIC PARTICLES (IONS OR NEUTRALS) WITH SOLIDS

Figure 24. Schematic showing the interaction of energetic particles with a solid surface. Particle bombardment of the surface results in the production of secondary electrons, sputtered atoms and high energy neutrals from the surface. The bombardment also results in the formation of lattice defects, interstitial atoms and trapped bombarding species in the near-surface region. Bombardment can also increase the surface mobility of adatoms and enhance the chemical reactivity of atoms on the surface.

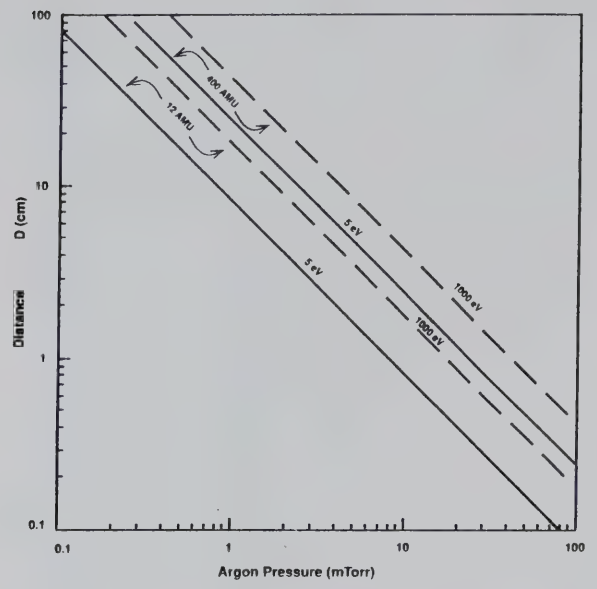

Figure 25. Distance for thermalization of a low mass (12 AMU) and a high mass (400 AMU) particle with low energy (5 eV) and high energy (1000 el) as a function of argon gas pressure (adapted from ref. 42).

target surface [45,46]. Preferential sputtering of one component of the surface can change the surface composition of an alloy, or compound material [47], or the composition of a film undergoing concurrent bombardment during deposition [48].

Most of the energy of the bombarding particles is lost as heat or in the displacement of atoms in the near-surface region. The displaced atoms leave lattice vacancies which may then trap bombarding species which have penetrated the near-surface region; this results in gas trapping [49]. This trapped gas can build up to a high concentration and create a high "chemical potential" between the near-surface region and the bulk of the material. This high chemical potential, along with heating, aids in diffusion of the gases into the bulk of the material if there is solid solubility. The displaced atoms are "stuffed" into the atomic lattice and create a compressive stress in the near-surface region. This process is sometimes called "atomic peening" [50].

Atoms sputtered from a surface at an oblique angle to the flux of bombarding species may be "forward sputtered" and can be deposited outside the bombarded area. This forward sputtering process increases the surface coverage on rough surfaces. Surface atoms or molecules may be struck by the bombarding species and be "recoil implanted" into the surface. Molecules on the surface can be dissociated and become more reactive. This dissociation aids in "bombardment-enhanced chemical reactivity" [31,32]. Bombardment can cause contaminant or unreacted species on the surface to be desorbed [15].

In ion plating, the bombarded surface is continually being buried by depositing material. Therefore the total residual film stress and incorporated bombarding gas increases with film thickness [51,52]. The increase of stress can result in residual compressive stresses great enough to cause spontaneous fracture and loss of adhesion ("deadhesion") of the film from the surface [37]. The trapped gas may coalesce to produce voids in the deposited film. Gas incorporation can be minimized by using low-energy (e.g., less than 300 eV) bombarding species, an elevated substrate temperature (300-400 °C) during deposition, a low deposition rate, and/or using higher atomic mass (e.g., Kr, Xe or Hg instead of Ar) bombarding species which also minimizes the "reflected energy per sputtered atom" carried by the reflected neutrals [30].

Bombardment allows the in situ cleaning of the surface prior to the beginning of the deposition by "ion scrubbing," physical sputtering ("sputter cleaning") or chemical etching [53]. This "cleaning" portion of the film deposition process allows good interfacial reaction for adhesion and the generation of ohmic contacts to semiconductor materials [54]. In addition to cleaning, bombardment can roughen the surface morphology and change the surface composition by preferential sputtering. Bombardment may also make the surface more "active" by the generation of reactive sites and lattice defects.

Nucleation of the depositing condensible atoms ("adatoms") on a surface is modified by ion bombardment by:

- cleaning the surface
- changing the chemical composition of the surface
- formation of defects and reactive sites
- recoil implantation of surface species
- introduction of heat into the near-surface region.

Generally these effects increase the nucleation density of the adatoms on the surface [55]. In addition, sputtering and redeposition of adatoms during ion plating allow film nucleation and growth in areas which would not otherwise be reached by the depositing adatoms.

The interface formation stage of film growth allows the formation of a desirable diffusion or compound type interface on the "clean" surface if the materials are mutually soluble. A "pseudodiffusion" type of interface can be formed due to the energetic particle bombardment during the initial deposition, if the materials are insoluble [40]. Interface formation is aided by defect formation and the deposition of energy (heat) directly into the surface without the necessity for bulk heating. In some cases the temperature of the bulk of the material may be kept very low while the surface region is heated by the bombardment. This allows the development of a very high temperature gradient in the surface region which limits diffusion into the surface [56]. The ion bombardment, along with a high surface temperature, can cause all of the depositing material to diffuse into or react with the surface giving an alloy or compound coating.

When atoms condense on a surface and have a low surface mobility, they develop a columnar morphology [57-59]. The development of the columnar morphology depends on the melting point of the depositing material, the substrate temperature, the angle-of-incidence of the adatom flux and the surface roughness. Bombardment during the growth of the film can modify a number of film properties by preventing the development of the columnar morphology, leading to the densification of the film [60-64]. Film properties that can be altered include: density, residual film stress, bulk morphology, surface morphology, surface area, grain size, crystallographic orientation, electrical resistivity, porosity, mechanical properties, chemical etch rate, contaminant retention, and corrosion rate.

Concurrent bombardment can improve surface coverage by increasing the surface mobility of the adatoms [65] and by sputtering and redeposition of the depositing material [66,67]. In the case of plasma-based ion plating, coverage is increased by gas scattering of the atoms before they reach the substrate surface [68] and the "forward sputtering" and backscattering of the sputtered atoms as shown in figure 26 [69]. By adjusting the bombardment parameters, a rough surface may be made smoother ("planarized") [70].

In reactive PVD processing, the depositing film species react with the gaseous ambient, an adsorbed species, or a co-depositing species to form a compound material such as TiC [71], TiN [72,73], BN [74], Si_3N_4 [75,76] or TiO_2. In reactive ion plating, bombardment enhances the chemical reaction ("bombardment-enhanced-chemical-reactions") [31]. In plasma-based ion plating, the plasma "activates" the reactive species by dissociation of molecular species and creates new species in the gas phase which may be more reactive (e.g., O_3 from O_2) or more readily adsorbed on the substrate surface (e.g., O_3 compared to O_2) [6]. The bombardment desorbs unreacted species [15]. In general, it has been found necessary to have concurrent bombardment in order to deposit hard and dense coatings of materials such as Si_3N_4 [75,76] and TiN [72,73] at low temperatures. Figure 27 shows the relative effects of heating and concurrent bombardment on the resistivity of TiN films [72]. By controlling the availability of the reactive gas, the film composition can be "graded" through the deposition. For example, titanium can be deposited as an underlayer (adhesion layer) for TiN by controlling the nitrogen availability during deposition. This "grading" is often necessary for the best adhesion.

In reactive IBAD, ions of the reactive gas can be used to bombard the growing film [77,78]. Energetic reactive gas ions have a high probability of reacting with the depositing film material. By controlling the amount of reactive species available, a variety of compositions may be produced. For example, in the Cu-O system the compounds of CuO, Cu_5O_4 or Cu_2O can be formed by controlling the copper-atom/oxygen-ion ratio.

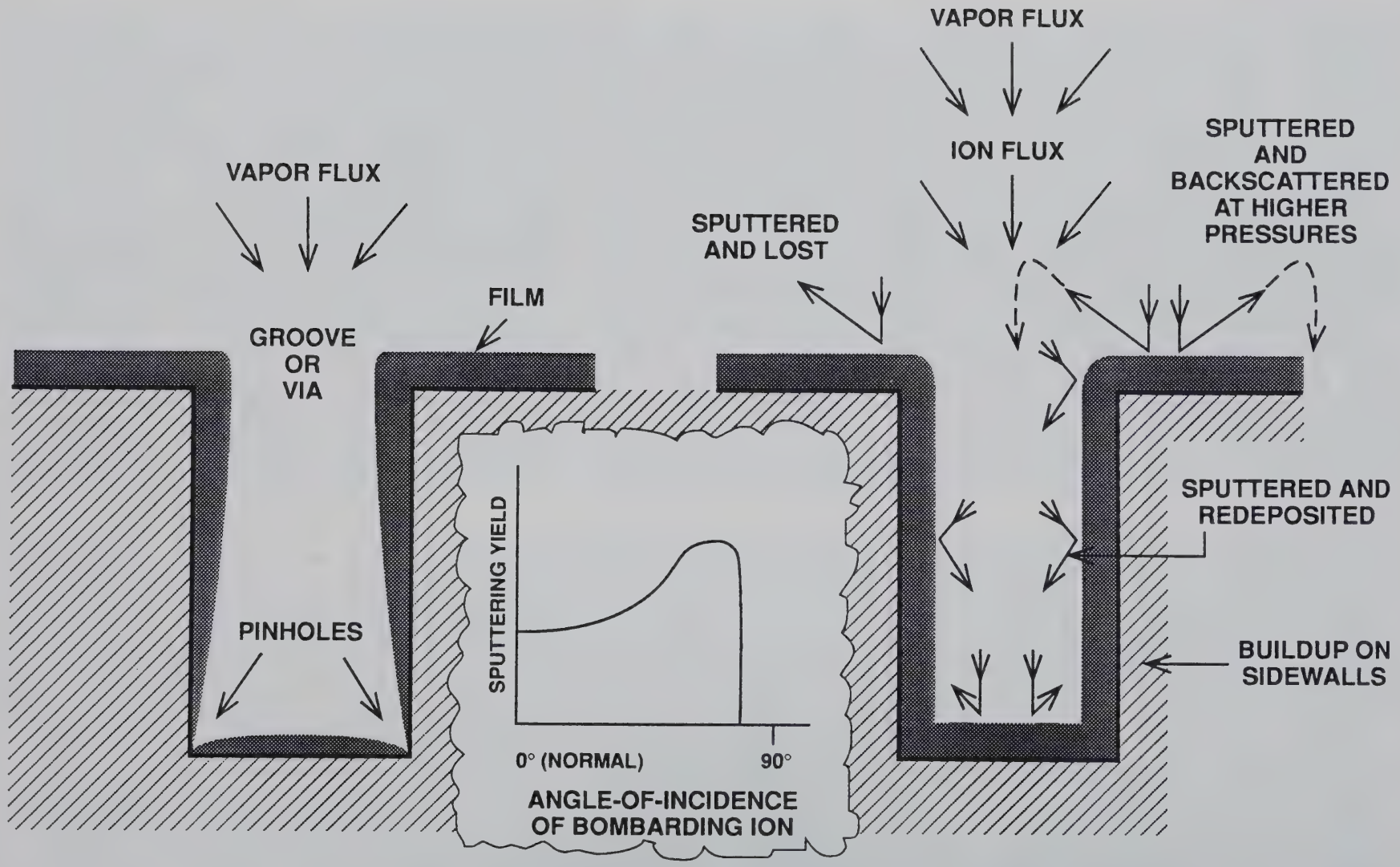

Figure 26. Effect of concurrent bombardment on surface coverage. In the case of no concurrent bombardment geometrical shadowing leaves pinholes at the base of the groove while in the case of concurrent bombardment, sputtering-redeposition and gas scattering fills in the geometrically shadowed regions. Also shown is the effect on the angle-of-incidence on the sputtering yield from a bombarded surface. At a high angle-of-incidence the sputtering yield drops to zero which allows build up on the sidewalls of the groove or via.

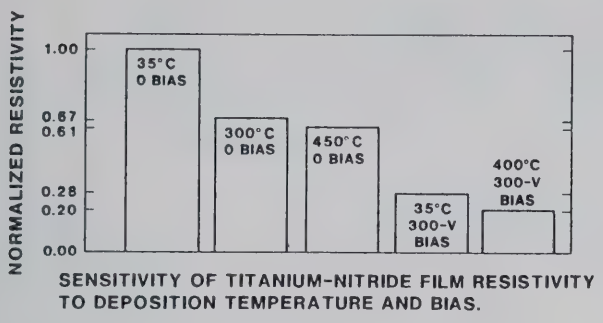

Figure 27. Relative effects of substrate temperature and ion bombardment (bias) on the resistivity of reactively sputter deposited Ti-N films (adapted from ref. 72). The resistivity of the Ti-N film depends on both the density and the composition of the film.

3. Sources of Vapor

The deposition sources for ion plating include:

- thermal evaporation and sublimation
- physical sputtering
- vacuum arc
- plasma arc
- chemical vapor precursor gases

Evaporation and sublimation sources are usually heated by resistive or electron beam heating, although other techniques such as rf heating, exploding wires or laser ablation may be used in special cases. Resistive or unfocussed low energy electron beam heating is used when the evaporation source material ("evaporant") vaporizes rapidly below about 1500-1800 °C. Figure 1a shows the use of a resistively heated thermal vaporization source. Figure 28 shows the use of a low-energy/ high-current electron beam to vaporize and ionize the gas and vapor species. For vaporization temperatures greater than about 1800 °C, focussed electron beam heating of the evaporant surface is generally used. Figure 29 shows the use of a high-voltage bent-beam electron beam evaporator where the filament region is differentially pumped to avoid ion erosion of the electron emitter filament [79,80]. In some cases, multiple vaporization sources are used to allow sequential deposition of different materials, special flux configurations (e.g., line source) or the gradual gradation from one material to another during deposition. The vaporization rate for thermal evaporation sources is suppressed by the presence of a gas.

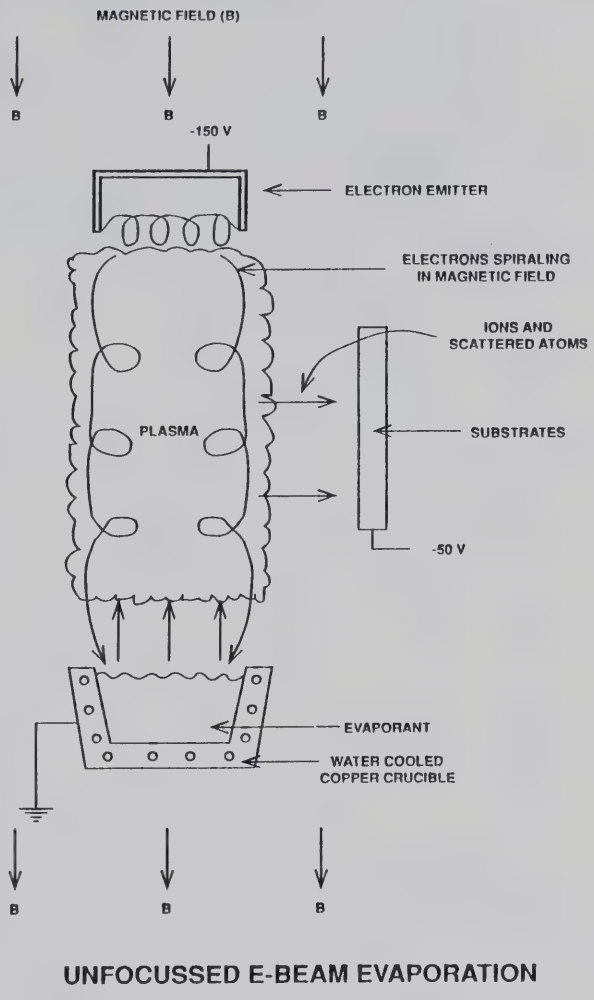

Figure 28. The use of an unfocussed low-energy high-current magnetically confined electron beam for evaporation and ionization. Ions of the plasma gas and the evaporant vapor are accelerated to the substrate by an applied bias.

Energetic ions from a plasma or ion gun may be used for sputtering a surface to provide the adatoms for deposition in ion plating. In many cases, the same plasma used as a source of ions for film bombardment may be used for bombarding the sputtering target. In other cases, a separate plasma must be established for the sputtering source. For example, in conventional magnetron sputtering (fig. 30) the plasma is confined near the target and there is no plasma near the substrate. To overcome this problem, an auxiliary discharge may be formed near the substrate or an unbalanced magnetron configuration (fig. 30) can be used

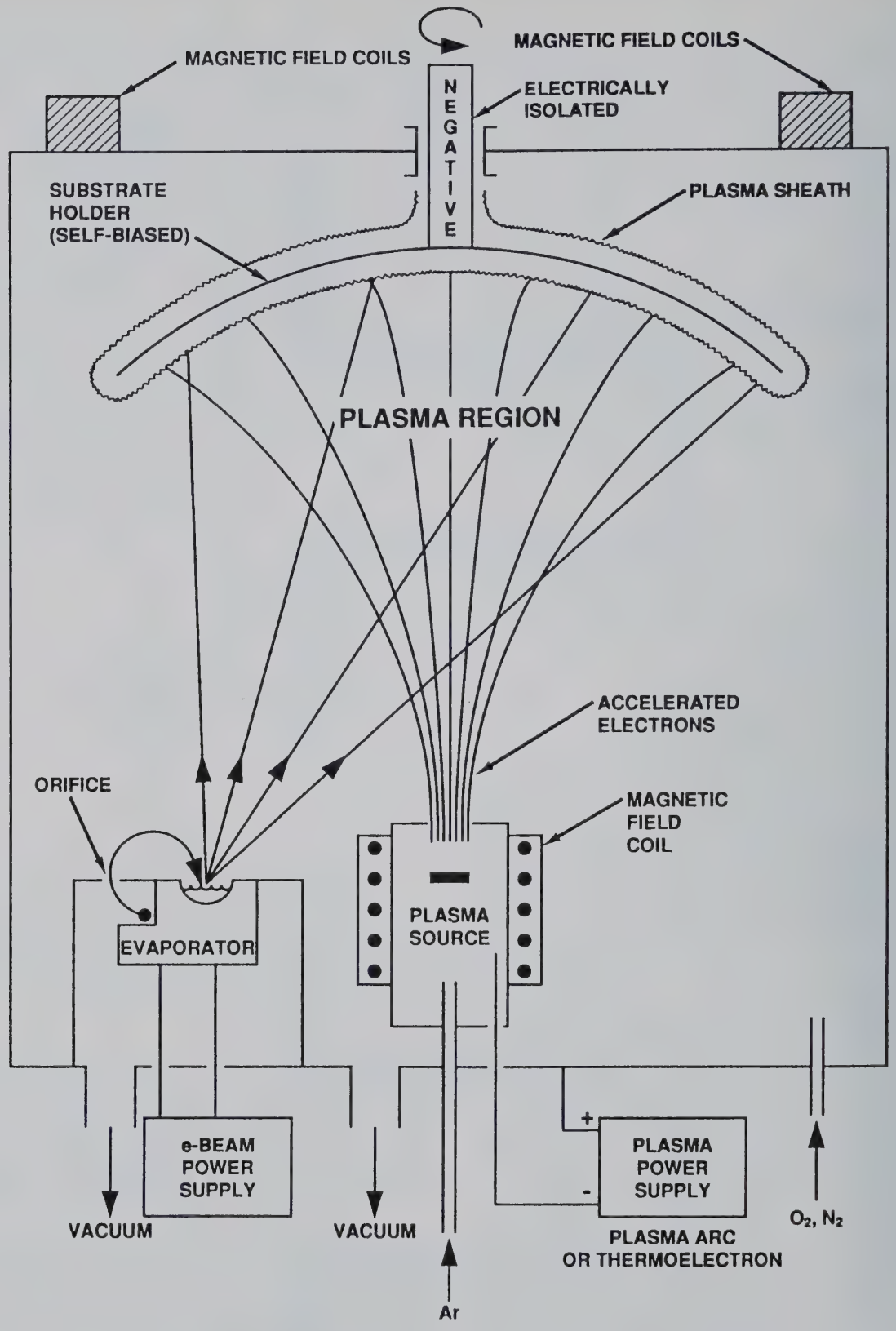

Figure 29. High-energy focussed bent-beam electron beam evaporation using a differentially pumped electron emitter source (see ref. 79). Also shown is a magnetically confined electron beam used to create a high self-bias on the electrically floating substrate holder (see ref. 115).

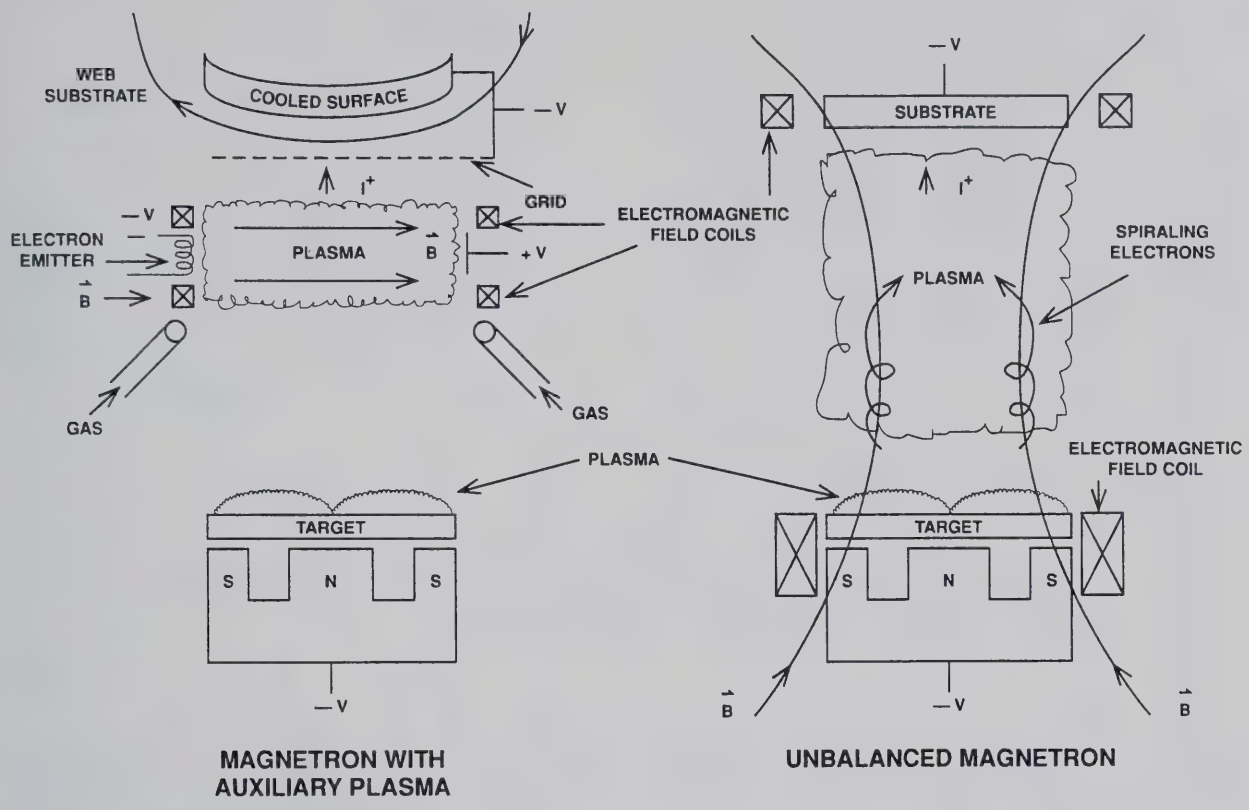

Figure 30. Ion plating using planar magnetron sputtering as the vaporization source. Conventional magnetron configuration with an auxiliary plasma source near the substrate, and an unbalanced planar magnetron sputtering configuration.

to establish a plasma near the substrate [81,82]. In the unbalanced magnetron configuration the escaping electrons can be used to impose a self-bias on the an electrically floating substrate.

Electric arcs may be established in a vacuum or in a gaseous atmosphere [83,84]. The high-current/low-energy electron flow between the electrodes gives a very high ionization probability for the vaporized material and gases in the space between the electrodes. Many of the ions are multiply charged. In a vacuum arc (fig. 31), the positive metal ions create a positive space charge between the electrodes and the positive ions are accelerated away from that region [85]. A substrate is then bombarded with energetic ions of the condensing film material ("film ions").

When a gas is present in the arc discharge region, thermalization by gas collision prevents the film ions, which have been accelerated away from the space charge region, from reaching the substrate with high energies. In this case, an accelerating substrate potential is necessary to attain bombardment. When a gas is present, the arc electrode separation is made large and ions of the gas are formed as well as ions of the arcing surface as shown in figure 31. The most general arc deposition configuration uses a cooled anode or the cooled chamber walls as the anode and the vaporization is from a solid cathodic. Often magnetic fields are used to cause the arc to move over the cathode surface. Arc sources can be operated in a reactive gas environment to allow the reactive deposition of compound films [86-88].

The arc vaporization of a solid surface ejects molten globules or "macros" of the surface material. These macros are generally undesirable and many techniques are being used to eliminate or minimize the deposition of the macros. Generally the number of macros decrease for the more refractory materials. Therefore arcing refractory materials or ones that form refractory materials with the ambient gas, produce the fewest macros than from lower melting point materials. For example, TiN from a titanium target will form fewer

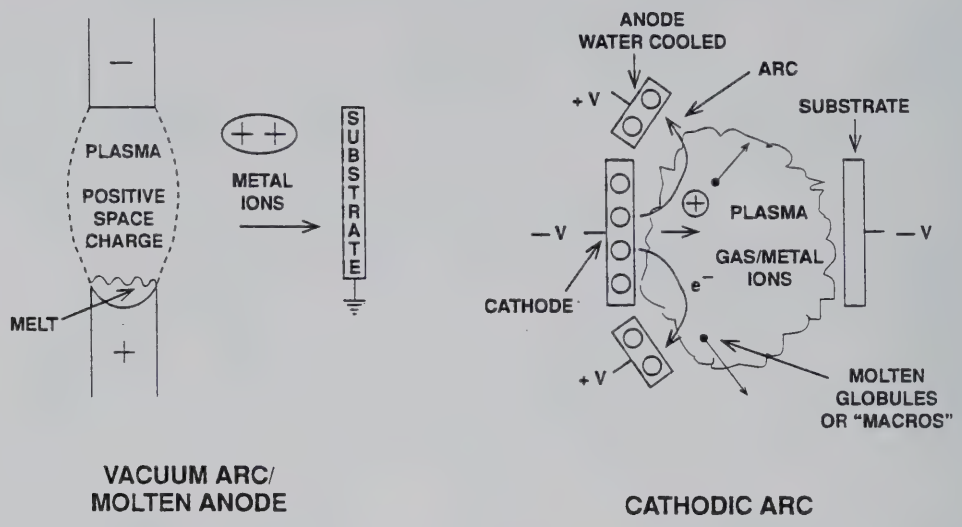

Figure 31. Arc vaporization in a vacuum and in a gaseous environment. In the vacuum arc positive ions are accelerated away from a positive space charge region between the two electrodes. In the gaseous plasma, ions are accelerated to the substrate by an applied negative bias.

macros than titanium in an inert gas [89]. In one technique, arc deposition is only used to form the initial film-substrate interface in order to attain good adhesion and unbalanced magnetron sputtering is then used for the balance of the deposition [90]. In ion plating, one of the major advantages of an arc vaporization source is the presence of the large number of "film ions" that may be used for bombardment without concern for gas incorporation in the film.

Gaseous chemical vapor precursor species containing the material to be deposited may be used as the source of the depositing material. Examples are: BCl_3, B_2H_6, CH_4, $TiCl_4$, SiH_4, WF_6, $Ni(CO)_4$, and $Al(CH_3)_3$. The precursor gas can be injected directly into the plasma as shown in figure 32 [11] or through an ion gun configuration where it is fragmented and ionized [91]. Using a chemical vapor precursor species in the plasma is similar to biased *P*lasma *E*nhanced *C*hemical *V*apor *D*eposition (PECVD), where the plasma is used to aid in the decomposition of the chemical vapor species and ions are accelerated to the substrate surface [14].

Laser vaporization (ablation) is performed with pulsed high-intensity excimer lasers [92]. Laser vaporization with concurrent ion bombardment has been used to deposit high quality, high-temperature superconducting films at relatively low substrate temperatures [93]. This technique has also been used to deposit hydrogen-free diamond-like carbon (DLC) films [94].

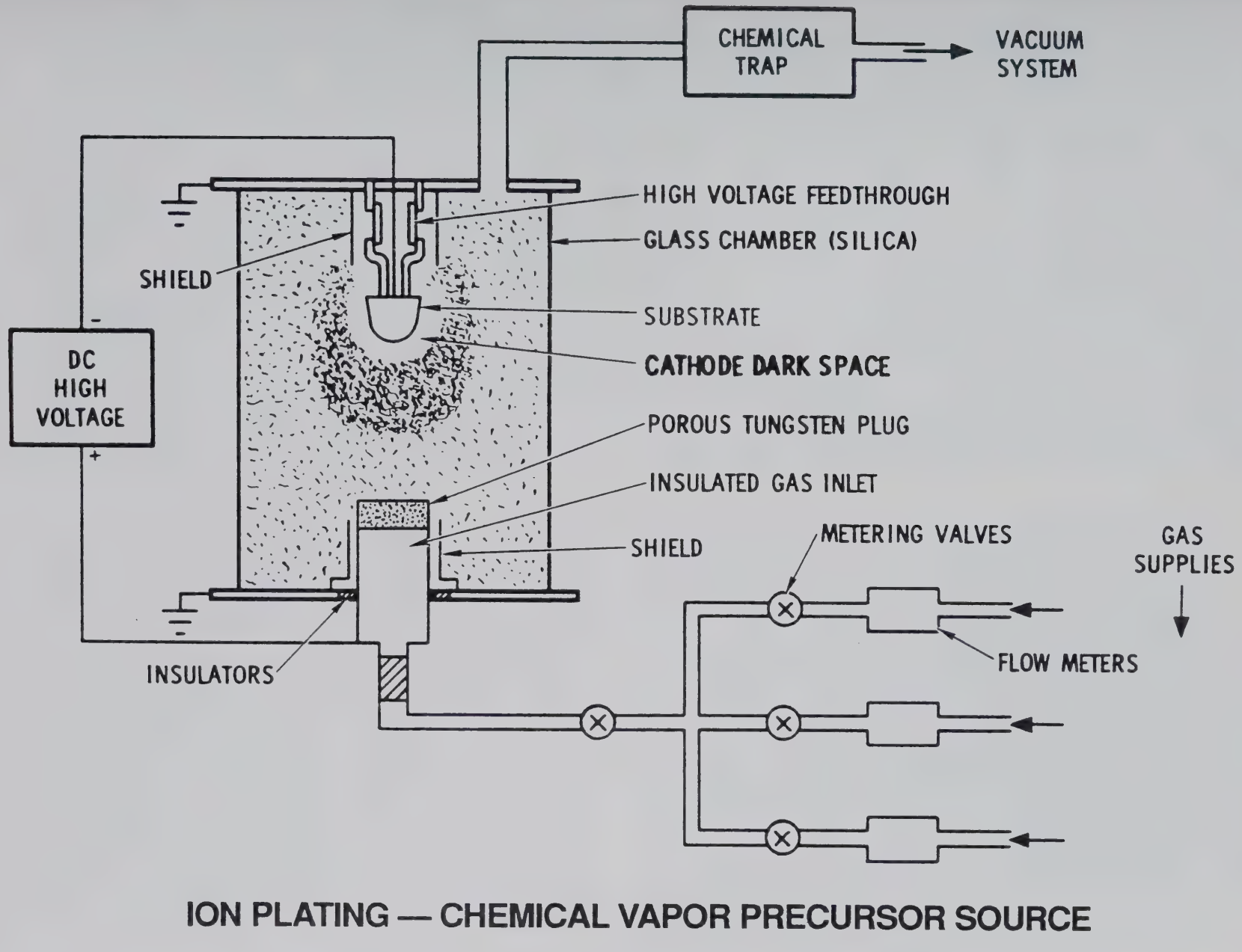

Figure 32. Plasma-based ion plating using a chemical vapor precursor gas in the plasma discharge.

4. Sources for Bombardment

In many applications of plasma-based ion plating, the gas density causes "thermalization" of energetic particles trying to pass through the gas [42]. Therefore, the energetic bombarding ions are generally accelerated toward the substrate due to a potential on the substrate or on a high-transparency grid surrounding the substrate fixture. This potential can be produced by applying a bias from an external source or by bombarding an electrically insulating or electrically floating surface with high-energy electrons ("self-bias"). In vacuum-based (or low-pressure) ion plating, the bombarding ions may be accelerated away from a surface or region (e.g., vacuum arc vaporization, or an ion gun) as well as being accelerated toward the substrate.

Energetic massive particles for bombarding surfaces and growing films may be in the form of inert or reactive gas species (ions or neutrals), charged fragments of chemical vapor precursor gases or charged species of condensing film material. The most common sources for energetic bombarding particles at gas (plasma) pressures above which there is thermalization of energetic particles between the vaporization source and the substrate are:

- ions from a DC, rf, plasma arc, or laser-induced [95] plasma being accelerated to the surface under an applied bias or "self-bias"
- high-energy neutrals originating from charge exchange processes in a gas [96].

Where the pressure is low enough so that there is little or no thermalization [97] between the source and substrate, additional sources of energetic particles are:

- reflected high energy neutrals which arise from energetic ions reflecting from a surface as neutrals [27-30], e.g., low pressure magnetron sputtering and ion beam sputtering
- acceleration of ions from the vacuum arc vapor source due to a space charge [85]
- acceleration of negative ions (e.g., O^-) away from a negatively-biased sputtering surface [98]
- energetic neutral sputtered species
- ion guns where ions are extracted from a confined plasma using a grid system [99-101].

Figure 33 shows some of the ion gun configurations that can be used in the IBAD processing.

Plasmas may be enhanced or generated in local regions by the addition of electrons to that region; however, this often leads to an inhomogeneous plasma [5]. These augmenting electrons typically come from a thermionic emitting surface [102] or a hollow cathode [103-106]. Often, magnetic fields may be used to confine electrons by trapping the electrons in the field direction which also causes them to spiral and thus increase their path length and ability to cause ionization. Plasmas may also be enhanced or generated in local regions in the system by electric field effects. For example, an rf electrode arrangement can be used to generate a plasma in a local region as shown in figure 34.

Irregular surfaces, points, edges and other geometrical effects cause distortion of the electric field in the vicinity of a surface and thus the plasma uniformity and the direction of accelerated ions (e.g., focussing effects). The plasma uniformity can often be improved by surrounding a complex surface with a grid electrically tied to the substrate—this provides a more uniform surface geometry. This "grid-surround" technique is used to coat loose items contained in a rotating "grid cage" or "barrel" as shown in figure 35 [107].

Substrates that are not electrically conductive require a self-bias, an rf-bias, or a grids placed in front of the non-conducting surfaces. The grid allow the surfaces to be bombarded by ions passing through the grid structure. The region between the grid and insulating surface is relatively field-free due to the presence of secondary electrons emitted from the bombarded surfaces. When using an rf-bias on an electrically insulating substrate, the substrate must completely cover the electrode. If a portion of the electrically conductive electrode is exposed, it provides a parallel electrical circuit which "shorts out" the capacitor formed by the electrode-substrate-plasma configuration.

Any surface in contact with a plasma develops a negative potential with respect to the plasma due to the high mobility of the electrons compared to the ions. This "self-bias" can range from several volts for weakly ionized "cold" plasmas to many tens of volts when the electrons are accelerated to the surface. Figure 29 shows a technique of creating a high self-bias by accelerating electrons away from an electron source, confining them along magnetic field lines, and causing them to impinge on an electrically floating substrate holder.

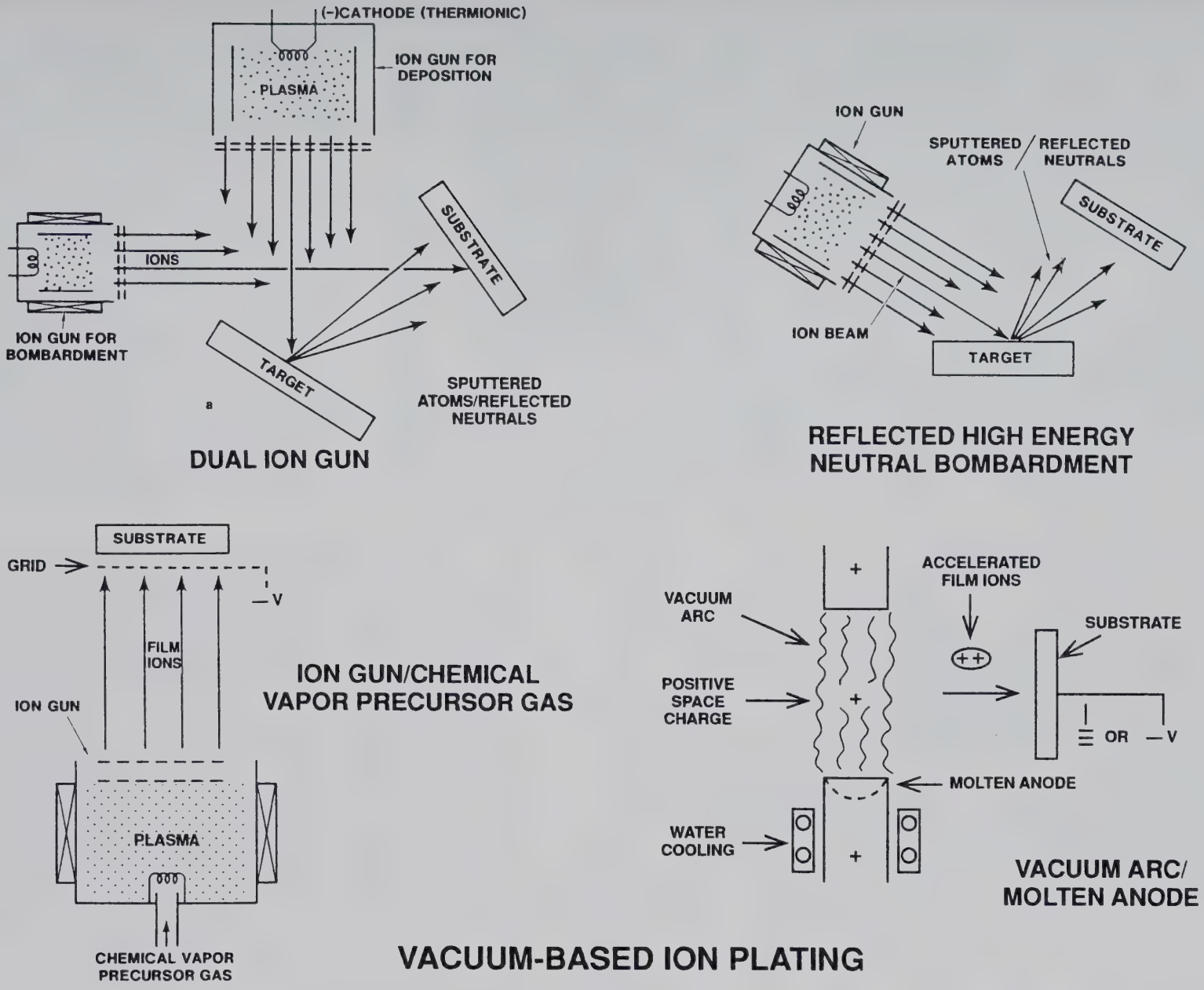

Figure 33. Bombardment sources and vaporization sources that can be used in IBAD processes.

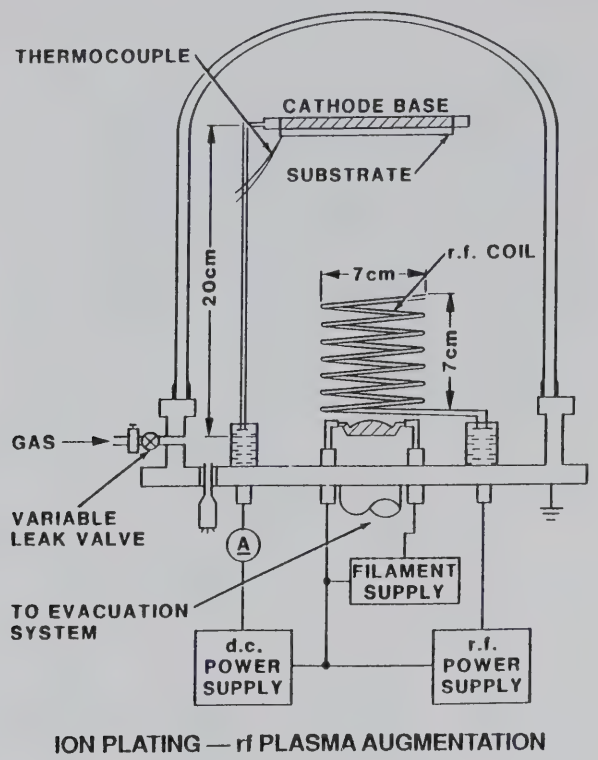

Figure 34. The use of rf plasma enhancement above a thermal vaporization source.

5. Ion Plating Processing Parameters

Ion plating conditions and film properties may be monitored as a function of 1) ion flux and energy vs. flux of depositing atoms (atom/ion ratio) [108-110], 2) the bombardment energy per depositing atom (typically 15-20 ev/atom) or 3) the "resputtering rate" (e.g., 40% resputtering) [111]. Each of these measurement techniques can be misleading. For example, when using method 1 or 2, high energy bombarding ions can become incorporated in the growing film and produce voids and porosity in the film. Also, in plasma-based ion plating, the ion and high-energy neutral fluxes and energy distribution are often uncertain. In method number 3, the measured "resputtering rate" is sensitive to the gas pressure since there is a great deal of backscattering to the film surface at higher pressures.

When using ion plating processes in production, the conditions necessary to obtain the desired film properties are usually determined empirically. Generally, ion plating is reproducibly performed by controlling and monitoring deposition parameters including:

- system geometry including the angle-of-incidence of the depositing adatom flux and the number of substrates (i.e., the "load")
- substrate bombardment power (watts/cm^2)
- deposition rate
- gas composition
- gas flow rate
- contaminants in the system

6. Ion Plating Systems

Ion plating essentially requires the same vacuum/plasma system as does sputter deposition. As with sputter deposition, an ion plating system should first be a good vacuum system since the effects of contaminants in the plasma are magnified by their activation. The enhanced surface coverage requires that the extra precautions need to be taken to shield high-voltage feedthroughs from the vapor flux.

At high vaporization rates in a high gas density, vapor-phase nucleation of ultrafine particles occurs ("gas evaporation") [112]. These ultrafine particles acquire a negative charge in the plasma and deposit on non-negative surfaces in the vacuum system giving a "sooty" deposit. If the material being deposited is oxygen-active, the ultrafine particles are pyrophoric and will burn if disturbed in air.

Fixturing of the substrate in ion plating is a major concern in that the fixturing should provide plasma uniformity over the substrate surface. The use of grids is desirable to provide a uniform field around fixtures.

7. Some Applications of Ion Plating and IBAD

The good adhesion obtained with ion plating allows the deposition of adherent coatings for demanding applications. Low shear metal lubricant and anti-seize films, such as silver, lead and indium that are deposited by ion plating, are used in x-ray tubes, for space applications by NASA, and on threads of piping used in chemical environments. M-Cr-Al-Y coatings, where M is Ni, Co, Fe or Ni + Co, are ion plated on aircraft engine turbine blades to provide high-temperature erosion/corrosion protection. Aluminum, copper, Ti-Au, Ti-Pd-Cu-Au, Cr-Au, etc., are used to metallize semiconductors, ferrites, glass and ceramics. Silver is deposited on beryllium to allow low-temperature solid diffusion bonding of high-tolerance beryllium parts. Ion plating is used to deposit biologically inert coatings of carbon, chromium, titanium and tantalum on body implants.

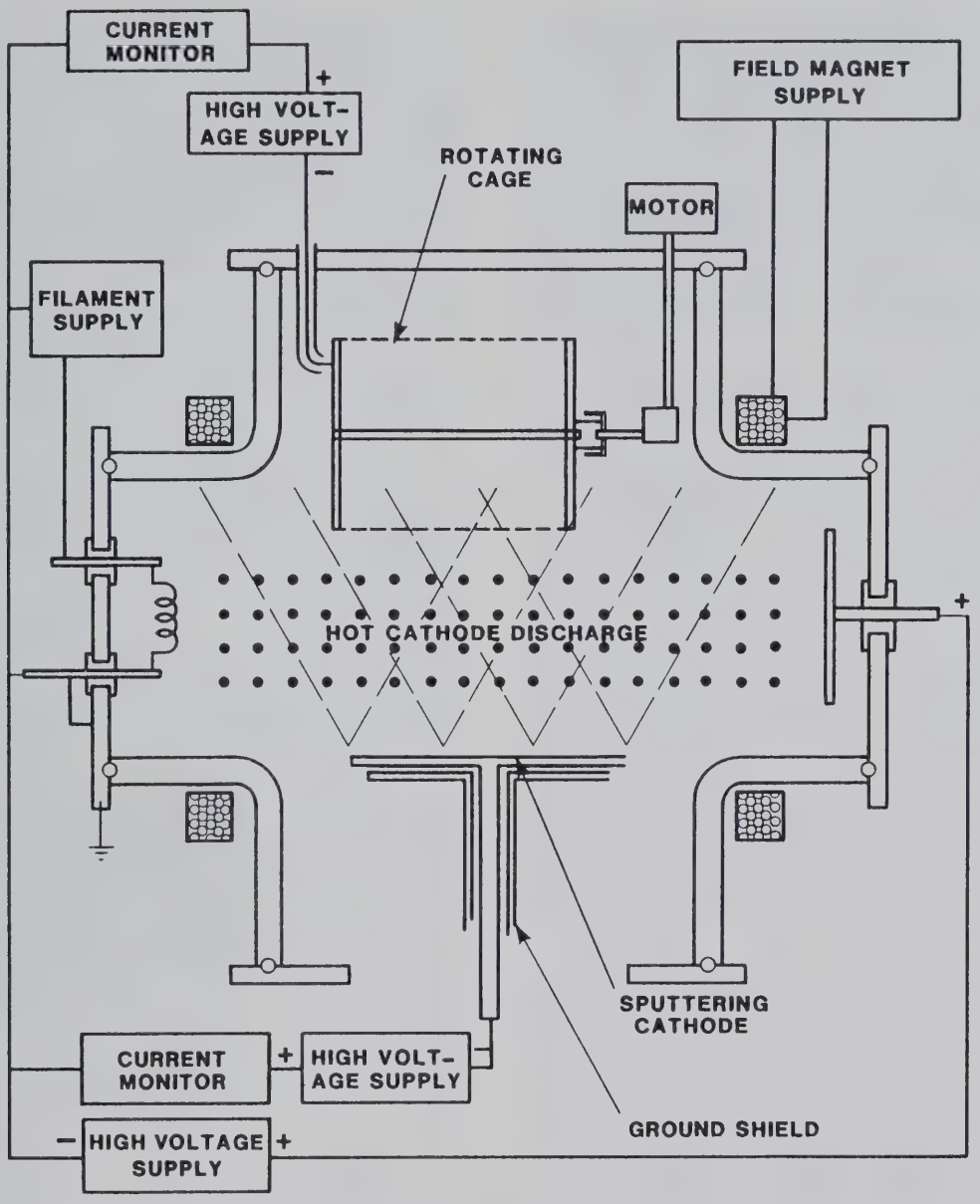

Figure 35. Barrel ion plating configuration (see ref. 107).

One interesting application of ion plating is to provide an adhesion layer for subsequent electroplating to a high thickness [113]. This combination of deposition techniques has been used to deposit thick copper layers on molybdenum for diamond point turning.

The good throwing power from gas scattering and sputtering/redeposition, along with film densification from the ion bombardment, allows coating over complex surface geometries and complex shapes with a minimum of pinholes and porosity and a minimum of fixture movement. In the semiconductor industry, the covering ability is used to smooth ("planarize") surfaces which have etch features on them.

Aluminum films are widely used for corrosion protection. For example, titanium aircraft fasteners are aluminum plated to prevent galvanic corrosion where they contact aluminum structures; and parts as large as small engine housings, aircraft landing gears and the inside of long pipes are plated with aluminum for corrosion protection. Uranium is

coated with aluminum to provide corrosion protection in nuclear reactor environments. Ultrahigh vacuum components are coated with gold and copper to reduce hydrogen desorption. The dense nature of the ion plated films allow the formation of good diffusion barrier films, such as TiN, on silicon under aluminum and tungsten metallization.

Ion plating allows the deposition of stoichiometric and dense films of compound materials at low-deposition temperatures and is used to deposit hard TiN, TiN/C, and TiC coatings on tool steel drill bits, gear teeth, high-tolerance injection molds, and aluminum vacuum sealing flanges. TiN or TiN overlayed with gold (gold color), ZrN (brass color), TiC (black) and Ti/Al-C/N (bluish-grey) are used as decorative coatings on metals and plastics [114]. In some cases corrosion-resistive coatings or diffusion-barrier coatings of nickel or nickel-palladium, deposited by electroplating, are used under the decorative coating. For example, electrodeposited Ni-Pd may be used on brass (Cu-Zn) to prevent zinc migration and to make the surface more smooth. Various compound films are used as optical coatings [115] and multilayer coatings are used as decorative coatings on stainless steel panels [114]. Multiple sequential deposition of a few monolayers of film material followed by reactive ion bombardment to form a compound with a cooling period between layers is used to deposit dense compound films on thermally sensitive substrates such as plastic ophthalmic devices [13,116].

At present, the principal applications of IBAD are to deposit dense optically transparent coatings for optical applications [26]. Often, this entails using bombarding ions of reactive gases, such as oxygen. In these applications, the densification of the film increases the index of refraction of the deposited material and gives a protective coating which is important when coating soft or environmentally sensitive optical components such as infrared optics.

8. The Future

As electroplating becomes more difficult to use because of pollution problems, PVD processes are being considered as replacement deposition processes. Ion plating, with its good surface coverage and good adhesion is a prime contender to coat complex surfaces. In addition, the use of TiN to replace gold, and ZrN to replace brass, provides improved durability over electroplated gold and brass coatings. The use of aluminum coatings to replace zinc and cadmium for corrosion protection is a growth area, and is being used to coat such diverse parts as small engine blocks, aircraft landing gear components, titanium fasteners, etc. [117]. The use of PVD processes to coat bulk materials such as strip steel, pipes and plastic webs will increase, and the use of coated bulk material will eliminate the need for coating fabricated parts in some instances.

The biggest deterrents to using ion plating are the high capital cost of high-volume production equipment, and the apparent complexity of the process. As more companies become involved in high-volume production, utilizing the process in order to retain market share, these deterrents will fade. At present, the use of ion plating is most applicable where high value-added processing is acceptable, such as in coating expensive injection molds, as compared to coating inexpensive drills. As the processing is refined and becomes more commonplace, ion plating will be used to coat less-expensive articles, particularly as high-volume equipment is developed, and the unit cost for coating is reduced.

The equipment needed for plasma-based ion plating is well in hand, and the main problems are associated with fixture design for specific applications. In general, the use of thermal vaporization is more cost-competitive than is sputtering as a vapor source for ion plating. The use of arc vaporization, with its high ionization, to form the initial bonding layer, is a very attractive process [90]. The equipment for IBAD processing could be greatly improved by the development of low-cost, high-current, large-area reactive ion beam sources.

9. Summary

Ion plating is particularly useful in applications where other deposition techniques do not provide optimal film properties, such as adhesion, surface coverage, film density, hardness or composition. The major processing problems are to obtain uniform bombardment over insulating surfaces, and over complex conductive surfaces, although these problems can generally be alleviated by using self-biasing techniques and grid structures. As electroplating becomes more environmentally unacceptable, it is expected that ion plating, which is classed as a "dry plating" process, will replace it in many applications where excellent adhesion and good surface coverage are required.

References

[1] D. M. Mattox, J Vac Sci Technol 10, 47, 1973.

[2] Ion Plating, D. M. Mattox, Chapter 13 in *Handbook of Plasma Processing Technology: Fundamentals, Etching, Deposition and Surface Interactions*, edited by Stephen M. Rossnagel, Jerome J. Cuomo and William D. Westwood, Noyes Publications, 1990.

[3] *Ion Plating Technology—Developments and Applications*, N. A. G. Ahmed, John Wiley 1987.

[4] H. K. Pulker, J Vac Sci Technol A10(4) 1669, 1992.

[5] K. S. Fancey and A. Mathews, Surf Coat Technol 36, 233, 1988.

[6] D. M. Mattox, Appl Surf Sci 48/49, 540, 1991.

[7] H. F. Winters, J. W. Coburn and T. J. Chuang, J Vac Sci Technol B1, 469, 1983.

[8] M. H. Jacobs, Surf Coat Technol 29, 221, 1986.

[9] Y. Murayama, J Vac Sci Technol 12(4) 818, 1975.

[10] R. P. Howson, J. N. Avaritsiotis, M. I. Ridge and C. A. Bishop, Thin Solid Films 63, 163, 1979.

[11] R. Culbertson and D. M. Mattox, 8th Conf on Tube Technol p101-107, IEEE Conf Record 1966 also Culbertson U.S. Patent 3,604,970 (1971) also Mattox U.S. Patent 3,329,601 (1974).

[12] S. Schiller, U. Heisig and K. Goedicke, J Vac Sci Technol 12(4) 858, 1975.

[13] R. P. Netterfield and P. J. Martin, Thin film synthesis by sequential magnetron sputtering and reactive gas bombardment, paper TF-FrM6 in 38th National Symposium of the AVS (1991).

[14] H. P. W. Hey, B. G. Sluijk, D.G. Hemmes, Solid State Technol 33(4) 139, 1990.

[15] L. I. Maissel and P. M. Schaible, J Appl Phys 36, 237, 1965.

[16] R. Frerichs, J Appl Phys 33, 1898, 1962.

[17] R. Conrad, R. A. Dodd, S. Han, M. Madapura, J. Scheuer, K. Sridharan and F. J. Worzala, J Vac Sci Technol A8(4) 3146, 1990 and references therein.

[18] K. E. Steube and L. E. McCrary, J Vac Sci Technol 11(1) 362, 1974.

[19] "Applications of ion vapor deposited aluminum coatings" D. E. Muehlberger p 75 in *Ion Plating and Implantation*, edited by Robert F. Hochman, Conference Proceedings American Society for Metals 1986.

[20] "Physical vapor deposition of metals, alloys and compounds" Rointan Bunshah, p. 200 in *New Trends in Material Processing*, American Society for Metals, 1974.

[21] S. Aisenberg and R. W. Chabot, J Vac Sci Technol 10(1) 104, 1973.

[22] D. van Vechten, G. K. Hubler, E. P. Donovan and F. D. Correll, J Vac Sci Technol A8(2) 821, 1990.

[23] D. van Vechten, G. K. Hubler, E. P. Donovan and F. D. Correll, J Vac Sci Technol A8(2) 831, 1990.

[24] F. A. Smidt, International Materials Reviews 35(2) 61, 1990.

[25] "Ion Beam Processing of Optical Thin Films" Ursula T. Gibson, p. 109 in *Physics of Thin Films* Vol. 13 edited by Maurice H. Francombe and John L. Vossen, Academic Press 1987.

[26] P. J. Martin, J Mater. Sci. 21, 1, 1986.

[27] D. W. Hoffman, J Vac Sci Technol A8(5) 3707, 1990.

[28] "Fundamentals of sputtering and reflection," David N. Ruzic Chapter 3, in *Handbook of Plasma Processing Technology: Fundamentals, Etching, Deposition and Surface Interactions*, edited by Stephen M. Rossnagel, Jerome J. Cuomo and William D. Westwood, Noyes Publications, 1990.

[29] S. M. Rossnagel, J Vac Sci Technol A7(3) 1025, 1989.

[30] H. F. Winters, H. J. Coufal and W. Eckstein, submitted to J Vac Sci Technol.

[31] G. A. Lincoln, M. W. Geis, S. Pang and N. Efremow, J Vac Sci Technol B1, 1043, 1983.

[32] J. W. Coburn and H. F. Winters, Nucl Instrum Method Phys Res B27, 243, 1987.

[33] S. Veprek and M. Heintz, Plas Chem Plas Proc 10(1) 3, 1990.

[34] S. Veprek and M.G.J. Veprek-Heijman, Appl Phys Lett 56(18) 1766, 1990.

[35] A. Leyland, K. S. Fancey and A. Matthews, Surf Eng 7(3) 207, 1991.

[36] R. W. Burger and L.J. Gerenser, 34th Annual Technical Conference Proceedings (Society of Vacuum Coaters) 1991 p. 192.

[37] "Residual stress, fracture and adhesion in sputter-deposited molybdenum films" D. M. Mattox and R. E. Cuthrell p. 141 in *Adhesion in Solids* edited by D. M. Mattox, J. E. E. Baglin, R. E. Gottschall and C. D. Batich Vol. 119 MRS Proceedings 1988.

[38] A. Matthews and D. T. Gethin, Thin Solid Films 117, 261, 1984.

[39] A. Matthews, Vacuum 32(6) 311, 1982.

[40] "Thin film adhesion and adhesive failure—A perspective" D. M. Mattox, p. 54 in *Adhesion Measurement of Thin Films, Thick Films and Bulk Coatings* edited by K. L. Mittal ASTM STP 640, American Society for Testing and Materials (1978).

[41] D. M. Mattox, J Vac Sci Technol A7(3) 1105, 1989.

[42] W. D. Westwood, J Vac Sci Technol 15, 1, 1978.

[43] W. J. Woo and Ch. Steinbruchel, J Vac Sci Technol A10(4) 1041, 1992.

[44] S. J. Choi, M. J. McCaughey, T. J. Sommerer and M. J. Kushner, paper PS-MoM6 at 38th National Symposium of the AVS (1991).

[45] D. M. Mattox, J Nucl Mat 122/123, 1267, 1984.

[46] S. M. Rossnagel, J Vac Sci Technol A6(6) 3049, 1988.

[47] "Bombardment-induced Compositional Changes with Alloys, Oxides, Oxysalts and Halides," R. Kelly, Chapter 4, p. 91 in *Handbook of Plasma Processing Technology: Fundamentals, Etching, Deposition and Surface Interactions*, edited by Stephen M. Rossnagel, Jerome J. Cuomo and William D. Westwood, Noyes Publications, 1990.

[48] H. F. Winters, D. L. Raimondi and D. E. Horne, J Appl Phys 40, 2996, 1969.

[49] D. Edwards, Jr. and E. V. Kornelsen, Rad Eff 26, 155, 1975.

[50] D. W. Hoffman and J. A. Thornton, Thin Solid Films 40, 355, 1977.

[51] D. M. Mattox and G. J. Kominiak, J Vac Sci Technol 8, 194, 1971.

[52] J. J. Cuomo and R.J. Gambino, J Vac Sci Technol 14, 152, 1977.

[53] "Adhesion and Surface Preparation," Donald M. Mattox, Chapter 3 in *Deposition Technologies for Films and Coatings*, edited by R.F. Bunshah, Noyes Publications 1982.

[54] J. L. Vossen, J. H. Thomas III, J.-S. Maa and J. J. O'Neill, J Vac Sci Technol A2(2) 212, 1984.

[55] D. G. Teer, *Coatings for High Temperature Applications*, edited by E. Lang, p. 83, Applied Science Publishers, 1983.

[56] R. T. Johnson, Jr. and D. M. Darsey, Solid State Electron 11, 1015, 1968.

[57] J. A. Thornton, J Vac Sci Technol A4, 3059, 1986.

[58] R. Messier, A. P. Giri and R. A. Roy, J Vac Sci Technol A2(2), 500, 1984.
[59] C. Fountzoulas and W. Nowak, J Vac Sci Technol A9(4) 2128, 1991.
[60] D. M. Mattox and G.J. Kominiak, J Vac Sci Technol. 9, 528, 1972.
[61] R. D. Bland, G. J. Kominiak and D. M. Mattox, J Vac Sci Technol 11, 671, 1974.
[62] "Modification of thin film properties by ion bombardment during deposition," J. M. E. Harper, J. J. Cuomo, R. J. Gambino and H. R. Kaufman Ch. 4 in Ion Bombardment Modification of Surfaces—Fundamentals and Applications, edited by Orlando Aucello and Roger Kelly, Elsevier, 1984.
[63] S. M. Rossnagel and J. J. Cuomo, Vacuum 38(2) 73, 1988.
[64] "Microstructural Control of Plasma-sputtered Refractory Coatings," David W. Hoffman and Robert C. McCune, Chapter 21 in Handbook of Plasma Processing Technology: Fundamentals, Etching, Deposition and Surface Interactions, edited by Stephen M. Rossnagel, Jerome J. Cuomo and William D. Westwood, Noyes Publications, 1990.
[65] "Low-energy ion/surface interactions during film growth from the vapor phase," J. E. Greene, S. A. Barnett, J.-E. Sundgren and A. Rockett, Chapter 5 in Ion Beam Assisted Film Growth (Beam Modification of Materials #3) edited by Tadatsugu Itoh, Elsevier 1989.
[66] D. W. Skelley and L. A. Gruenke, J Vac Sci Technol A4(3) 457, 1986.
[67] J. K. G. Panitz, B. L. Draper and R. M. Curlee, Thin Solid Films 166, 45, 1988.
[68] K. S. Fancey and J. Beynon, Vacuum 34, 591, 1984.
[69] I. Abril, A. Gras-Marti and J. A. Valles-Abarca, Vacuum 37, 394, 1987.
[70] H. P. Bader and M.A. Lardon, J Vac Sci Technol A3(6) 2167, 1985.
[71] M. Fukutomi, M. Fujitsuka and M. Okada, Thin Solid films 120, 283, 1984.
[72] A. J. Aronson, Microelectron Manuf Testing 11, 25, 1988.
[73] S. Benhenda, J. M. Guglielmacci, M. Gillet, L. Hultman and J.-E. Sundgren, Appl Surf Sci 40, 121, 1989.
[74] Rother, H. D. Zscheile, C. Weismantel, C. Heiser, G. Holzhuter, G. Leonhardt and P. Reich, Thin Solid Films 142, 83, 1986.
[75] J. Chin and N. B. Elsner, J Vac Sci Technol 12(4) 821, 1975.
[76] A. Day, L. Wamboldt and F. Jansen, paper TF-FrM7 in 38th National Symposium of the AVS (1991).
[77] "Synthesis by reactive ion beam deposition" J. J. Cuomo, in Ion Plating and Implantation: Applications to Materials, edited by Robert F. Hochman, ASM Conference Proceedings 1986.
[78] J. M. E. Harper, J. J. Cuomo and H. T. G. Henzell, J Appl Phys 58, 550, 1985.
[79] D. L. Chambers and D. C. Carmichael, 14th Annual Technical Conference Proceedings (Society of Vacuum Coaters) 1971, p. 13.
[80] H. R. Harker and R. J. Hill, J Vac Sci Technol 6, 1395, 1972.
[81] B. Window and G. L. Harding, J Vac Sci Technol A8(3), 1277, 1990.
[82] R. P. Howson and H. A. Ja'fer, J Vac Sci Technol A10(4) 1784, 1992.
[83] "Vacuum Arc-Based Processing," David Sanders, Chapter 18 in Handbook of Plasma Processing Technology: Fundamentals, Etching, Deposition and Surface Interactions, edited by Stephen M. Rossnagel, Jerome J. Cuomo and William D. Westwood, Noyes Publications, 1990.
[84] J. Vyskocil, and J. Musil, J Vac Sci Technol A10(4) 1740, 1992.
[85] R. L. Boxman and S. Goldsmith, Surf Coat Technol 44, 1024, 1990.
[86] "TiN Deposition Using a Vacuum Arc Source," Clark Bergman, p115 in Ion Plating and Implantation, edited by Robert F. Hochman, Conference Proceedings American Society for Metals 1986.
[87] P. J. Martin, paper VM-WeM4 at 38th National Symposium of the AVS (1991).
[88] Y. Tanaka, T. M. Gur, M. Kelly and S. B. Hagstrom, J Vac Sci Technol A10(4) 1749, 1992.
[89] H.-D. Steffens, M. Mack, K. Moehwald and K. Reschel, Surf Coat Technol 46, 65, 1991.
[90] W.-D. Munz, F. J. M. Hauser, D. Schulze and B. Buil, Surf Coat Technol 49, 161, 1991.
[91] T. Mori and Y. Namba, J Vac Sci Technol A1(1), 23, 1983.
[92] Pulsed Laser Deposition, G. K. Hubler, guest editor, MRS Bulletin 17(2) February 1992.
[93] A. Kumar, L. Ganapath, P. Chow and J. Narayan, Appl Phys Lett 56(20) 2034, 1990.
[94] F. Davanloo, E. M. Juengerman, D. R. Jander, T. J. Lee and C. B. Collins, J Mater Res 5(11) 2394, 1990.
[95] W. Pompe, H.-J. Scheibe, P. Siemroth, R. Wilberg, D. Schulze and B. Bucken, Thin Solid Films 208, 11, 1992.
[96] J. Machet, P. Saulnier, J. Ezquerra and J. Gulle, Vacuum 33, 279, 1983.
[97] A. Bessaudou, J. Machet and C. Weismantel, Thin Solid Films 149, 225, 1987.
[98] R. L. Sandstrom, W. L. Gallagher, T. R. Dingle, R. H. Koch, R. B. Laibowitz, A. W. Kliensasser, R. J. Gambino, B. Bumble and M. F. Chisolm, Appl Phys Lett 53, 444, 1986.
[99] Handbook of Ion Beam Processing Technology edited by J. J. Cuomo, S. M. Rossnagel and H. R. Kaufman, Noyes Publications 1989.
[100] "Broad-beam Ion Sources," Harold R. Kaufman and Raymond S. Robinson Chapter 7 in Handbook of Plasma Processing Technology: Fundamentals, Etching, Deposition and Surface Interactions, edited by Stephen M. Rossnagel, Jerome J. Cuomo and William D. Westwood, Noyes Publications, 1990
[101] J. M. E. Harper, J. J. Cuomo and H. R. Kaufman, Ann Rev Mater Sci 13, 413, 1983.
[102] D. M. Goebel, Y. Hirooka and T. A. Sketchley, Rev Sci Instrum 56(9), 1717, 1985.
[103] J. R. Morley and H. R. Smith, J Vac Sci Technol 9(6) 1377, 1972.
[104] Y. S. Kuo, R. F. Bunsah and D. Okrent, J Vac Sci Technol A4(3) 397, 1986.
[105] "Hollow cathode etching and deposition" Cris M. Horwitz Chapter 12 in Handbook of Plasma Processing Technology: Fundamentals, Etching, Deposition and Surface Interactions, edited by Stephen M. Rossnagel, Jerome J. Cuomo and William D. Westwood, Noyes Publications, 1990.

[106] D. F. Dawson-Elli, A. R. Lefkow and J. E. Nordman, J Vac Sci Technol A8(3) 1294, 1990.
[107] D. M. Mattox and F. N. Rebarchik, J Electrochem Technol 6, 374, 1968.
[108] D. W. Hoffman and M.R. Gaertner, J Vac Sci Technol 17, 425, 1980.
[109] D. Van Vechten, G. K. Hubler, E. P. Donovan and F. D. Correll, J Vac Sci Technol A8(2), 821, 1990.
[110] G. K. Hubler, D. Van Vechten, E. P. Donovan and F. D. Correll, J Vac Sci Technol A8(2) 831, 1990.
[111] J. A. Thornton, Thin Solid Films 40, 335, 1977.
[112] J. K. G. Panitz, D. M. Mattox and M. J. Carr, J Vac Sci Technol A6(6), 3105, 1988.
[113] J. W. Dini, Plat Surf Finish 72(7) 48, 1985.
[114] U. Kopacz and S. Schulz, 34th Annual Technical Conference Proceedings (Society of Vacuum Coaters) 1991 p. 48.
[115] S. Pongratz and A. Zoller, J Vac Sci Technol A10(4) 1897, 1992.
[116] U.S. Patent 4,851,095 (July 25, 1989).
[117] B. Nevill, Plating and Surface Finishing, January (1993), to be published.

About the Author: *Donald M. Mattox is the Technical Director of the Society of Vacuum Coaters and is a consultant on thin film technology. Before retirement he was the Supervisor of the Surface and Interface Technology Division at Sandia National Laboratories in Albuquerque, NM.*

Cathodic Arc Evaporation

Richard H. Horsfall and Raymond P. Fontana

Multi-Arc Scientific Coatings
200 Roundhill Drive
Rockaway, NJ 07866
Phone: (201) 625-3400
Fax: (201) 625-2244

Cathodic arc evaporation is a relatively new commercial coating process for industrial coating applications. This paper compares this process and points out some of the advantages compared to other physical vapor deposition techniques. It also discusses the interrelationship between coating properties and application requirements. Included are discussions on major markets where cathodic arc evaporation has found wide success as well as discussions on emerging opportunities for new coatings and applications of existing coatings. The paper closes with a brief description of a major new advance in cathodic arc technology.

Key words: arc; arc coating; cathodic arc; PVD; vapor deposition.

1. Introduction

Cathodic arc evaporation is a physical vapor deposition technology (PVD). Among the industrial PVD technologies it is the newest and most flexible in providing well-adhered thin film coatings on a wide array of materials. In 1979, Multi-Arc acquired the free world rights to the Sablev patent and access to the Snaper patent. Both of these patents are core patents to the arc PVD process. Multi-Arc's contribution has been to commercialize these patents into an effective PVD process. In 1992, Multi-Arc and other companies using arc evaporation machines provided coatings on tools and parts with an estimated coating value of $100 Million annually.

To understand the potential of cathodic arc technology, it is helpful to review the features of this process and compare these features to electron beam evaporation (e-beam) and magnetron sputtering technologies—both PVD processes. Table 1 and figures 36–38 provide this comparison. The two major features of conventional arc technology are its ability to generate highly charged metal ions in the range of 1.7 eV with 80% metal ionization (Ti), and to do so from a solid quickly to a vapor state without secondary plasma enhancement devices. This latter feature allows for very practical commercial chamber designs and simplified fixturing of substrates to be coated.

The above two basic features of cathodic arc technology produce extremely well-adhered coatings with intermixing of metal ions with the substrate [1,2]. An almost infinite number of metals and alloys can be evaporated with this technology. Due to the high ionic energy generated in combination with negative biasing of substrates, low temperature deposition is possible and practical. Cathodic arc deposition, therefore, expands the range of materials that can take advantage of thin film coatings. Cathodic arc produces coatings that are adherent and that can be deposited at various thicknesses to meet a particular application requirement.

Table 2 and figure 39 provide information that lists and compares the suitability of various PVD techniques for producing a variety of simple and complex coatings.

Table 1. Comparison of PVD process parameters

Criteria and Coating Parameters	Type of Source		
	Anodic	Cathodic	
	Low Voltage Electron Beam Source	Magnetron Source	Arc Source
State of source material	Liquid	Solid	Solid
Type of source materials	Metals	Metals, alloys compounds (insulators)	Metals, alloys (compounds)
Direction of material flux	Upward	Universal	Universal
Composition of material flux	Atoms, ions	Atoms, ions	Ions, atoms clusters (droplets)
Working gas pressure (mbar)	–	$(7–50)\times10^{-3}$ (Ar)	–
Reaction gas pressure (mbar)	5×10^{-3} (N_2)	$(2–10)\times10^{-4}$ (N_2)	$(5–500)\times10^{-4}$ (N_2)
Source voltage (V)	70–100	300–800	10–40
Source current (A)	140	< 10	40–400
Mean particle energy (eV)	< 50	10–40	50–150
Degree of ionization (%)	10–50	< 20	50–80
Substrate voltage (V)	100	100–2000	50–1000
Substrate current density (mA cm^{-2})	< 5	2–6	< 7.5

2. Using Cathodic Arc Deposition

It is important for the user of this technology, whether it be for a purchase of a cathodic arc coating system or for using a coating service, to understand how the process of preparing a part or tool for coating is as important as the parameters selected to coat it. Whereas chemical vapor deposition accomplishes its final cleaning step at 1000 °C with hydrogen as the final reducing agent, cathodic arc (in common with other PVD processes) relies more on understanding how a part or tool is actually manufactured, so that adjustments can be made to the cleaning and conditioning process prior to coating. Since cathodic arc produces very high ionization rates and higher energy levels of

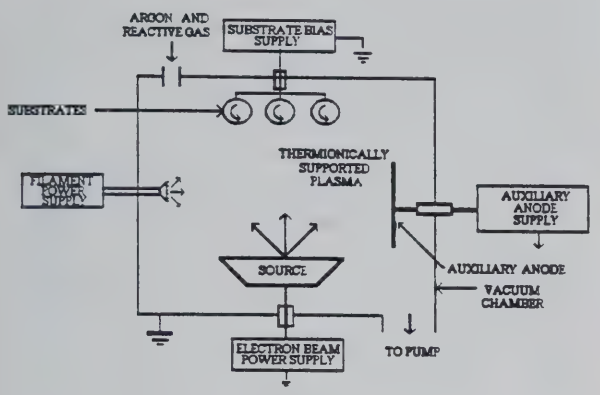

Figure 36. Schematic of components in a thermionically-enhanced triode ion plating system.

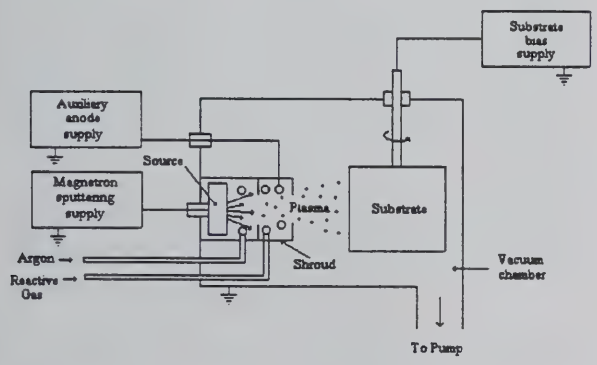

Figure 37. Schematic of components in a magnetron sputtering system.

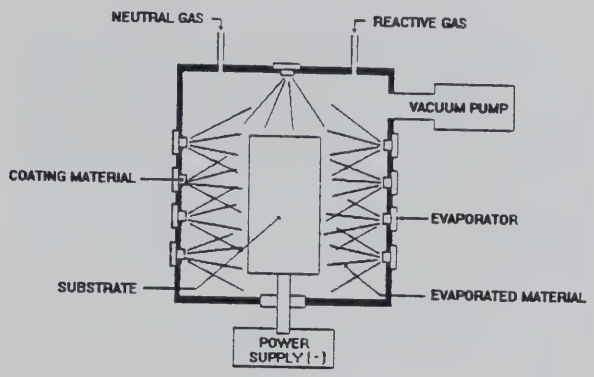

Figure 38. Schematic of components in a vacuum arc system.

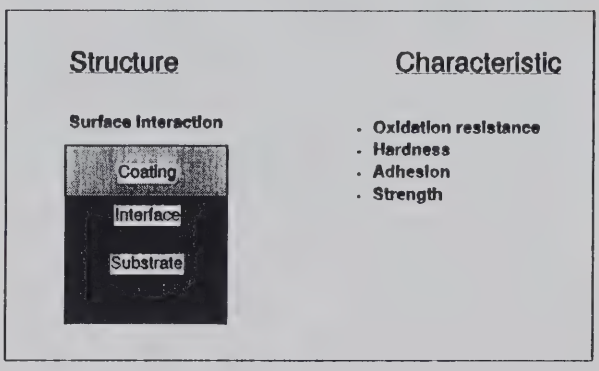

Figure 39. Important properties of the coating/substrate system for wear resistance applications.

Table 2. Suitability of various PVD coating techniques for the evaporation of advanced films

Type of Coating	Type of Structure	Ion Plating Sources: Anodic E-Beam	Cathodic Arc	Cathodic Sputtering
	Multicomponent	•	•	•
MG1G2	Multilayer	•	•	•
	Graded-layer	•	•	•
	Multicomponent	•+	•	•
M1M2G	Multilayer	•+	•+	•+
	Graded-layer	•+	•	•+

Mi: Metal
Gi: Metalloid
• Possible with single source
•+ Need multiple sources

the metallic atoms (as opposed to mostly ionic gas atoms in electron beam and sputtering), a wide range of substrates can be successfully coated at temperatures of 350 °F to 1000 °F. To utilize this coating at low coating temperatures, a good understanding of the manufacturing process of the part or tool to be coated is needed.

Almost all commercial cathodic arc deposition systems utilize multiple arc sources. Understanding the critical areas to be coated as well as the geometry of the parts are important in determining cathode placement and utilization in a chamber and/or the fixturing to be used. Fixtures can be as simple as a rotary table in vertical or horizontal orientation, or more complex double and/or triple planetary rotation devices. Since Multi-Arc's multiple cathodic arc sources can be individually controlled (manual or automatic), plasma density profiles can also be maintained that ensure consistent part-to-part uniformity within a load, as well as load-to-load uniformity.

The cathodic arc process differs substantially from electron beam and magnetron sputtering through its ability to produce high ratios of ionized metal species compared to neutrals. This high ratio not only affects film growth and its deposition rate but also serves two other useful purposes.

Firstly, ion bombardment of the substrate can be accomplished with metallic ions, which in combination with high substrate negative voltages (approaching -1000 to -1500 V) bombards the parts/tools with sufficient energy to sub-atomically clean them prior to the coating cycle. This technical advantage promotes superior adhesion.

Secondly, as reported by Munz, et al., STEM analysis demonstrates that in the instance of titanium ion bombardment, Ti ions penetrate the steel substrate and a very thin (100 to 200 Å) intermixed layer of an intermetallic compound of Ti-Fe is formed. Such intermixing promotes excellent adhesion and critical shear stress levels [1,2].

By understanding how a part/tool is manufactured and what property a coating is intended to provide—whether it is wear, low friction, or corrosion protection—the cathodic arc system can be tuned to deposit the coating thickness and uniformity required to optimize the part/tool function. Successful coating applications have coating thicknesses ranging from 0.5 μm to as high as 15 μm of titanium nitride (TiN). Different properties of various coatings influence practical coating thicknesses. For example, titanium carbonitride (TiCN) coatings tend to be very thin (1 to 2 μm), whereas titanium aluminum nitride (TiAlN) can be relatively thick (5 to 12 μm). Among the binary coatings, chromium nitride (CrN) can be deposited successfully to over 20 μm. In the case of CrN deposited via cathodic arc, this is due to lower stresses in the coating compared to TiN.

In the early 1980's, cathodic arc was criticized for the inclusion of macro droplets in its thin films. Although arc coatings have more macros than other types of PVD coatings, they have not had any significant performance debit in the fields of metal cutting, metal forming, plastic molding and medical products. In some sliding wear applications, macros have been shown to be beneficial by providing wear debris (TiO_2) which improves lubricity; thus, improving wear resistance [3]. Since the early 1980's, continued research work and improvement in ancillary production support systems has led to a better understanding of the mechanics controlling the evaporation process. This has resulted in reduction of the quantity and size of macro droplets in cathodic arc coatings. This in turn has led to the expansion of viable applications for cathodic arc technology. Cathodic arc can now compete in decorative applications with good cosmetics and in wear components where sliding wear and/or corrosion resistance properties in coatings are required.

Multi-Arc uses, depending upon the coating applications, one or a combination of various substrate conditioning techniques. Metallic ion bombardment, poison cathode bombardment, glow discharge and radiant heating are all used to maximize adhesion and reduce droplets. The latter three techniques improve visual coating appearance and control droplet formation when necessary.

At the 1991 International Conference on Metallurgical Coatings, Multi-Arc introduced the enhanced arc, which promises to expand cathodic arc technology into such fields as optics, the development of diamond-like coatings (DLC) and diamond coatings [4,5]. Enhanced arc technology promises high adhesion levels, dense coatings, little or no droplets in the film and high production coating rates.

3. Equipment Design

Typical equipment costs can range from a purchase of a conventional cathodic arc source, including power supply and electronic controls, for $15,000 to a three meter system, complete with cleaning line, for over $1,700,000. Prices have been quoted for an in-line, load lock system of $2,500,000 not including the cleaning system. The ability to place individual arc sources almost anywhere in a chamber means that the building of unique turnkey systems is practical.

The vast majority of cathodic arc systems built for service or in-house customer use are units that have outside chamber dimensions of 33 in × 33 in ×

44 in high. A typical coating zone is 20 in in diameter by 26 in high. Figure 40 shows a typical footprint. Chambers have been built for R&D purposes as well as special applications. Multi-Arc has built 2 and 3.5 meter machines to coat printing rolls and broaches.

These chambers are in most cases front door loading with full access to the interior chamber. Many of the other features are standard options. For example, operating controls can be manual and/or computer controlled. Fixturing is dictated by the type of work and uniformity requirements. Likewise, pre-conditioning options are available depending on the application and performance requirements.

One of the important areas in arc technology, particularly in how it relates to equipment design, has been the design of the cathode apparatus (arc source) itself. Multi-Arc has continued to evaluate cathode designs for a number of years. There are several designs in use worldwide—circular, rectangular, random and steered arc sources.

The majority of systems use circular arc sources that range in size from 2.25 in to 3 in in diameter. Also, most systems use the "random" arc. The descriptive word, "random" is actually a misnomer. All "random" systems use permanent magnets that are placed behind the circular cathodes to "control" the arc. The proper placement of these magnets sets up magnetic force fields which keep the arc on the source (or cathode) face and also assure even erosion of the source material. The use of small arc sources in combination with properly sized and placed permanent magnets assures even erosion.

The development of the "steered" arc is an attempt to control macro particle size and narrow the bell curve distribution of macros compared to "random" arc sources. This is accomplished by attaching movable electromagnets behind the cathode face. The electromagnet field steers the arc around the face forcing the arc spot to move from one location to the next.

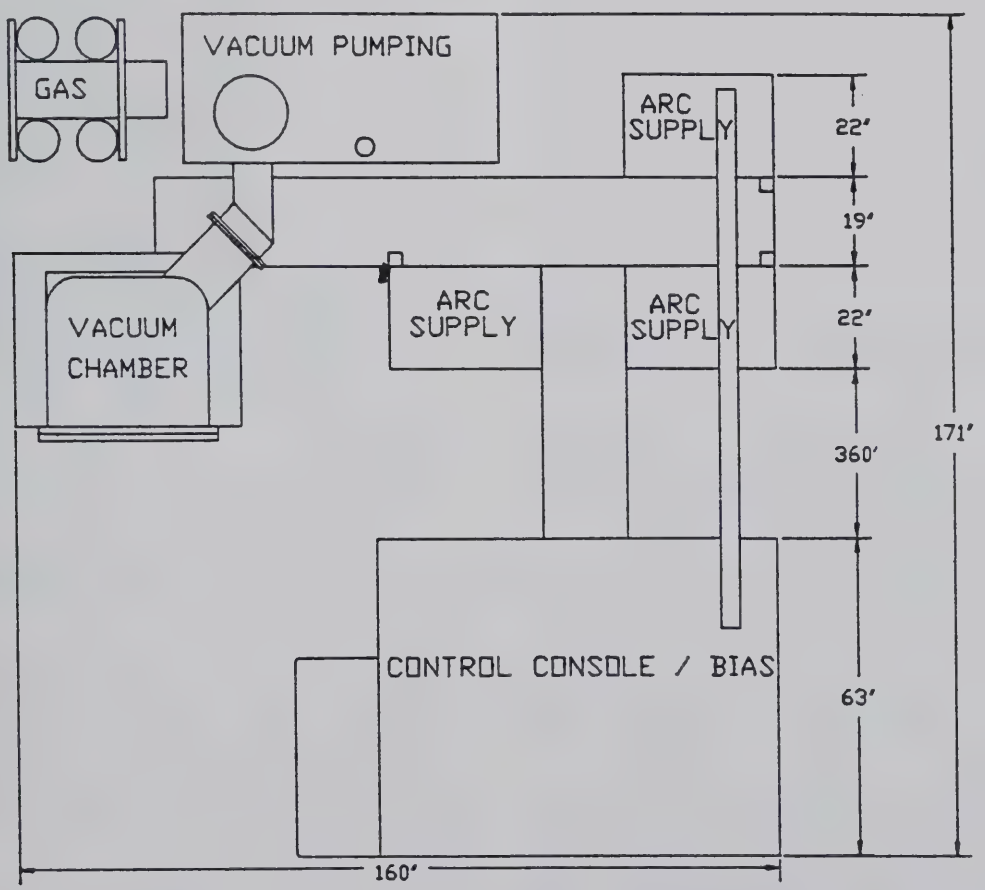

Figure 40. Footprint of a Multi-Arc 334 System, not including cleaning line.

The "steered" arc has produced smoother coatings compared to "random" arc but from a commercial point of view has not proven an attractive alternative for several reasons. To retrofit a commercial coating machine with separate electromagnetic motors is quite expensive, and it is cumbersome to maintain. The improvement of performance of these coatings is not significantly measurable in such markets as cutting and forming tools. Finally, most macros are produced in the conditioning or heat-up phase with the random arc. A number of practical methods exist to reduce droplets using alternative heat-up methods with the random arc which are more commercially practical, less expensive and easier to operate and maintain.

Over the last 10 years a number of machines have incorporated large rectangular cathode designs. Large cathode designs have had problems. The most common has been lack of even cathode erosion, leading to short cathode life and greater non-uniformity of coating distribution. This has occurred due to the inability of the arc to move evenly over the larger surface area of the cathode. Source to substrate variations inherent when fixturing commercial size cycles of cutting tools also cause the arc to preferentially operate on the cathode surface. This leads to poor erosion profiles and inefficient material utilization. With large cathodes the macro problem is more difficult to control but can be reduced through alternative means of substrate heating and conditioning.

Please refer to the discussion of the enhanced arc as a future improvement in cathode design, deposition and the elimination or near elimination of macros depending on the material to be evaporated.

Cathodic arc equipment has been well accepted worldwide. There are over 50 coating service centers around the world. Turnkey systems have been sold to over 50 in-house users worldwide.

Specific applications where cathodic arc PVD has found wide acceptance are:

- Original equipment high speed steel cutting tool manufacturers
- Original equipment carbide cutting tool manufacturers
- Fabricators of cutting tools
- End users of cutting tools, first time coats and recoats
- Press tooling, such as progressive dies, cut off/blank/trim/flange steels and draw dies
- Aluminum can tooling, body end and seam tooling
- Plastic injection molds, cores, pins, extrusion screws
- Medical instruments, orthopedic instruments and implants
- Anilox and gravure rolls
- Decorative applications including rings, sports equipment, pens and hardware
- Wear components for the oil and gas industry, and the automotive and aerospace industries
- Semiconductor molds.

4. Cathodic Arc Coatings and Applications

Cathodic arc technology is capable of producing a very wide variety of coatings. Presently binary coatings such as TiN, ZrN, and CrN are commonly available. Ternary coatings such as TiAlN, TiCN, and TiZrN are being used today in increasingly sophisticated applications. These ternary coatings are extremely flexible. By understanding how the cathodic arc process can affect the coating composition on the substrate, these coatings can be optimized for a specific use. It is important to review microstructure and mechanical characteristics of cathodic arc coatings when selecting a coating for a specific use.

In general, cathodic arc coatings have small grain, dense structures, and although they possess high residual compressive stresses they are less stressed than electron beam PVD coatings. Arc coatings have more macrodroplets affecting stress, but due to the high energy of the arc technique they have finer grain structures. Arc coating crystallography shows a preferential {111} orientation. Again, the film-substrate interface is improved through the energetic ion bombardment, causing in some cases a mixing at the interface, depending on the metals being evaporated and deposited.

The above characteristics help define the coating and influence various cathodic arc coatings by affecting residual stress, which influences hardness, adhesion and hot hardness. It is valuable to understand these factors when determining the suitability of cathodic arc for various applications. See figures 41–44 for hardness, critical load, coefficient of friction and hot oxidation values for arc deposited coatings.

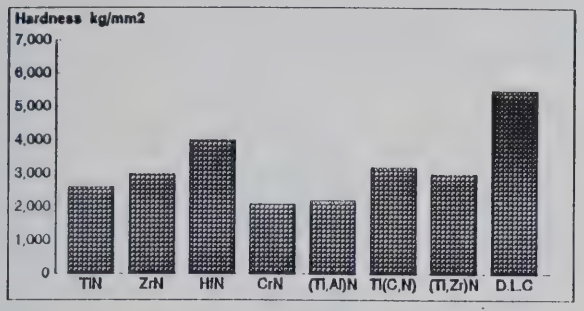

Figure 41. Microhardness of PVD arc coatings at room temperature.

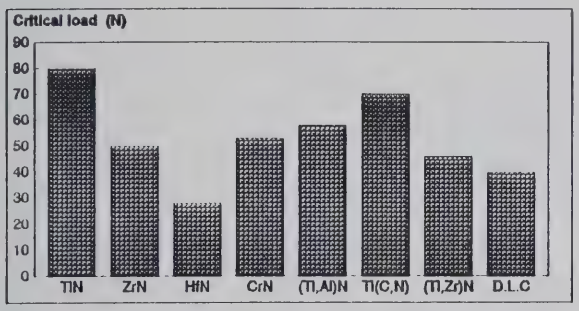

Figure 42. Critical load comparison of PVD arc coatings deposited on HSS substrate.

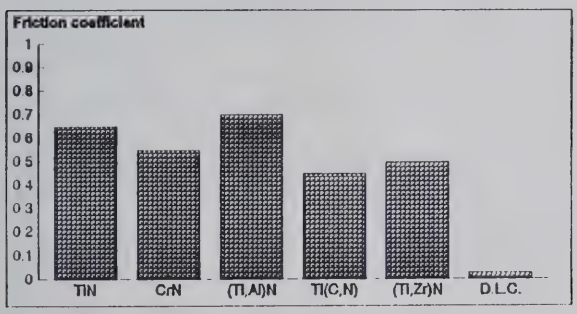

Figure 43. Friction coefficient of PVD arc coatings (100C6 ball against uncoated HSS disc).

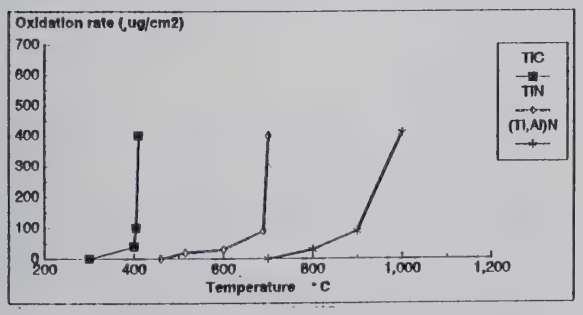

Figure 44. Hot oxidation comparison of PVD TiC, TiN, (Ti,Al)N, and CrN coatings.

4.1 Cutting Tools

In the mid-1980's the cutting tool market (or more specifically the high speed steel cutting tool market) provided the base volume to permit this technology to be developed for other applications. As this market has become more knowledgeable about thin film coatings, cathodic arc technology has become more widely used. PVD arc coatings are now being routinely used on round shank carbide tools and inserts. PVD arc coatings are replacing CVD coatings used on cut-off, threading and grooving carbide inserts. See Table 3 for a comparison of coatings vs. material to be machined.

Table 3. Coatings selection as a function of machined material for round shank cutting tools and indexable insert applications

	TiN	Ti(C,N)	(Ti,Al)N
Alloyed steel	***	***	***
Stainless steel	***		***
Nickel based alloy			***
Titanium and titanium alloy			***
Cast material		***	***
Non ferrous materials (Al, Brass, Copper)			

Asterisk–good application, Shaded–poor.

The cathodic arc's high ionization rates, which produce superior adhesion and highly compressive coatings with remarkably good ductility, allow coatings to be deposited with greater thicknesses compared to other PVD techniques. The flexibility of this technique allows for multi-layer designs and the deposition of coatings with high oxidation resistance and hot hardness. These characteristics will continue to allow for the development of PVD coatings that can compete with CVD.

Cathodic arc TiAlN is now being used to cut hard-to-machine materials such as aerospace alloys and cast iron. The physics of the cathodic arc makes evaporation of alloyed cathodes very practical. The evaporation, transportation, and deposition of metallic ions from alloyed cathodes, and a coating's final composition (such as TiAlN) can be closely controlled via the cathodic arc. Table 4 shows examples of application successes.

The recoating of expensive resharpenable cutting tools has become a widely used process within the metal removal industry. Maximum tool life with its productivity gains through recoating is now commonplace. Cathodic arc's high energies allow (along with specialized know how) successive coatings to be deposited on older coatings without

Table 4. Cutting tool application successes

Coating: TiN Tool	Material cut	Uncoated	Coated
Broach	Waspalloy	63 pcs.	126 pcs.
Dovetail	C-1117/C-1144	800 pcs.	2,400 pcs.
Keyway cutter	8620	1,000 pcs.	2,000 pcs.
Slitting saw	Copper	1,200 pcs.	12,000 pcs.
Cut off blades	Cold rolled steel	5,000 pcs.	40,000 pcs.
Milling cutters	8620	70 pcs.	160 pcs.
Gun drills	Chrome moly	70 pcs.	323 pcs.
Circular saw	1018 blade	3/Shift	1 blade every 5 shifts
Coating: TiAlN Tool	**Material cut**	**Uncoated**	**Coated**
HSS Co end mills	Titanium 6A1-4V	4 hrs.	8 hrs.
Cobalt drills	Titanium 6A1-4V	1.5 holes	5 holes
HSS end mills	Inconel	TiCN 6.5"*	8.0"*
Taper length drills	17-4 PH	TiN 10 pcs.	25 pcs.
Carbide milling Inserts	Cast iron	800 pcs.	3,400 pcs.
Carbide dovetails	52100	TiN 1,100 pcs.	2,400 pcs.
Carbide end mills	Titanium 6A1-4V	500 pcs.	4,400 pcs.
Carbide end mills	Waspalloy	TiN-15"*	30"*

* Material removed

creating distinct layers. The high mobility of the ions and their high kinetic energy produce a continuous layer of original and new coating. Original tool performance is restored. Table 5 illustrates a recoated tool/part's return on investment.

4.2 Press Tooling

Cathodic arc coatings have produced outstanding economic returns to their users in metal fabrication. This technology is unique in its ability to deposit adherent coatings at temperatures as low as 350 °F, and has expanded the use of coatings to virtually all commonly used tool and die steels. Most tool and die steels are tempered between 350 °F to 600 °F, compared to cutting tools where the substrates are either carbide or high speed steels with 1000 °F tempering ranges. To maintain hardness and support for the coating, the coating process must have enough energy to impart good mechanical bonding without affecting the hardness of the alloyed steel. Table 6 provides typical examples of application successes in press tooling.

New developments of coatings via cathodic arc are expanding the use of coatings in medium hot forging. The hot hardness of TiAlN is providing life extension in hot heading applications. Here the hot hardness and the elevated oxidation resistance of the coating is reducing abrasive wear and retarding the oxygen reaction with the coating. In the last example in Table 6, the poor thermal conductivity of this coating protects the ion nitride layer which is supporting the TiAlN film. The excellent ductility of the cathodic arc TiAlN coating enables this coating to be applied when necessary in thicknesses in excess of 10 μm for heavy impact applications. Figure 45 compares wear of uncoated, TiN coated, and TiAlN coated tools in punching silicon steel sheet.

CrN coatings in thicknesses of 15 to 30 μm are practical using the cathodic arc technique. This capability, in addition to its favorable resistance to hot air oxidation, has opened new application opportunities. These areas include:

- Hot forging
- Draw dies
- Replacing electroplated chrome in some sliding wear applications
- Replacing electroplated chrome in some corrosion applications.

CrN arc deposited films exhibit relatively low internal stresses, have excellent coefficient of friction characteristics, and have good corrosion resistance. The micro-porosity existing in all PVD coatings

Table 5. Return on investment using recoating

Tool		Machine	
Tool material		RPM	
Dimension		Feed	
Tool mfgr	$439.00	* Cycle time (minutes)	1.450
* Tool cost (coated)	$35.00	* Tool setup time (minutes)	10.00
* Cost to recoat	0.2550	* Operator cost/hr.	$35.00
* Max grind stock	$9.90	* Pieces/grind	378
* Cost to regrind		* Pieces/grind (recoat)	1134
Part name		* Total shrpngs	15
Part number		* Total shrpngs (recoat)	15
Workpiece material		* Wear/shrpng	0.0170
Workpiece hardness		* Wear/shrpng (recoat)	0.0170
* Pieces/year	4720000	Coolant	

* This information is required.

		Uncoated	Coated
Tool savings	Pieces/grind	378.0000	1134.0000
	Average wear	0.0170	0.0170
	Available changes	15.0000	15.0000
	Actual changes	15.0000	15.0000
	Pieces/tool	6048.0000	18144.0000
	Recoat cost	N/A	525.0000
	New tool cost	439.0000	439.0000
	Tool cost/PC	0.0726	0.0531
	Savings/PC		0.0195
	Annual savings		$91,830
Grinding savings	Tools per year	780.4233	260.1411
	Grinds per year	12486.7725	4162.2575
	Cost per grind	9.9000	9.9000
	Grind/cost piece	0.0262	0.0087
	Savings/PC		0.0175
	Annual savings		$82,413
			0.4167
Direct labor savings	Operator cost/min	0.4167	
	Annual set up time	124867.7249	41622.5750
	Annual cycle time	**********	*********
	D/L per piece	0.0412	0.0339
	Savings/PC		0.0073
	Annual savings		$34,685
Total cost/piece	.....	$0.1400	$0.0957
Annual totals	Increased production	1.22%	57,410 pcs
	Tool cost savings		$91,830
	Grinding cost savings		$82,413
	Direct labor savings		$34,685
	Annual tool savings		$228,404
	Total annual savings		$437,332

makes thick CrN coatings attractive for applications where sliding wear and corrosion are both failure mechanisms.

4.3 Medical Applications

Cathodic arc has also expanded the use of coatings within the medical industry. Table 7 lists the types of tools being coated with arc deposited TiN. The Food and Drug Administration (FDA) approves TiN by individual application, and not the coating per se.

Many surgical tools utilize a 400 series stainless steel which has some corrosion resistance, but is used in preference to 300 series stainless steel because it provides a sharper cutting edge due to its

Table 6. Press tool application success

Coating: TiN Tool	Material	Uncoated	Coated
Profile punch	Copper	330,000 pcs.	1,400,000 pcs.
Cold forming punch	1018	30,000 pcs.	300,000 pcs.
Punch	17-4 stainless	20,000 pcs.	250,000 pcs.
Draw ring	1018	350 pcs.	180,000 pcs.
Extrusion punch	1018	1,000 pcs.	15,000 pcs.
Flange die	Cold rolled steel	50,000 pcs.	480,000 pcs.
Blank die	Hot rolled steel	55,000 pcs.	300,000 pcs.
Seaming roll	Tin plated steel	10,000,000 pcs.	45,000,000 pcs.
Beading roll	TFS with lacquer	Polish 4×/shift	1×/3 shifts
Deep draw	Aluminum	10,000 pcs.	130,000 pcs.
Score knife	Aluminum	2–15 days	4–30 days
Pre-curl	Aluminum	3 months	12 months
Hot heading	1040	50,000 pcs.*	150,000 pcs.**

* H13 ion nitrided with TiN.
** H13 ion nitrided with TiAlN.

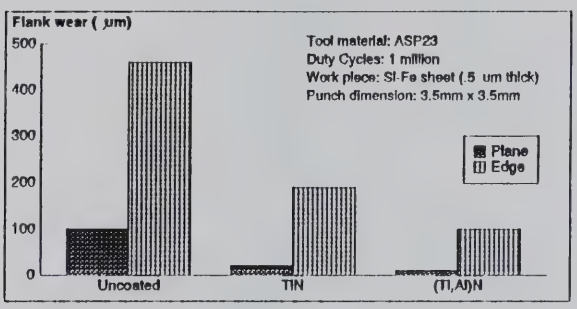

Figure 45. Flank wear of coated punches for stamping applications in Si-Fe sheet. Influence of the coating as a function of the wear location.

Table 7. Types of tools coated via Arc TiN in the medical industry

Surgical Instruments	Orthopedic implants
Aspirator tips	• Hips
Broaches	Acetabular cups
Curettes	Femoral heads
Drills	Stems
Drill guides	• Knees
Driver heads	Femoral component
Forceps	Patella plates
Knives/scalpels	Tibial platforms
Osteotomes	• Trauma
Planers	Plates
Rasps	Rods
Reamers	Screws
Rongeurs	
Scissors	

higher hardness. The high ionic energy of the cathodic arc allows for the low temperature coating of 400 series steel without affecting the hardness of the substrate. The low temperature of the arc process also maintains the anti-corrosive properties of the 400 series stainless. The cathodic arc process also coats well on passivated stainless steels.

Table 8 provides a case history of how cathodic arc TiN coating improves cutting conditions in bone-simulated material (note temperature reduction).

Various medical research studies illustrate how the microstructure and mechanical properties of cathodic arc TiN make it a suitable choice for an implant coating. See Table 9 for referenced studies.

4.4 Decorative

Color matching, along with good adhesion, and wear and corrosion resistance, is a prerequisite for significant portions of this market. Cathodic arc's capability of evaporating alloyed material, along with gas mixing, and coupled with low temperature deposition makes arc technology an attractive coating technique in this market. The preferred method for depositing attractive "life time" thin films on class and champion series rings has been cathodic arc. Improvements in techniques to reduce droplet emission has resulted in higher reflectance coatings which, with high ionic energy, has enabled low temperature substrates to be successfully coated.

Table 8. Medical reamer performance

Reamer Cutting Performance

Reamer size (mm)	TiN coated	Uncoated
12 mm	13 sec.	20 sec.
13 mm	11 sec.	25 sec.
14 mm	9 sec.	22 sec.
15 mm	10 sec.	21 sec.
16 mm	10 sec.	20 sec.

Note: Seconds (avg. to ream 1.4" deep hole. 1 mm depth of cut.

Tip Temperature—14 mm Reamers

Hole #	TiN coated	Uncoated
1	114.9 °F	168.8 °F
2	131.1 °F	184.4 °F
3	146.6 °F	190.9 °F
4	153.6 °F	189.5 °F
5	154.2 °F	194.9 °F

Note: 5 holes reamed consecutively.

Conclusions:

1. Titanium Nitride (TiN) coatings improve the ease of cutting and cutting speed of intramedullary reamers.
2. Material removal rates are up to 127% higher with TiN.
3. TiN coated reamers cut more cooly and exhibit better chip flow than uncoated reamers.
4. Edge rounding at the reamer tip is substantially reduced with TiN.

Table 9. TiN reference studies in medical industry

1. Coll et al.: Surface Coating Technology, 1988, 36 (3–4), 867–878.
2. Pappas, et al.: Comparison of Wear of UHMWPE Cups Articulating with Co-Cr and TiN Coated Femoral Heads; Transactions of the Society for Biomaterials, Vol. XIII, May 1990.
3. Streicher et al.: New Surface Modification for Ti-6Al-7Nb Alloy: Oxygen Diffusion Hardening (ODH); Biomaterials 1991, Vol. 12, March.
4. Davidson et al.: Friction, Abrasion, Resistance, and Attachment Strength of Various Modified Implant Bearing Surfaces; Combined Meeting of the ORS of USA, Japan & Canada, October 1991.
5. Davidson et al.: Surface Modification Issues for Orthopaedic Implant Bearing Surfaces; Advanced Materials & Manufacturing Processes, March 1992.
6. Brown et al.: Effects of Different Surface Treatments of Fretting Corrosion of Ti6Al14V; 38th Annual Meeting of the ORS, Vol. 17, Section 1, February 1992.

Two well-known watch makers are using cathodic arc technology to coat watch bezels. One is coating over a stainless steel bezel while the other is depositing onto specially prepared zinc die cast bezels. A thin layer of gold is sputtered over the arc deposited film. This combined technology has created a new market opportunity by saving gold, and providing a "life time" matched (to the gold) hard coating.

The above examples illustrate the merging of two technologies to serve a market need. The manufacturer can now provide a "pollution free" wear resistant coating by using cathodic arc's high ionic plasmas to apply low temperature well-adhered PVD coatings.

Cathodic arc has also demonstrated capability in providing a wear and corrosion resistant decorative coating for hardware fixtures and automotive exterior components. In this latter case, the cathodic arc has been successful in coating over metallized plastics. The benign, non polluting nature of the cathodic arc process, coupled with flexible chamber design and high deposition rates, has opened new opportunities in this decorative market niche.

4.5 Wear Components

The opportunities in this field are virtually limitless. End users are becoming more knowledgeable concerning potential collateral applications within their companies. Second, EPA regulations concerning waste disposal sites and compliance costs are causing companies to explore all surface treatment technologies.

Cathodic arc technology is particularly well suited. Cathodic arc coatings are already solving sliding wear and galling failures in automotive and aerospace applications. Many customers can retain their lower cost substrates via the arc technique. Work is also progressing with thicker coatings of CrN to replace thin coatings of electroplated hard chrome. CrN via arc deposition has the added feature of having no cracks, which are often found in hard chrome. Arc-deposited CrN has hardness values in 1700–1800 Vickers range, compared to 800–1000 Vickers for hard chrome. With arc CrN in compressive stress, crack free and possessing superior adhesion, chrome nitride via cathodic arc is a very plausible replacement for hard chrome. See Table 10, comparing coatings and the relative mechanisms of wear.

Table 10. Coating behavior as a function of the various mechanisms of wear

Mechanisms of wear	TiC	Ti(C,N)	TiN	(Ti,Al)N
Diffusion	••	••	•••	••••
Adhesion	••	••	••••	•••
Abrasion	••	•••	••	•••
Oxidation	•	••	•••	••••

• poor / •• medium / ••• good / •••• excellent.

5. New Technical Developments

5.1 Enhanced Arc

This latest advance in cathodic arc technology opens up new opportunities for potential users. This major step forward shows promise in developing diamond-like coatings (DLC) and diamond coatings for the cutting tool, medical and wear component industries. This development also produces coatings that eliminate, or virtually eliminate, macros in the coating. Now the advantages of arc technology, such as superior adhesion, can be used in applications that require "defect free" thin films. The following is a brief description of this technology.

The enhanced arc, as developed by Multi-Arc Scientific Coatings, uses a magnetic solenoid which is placed in line along the same axis as the cathode. In this way, the metal ions, electrons and other plasma species which are generated at the cathode surface are forced to pass axially through the center of the magnetic field. A schematic representation of this device is shown in figure 46. Soft magnetically permeable core pieces are used inside the magnetic solenoid to complete a magnetic circuit which can act on the plasma. Depending on the location and configuration of these core pieces within the solenoid, various interesting properties can be imparted to the three main areas which constitute coating. These areas are the generation, transportation, and condensation phases of the deposition process.

In the generation phase the enhanced arc imparts a higher current density on the surface of the cathode. This leads to a higher level of heating of the surface, which aids in causing the arc spot to split into several spots, which further enhance the amount of material generated. These arc spots are more diffuse and move rapidly over the cathode surface, thereby causing the macroparticles which are generated to be much smaller in size.

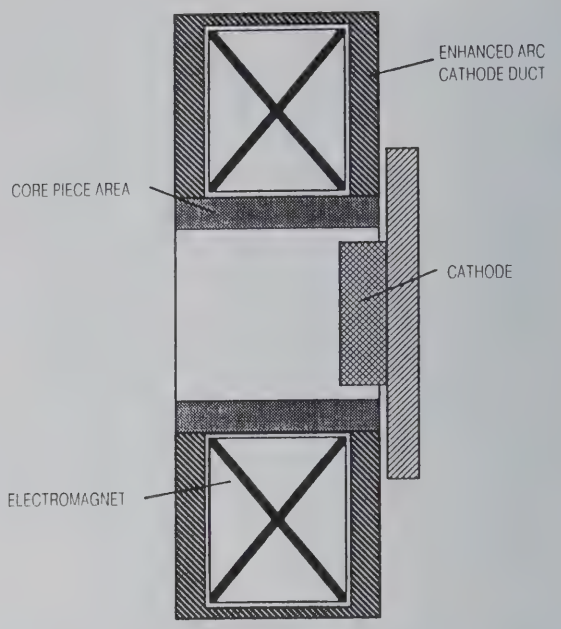

Figure 46. Schematic representation of the Enhanced Arc System.

In the transportation phase, as the plasma material passes through the enhanced arc apparatus higher energy is imparted to the ions which are generated. Conventional arc evaporation imparts an average energy of 1.7 eV to titanium ions which are generated. The enhanced arc raises this to over 2.1 eV for titanium. In addition, the disassociation and ionization of nitrogen takes place in this stage, which does not happen with the conventional process. We theorize that the high electron bombardment of already reduced macros which are generated causes them to become vaporized in this phase of the process. In the conventional arc evaporation process about 75% to 80% of the titanium metal vapor which is generated is ionized. With the enhanced arc system we have shown that there is 100% ionization of the generated metal vapor.

The last and most important phase is the condensation phase. The substrate to be coated is biased by a negative potential. This negative potential provides an additional attractive force to capture the high energy arriving ions. These high energy arriving ions in and of themselves will lead to well-adhered, dense, compacted films. In addition, the bombardment of the film by the ionized gas species which can be generated will further aid in the formation of dense, defect-free films. This can be seen in figure 47.

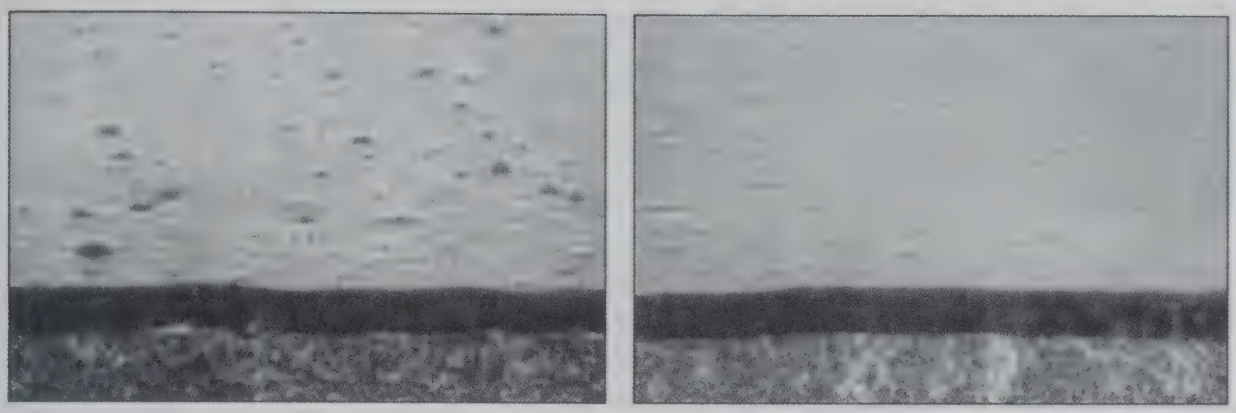

Figure 47. Fracture cross section and surface of a 7 μm TiN coating at 1000×, using (a) conventional arc, (b) enhanced arc.

One of the most significant advantages of the enhanced arc system is its ability to sustain an arc spot on the surface of a graphite cathode. Due to the negative resistivity as a function of temperature for this material, it is extremely difficult to evaporate with the conventional arc process. The enhanced arc system allows for the evaporation of the material. Dense well-adhered DLC films have been evaporated and deposited onto high speed steel substrates. This newest advancement of the arc evaporation technology promises to open up many new areas of application for arc evaporated coatings.

6. Evolution of Arc Technology

The major strengths of arc technology are that it is simple in concept and can be translated into very rugged and reliable equipment. Its ability to highly ionize the metal species allows for superior adhesion of coatings compared to other PVD technologies. Arc evaporation has a wider "coatings window" because good adhesion can be achieved (depending on application requirements) as low as 350 °F, which allows the coating to be applied to a broad range of substrate materials.

As stated earlier, a "good" or "bad" coating is application dependent. It is how the coating performs in the final analysis that counts. A purist would say that macros are undesirable. Concern over macros is application dependent. We have had several applications where they have provided certain advantages.

An area requiring further development is the building of models that can predict coating thickness and uniformity, given the variabilities of part configurations, distances from the substrate, bias voltage, pressure, temperature, etc. Today, educated guesses and trial cycles are run on specific parts/applications to optimize coatings. Mathematical models that could predict actual results would shorten development time. Understanding the physics and interrelationships of the process as related to specific part geometries, surface conditions and spacing of parts is required to develop practical mathematical models.

Arc technology, as can other PVD processes, can benefit from refinements in arc sensing, bias power supplies, fixturing, computer technology, vacuum pumps, etc.; however, our experience points to an educated customer and an educated arc technology supplier in adapting the technology to the application. After this understanding is reached, a determination can be made as to whether the current technology is suitable or can be modified, or whether the current state of development is not adequate to perform in a specific application. Lack of fit could be either technical and/or economic, such as cost per piece not being competitive with an alternative process or manufacturing method.

7. References

[1] G. Hakanson, L. Hultman, J. E. Sundgren, J. E. Greene, and W. D. Munz, Surface and Coatings Technol. **48**, 51–67 (1991).

[2] W. D. Munz, Surface and Coatings Technol. **48**, 81–94 (1991).

[3] S. E. Franklin and J. Beuger, Phillips CFT, "A Comparison of Tribological Behaviors of Several Wear Resistant Coatings," ICMC (1992), San Diego, CA.

[4] P. Sathrum, B. F. Coll, Surface and Coatings Technol. **50**, 103–109 (1992).

[5] B. F. Coll, P. Sathrum, R. Aharonov, M. A. Tamor, Thin Solid Films **209**, 165–173 (1992).

About the authors: *Richard H. (Rick) Horsfall has been involved with hard thin film coatings (CVD and PVD) for almost 10 years. Rick started a coatings service in Dallas, Texas which he later sold to Multi-Arc Scientific Coatings. Mr. Horsfall has remained with Multi-Arc Scientific Coatings where he is Vice President of Sales & Marketing.*

Prior to thin film coatings, Rick has held positions of Vice President of Marketing at Reed Mining Tools, Thomsen Equipment and Division Manager at Cummins Engine Company. This co-author has a BA from Ohio Wesleyan University and an MBA from Ohio State University. He is a member of ASM International and SME.

Raymond P. (Ray) Fontana is the Director of Research & Development for Multi-Arc Scientific Coatings. He holds a BS in Mechanical Engineering and an MS in Management Science from Fairleigh Dickinson University. Mr. Fontana has 18 years of experience in thin film optical and metallic vacuum coatings deposited by sputtering, reactive magnetron sputtering, and cathodic arc evaporation. In addition, he has extensive experience in vacuum technology related to processing and systems design. He is a member of ASM International, SME and SVC.

Chemical Vapor Deposition and Plasma Enhanced Chemical Vapor Deposition

Jack Chin

Consultant
2437 Unicornio Street
Carlsbad, CA 92009
Tel/Fax: (619) 438-2535

The demands for materials with improved mechanical, thermal, optical, electrical, magnetic, and chemical properties have forced the development of technologies such as chemical vapor deposition (CVD) and plasma enhanced chemical vapor deposition (PECVD). These technologies are used not only as surface treatments to improve properties of the base materials but to form materials which are not readily made by other means. An overview of the basic principles behind CVD and PECVD is presented and comparisons are made of the technologies and materials that result from them. These comparisons highlight the similarities and differences of the two technologies. A few CVD and PECVD processes are described and the limitations, advantages, and technical gaps associated with each technique are discussed.

Key words: Chemical vapor deposition; CVD; ECR-PECVD; LPCVD; PACVD; plasma enhanced chemical vapor deposition; PECVD; RF-PECVD; vapor deposition.

1. Introduction

Readers of this book are already aware that many vapor deposition processes are available to form the same materials. This chapter does not present a comprehensive review of CVD and PECVD developments. Its purpose is to provide basic information about each of these vapor deposition processes that will allow readers to recognize where technology gaps exist which could be appropriately addressed by the capabilities and objectives of their organizations.

Electrodeposition, vapor deposition, sol gel, solution, and melting processes are all methods for forming materials from their basic building blocks of atoms, ions, and molecules. Vapor deposition includes any process in which materials put into a vapor form, by some condensation, chemical reaction, or conversion step, are made to form a solid material. These processes are used to form coatings to alter the mechanical, electrical, thermal, optical, corrosion resistance, and wear properties of the substrates upon which they are deposited. They are also used to form free-standing bodies, films, and fibers and to infiltrate fabric to form composite materials. Vapor deposition provides methods of preparing materials which may be fabricated by other techniques but because of needed properties or economic considerations are best produced by vapor deposition processes. An example is the miniaturization of electronic circuits. Alternate processes for forming the complex circuits of computer chips have not developed. Without vapor deposition techniques to form materials with controlled microstructures and chemistry, progress in this and related technologies would have been very difficult.

The term physical vapor deposition (PVD) was used in early experiments in which materials were vaporized and then recondensed to form coatings. Chemical vapor deposition (CVD) was the term used when the chemical composition of the precursor gases differed from that of the deposit. In CVD processes a gas or mixtures of gases are fed into a deposition chamber where the material is to be deposited. To make the process work, energy is

supplied to the gas to decompose it or to convert the stable molecules of the gas to ions, free radicals, or energetic neutrals. This then generates the reactive gas mixture from which the deposits are formed.

The world-wide proliferation of vapor deposition developments made the designations PVD and CVD too limiting. As modifications of these early processes progressed, experimenters began adding clarifying words to describe how the precursor gases were converted into the reactive gas mixtures. Sputtering, ion plating, plasma enhanced chemical vapor deposition (PECVD—sometimes called plasma assisted chemical vapor deposition (PACVD)), low pressure chemical vapor deposition (LPCVD), laser enhanced chemical vapor deposition, active reactive evaporation (ARE), ion beam sputtering, laser evaporation, and electron cyclotron resonance (ECR) enhanced vapor deposition are terms now used to describe modifications of the early PVD and CVD processes. For example, LPCVD processes are those in which the total pressure in the deposition chamber is less than 1 Torr.

1.1 CVD and PECVD Processes

In both CVD and PECVD processes, a reactant gas mixture is allowed to impinge on a substrate upon which a deposit is to be made. The two processes differ in the manner by which the reactants used to make the deposit are formed. In CVD processes gas precursors are heated to form the reactant gas mixture. The molecular fragments, free radicals, and atoms thus formed react with one another in the gas phase and/or on the substrate to form the desired solid. Temperature plays two roles in this process. First, it provides the activation energy for the decomposition of the precursor gases. Second, it (along with pressure and the starting gas composition) determines the chemical makeup of both the reactant gas mixture and deposited solid. The properties of deposits formed by CVD processes are dependent not only upon the process parameters, but also upon the temperature profiles and gas dynamics of the deposition system.

The formation of the reactive gas mixture is more complex in PECVD than in thermal CVD processes. Energy is added to electrons by an electric field in a low temperature plasma. Collisions of these energetic electrons with neutrals produce ions. These ions also gain kinetic energy in the electric field of the plasma. When these ions collide with neutrals, ions, free radicals, molecular fragments, and agglomerated macromolecules can result. Deposits form as a result of the reaction of these energetic species of the plasma with each other or with the substrate. Since the substrate in PECVD processes is heated by the impinging ions, additional heating or cooling of the substrate may be required to optimize the desired properties of the deposit. While the purpose of this heating or cooling is not to form the active gas species, as it does in CVD processes, temperature does influence the composition of the reactive gas in the glow discharge plasma and thus the microstructure and deposit chemistry.

1.2 CVD and PECVD Applications

The first CVD processes were operated at atmospheric pressures in isothermal systems. Deposition of carbon by the thermal decomposition of hydrocarbon gases and the hydrogen reduction of halides to form refractory materials dominated the early CVD developments. Examples of early applications include deposits for semiconductor developments in the electronic industry [1–5], tribology applications [6–14], corrosion protection [15–19], and optical applications [20–21]. Early CVD deposits were also used for refractory materials in the High Temperature Gas Cooled Reactor (HTGR) programs, thermionic reactor experiments, and high temperature composite material development studies. A wider variety of materials are now being deposited by CVD and PECVD processes. A partial list of these materials is shown in Table 1. Formation of materials by CVD or PECVD processes is usually done because specific properties of materials of interest are difficult to obtain by other means. The uniqueness of vapor deposition processes lies in their ability to control the microstructure and/or chemistry of the deposited material. CVD and PECVD processes are used not only for the deposition of coatings but also to form foils, powders, composite materials, free-standing bodies, spherical particles, filaments, and whiskers. Some examples of problems solved using CVD and PECVD are described below.

Carbon foils 200 to 1000 A thick were made for high energy, high intensity negative ion beam neutralization studies. The foils were formed by depositing thin carbon films on soluble substrates by an RF-PECVD process and then selectively dissolving away the substrates [22].

Table 11. Partial list of materials deposited by CVD and PECVD processes

MATERIALS	DEPOSITION PROCESS					
METALS	CVD	LPCVD	RF-PECVD	Remote RF-PECVD	Microwave	ECR-PECVD
Al	X					
Cu	X					
Cr	X					
Fe	X					
Mo	X	X	X			
Nb	X					
Ge		X	X			
Ni	X		X			
Ti	X					
Re	X					
Ru	X					
V	X					
W	X	X				
Zr	X					
Co		X				
NbAl	X					
TiAl	X					
Ta10W	X					
WRe	X					
NbZr	X					
Nb_3Ge	X					
Cr_2Co			X			
Nb_3Sn	X					
Nb_3Ga	X					
CARBON CARBIDES SILICIDES						
Carbon/graphite	X		X		X	X
Diamond-like			X		X	X
Diamond	X		X		X	X
B_4C	X		X			
SiC	X		X		X	
TiC	X		X			
ZrC	X					
TaC	X					
HfC	X					
NbC	X					
W_xC	X					
Cr_3C_2	X	X				
Cr_7C_3	X	X				
C-Si alloys	X		X			
Si	X	X	X	X		X
Nb_3Si	X					
V_3Si	X					
$TiSi_2$	X	X	X			
$MoSi_2$	X	X	X			
WSi_2	X	X	X			
$TaSi_2$	X		X			
Cu_5Si	X					
Ti_5Si_3	X					

Table 11. Partial list of materials deposited by CVD and PECVD processes—Continued

MATERIALS	DEPOSITION PROCESS					
Nitrides Oxides	CVD	LPCVD	RF-PECVD	Remote RF-PECVD	Microwave	ECR-PECVD
BN	X	X	X		X	
Si_3N_4	X	X	X	X	X	X
Si_3N_4-TiN	X					
TiN	X	X	X			
AlN	X	X	X			
ZrN	X					
NbN	X					
HfN	X					
VN	X					
GaN			X			
Al_2O_3	X		X			
SiO_2	X		X	X	X	
MoO_2	X					
TiO_2	X					
ZrO_2	X					
Cr_2O_3	X					
Fe_2O_3			X			
CeO_2	X					
Y_2O_3	X					
SnO_2			X			
RuO_2	X					
GeO_2			X			
Ta_2O_5	X					
SiO_2-GeO_2			X			
$Bi_4Ti_3O_{1.2}$	X					
$YBa_2Cu_3O_{7-x}$	X					
Borides Miscellaneous						
B	X		X			
TiB_2	X					
HfB_2	X					
ZrB_2	X					
NbB_2	X					
TaB_2	X					
MoB	X					
Mo_2B	X					
Mo_2B_5	X					
MoB_2	X					
W_2B_5	X					
GaAs	X		X			X
GeAs	X					
$Ga_{1-x}Al_xAs$	X					
Nb(C,N)	X					
Ti(C,N)	X					
Si(C,N)			X			
$SiON_2$			X	X		
Cr_2CO			X			
CdS			X			
SmS	X					
ZnS	X					
BP	X					
GaP	X			X		
GaP/Si	X					
InGaAsP	X					

Advantage has been taken of the high product purity of CVD processes in the preparation of powders [23–25]. High gas pressures and high concentrations of reactant in the gases favor the formation of powders [26–28] by both CVD and PECVD processes. Both chemical vapor infiltration (CVI) [29–31] and plasma enhanced chemical vapor infiltration (PECVI) [32,33] are being targeted as potential commercial processes to produce high temperature, fiber reinforced composite materials. Most of the advancements have been by CVI processes. Developments in vapor infiltration of composites are dependent on the geometry of the parts to be infiltrated, the chemical compositions of both reinforcement and matrix materials, and the operating environments of the composites. Progress in CVI technologies has been slow. Innovative CVI approaches are needed for the commercialization of high temperature composites to become economically feasible.

An example of a specialized free-standing body formation is the fabrication of emitters for thermionic reactor experiments [34–39]. Tungsten emitters were deposited by the hydrogen reduction of WF_6 on molybdenum substrates in a CVD process. The process parameters were used to restrict the fluorine contents of these emitters to between 5 and 15 ppm. These fluorine levels were found to maximize the mechanical properties of the emitters while maintaining fast neutron damage resistance. A [110] high work function coating of tungsten from the hydrogen reduction of tungsten chloride [40,41] was deposited over the fluoride tungsten to complete the emitter. Emitters were closed end cylinders with up to 12 cm lengths, 3 cm diameters, and 0.5 cm thick walls.

The development of coated nuclear fuel particles is another example of vapor deposition processing solving a problem that would have been difficult to solve by other means. In nuclear reactors the products of fission reactions must be contained and retained in some manner that will permit them to be removed either continuously or periodically when the fuel is spent. In either case it is imperative that fission products do not leak out of the reactor. Fission reactors normally use primary and secondary containment of the fission products to prevent this leakage. In helium cooled, high temperature reactors, this problem was solved by encapsulating UC_2, UO_2, ThO_2, and other nuclear particles in multilayered carbon and silicon carbide coatings as shown in figure 48. The inner coating was made of low density amorphous carbon to provide space for fission products. Two isotropic carbon coatings with silicon carbide sandwiched between them completed the fuel particle coating. The carbon coatings were isotropic for stability in the neutron environment of the reactor. They also were pore free and able to withstand fission product gas pressures of approximately 300 atmospheres that accumulate during the life of the fuel element. The silicon carbide layer retained those fission products which diffuse through carbon. All coatings were applied in a fluidized bed of particles, typically 100–1000 μm diameter, of the nuclear materials [42–45].

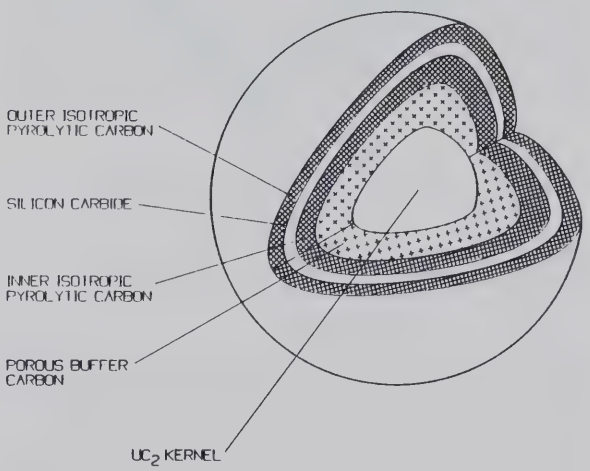

Figure 48. Multilayered carbon and SiC coatings used on General Atomics' UC_2 fuel particles for fission product retention [see refs. 42–44].

Vapor-liquid-solid (VLS) is a catalyzed CVD process that is used for the deposition of filaments and whiskers. Carbon filaments are formed by the catalytic reduction of hydrocarbons in the VLS process [46–48]. Iron or nickel fine powders are typically used as the catalyst for this process. Amorphous carbon preferentially deposits on the catalyst and diffuses into it, forming a low melting carbide. Graphite precipitates on the substrate side of the catalyst, forming the filament as shown in figure 49. Deposition of anisotropic pyrolytic carbon increases filament diameters and the growth ring appearance of filament cross sections. The free energy difference between the deposited amorphous carbon and the precipitated graphite provides the driving force for the continued transport of carbon through the catalyst. Whiskers of silicon carbide are formed by a similar VLS process on substrates peppered with a transition metal catalyst [49].

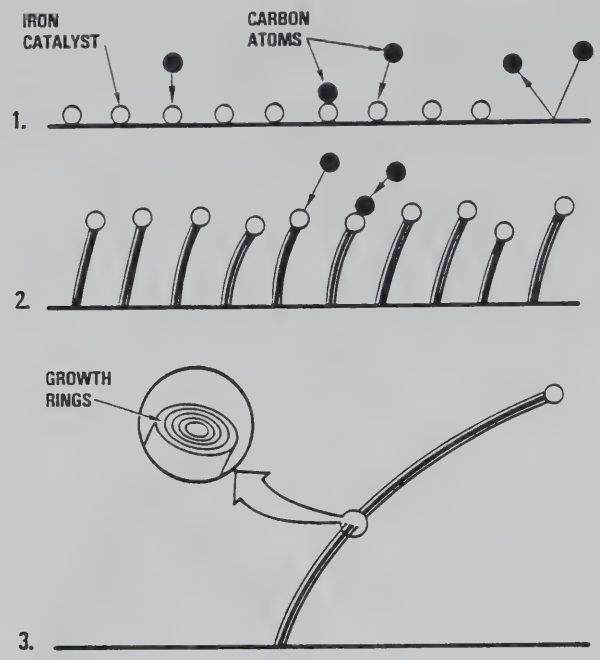

Figure 49. Growth steps for the catalyzed nucleation and growth of carbon filaments by the VLS deposition process.

The CVD processes discussed so far require high temperatures, typically 1100 °C and higher. When attempts were made to lower process temperatures by using more reactive precursors such as hydrides and metal organics, the processes generated poor quality, frequently contaminated, often sooty deposits. Cold-walled reactors provided the first improvements over the early processes.

Cold wall CVD created sharp thermal gradients and reduced gas phase reactions which produce sooting and improved the uniformity of film coverage. Both microstructure and impurity contents were more controllable by cold wall CVD processes. Reducing processing pressures to less than 1 Torr further improved the quality of deposits formed by cold wall CVD processing. This allowed the use of more reactive hydride and metal organic precursors. Epitaxial silicon could then be deposited at 600 °C by LPCVD processes [50] instead of the 1100 °C+ [51–53] temperatures used in early epitaxial silicon depositions.

Process developers began looking at plasma enhanced processes to further reduce deposition temperatures. The first plasmas used were DC and low frequency RF, which allowed epitaxial silicon film formation to occur at temperatures lower than 300 °C [54]. These lower temperature deposits, however, had several drawbacks. It was more difficult to control contamination, microstructure, and as-deposited stresses in these deposits than in the higher temperature CVD processes. Improvements have been, and are being, made by switching to 13.56 MHz and 2.54 GHz plasmas and through the use of remote plasma processes. Remote plasma processes are those in which the substrate is remote from the plasma where the reactive gas mixture is formed [55–57].

These efforts to improve control of the deposition processes are continuing. Work is also being done to apply these newer technologies in the development of high temperature superconducting materials, the vapor deposition of diamond, and the development of functionally gradient materials.

2. Operating Principles in Chemical Vapor Deposition and Plasma Enhanced Chemical Vapor Deposition Processes

2.1 Chemical Vapor Deposition

Conceptually the CVD process is one in which a mixture of gases is forced through tubing into a heated deposition chamber. The heated gas mixture undergoes chemical reactions in the deposition chamber to form a deposit on a strategically located substrate within the chamber. A typical CVD process can be broken down into the following steps:

- formation of the reactive gas mixture,
- mass transport of the reactant gases through a boundary layer to the substrate,
- adsorption of reactants on the substrate,
- reaction of the adsorbents to form the deposit, and
- desorption of the gaseous decomposition products of the deposition process.

The thermodynamics and kinetics of the chemical reactions within the reactive gases and between the reactive gases and adsorbents on the substrate are complex. Equally complex are the flow dynamics which control temperatures, pressures, gas flow rates, and gas compositions at the gas-substrate interface. Abrupt changes in the dimensions of the gas flow from tubing to deposition chamber, thermal gradients in the heated gases, dynamic chemical reactions in the heated gases, and the size and configuration of the exhaust system all contribute to the flow dynamics of the processes. The design of the deposition system and selection of process parameters must be tailored to suit the material

being deposited. This will allow one to control the thermodynamics, kinetics, and transport properties of the process.

2.1.1 CVD Thermodynamic Models A CVD process may be primarily due to the unimolecular decomposition of a precursor gas, as is the case in $C_3H_6 = 3C + 3H_2$ for the deposition of carbon from a hydrocarbon. However, this is not the only reaction that occurs, as thermodynamic examination of the process would show. For example, as figure 50 [58] shows, the continued collisions of the molecular fragments at elevated temperatures allow other possible reactions to occur.

The deposition process may be bimolecular, requiring the decomposition of two compounds and the interaction of products of these decomposition processes to form the deposit. An example is the deposition of Si_3N_4 from the reaction of SiH_4 with NH_3. The desired deposit is formed if thermodynamics favor the deposition process and when the temperature is high enough that the required activation energy for the reaction to occur is exceeded. Whether or not these materials are actually formed depends on the kinetics of the reactions.

The goal of thermodynamic modeling is to determine a window of process parameters which will favor the deposition of the material of interest. For simplicity it is usual to limit the thermodynamic modeling to isothermal, isobaric equilibrium reactions [59–61]. The assumptions are made that if time is not limited, chemical equilibrium will be achieved and can be estimated from thermodynamic calculations. Thermodynamic calculations provide process guidance in the selection of precursor

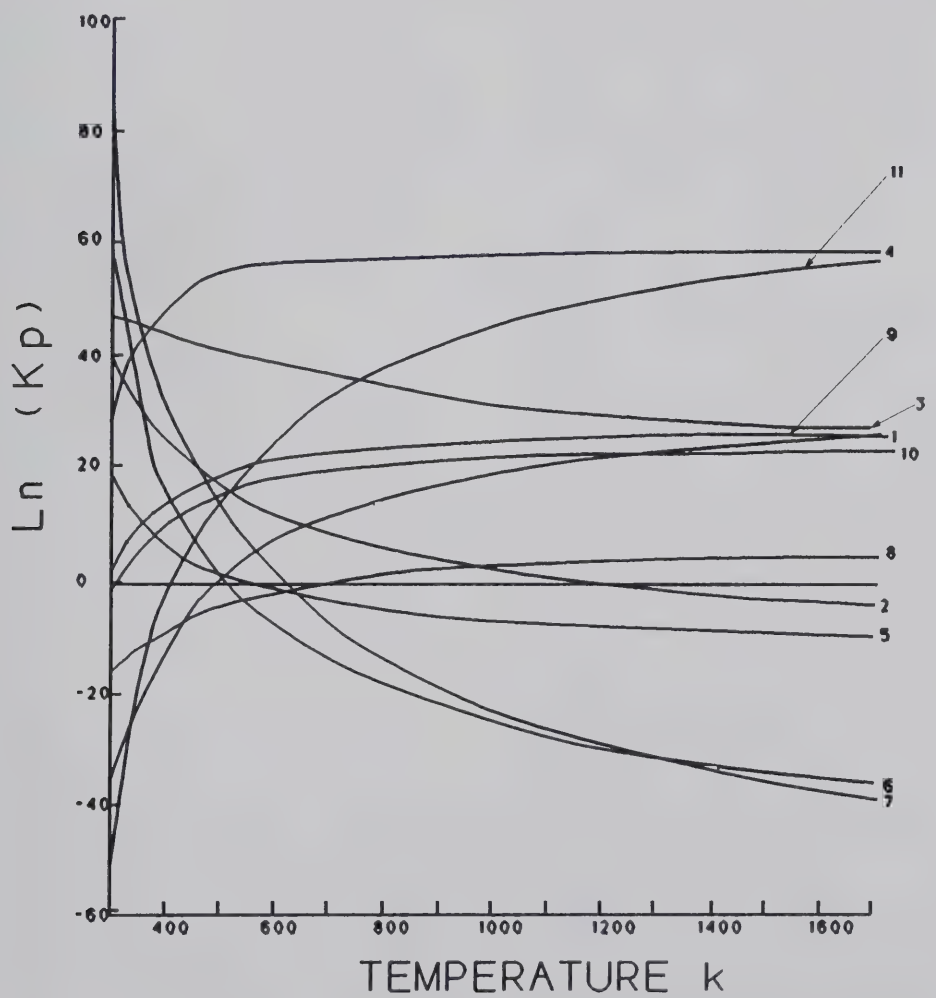

Figure 50. Effect of temperature on the equilibrium constant for reactions involving C_3H_6 (after Grower and Hill [58]). Curve 1, $C_3H_6 \rightleftharpoons CH_4 + C_2H_2$; Curve 2, $C_3H_6 \rightleftharpoons CH_4 + 2C + H_2$; Curve 3, $C_3H_6 \rightleftharpoons 3C + 3H_2$; Curve 4, $C_3H_6 + H_2 \rightleftharpoons CH_4 + C_2H_4$; Curve 5, $C_3H_6 + 3H_2 \rightleftharpoons 3CH_4$; Curve 6, $C_3H_6 \rightleftharpoons 3/2\ C_2H_4$; Curve 7, $C_3H_6 \rightleftharpoons 1/2\ C_6H_6 + 3/2\ H_2$; Curve 8, $C_3H_6 \rightleftharpoons C_2H_2 + C + H_2$.

gases, temperatures, and pressures. CVD phase diagrams are generated from these calculations [62–69]. Examples of such CVD phase diagrams are shown in figure 51. These diagrams provide equilibrium gas composition limits that allow the experimenter to estimate the range of process parameters which will deposit materials of the desired chemical composition.

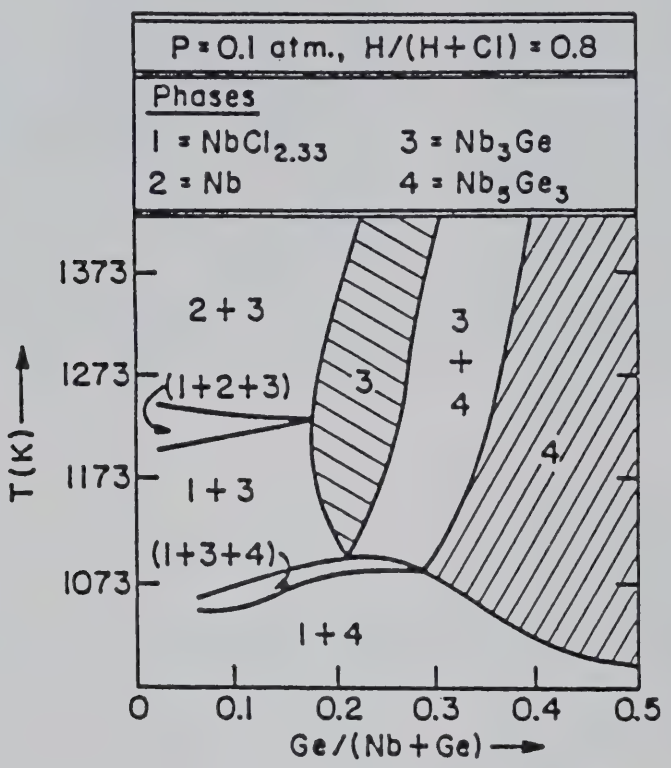

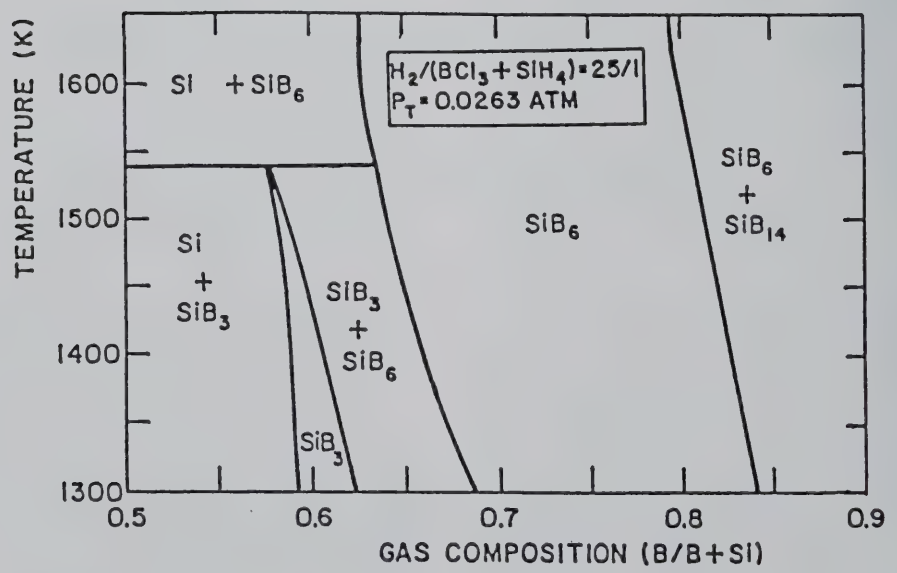

Figure 51a. Equilibrium CVD phase diagram for a portion of the Nb-Ge-H-Cl system (after Spear [59], reprinted with permission of The Electrochemical Society).
Figure 51b. Equilibrium CVD phase diagram for a portion of the SiH_4-BCl_3-H_2 system (after Spear and Dirkx, Ref. [60], reprinted with permission of The Materials Research Society).

Several computer programs have been developed to generate these CVD diagrams. Two examples are SOLGASMIX [70,71], and NASA CEC [72]. These programs are quite valuable in planning CVD processes as long as the model limitations are understood. Three of these limitations are

(1) the availability of thermodynamic information needed to make thermodynamic calculations,
(2) the accuracy of the existing thermodynamic data base, and
(3) the ability to relate thermodynamic calculations to the dynamically changing temperature environments of real CVD reactors.

2.1.2 CVD Kinetic Models Kinetic modeling of CVD processes has not received the same attention as thermodynamic and transport modeling. Difficulties in experimentally verifying theoretical models are the primary reason. It is also difficult to combine mass transport and kinetic models owing to differences in time for rates of reactions and transport processes [73]. Most kinetic models of CVD processes [26,28,73–92] are based on indirect information about the kinetics of the reactions. An example of this type of information is the rate of deposition. These kinetic models fall into three categories:

(1) those which look at homogenous reactions in a nearly stagnant boundary layer where diffusion across this layer is the rate controlling step in the CVD process [80];
(2) those which look at heterogenous reactions on the substrate where the kinetics of these reactions is rate controlling [73,76,83,86]; and
(3) those which consider the deposition process in terms of a flux of gas phase species and a sticking coefficient for these impinging species [28,75,79,83].

In boundary layer models of CVD processes [84], the precursor gases must react in the gas or on the substrate to form the molecular species from which the deposit is made. These gas mixtures contain molecules, atoms, ions, or free radicals which can do one or both of the following:

(1) undergo homogenous reactions in the gas mixture;
(2) diffuse to the substrate, adsorb on the substrate, and undergo heterogeneous reactions with other adsorbed molecules or with molecules of the substrate.

Which reactions occur depends not only on favorable thermodynamics but on the activation energies required for the reactions to begin. The rate controlling steps in the complex deposition process also affect the deposition process path. Not only are precursor gases involved in the reactions but also metastable intermediates and gaseous products of the deposition process. A counter flow of these gaseous products must diffuse away from the substrate surface. Their presence thus increases the complexity of the gas phase chemistry at the gas-substrate interface. Gas pressures as well as gas temperatures and gas composition affect the chemical kinetics of CVD processes [28,74–79].

High collision frequencies of molecules in near isothermal, atmospheric pressure, viscous flow gases promote homogenous reactions. These reactions occur primarily in the boundary layer of nearly stagnant gas above a heated substrate but can also occur in the heated fast-flowing feed gas [26,27,80]. Homogenous reactions can result in gas phase nucleation of macromolecules and formation of particulate by agglomeration of macromolecules. Diffusion of these macromolecules and other reactants at atmospheric pressure can be slow compared with the reaction kinetics on the substrate. When this occurs, diffusion across the boundary layer is the rate controlling step in the deposition process [74,76–78,80,81]. When both gas temperature and pressure are reduced, not only is the collision frequency reduced but also the number of collisions which result in gas phase macromolecule formation. Eventually the rate of reaction between adsorbed reactants on the substrate becomes slower than the mass transport of reactants to the substrate. The deposition process is then controlled by the rate at which surface diffusion and reaction of adsorbed atoms with one another and/or the substrate occur. The effect of these changes in the rate controlling step is shown in a plot of the deposition rate versus 1/T (fig. 52).

Although the boundary layer thickness may not change with pressure [77,78], diffusion of reactants across this boundary layer is more rapid as deposition pressures are lowered. Diffusion is roughly inversely proportional to pressure. Thus, gas phase nucleation and formation of macromolecules or particulates are correspondingly less. When the mean free path for molecular collisions exceeds approximately half the diameter of the deposition chamber, gas phase nucleation is eliminated [83].

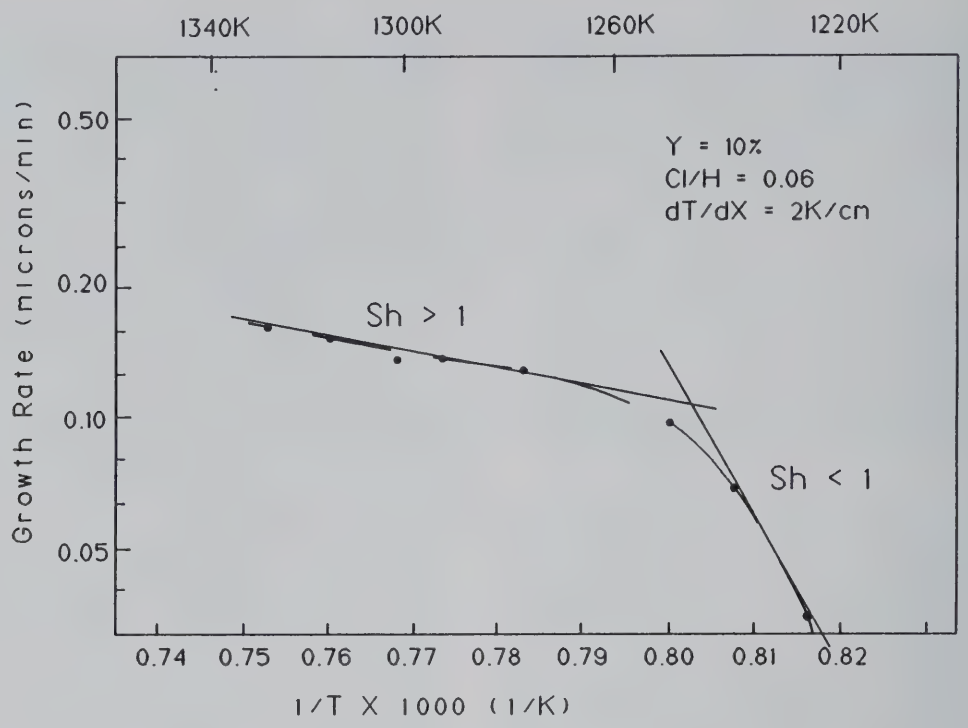

Figure 52. CVD silicon growth rate change as a function of 1/T as the Sherwood number changes from Sh < 1 to Sh > 1 (after Bloom et al., Ref. [50]).

2.1.3 CVD Transport Models Thermodynamic calculations provide an upper limit of possible reactions if temperatures and pressures are known and if the kinetics favor the reaction. Neither thermodynamic nor kinetic calculations provide guidance in the design of apparatus needed for commercial CVD. Control of deposit composition, uniformity, and reproducibility needed to produce modern materials requires a sophisticated understanding of the transport phenomena within the CVD reactor. Both 2D and 3D modeling of CVD processes are being developed to provide information about gas velocity, gas composition, and thermal variations within the CVD reactor [84,93–113].

CVD transport models address problems that system engineers must overcome in designing deposition environments which provide reproducible control over the process parameters. Temperature distributions within the reactive gas mixture, transport of the reactants to the substrate, the substrate temperature, and the dwell time for reactants in the vicinity of the substrate are process parameters which must be known and controlled. The transport parameters which are addressed in these models include the following: T, temperature; v, gas velocity; l, path length for gases in the hot zone of the deposition reactor; η, gas viscosity; g, gravity; ρ, gas density; D, the diffusion coefficients for the gases; k, the mass transfer coefficient; and C_p, the specific heat at constant pressure. These transport parameters are often grouped together in dimensionless numbers as a convenient way of providing numerical guides to the flow dynamics of selected deposition hardware and processes. Some of the dimensionless numbers of interest in CVD processes are:

1. Reynolds Number, $Re = \rho v_o l/\eta_o$.
   $Re < 2300$ in the vicinity of the substrate indicates laminar flow.
2. Gr/Re^2, where the Grashof number $Gr = g\rho_o \Delta\rho_o l^3/\eta^2$.
   $Gr/Re^2 > 0.3$ is indicative of combined, or if > 16 free, convection flow [93,111].
   $Gr/Re^2 < 0.3$ is indicative of forced convection flow. For deposit uniformity, this is desirable.
3. Sherwood Number, $Sh = kr/D$ for a first order process in a reactor of radius, r.
   $Sh > 1$ is indicative of the deposition rate being limited by the rate of diffusion of the reactants through a boundary layer above the substrate [76].
   $Sh < 1$ is indicative of a surface diffusion and reaction kinetics, rate controlling process. When uniformity is more important than deposition rate, it is desirable to operate in an $Sh < 1$ mode.

4. Pe/Sh, where the Peclet number Pe = vl/D. Pe/Sh > 850 is indicative of uniform deposition [84].

Temperature gradients in cold wall systems can be > 1000/K. These gradients can significantly alter model predictions and must be considered when making transport calculations. When heat transfer corrections are included in transport models, flow patterns in both vertical and horizontal reactors can be drastically altered [107]. In cold wall CVD systems involving gas species with disparate molecular species, Soret (thermophoretic) diffusion can change the expected chemistry at the gas-substrate interface. These and other corrections to the transport models are system design dependent and are thus more easily determined experimentally than theoretically.

The mean free paths for collisions of gas species in the reactive gas mixtures of both CVD and PECVD processes are inversely proportional to the pressure, P. Pressure therefore has a direct bearing on the gas phase chemistry. As pressures are lowered, the diffusion coefficients for reactants impinging on the substrate, D_r, are lowered since $D_r \alpha 1/P$. The boundary layer thickness increases with decreasing pressure, but at a slower rate than D_r increases.

2.2 Plasma Enhanced Chemical Vapor Deposition

Gas phase chemistry, adsorption, surface chemistry kinetics, and mass transport in PECVD processes are all skewed when compared with CVD processes by the existence of the plasma. Glow discharge plasmas rather than temperatures are used to provide the activation energy to initiate gas phase chemical reactions in PECVD processes. Control of the gas phase chemistry in PECVD processes therefore requires control of the plasma properties. Excellent reviews on this subject are available [114–132]. The following sections give a brief description of glow discharge plasmas and an overview of those plasma properties which influence PECVD processes.

2.2.1 Glow Discharge Plasmas Glow discharges are generated when an electric field of sufficient strength is applied across a gas that breakdown of the insulating properties of the gas occurs. Electrons gain energy during their fall through the potential gradient of the electric field. The momentum and thus the energy of the electrons responding to this electric field are transferred to the atoms or molecules of precursor gases through collisions. These collisions result in the formation of ions, molecular fragments, energetic neutrals, atoms, and free radicals. A plasma is formed when the number density of ions and electrons is everywhere equal. This condition of quasi-neutrality is maintained by the continued presence of energetic electrons.

Plasmas differ from neutrals in their collective behavior. This collective behavior is in the form of both particle and wave motion. Particle motion results from the movement of ions in the electric and magnetic fields of the plasma. Wave motion is the result of the response of electrons of the plasma to electric and magnetic fields. Wave motion occurs when the degree of ionization in the plasma is high enough that charge bunching and separation occur. Since the concentration of energetic electrons controls the number of ions formed from electron-neutral particle collisions, wave motion alters the distribution of ions in the deposition chamber. Thus, both particle and wave motions can influence the deposition of materials in PECVD processes.

To maintain a capacitively coupled plasma, electric field strengths and gas pressures must be adjusted not only to add sufficient kinetic energy to electrons to ionize neutral atoms, but to allow the ions to accumulate sufficient kinetic energy to generate secondary electrons when impacting the cathode. The quasi-neutral state can continue if the quantity of secondary electrons exceeds that needed for the formation of ions and the replacement of those electrons lost to walls and other parts of the deposition system. Plasmas which meet these criteria are glow discharges where the average electron energy is the order of 1 to 30 eV in an electron cloud whose density ranges from approximately 10^8 to 10^{12} cm^{-3}.

In DC plasmas and low frequency capacitively coupled RF plasmas, electrons increase their energy in the cathode sheath. The cathode sheath is a positive space charge region which forms near the cathode as a result of differences in electron and ion mobilities. The sheath forms a potential barrier which repels electrons and maintains the electron flux-ion flux equilibrium. The potential gradient between the plasma and wall is primarily the potential gradient across the cathode sheath. The potential gradients across both the cathode and anode plasma sheaths of capacitively coupled plasmas are dependent on the potential drop across the electrodes, plasma frequency, gas pressure, gas flow velocity, gas composition, electrode size, and electrode configuration.

When the collision frequency is high, as is the case for electrons and neutral gas species in near atmospheric pressure gases, the average energy accumulated by the electrons is small. Under these circumstances the average electron temperature and neutral gas molecule temperatures are approximately the same. It then becomes difficult to apply an electric field of sufficient strength to cause ionization without creating an electron avalanche and arcing.

The key to sustaining a plasma is thus to increase the mean free path for electron-electron and electron-atom collisions while minimizing electron wall loses. Lowering pressures used in the deposition process is one way of increasing the mean free path. There are limits, however, to the adjustments one can make with pressure alone and still sustain the plasma. The mean free path for electron-atom collision will become a significant fraction of the dimensions of the coater chamber as pressures are lowered. When this occurs, electron density reduction by low electron-atom collision frequencies and electron loss by wall collisions will quench the glow discharge.

2.2.2 Control of the Plasma Properties The plasma properties which control the gas phase chemistry in PECVD processes are:

- the collision frequency,
- the mean free path,
- the electron density, and
- the electron energy distribution function.

The deposition rate is dependent on the number of active species in the plasma and thus the collision frequency of energetic electrons with neutrals in the precursor gas. The degree of ionization of neutrals in a plasma depends on the electron energy distribution and the electron density.

The collision frequency of electrons with neutral gas species **a** for momentum transfer ν_a can be described by the expression:

$$\nu_a = \rho_T \sigma_a v_e \quad (1)$$

where v_e is the average electron speed; ρ_T is the density of all atoms, molecules, ions, free radicals, and electrons in the gas; and σ_a, the collision cross section of gas species a, is assumed to be independent of energy. Since

$v_e \propto (T_e)^{1/2}$, expression (1) can be written

$$\nu_a = K_e \rho_T \sigma_a (T_e)^{1/2} \quad (2)$$

where K_e is a proportionality constant and T_e is the electron temperature.

The collision frequency depends on the mean free path of the electrons. The mean free path, λ_a, is the average distance electrons travel before they collide with a neutral species. For electrons passing through a gas of species density ρ_T,

$$\lambda_a = 1/\rho_T \sigma_a \quad (3)$$

where σ_a is the collision cross section for momentum exchange. The collision cross sections are electron energy dependent. For argon, the maximum cross section for momentum exchange is approximately an order of magnitude larger than the cross section for ionization to Ar^+ and requires an order of magnitude lower electron energy.

Another way of increasing the average energy of electrons in a plasma is to alter the plasma properties with an applied magnetic field. When a magnetic field is applied normal to the applied electric field, an **E X B** drift will cause the electrons to describe a cyclic motion around electric field lines. This change in electron direction increases the mean free paths and thus increases electron energies. Cyclic electron motion in response to magnetic fields cuts electron wall losses. This lowers the threshold pressures needed to sustain the plasma and broadens the window of allowable PECVD process parameters. Magnetic field strength affects the spatial distribution and reactive gas phase species density [200].

2.2.3 Electromagnetic Frequency Effects on Cold Plasmas Plasma excitation frequencies have a direct influence on the properties of glow discharges and therefore the gas phase chemistry in PECVD processes. They affect the minimum voltage required to sustain a plasma. Frequency determines the spatial distribution of species and how their energies and concentrations change with time. The shape of the electron distribution function may change with frequency.

Changing from low to high RF plasma frequencies causes an increased oscillation of electrons in response to changes in the direction of the electric field. The energy distribution and collision frequency of electrons with neutral atoms and molecules in plasmas of DC, RF, and microwave glow discharges control the gas phase chemistry and hence the composition of the deposits which result from these processes [114,119,135]. Both the electron energy distribution function (the probability of finding electrons at a given interval of energy) and electron density vary with the discharge

stimulating frequency. Even when used only for biasing the substrate, frequency affects the ion energy distributions (fig. 53 [123]).

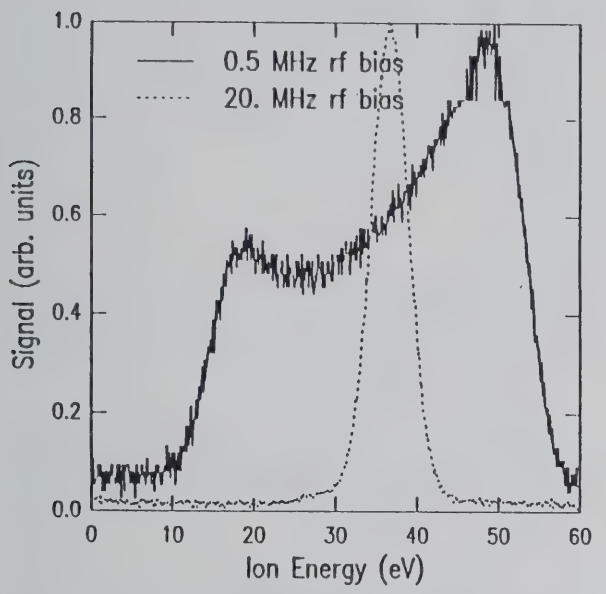

Figure 53. Effect of RF bias frequency on the ion energy distribution at the substrate in an ECR-PECVD system (after Holber and Forster, Ref. [123], reprinted with permission of the American Institute of Physics).

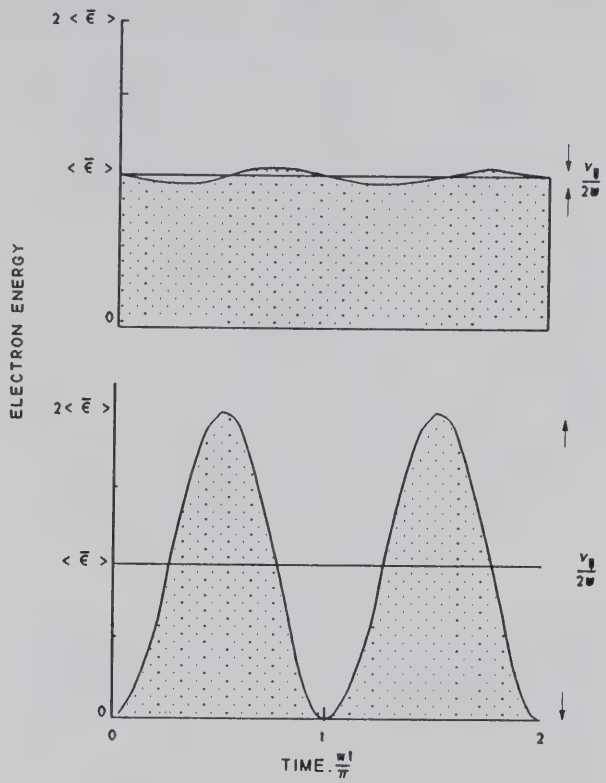

Figure 54. Electron energy as a function of ωt at (a) RF and microwave frequencies i.e. $\nu/\omega < 1$, and (b) low frequencies i.e. $\nu/\omega > 1$ (after Flamm, Ref. [120], reprinted with permission of the American Institute of Physics).

Ferreira and Loureiro have shown for argon [122] that the average input power per electron at unit gas pressure required to sustain a discharge decreases as ω (the angular frequency of the applied electromagnetic field) increases. Thus, at a specific power input and constant pressure, the ionization efficiency of the plasma increases as ω increases. They showed that the shape of the electron distribution function, f(u), depends on ν_a/ω. When $\nu_a/\omega > 1$, the electrons act as if they are in a DC plasma. For $\nu_a/\omega < 1$ (RF and microwave frequencies), f(u) is not Maxwellian. In low frequency RF discharges, the low electron collision frequency does not allow the mean electron energy to respond to field changes. At higher excitation frequencies (high collision frequencies between electrons), the mean electron energy will respond to the instantaneous field intensity and be in equilibrium with it. These differences can be seen in figure 54 [120].

Moisan et al. [119] showed that the electron energy distribution function was also sensitive to ω. They found the density of dissociated molecules, free radicals, ions, and excited atoms produced from collisions of energetic electrons with neutrals to be ω sensitive. Wertheimer and Moisan [135] estimated f(u) for different values of ν_a/ω for DC, RF, and microwave plasmas. Their work shows that the population of higher energy electrons increases as the plasma frequency increases.

At constant power, the average energy of the electrons, (u), decreases as the plasma frequency increases. This compensates for the higher population of high energy electrons with increasing plasma frequency than a Maxwellian distribution would suggest. The consequence of these skewed electron energy distributions is differences in gas phase chemistry and thus deposits formed by RF and microwave frequencies. Properties of deposits formed at microwave frequencies differ from those of 13.56 MHz RF frequency plasmas [136–140]. An example of this can be seen in figure 55, for the hydrogen contents of Si_3N_4 deposited by CVD, RF-PECVD, ECR-PECVD, and RF biased ECR-PECVD processes. The figure shows that the total hydrogen uptake by RF-PECVD at 300 °C is not too different from the hydrogen uptake by an ECR-PECVD process at 25 °C. This is counter to the normal trend in which the hydrogen uptake decreases with increasing temperature [138,174].

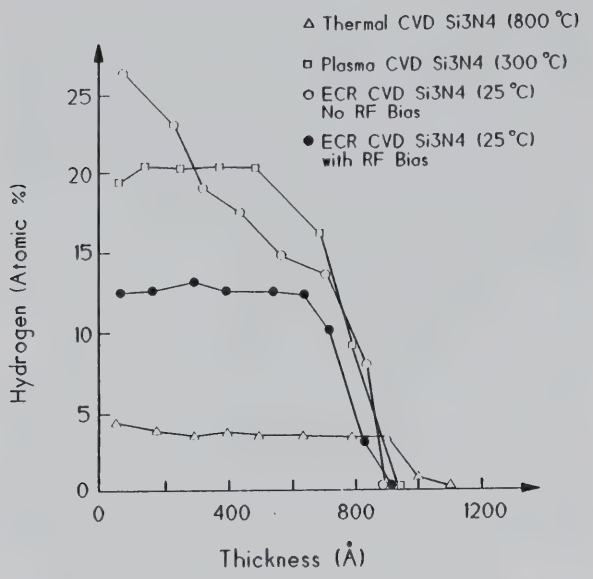

Figure 55. Hydrogen contents of Si_3N_4 films, deposited by CVD, RF-PECVD, and ECR-PECVD processes, as a function of film thicknesses and substrate temperatures (after Nguyen and Albaugh, Ref. [136]).

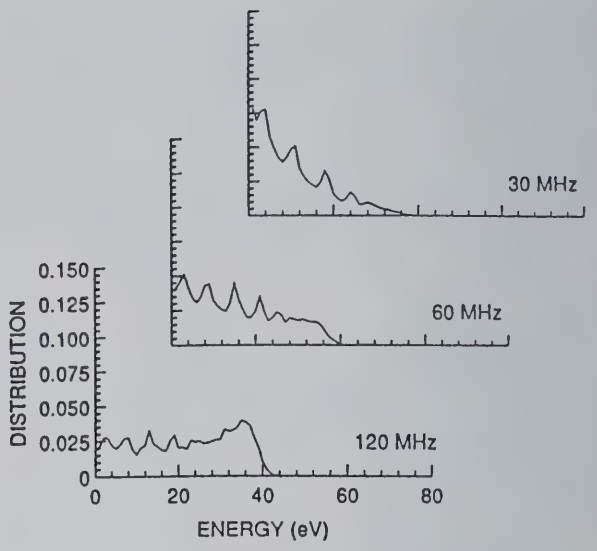

Figure 56. Effect of frequency on ion energy distributions at the electrode in a 250 mtorr, 4 cm thick helium glow discharge (after Surendra and Graves, Ref. [14], reprinted with permission of the American Institute of Physics).

Surendra and Graves' Monte Carlo simulation of ion energies in a capacitively coupled parallel-plate electrode system (fig. 56 [141]) shows how frequency affects ion energy distributions in helium glow discharges. Regardless of the plasma frequency selected for the deposition process, both the electron energy and energy density of the glow discharge are dependent on the gas composition, pressure, and system configuration.

2.2.4 Modeling PECVD Processes Modeling of PECVD processes has been very limited because of the complexity of and lack of detailed knowledge concerning the plasma environment. The PECVD processes can be broken down into the same steps as CVD processes:

- formation of the reactive gas mixture,
- diffusion of the reactants to the substrate,
- adsorption-reaction on the substrate, and
- desorption-diffusion away from the substrate of the products of the deposition process.

Each step in the process is skewed by the presence of the plasma environment. Thus, PECVD analysts concentrate on developing models which allow one to understand how the plasma properties of the electron energy distribution function, electron densities, ion energy distribution, and ion flux are affected by process parameters. Process parameters of concern are pressure, RF power, plasma frequency, substrate bias voltage, chemical composition of the precursor gases, gas flow rates, magnetic field strengths, electric field strength, and geometry of the plasma system. Some modeling studies address specific regions such as the plasma sheath [134,144,145] or the plasma-substrate interface [89,122,143,146,147]. Gas phase chemistries at different locations relative to electrodes within the plasma environment [142] are different. Thus, the gas phase chemistry in the plasma is quite different from that in the sheath. Economou et al. [134] developed a simplified time average model of the plasma sheath for RF plasmas, applicable to >10 MHz plasmas, with average ion energies. The model shows that ion flux increases as reactor pressures are lowered. The higher the RF power levels, the higher the rate of increase in ion flux with decreasing coater reactor pressures. The model also shows a nearly linear relationship between the ion bombardment energy and the ratio E/p, where E is the electric field and p is the deposition reactor chamber pressure.

Some modeling studies examine the influence of magnetic fields [131,148,149] on plasma properties. These models show that applied magnetic fields affect the spatial distribution of reactive gas phase species and the transport properties of the gases. Other models show the influence of plasma frequencies [119,120,122,135,141]. These models show that the ion current and plasma density are roughly proportional to ω^2. The sheath thickness scales approximately with $1/\omega^{0.87}$.

3. Implementing CVD AND PECVD Processes

CVD and PECVD system designs are continually changing. Commercial custom systems for electronics, tribology, and decorative coating applications are available. Most research and development groups build their own systems or buy hardware which can be modified to meet their needs.

3.1 CVD Systems

The spectrum of CVD system designs represents different responses to the need to improve control of the deposition environment for a specific deposition requirement. CVD deposition systems fit into the broad categories of hot wall CVD or cold wall CVD based on the method used to heat the substrate. Most modifications of the equipment used for either hot wall or cold wall depositions are efforts to

- improve the uniformity of the gas flow over the substrate,
- control the gas flows in the system, or
- increase the size or quantity of parts to be coated.

In hot wall CVD reactors, substrates are immersed in an externally heated reactive gas mixture. These substrates are supported in an isothermal region within the deposition chamber where temperatures and gas flows can be approximated and controlled. Both horizontal and vertical deposition chambers are common. Gas pressures used for these CVD processes are typically 2 to 760 Torr. Examples of hot wall CVD deposition systems are shown in figure 57. A variant of the hot wall system is the heated fluidized bed of particles [150] (fig. 58). The substrate in these processes can be the particles of the fluidized bed or a material suspended within the fluidized particles.

Cold wall CVD reactors were developed to reduce the time during which reactive gases are in contact with a heated substrate and the quantity of gas that is heated to deposition temperatures. These factors reduce the quantity of particulate that can form and be encapsulated into the growing deposit. Typical cold wall CVD reactors are shown in figure 59. A common way to heat the substrate in cold wall CVD is by induction coupling the substrate to an RF power supply. This allows for rapid heating and cooling of the substrate and thus

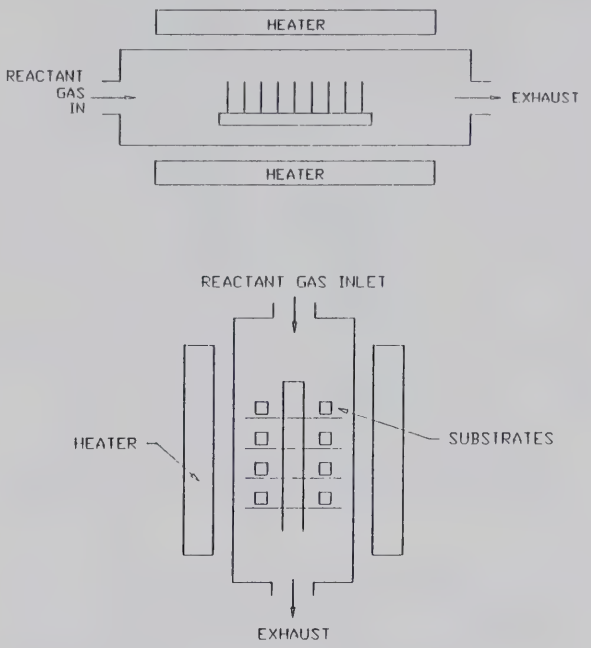

Figure 57. Typical hot wall CVD reactors used for (a) wafer processing and (b) tribology applications.

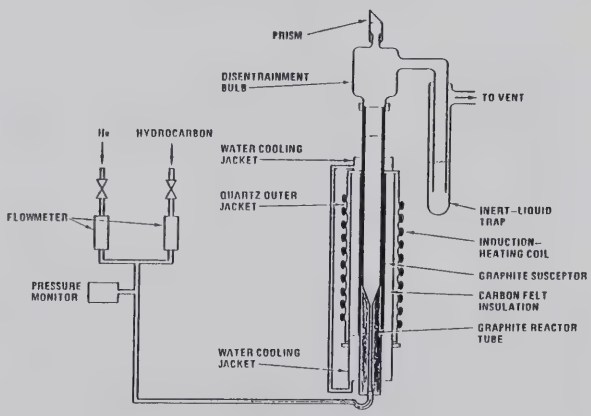

Figure 58. Hot wall, fluidized particle bed CVD reactor (after Bokros, reprinted from Ref. [150], with permission from Pergamon Press Ltd., Headington Hill Hall, Oxford OX3 OBW, UK).

minimizes deposition of undesirable morphologies and compositions at intermediate temperatures during substrate heating to reach processing temperatures. Another application of cold wall CVD reactors is in CVI of composite materials. For optimum densification by infiltration it is desirable to use both a thermal gradient and a pressure gradient in CVI processing whenever possible [29]. Examples of CVI systems for pressure gradient and pressure gradient plus thermal gradient operation are shown in figure 60.

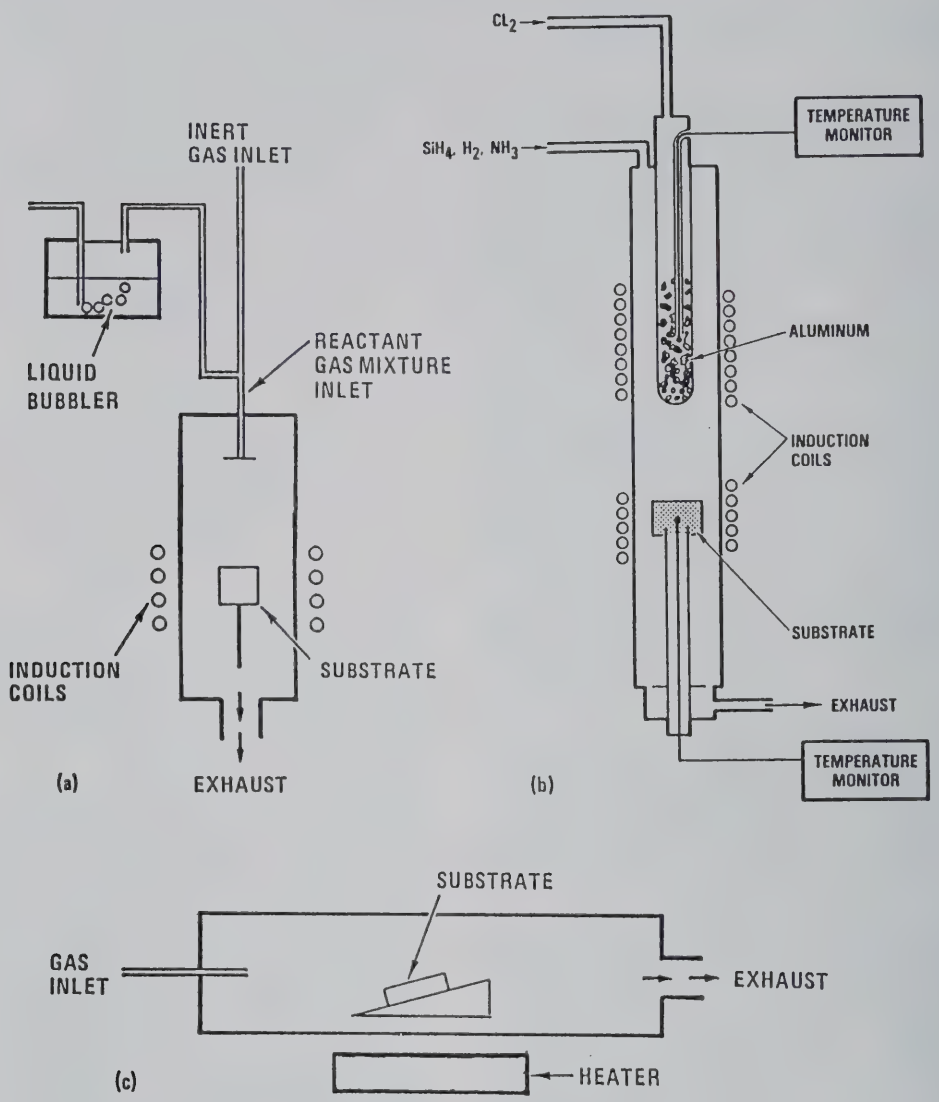

Figure 59. Typical cold wall CVD reactors used for (a) liquid precursor reactant, (b) in situ reactant gas formation, and (c) horizontal displacement flow experiments.

Newer systems utilizing low pressure chemical vapor deposition (LPCVD) are designed to improve film uniformity and lower impurity contents by reducing pressures to <1 Torr to minimize asymmetric thermal gradients and gas flow patterns [91].

3.2 PECVD Systems

Glow discharges used in PECVD processes include DC, RF, and microwave plasmas. PECVD systems are designed around the plasma to be used in the deposition process. The normal operating pressures for PECVD processes are dictated by the requirements for the maintenance of plasmas in these systems. DC plasmas operate in a narrow pressure regime for deposition of noninsulating materials. Their use is thus limited and they are not normally chosen for PECVD systems. Two types of PECVD systems are being built. RF-PECVD systems are those which use moderate frequency RF power supplies. Microwave-PECVD systems are those which use microwave power supplies. Federal regulations currently authorize 13.56, 27.12, 40.68, 915, and 2450 MHz frequencies for non-broadcast usage. The availability of relatively inexpensive power supplies which comply with these regulations, 13.56 and 2450 MHz, makes these the choice for most RF and microwave PECVD processes in the United States. However,

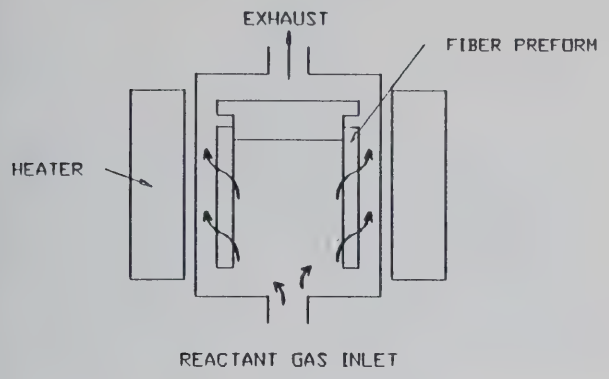

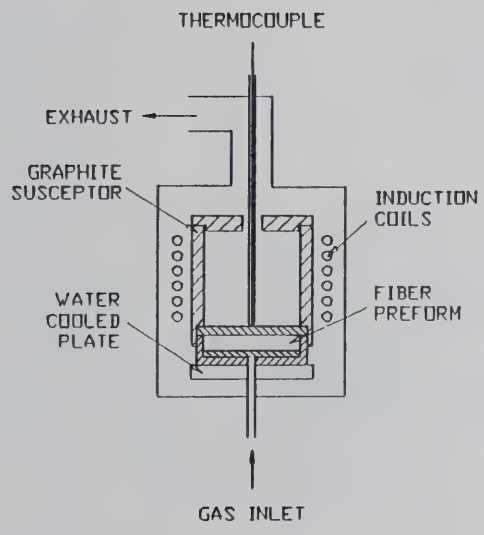

Figure 60. Apparatus used for (a) pressure gradient CVI and (b) pressure gradient and thermal gradient CVI studies.

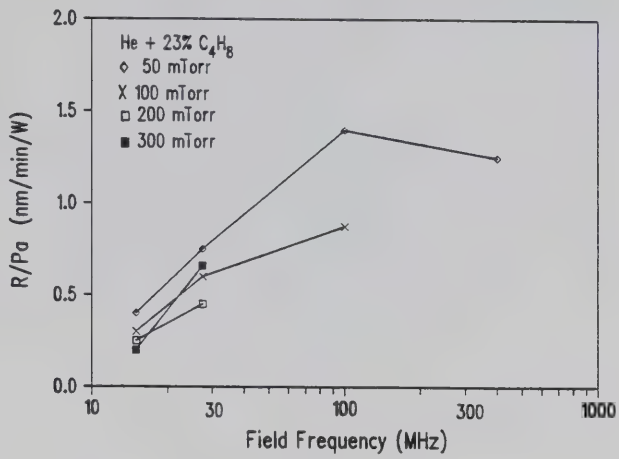

Figure 61. Effect of frequency and total gas pressure on the PECVD growth rate of polymer thin films (after Moisan et al., Ref. [119]).

as figure 61 shows, the optimum frequency for PECVD processing is not necessarily one of these authorized frequencies nor the highest frequency [119].

3.2.1 RF-PECVD Most of the developments in RF-PECVD systems have come from the commercialization of these processes for the electronics industry. Early emphasis on maximizing the quantity of wafers processed has given way to the greater need for contamination control and step coverage uniformity. To meet these needs vertical deposition systems with the substrates between parallel plate electrodes have replaced many of the early hot wall barrel systems. Examples of RF-PECVD systems are shown in figure 62. A variant of RF-PECVD systems is remote-PECVD systems in which the substrate is isolated from the plasma where the reactive gas mixture is formed. The purpose of this isolation is to avoid the high energy ion impingement on the deposit. This minimizes encapsulation of contaminants, stresses, disordered microstructures, and metastable phases in the newly formed deposit. A disadvantage of these processes is the low deposition rates [57,151], which are nearly an order of magnitude lower than those in traditional PECVD processes.

3.2.2 Microwave PECVD Many recent PECVD experimental studies use electron cyclotron resonance (ECR) microwave systems. Deposition systems which use microwave frequencies differ from RF systems in the manner by which they transmit power from the oscillator to the deposition chamber (applicator-plasma load region). The transmission line can be a coaxial cable or a waveguide. Both microwave and cavity applicators are used with mirror and cusp geometry magnetic fields (fig. 63) [128]. The magnetic mirror fields have also been used for DC and AC plasmas by Varga [201] (fig. 63) to deposit diamond-like carbon (DLC). Common forms of those microwave deposition systems, some which use applicators, are shown in figure 64.

Designs of ECR-PECVD systems are more complex and less well developed than those of CVD and RF-PECVD systems. The potential exists for greater control of the plasma environment in ECR-PECVD systems than in RF-PECVD systems. The electroless ECR plasma allows separation of the power input to the plasma from that of substrate biasing. This decoupling permits separate control of ion energies. It also allows broader control of the plasma density through adjustments in pressure and magnetic field strengths than is achievable with RF-PECVD systems. In spite of these poten-

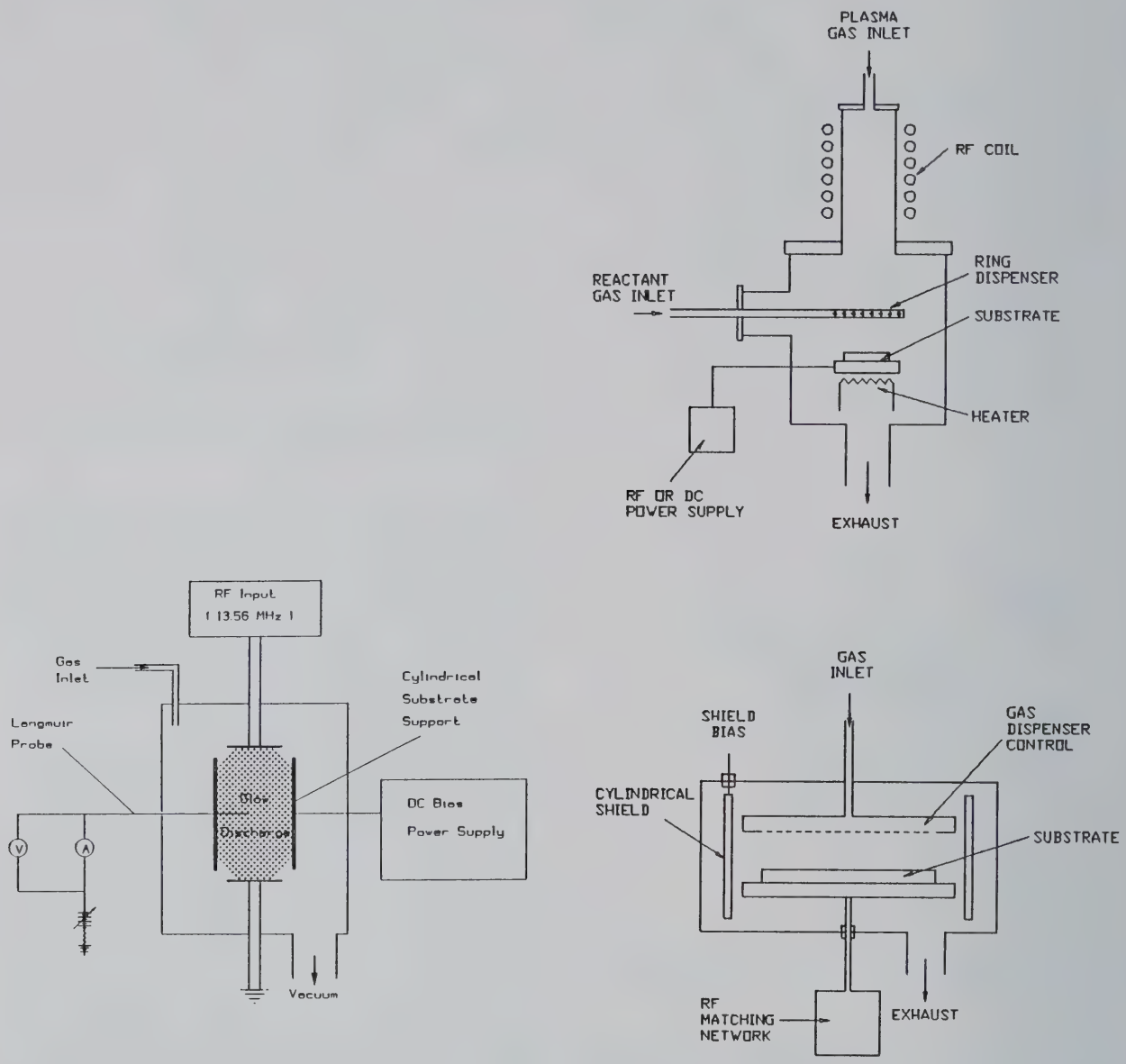

Figure 62. Typical RF-PECVD reactors used for (a) separate substrate bias studies, (b) remote plasma experiments, and (c) large diameter silicon wafer epitaxial thin film formation (after Matsuoka and Ono, Ref. [128]).

tials it has been difficult to reproducibly tie deposit properties to process parameters. The primary reason is the difficulty in obtaining a uniform plasma environment for the substrate that does not change with modest changes in process parameters and is flexible enough to be of practical use in commercial applications. ECR conditions do not exist throughout the plasma region [152] and are spatially sensitive to pressure [128], substrate bias [123,125], magnetic field strength [128,152], and magnetic field geometry [202].

3.2.3 Supporting Hardware In both CVD and PECVD systems gases are fed into the deposition chamber through a gas flow control panel. When liquid reactants are used in the deposition process, they are normally placed in a bubbler and transported to the reaction chamber with a carrier gas. This sometimes requires a separate temperature control system for the bubbler and gas lines to the deposition chamber. Gas flow and exhaust systems used for PECVD processes are the same as those used in CVD depositions operating at equivalent

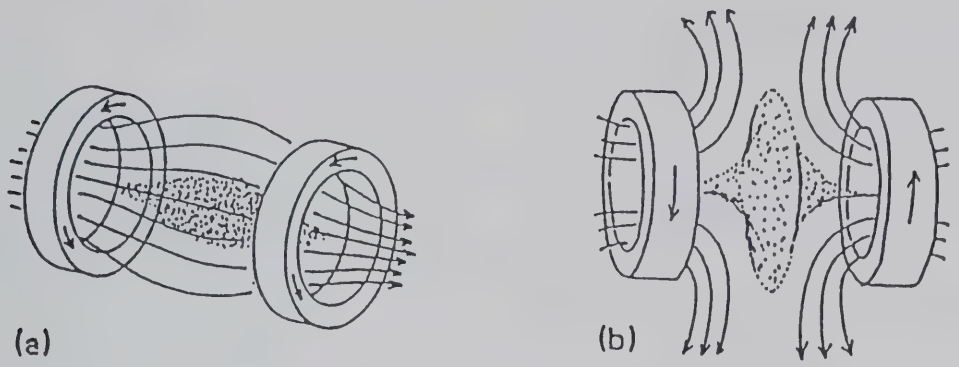

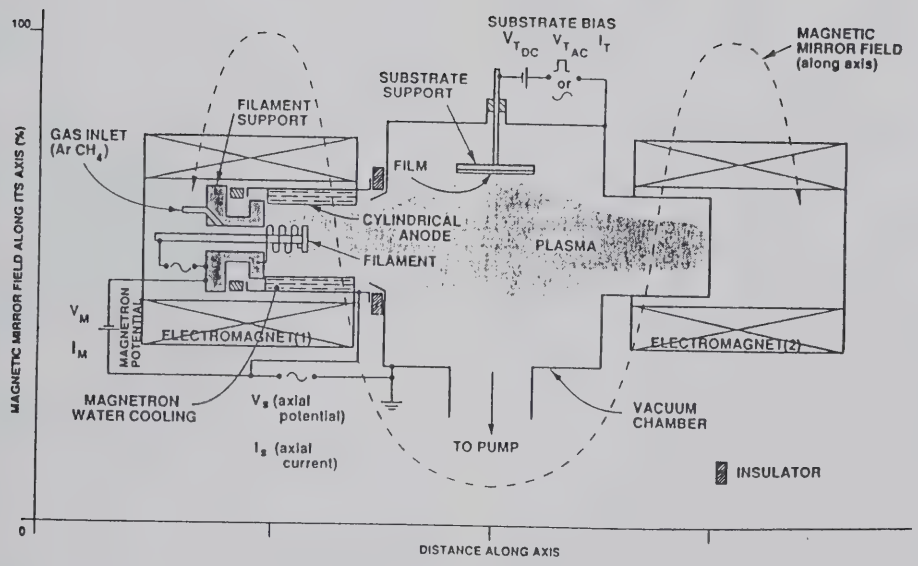

Figure 63. Electromagnetic coil current arrangements for (a) mirror, (b) cusp field applicators, and (c) the effect of a magnetic mirror field on a 50 Hz glow discharge used for diamond-like-carbon formation (after Varga, Ref. [20], reprinted with permission of the American Institute of Physics).

pressures. The purity of gases used in the deposition processes impacts both the purity of the deposit and the formation of unwanted gas phase particulates. Where high purity particulate free gases are essential, such as in wafer manufacture, the gas delivery hardware can be as important as gas purity [203]. Gas delivery systems for ultra-clean operation must have straight tubing, bakeable valves, and filtration to remove both water and particles.

Systems that operate only at atmospheric pressures are usually easier to build and operate but lack the flexibility for microstructure, chemistry, and property control that reduced pressure depositions offer. The sophistication of exhaust systems for reduced pressure depositions depends on the targeted properties of the materials to be deposited. For some processes, roughing pumps with suitable gas scrubbing systems are sufficient. For others, roots pumps or even high vacuum, cryogenic, or oil-less turbomolecular pumps are needed.

Auxiliary equipment needed for controlling the plasmas and in situ diagnostics in both CVD and PECVD processes is dictated by which process parameters are crucial to the formation of the desired deposit.

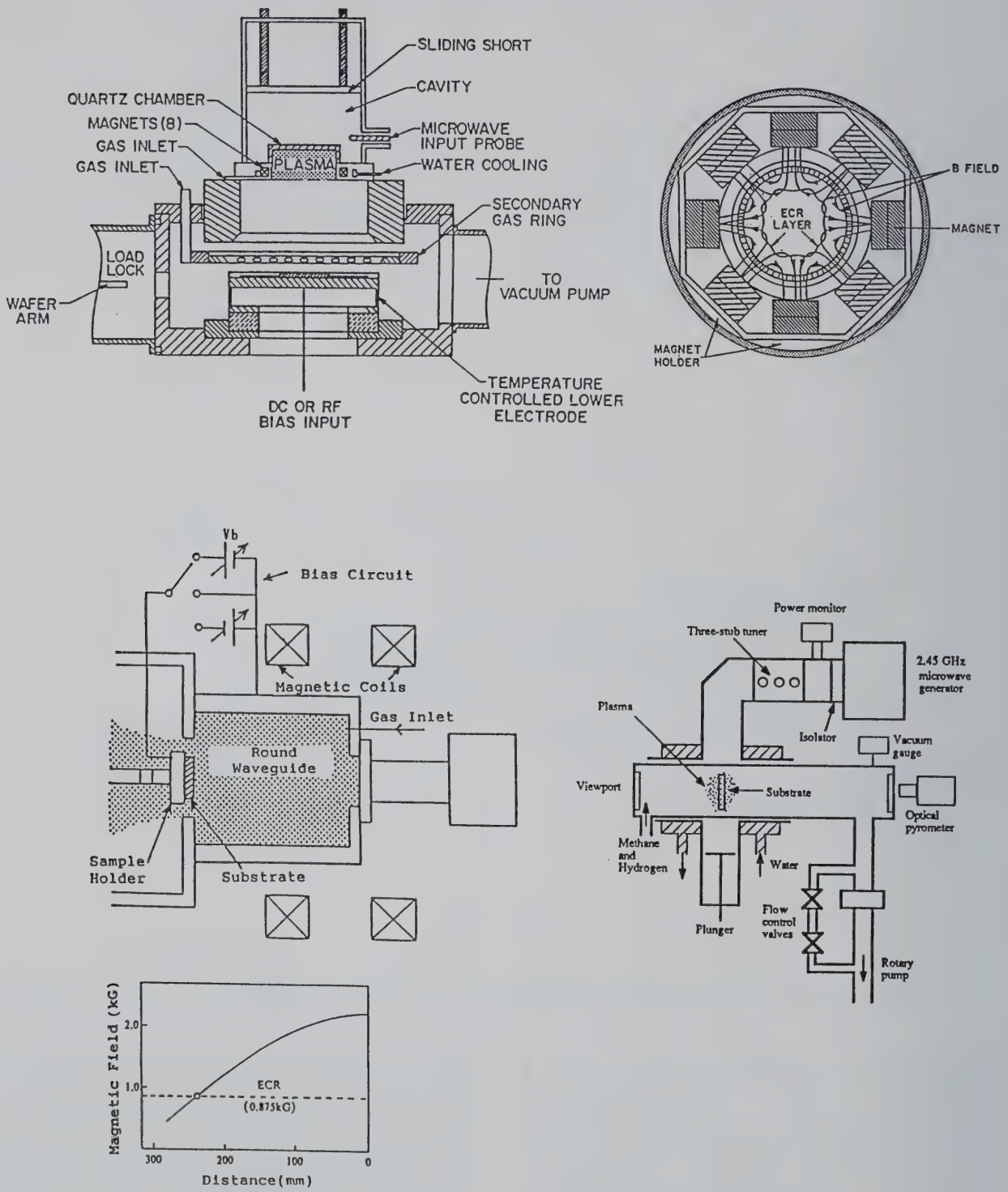

Figure 64. Typical microwave-PECVD systems with (a) a cavity multicusp ECR applicator (after Asmussen [204] and Buckle et al. [205]), (b) axial mirror magneto-ECR applicator (after Ma et al. [206]), and (c) no magnetic field applicator (after Glass et al. [207]).

3.3 Substrate Preparation

Substrate preparation is important to the nucleation of new growth, deposit uniformity, morphology, and substrate-deposit adhesion. In both CVD and PECVD processes surface imperfections, dirt particles, and foreign atoms can be nucleation sites for new deposit growth. Thus, pretreatment of the surfaces involves minimizing surface contamination by mechanical and chemical means before mounting the substrate in the deposition reactor. Substrates must be cleaned just prior to deposition to minimize adsorption of contaminants from room air. For some applications this means clean-room handling of substrates.

The deposition reactor chamber must be clean, leak-tight, and free from dust, moisture, and foreign contaminants. Once deposition begins, surface cleanliness is usually maintained in CVD processes by the gas-substrate chemical reactions at substrate temperatures. Deposition and sputter removal of contaminants occur simultaneously in PECVD processes. This continually removes physically adsorbed contaminants but does not control particulate encapsulation. Particulates can form from contaminants in the precursor gases or as a result of selecting the wrong processes. Dust in the reactor chamber, precursor gas purity, and process parameters must be controlled to control particulate encapsulation in the deposit.

3.4 Process Diagnostics

Diagnostic tools used for in situ monitoring of CVD deposition processes include thermocouples, optical pyrometers, oxygen monitors, and moisture analyzers. Diagnostics used for PECVD processes include gas phase Langmuir current-voltage measurements, optical pyrometer and/or shielded thermocouple temperature monitoring, substrate bias measurements, current density measurements, and mass spectrometer examinations. The diagnostic tool chosen for each process depends on the critical process parameters of the deposit to be made. Descriptions of some diagnostic tools are given in the following paragraphs.

Temperature measurements in CVD systems are made with thermocouples whenever possible. When the substrate is heated inductively with an RF power supply, thermocouples must be electrically isolated from the substrate. Thermocouples can be used in PECVD processes if blocking capacitors shield the substrate and thermocouples from the effects of RF leakage. Surface currents make 13.56 MHz frequencies more difficult to shield against than the <500 KHz frequencies used in RF inductive heating. Thermocouples must also be isolated from the reactive gas mixtures, or alternative means of in situ monitoring temperatures must be used.

Optical pyrometers are used for high temperatures (>1400 °C) when either thermocouples react with other materials used in the CVD process or temperatures are above thermocouple operating temperatures. Fourier transform infrared spectroscopy (FTIR) rotational temperature measurements are another temperature monitoring option [90].

Plasma properties must be monitored in PECVD processes. A device commonly used for these measurements is the Langmuir probe. The probe consists of one or two fine wires that are floated electrically with respect to ground. Electron temperature, plasma density, electron distribution function, and ion distribution functions are measured with these probes. Langmuir probe measurements are affected by the plasmas being studied, the probe geometry, the probe location, and the materials being deposited [153–157].

The quadrupole mass spectrometer (QMS) is another common diagnostic tool for PECVD processes [158–163]. This instrument ionizes the system gas by electron impact and resolves the masses of the resulting ions. Atoms can be recognized by their characteristic parent and daughter fragmentation peaks. In principle, ions can be extracted with a tube directly from a plasma, skipping the normal ionization step [161,162,164]. However, this may not give an accurate picture of the gaseous species within the plasma. Problems encountered in localized mass spectrometer sampling are inherent in any probe inserted into the plasma. The typical QMS operates at lower pressures than most deposition pressures, so sample extraction must remove atoms, ions, free radicals, or molecules from the deposition chamber for analysis in the QMS system. Inserting a tube into a plasma to sample its contents perturbs it and alters the local volume chemistry in the vicinity of the probe. Temporal, temperature dependent, frequency dependent sheaths form adjacent to the sampling tube in an RF plasma which attract or repel ions in the plasma [145]. In either case, the accuracy of the measurement is compromised. Thus, extraction and examination of process gases are normally done away from the plasma in the effluent gases. A disadvantage of this technique is the loss of short-lived metastable intermediates of the deposition process.

Optical emission spectroscopy (OES) analyzes light emitted from the plasma to identify ions and atoms [151,165–167]. FTIR analyzes infrared emission from the plasma to detect molecules and molecular fragments in the plasma environment [168]. Laser induced fluorescence (LIF) is used to determine the rotational, vibrational, or electronic state of a molecule or atom [169–171]. Raman spectroscopy can be used to measure reactant species concentrations and electron temperature [169]. All of these nonintrusive techniques require windows which minimize attenuation and distortion of optical or infrared transmission. One side of these windows must be in the deposition chamber. The windows must be kept clean, which is often difficult to do since walls and windows become coated during the deposition process.

4. Process Comparisons

The gas phase chemistry in PECVD processes depends on the composition of the active gas species and their collision frequency. It is thus dependent not only on the gas pressure, gas temperature, and gas composition as in CVD processes, but also on the electric field strength, the presence or absence of magnetic fields, and, in the case of RF plasmas, the plasma frequency.

4.1 Deposition Rates

Deposition rates are sometimes different and sometimes nearly the same for CVD and PECVD processes. One rarely uses comparable deposition temperatures to deposit the same materials by CVD and PECVD processes. While it is common to discuss CVD rates in terms of temperature, this is not always meaningful with PECVD processes. More appropriate for PECVD rates are the electron densities and electron energy distributions within the plasmas. By keeping the plasma properties constant and examining deposition rates as a function of temperature with and without a plasma, Comfort and Reif [92] were able to compare the two processes. Arrhenius plots of their results (fig. 65) which compare the deposition rates for silicon on silicon versus temperature, with and without a plasma, show the activation energies for the two processes to be comparable. The curves show that while deposition by PECVD processes begins at lower temperatures, the deposition rates at these lower temperatures are correspondingly lower. The step difference in the rate of deposition for PECVD silicon over CVD silicon at any temperature is due to the plasma enhancement. The location of the substrate relative to the plasma must also be considered. The deposition rates in remote plasma RF and ECR processes are normally slower than in conventional CVD and PECVD where the substrates are not in the plasmas. The deposition rates and the properties are thus only indirectly related to the plasma properties.

Deposition rates not only provide information about activation energies but indirect gas phase chemistry information. An example is the comparison of helium and argon dilution in the deposition of Si_3N_4 from NH_3 and SiH_4 plus He or Ar by a remote plasma process. According to Tsu and Lucovsky, Ar is more effective than He in causing the incorporation of SiH in the growing deposit and causes the difference in deposition rates for processes which use He or Ar as a diluent [174].

The diluent used in the deposition process not only affects the deposition rates but also affects the properties of the deposit. Claassen et al. showed (fig. 66) that the refractive indexes of Si_3N_4 deposits made by RF-PECVD processes are strongly dependent on whether the diluent is Ar, H_2, or N_2 [137].

4.2 Microstructure

Morphologies of deposits depend on whether the reactions to form the deposits occur in the gas phase or on the substrate. Morphologies are also influenced by which step in the deposition process is rate controlling. The rate controlling step is dependent on the gas velocity, pressure, and temperature of the deposition process.

The microstructures of deposits formed by both CVD and PECVD processes depend upon:

- chemical makeup and energy of atoms, ions, or molecular fragments impinging on the substrate,
- chemical composition and surface properties of the substrate,
- substrate temperature, and
- presence or absence of a substrate bias voltage.

These factors determine whether adsorption, sputter removal of substrate atoms, or implantation of impinging gas phase species occurs.

Molecules and atoms impinging on the substrate react in several ways. Nonlocalized physical adsorption can occur where adatoms or molecules are stable at every point on the substrate. Molecules

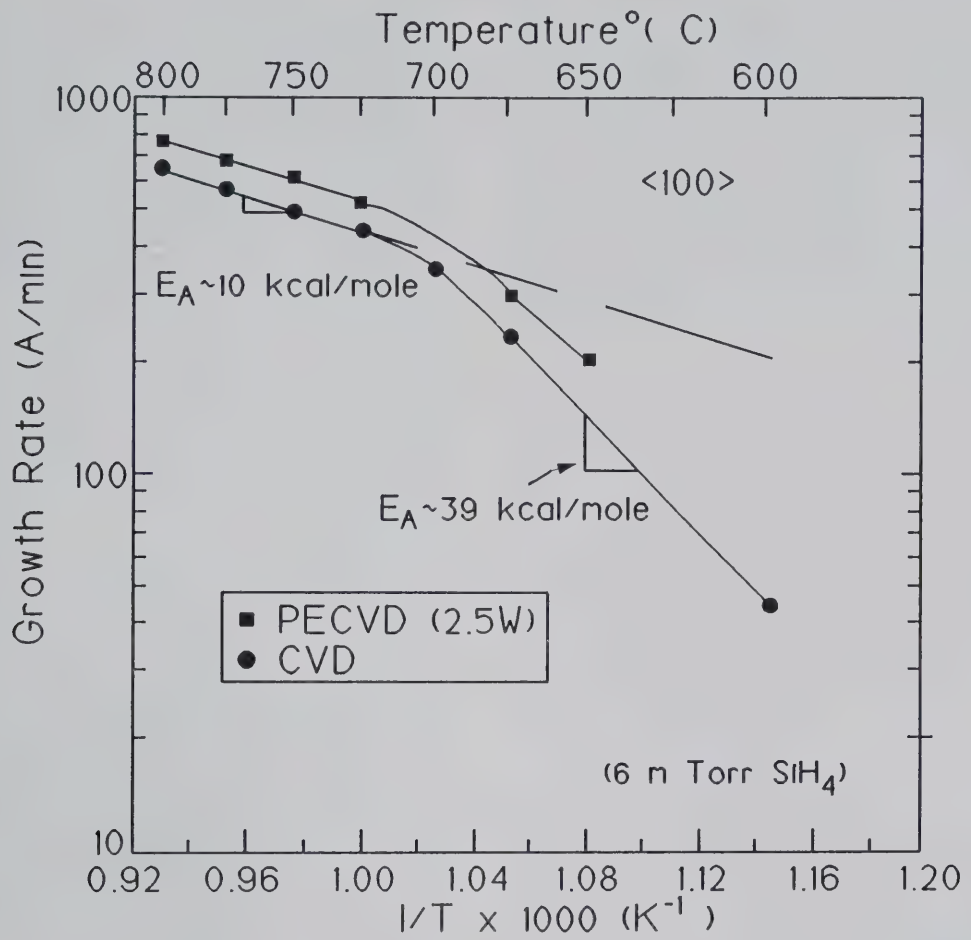

Figure 65. Arrhenius plots comparing growth rates of CVD and RF-PECVD silicon as a function of 1/T (after Comfort and Reif, Ref. [92]).

and atoms thus adsorbed are free to move about the surface very much like a two-dimensional gas. Nonlocalized adsorption provides high surface mobility for impinging atoms. Impinging atoms may chemisorb in localized areas where adatoms or molecules occupy fixed minimum potential sites. While this restricts movement of the adsorbed species, it does not prevent it. Movement of the chemisorbed species is possible by site jumping but this movement is normally very limited. Chemisorbed atoms form nucleation sites where further chemisorption and growth of clusters can occur. Growth can be by island formation in nonlocalized adsorption when mobile condensing adatoms react with one another and are more strongly bound to each other than to the substrate. Chemical composition and substrate temperature play a strong role in the relative amounts of localized and nonlocalized adatoms in the deposition process. Both types of adsorption are normal during the deposition process. Low temperatures favor nonlocalized physical adsorption and high nucleation rates. Higher temperatures favor chemisorption and lower nucleation rates. At these higher temperatures physical adsorption with weak van der Waals forces limits both the quantity of adatoms and their dwell time on the surface. Thus, random polycrystalline deposits are formed at low temperatures and large crystals and epitaxial growth are favored at elevated temperatures. The effect of temperature on the morphology can be clearly seen in CVD SiC deposits (fig. 67). Similar microstructural changes with substrate temperature can be expected in PECVD deposits [189].

As previously mentioned, formation of the reactive gas mixture is not the only reaction occurring in the gas above the substrate. Nucleation and agglomeration of macromolecules can lead to growth of particles in the gas phase. Particle formation is favored by high collision frequencies among gas phase species and the long total time agglomerated molecules are in contact with reactive gases at ele-

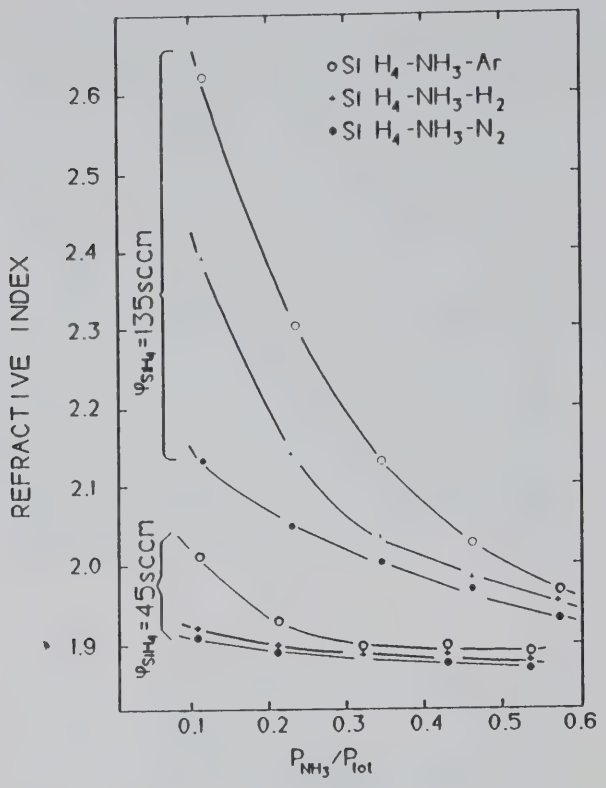

Figure 66. Effect of diluent gas composition on the refractive indexes of Si_3N_4 deposits formed from SiH_4-NH_3-diluent gas mixtures (after Claassen et al., Ref. [137]).

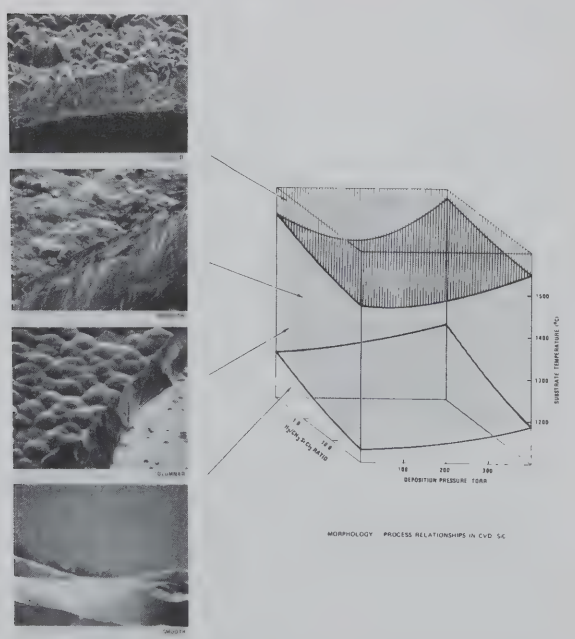

Figure 67. Morphology-process relationships in CVD SiC [177].

vated temperatures where deposition can occur. Thus, high pressures and long contact times between the flowing gases and the heated substrate or wall of the deposition reactor promote gas phase nucleation and particle growth. Incorporation of both macromolecules and particulates in the deposit affects the microstructure of the deposit.

Examples of the influence of gas phase nucleation on the microstructure of CVD deposits can be seen from an examination of morphology changes in CVD carbon deposition. In isothermal, fixed substrate carbon deposition from hydrocarbons, gas phase nucleation generally results in the deposition of powder and dust. When process conditions are adjusted in such a manner that deposit growth on the substrate occurs, anisotropic carbon is formed.

When carbon is deposited in a bed of fluidized particles, gas phase collisions of macromolecules with the substrate occur as well as collisions between atoms and molecules. One is thus able to control the size of macromolecules and particulate that are formed in the gas phase by controlling the fluidized bed area, the hydrocarbon concentration, and the temperature. Deposits which result from this control of gas phase nucleation and growth can then vary in their apparent microstructure from anisotropic to isotropic [150].

Increasing deposition temperature not only changes the grain structure in CVD deposits but also allows preferred orientations of growing crystals to form. Large crystal growth is due to the lower probability of atoms adsorbing on non-lattice sites and the increased mobility of chemisorbed atoms at elevated temperatures. These microstructure changes are readily seen in diamond [175], silicon nitride [176], and silicon carbide [177,178] deposits.

4.3 Chemical Composition and Impurity Content

Chemical composition in both CVD and PECVD processes is controlled by the precursor gases and the deposition process parameters. In CVD processes, the substrate temperature and the temperature of gases in the immediate vicinity of the substrate control the gas phase chemistry and dictate the chemical composition of the deposit. In PECVD processes, one must not only control the gas composition and substrate temperature but also the plasma parameters to control the chemical composition of the deposit. In both processes unwanted products of the deposition process can become encapsulated in the deposit. The quantity of

this contamination is dependent on the choice of precursor gases used in the deposition process [173,174,179–181]. An example of this can be seen from the effect of H_2/WF_6 ratio on the fluorine content of CVD tungsten (fig. 68). The quantity of contaminant in the deposit, for most of these deposition processes, is inversely proportional to the substrate temperature.

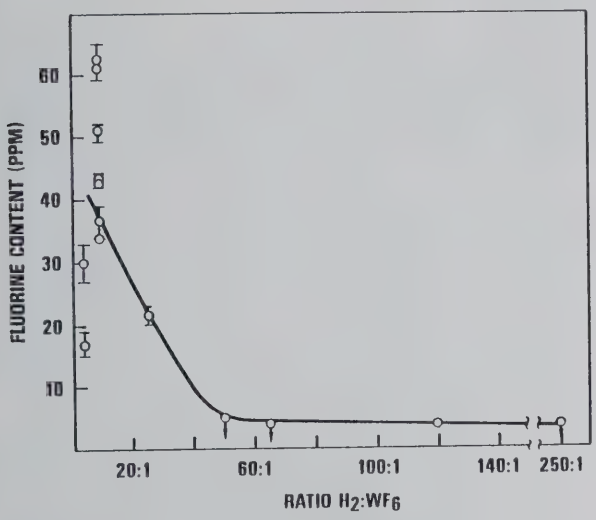

Figure 68. Effect of the ratio H_2/WF_6 on the fluorine content of CVD tungsten [38].

The ion current generated in a plasma differs for each gaseous species with pressure and with power into the plasma (fig. 69) [182]. Thus, in PECVD processes the power input to the plasma can have a direct influence on the gas phase chemistry [183] and hence the chemical composition of the deposit. In ECR-PECVD processes the presence of a bias voltage not only altered the Si/N ratio [184] in deposits made from SiH_4, but also the quantity of adsorbed hydrogen.

4.4 Stresses in Deposits

Intrinsic stresses in deposits can originate from differences in coefficients of thermal expansion between the substrate and deposit. Coefficients of thermal expansion must always be considered when depositing a coating. According to Powell [185], if the elastic modulus of the deposit is approximately equal to the elastic modulus of the substrate, $E_d \approx E_s$, and if the thickness of the deposit is much less than that of the substrate, then stress in the deposit is

$$\delta_d \approx E_d \Delta T(\alpha_s - \alpha_d), \tag{4}$$

where α_s and α_d are the coefficients of thermal expansion in the substrate and deposit, respectively, and ΔT is the temperature change from the deposition temperature. A positive sign indicates tensile

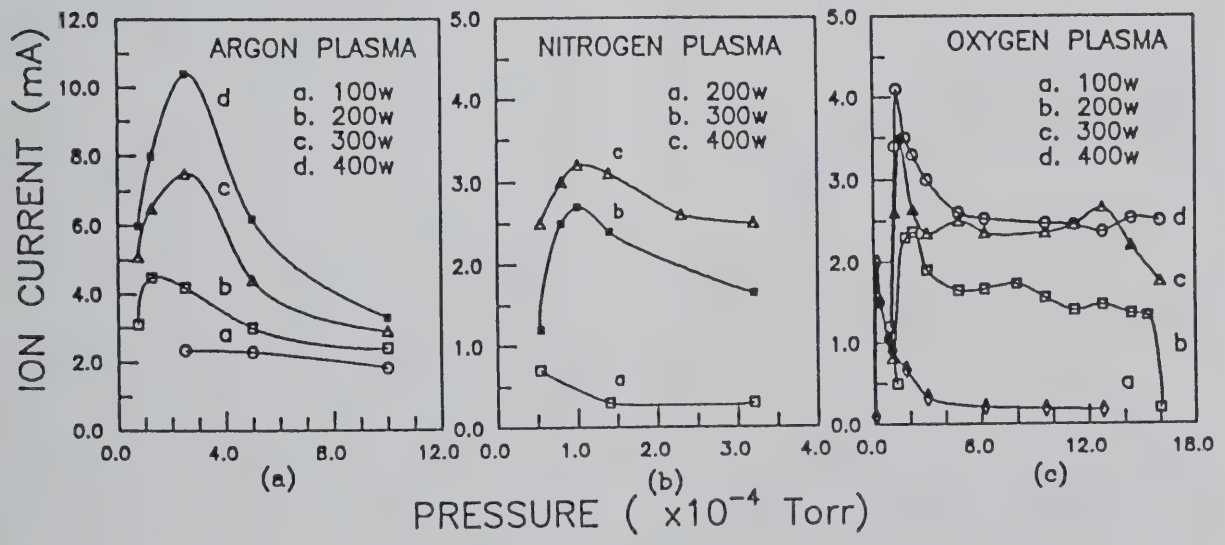

Figure 69. Effect of gas composition, gas pressure, and microwave power on the ion current in microwave ECR plasmas (after Hu et al., Ref. [182], reprinted with permission of The Electrochemical Society).

stress, a negative stress indicates compressive stress. Intrinsic stress is a stress which develops in all deposits in which the substrate is of a different material or different crystal structure than the deposit. The magnitude of these stresses can be especially large in CVD deposits where the deposition temperatures are high. An example is the 920 MPa compressive stress in Ti(C,N) films deposited on high-speed steel by a CVD process [186].

The source of intrinsic stresses can determine whether they are compressive or tensile. Intrinsic stresses develop from

- encapsulation of foreign atoms into the deposit [181,187–191],
- formation of disordered structures [181,187, 192–194],
- deposition of metastable phases [195],
- surface tension effects [185,191,196],
- the melting points of the deposit [197], and
- the molecular weights of the deposit and impinging ions on the substrate [198].

A common contaminant in CVD and LPCVD films is chlorine. Intrinsic compressive stresses in both SiO_2 and SiO_xN_y films were found to increase as the chlorine contents of the deposits increased [199]. PECVD processes are especially prone to the development of intrinsic stresses in the as-deposited films due to substrate biasing and encapsulation of contaminants. The low deposition temperatures used in PECVD processes generally increase the amount of encapsulated contaminant plus substrate biasing causes encapsulation of cations of both reactant gases and precursor diluents such as hydrogen and argon. Again, the result of these encapsulations is increased intrinsic compressive stresses in the deposit. Volume strain energy produced during the formation of grain boundaries in polycrystalline film formation and growth is another source of intrinsic compressive stress in vapor deposited films [196].

5. Technology Gaps

CVD and PECVD applications are expanding both in number and sophistication. The U.S. market in 1988 for CVD applications, as seen in Table 12, was 1.2 billion dollars [209]. Of that, 77.6% was for electronics applications. The annual growth of these vapor deposition markets is expected to range from 10–25% depending upon the application. The dominant expenditures for CVD and PECVD applications will continue to be in electronic applications. Annual expenditures for CVD and PECVD electronics applications are tied mostly to semiconductor sales. As Table 13 shows, United States semiconductor sales between 1988 and the forecasted end of 1993 will change from 13.42 to 20.42 billion [210]. It is not surprising that the major advances in CVD and PECVD technologies have come from developments for electronics applications. This trend is expected to continue. Recent developments in vapor deposition processes for composite materials, tribological applications, high temperature materials, optical films, and erosion protection, mirror past developments of the electronics industry. It is thus reasonable to assume that a significant amount of the processing information gained from electronic material developments can be used to guide developments for other CVD and PECVD applications.

Table 12. United States CVD Market

APPLICATION	1988 (MILLIONS)	1993 (PROJECTED, IN MILLIONS)
Chemical	12	19
Photovoltaic	17	34
Optoelectronics	42	140
Optical	55	167
Structural	145	233
Electronics	940	2330

Implementation of CVD and PECVD processing solutions to solve materials problems is forecasted to continue into the foreseeable future. Each new application of these vapor deposition technologies is expected to have its own development history. The degree of sophistication for each process development will depend on the demands of the final product. The reasons vapor deposition processes are chosen for most new applications are for the specialized property requirements of the final materials or the cost constrains for producing them. Examples of applications in which CVD and PECVD processing is being used, immediate concerns, and processing solutions are shown in Table 14. The diversity of vapor deposition processing solutions in these few examples shows one must ultimately tailor the fabrication method to the targeted properties of the final product. There is no universal CVD or PECVD research hardware, or production facility that solves all problems. However, with detailed end product goals, vapor deposition processing recommendations can be made to small organizations that should solve most of their current and immediate future needs.

Table 13. Semiconductor sales and trends

REGION	1988	1989	1990	1991	1992	1993 (forecast)
World wide	44.95	48.76	50.52	54.61	58.22	66.60
USA	13.42	14.83	14.45	15.38	17.60	20.42
Japan	18.11	19.15	19.56	29.94	19.90	21.78
Europe	8.05	8.94	9.60	10.11	10.63	11.67
Rest of world	5.37	5.85	6.91	8.18	10.06	12.73

While most technology gaps are application specific, there are those which are common to many CVD and PECVD applications. Listed in the paragraphs that follow are some of these generalized technology gaps.

5.1 Process Planning Through CVD and PECVD Modeling

CVD and PECVD processing are well known and are commercial realities for only a few materials and applications. Start up costs for new applications of CVD or PECVD technologies can be very expensive. There is a continuing need to minimize these start up costs. One way to reduce commercialization costs for new materials and applications is to develop models based on theoretical and experimental data which can be used to optimize the design of production vapor deposition systems before investments are made in their construction. Formation of the reactant gas mixture and mass transport of the reactant gases to the substrate are both dependent on CVD or PECVD system design and the targeted process parameters. Since each of these process steps influences the microstructure, composition, and properties of the deposit, they must be known and controlled. The more complex the process the more urgent is the need for modeling. Dynamic models show and experiments verify the complexity of the flow patterns and temperature profiles in both CVD and PECVD processes. While there is more experimental information relative to the development of CVD hardware than of PECVD hardware, the need to improve the reproducibility for both processes through system design optimization still exists.

Two vapor deposition process planning steps are aided by CVD and PECVD modeling. First process operating limits can be determined from thermodynamic and kinetic modeling. These calculations, together with available experimental data, should provide information about pressures, temperatures, precursor concentrations, plasma parameters and times needed to form the targeted material. Hardware configurations needed to provide the predetermined deposition environment can then be evaluated from fluid dynamic and plasma profile models. These models should provide information about gas flow patterns, allowable gas flows, temperature profiles, permissible time-temperature histories, plasma uniformity, and plasma parameter limits.

The data base used in thermodynamic and kinetic calculations is inadequate to permit reliable processing decisions for most CVD and PECVD applications. More comprehensive, updated data bases are needed to improve the reliability of thermodynamic and kinetic predictions. Improvements in predicting which process parameters will control the kinetics of the processes for most CVD and PECVD applications are needed through both experimental and theoretical studies.

The need exists to develop new ways of measuring the kinetics of vapor deposition processes. Modeling of kinetic processes, especially for plasma processes, are not as advanced as thermodynamic modeling. It is difficult to monitor the kinetics of vapor deposition processes experimentally and thus hard to verify kinetic model predictions with experimental results.

5.2 In-situ Process Monitoring

Where material properties are the prime concern of the vapor deposition application, trends in process development have been toward lower processing temperatures, lower reaction chamber pressures, better control of contaminants in the deposition reactor, and improved in-situ diagnostics to control the deposition process. For most new applications of CVD and PECVD technologies, it is imperative that one controls the nucleation, chemistry, microstructure, and growth rate of the deposit. In spite of past developments, deposition conditions for most CVD and PECVD processes are quite variable with processing time and

Table 14. Examples of current and forecasted CVD and PECVD development trends

APPLICATION	CURRENT DEVELOPMENT CONCERNS (PARTIAL LIST)	PROCESSING SOLUTIONS, (CURRENT OR FUTURE FORECASTED)
Semiconductor wafers	Step coverage. Particle contaminations.	LPCVD, ECR-PECVD processes.
	Uniformity of properties. Minimum feature size.	Ultra-clean facilities, cluster deposition systems
	Trench filling.	Single wafer processing. Cluster deposition systems. In-situ monitoring of process parameters and contamination. PECVD, TEOS based precursors.
Tribology	Adhesion and compatibility, coating to substrate.	Intermediate coating materials.
	CTE match, coating to substrate.	Functionally graded hard coatings.
	Friction, coating to work piece.	Outer layer materials.
Corrosion barrier coatings	Al_2O_3, TiN, TiC, coatings for AISI403 SS erosion/corrosion protection	PECVD multilayers.
	Low cost Ti-based and silicide coatings for copper tubing.	Fluidized mixed powders of Ti or Si with $CuCl_2$, H_2, and HCl.
Diamond films	Nucleation uniformity.	Mechanical abrasion, electron or ion beam processing.
	Graphite inclusions.	Precursors containing oxygen or a halide.
	Adhesion to substrates.	Interface materials.
Composite materials	Infiltration of matrix materials.	Thermal and/or pressure gradient processing.
	Matrix/fiber interface compatibility.	Filament coatings.
	Oxidation resistance.	Filament or composite coatings.
Optical films	Precise thickness control.	In-situ monitoring of LPCVD processes.
	Color control in ZnS infrared windows.	High temperature, high H_2S/Zn molar ratio.
High T_c materials	Multicomponent codeposition.	β-diketonate chelate precursors.
	Low contamination, controlled microstructure.	LPCVD processing.

Table 14. Examples of current and forecasted CVD and PECVD development trends—Continued

APPLICATION	CURRENT DEVELOPMENT CONCERNS (PARTIAL LIST)	PROCESSING SOLUTIONS, (CURRENT OR FUTURE FORECASTED)
In-core thermionic emitters	Fast neutron tolerance.	Low F_2 content tungsten from WF_6.
	High work function surface.	[110] Tungsten from WCl_x.
CdTe photovoltaic films	Deposition temperature. Thickness uniformity, stoichiometry, pinholes, porosity.	MOCVD 400 °C. CVD from vaporization of precursors at 700 °C.
Amorphous Si:H photovoltaics	Large area, uniformity, composition.	PECVD processing.
	Light induced degradation.	a-SiC:H interlayer deposition.
Fusion first wall materials	Damage tolerance to high energy plasma particle impacts.	TiC or SiC coated graphite tiles.
High temperature gas cooled reactor fuel coatings	Stability to thermal neutron damage.	Isotropic, fluidized bed CVD C.
	Fission product retention.	Isotropic C, SiC.
	Fuel swelling tolerance.	Porous C fuel/coating. Interface layer.
Medical products	Wear resistance, (heart valves).	Fluidized bed CVD C, C-Si alloys.
	Hardness, wear resistance, (teeth).	TiN coated Co, Nb, Ti, Co alloys.
	Thromboresistance, (heart valves).	C, C-Si alloys.
	Biocompatibility, (teeth).	TiO_2, TiN multilayers on Ti.

location along the substrate-gas interface. Even on a macroscopic scale, the properties of thick film deposits can be quite different from point to point on the substrate. Reproducible CVD or PECVD processing can be achieved only if one knows the temperature, pressure, and gas composition in the near region of the precursor gas-substrate interface and can control the parameters critical to the deposition process. In CVD processing this means in-situ monitoring and controlling temperatures, precursor gas composition, deposition chamber pressure, and flow dynamics during the deposition process. For PECVD processes one must not only monitor and control temperatures, precursor gases, and deposition chamber pressures, but also the plasma properties of electron density, electron energy distribution, plasma frequency, and the mean free path for electron-neutral collisions.

New in-situ diagnostic techniques are needed to monitor process parameters during CVD and PECVD processing. The challenge is to determine temperature plasma properties and gas flow profiles at the gas-substrate interface and to develop in-situ diagnostics to monitor gas phase and substrate-gas phase reactions. Different materials and processes will require different solutions to in-situ diagnostics and process control. Control of plasma properties at the plasma-substrate interface in most PECVD processes is especially difficult and remains as the main barrier to the commercialization of ECR-PECVD processing. Some successes are being reported in these areas, especially

through the use of newer plasma sources where control of plasma density is separated from control of ion impact energies, but more work is needed.

5.3 Process Costs, Environmental Sensitivity

There is a generalized need to improve product properties and lower processing costs. For most applications this translates to lower deposition temperatures, improved deposition uniformity, better control of composition, reduced impurity contents, and higher production yields. These goals are being achieved for a few materials by reducing pressures in CVD processes and using organometallic in both CVD and PECVD processes to replace traditional halide precursors in the deposition processes. The replacement of traditional halide precursors with organometallic precursors lowers the temperature of the deposition processes and replaces these chemical hazards with materials that are less destructive to the environment. This potentially lowers costs by reducing the amount of waste removal hardware needed in the production process. Several problems must be addressed in a switch to organometallic precursors. These include the need to develop new organometallic materials with appropriate vapor pressures for use in vapor deposition processes and the need to minimize contamination of the of the deposit resulting from the decomposition and encapsulation of precursor fragments.

Developments of new plasma sources are needed. Traditional RF plasmas have limited plasma densities and operating pressures. Microwave plasma sources pose uncertain health hazards and require large magnets, microwave wave guides and complex field coils. Control of plasma properties and plasma uniformity over large area substrates is the goal of present day plasma source developments. Meeting these goals would not only improve the properties of the materials produced with these sources but would also lower processing costs. Work is being done on the development of helicon plasma sources, continuous, modulated, and distributed ECR's, and inductively coupled discharges. No plasma source is best for all PECVD applications. Thus the need for new plasma sources is likely to continue.

5.4 Automated CVD and PECVD Processing

Minimizing contamination from the products of CVD and PECVD processing is an unending quest. In the semiconductor industry particle contamination is a major concern. The size of a particle contaminant determines the minimum size of a wafer feature that is influenced by it. Particles >10% of a feature size are normally a wafer killer. The maximum allowable particle size of a contaminant in the year 2002 is projected to be 0.02 μm. Conventional sequential processing where wafers are hand carried from one process station to another cannot meet this particle size limit. Wafer transport, geometry of the deposition chamber, gas flows, moving parts above the substrate, gas turbulence, and vibration can all be sources of particle contamination. To overcome this, cluster tooling has been developed in which each processing step is done in a separate module. The modules are joined together to allow automated transfer between modules without removing the wafer from the system. CVD cluster systems are not cheap, costing about $1,000,000 for a three module array. These systems have been in use since 1985 and have taken 2–3 years to develop. What is needed for the electronics industry is standardization of the cluster modules and the module interfaces. All aspects of cluster tooling are being upgraded and the targeted minimum particle contamination levels are possible with these systems.

It is likely that some form of cluster tooling will be appropriate and needed for other CVD and PECVD applications. Formation of deposits for photovoltaics, functionally graded materials, high T_c superconductors, and nanostructure multicomponent materials are examples of applications which might benefit from cluster processing.

6. Comments

This chapter has discussed the variability one might expect to find in CVD and PECVD processes and in the properties of deposits that result from them. The intent of this effort was to direct readers to those processes which might be most appropriate for their needs. To aid in the understanding of CVD processes, thermodynamic, fluid dynamic, and kinetic model studies have paralleled experimental developments. While sometimes imprecise because of simplifying assumptions, these models have nevertheless provided insight into the control of the chemical composition, microstructure, and properties of CVD deposits.

Experimenters have examined alternative processes to reach the improvements sought in CVD deposits. One of these processes is PECVD. Achievement of these improvements by PECVD

processes requires not only control of temperatures, pressures, gas composition, and gas flows but also improvements in the control of the plasma properties. Plasma properties of mean free path, collision frequency, electron energies, and electron energy distributions must all be controlled to control ion energy distributions, density, and direction. These controls are being sought by optimization of plasma frequencies, utilization of magnetic fields, and development of models to guide the design of PECVD systems.

While experimental trials can provide estimates of temperature profiles and gas velocity distributions within CVD and PECVD systems, these conditions are everchanging with adjustments in temperatures, pressures, gas flows, and plasma properties. The most practical way of overcoming these uncertainties is to design the deposition system to operate under conditions which will minimize nonuniformity in gas flows, temperature profiles, and plasma properties at the substrate-reactive gas interface. This usually means low pressure (<100 Torr) operation. For many vapor deposition applications, this is acceptable.

This chapter has attempted to clarify the reasons for selecting either CVD or PECVD and the types of systems needed to utilize these processes. Once a few fundamentals of each of these processes are understood, and the advantages and limitations of each process are known, process judgements can be made concerning the applicability of each technology to the needs of your organization. When one reviews the work of others, it is obvious that these processes are fundamentally very complex. Careful thought should be given to the selection of a process and deposition system before buying even a "turn key" deposition system. A few guidelines which might be helpful in selecting a process and system are:

1. Let the material to be deposited, the properties needed from this material, and the substrate upon which it is to be deposited dictate the process selected to form the material.
2. When several vapor deposition processes appear equivalent, screen recent literature studies to determine which process most nearly matches the expertise, time, and cost constraints of your organization. If CVD or PECVD is the process of choice for the material to be deposited, and relevant experimental information is available, let these studies guide the process parameter and equipment selection.
3. Allow for equipment modifications as you gain experience in the operation of the deposition system.
4. Be aware that there is no universal deposition process that is best for all deposition applications and there is no universal equipment that meets the requirements of the spectrum of deposition variables critical to the formation of all materials formed by either CVD or PECVD processes.
5. Consider that the cost gain from attempts at increasing either the types of materials, substrate sizes, or number of the parts that can be processed in one deposition system is often lost in the complexity and cost of operating that system.

7. References

[1] C. F. Powell, J. H. Oxley, and J. M. Blocher Jr., Vapor Deposition, John Wiley and Sons, New York (1966).

[2] R. C. Bracken, Chemical Vapor Deposition, Second International Conference, J. M. Blocher, Jr. and J. C. Withers, eds., Electrochemical Society, New York (1970), pp. 731–752.

[3] S. Mendelson, Chemical Vapor Deposition, Second International Conference, J. M. Blocher, Jr. and J. C. Withers, eds., Electrochemical Society, New York (1970), pp. 753–765.

[4] H. B. Pogge, D. W. Boss, and E. Ebert, Chemical Vapor Deposition, Second International Conference, J. M. Blocher, Jr. and J. C. Withers, eds., Electrochemical Society, New York (1970), pp. 767–793.

[5] W. Kern and V. S. Ban, Thin Film Processes, J. L. Vossen and W. Kern, eds., Academic Press, Inc., Orlando, FL (1978), pp. 309–315.

[6] B. E. Barry, Thin Solid Films **39**, 35–53 (1976).

[7] W. Ruppert, The Third International Conference on Chemical Vapor Deposition, F. A. Glaski, ed., American Nuclear Society, Hinsdale, IL (1972), pp. 340–351.

[8] H. E. Hintermann, H. Gass, and J. N. Lindstrom, The Third International Conference on Chemical Vapor Deposition, F. A. Glaski, ed., American Nuclear Society, Hinsdale, IL (1972), pp. 352–368.

[9] J. J. Nickl, M. Reiche, R. Vesper, and A. Weiss, The Third International Conference on Chemical Vapor Deposition, F. A. Glaski, ed., American Nuclear Society, Hinsdale, IL (1972), pp. 369–382.

[10] R. Ljungqvist, The Third International Conference on Chemical Vapor Deposition, F. A. Glaski, ed., American Nuclear Society, Hinsdale, IL (1972), pp. 383–396.

[11] G. W. Wakefield and J. A. Bloom, The Third International Conference on Chemical Vapor Deposition, F. A. Glaski, ed., American Nuclear Society, Hinsdale, IL (1972), pp. 397–403.

[12] J. R. Peterson, J. Vac. Sci. Technol. **11** (4), 715–718 (1974).

[13] H. O. Pierson, Thin Solid Films **40**, 41–47 (1977).

[14] W. Ruppert, Thin Solid Films **40**, 27–40 (1977).

[15] J. R. Rairden and M. R. Jackson, Thin Solid Films **40**, 291–298 (1977).
[16] P. C. Felix and H. Beutler, The Third International Conference on Chemical Vapor Deposition, F. A. Glaski, ed., American Nuclear Society, Hinsdale, IL (1972), pp. 600–617.
[17] W. Hanni and H. E. Hintermann, Thin Solid Films **40**, 107–114 (1977).
[18] J. B. Stephenson, D. M. Soboroff, and H. O. Mcdonald, Thin Solid Films **40**, 73–80 (1977).
[19] G. A. Saltzman, Thin Solid Films **39**, 287–295 (1976).
[20] B. O. Seraphin, Thin Solid Films **39**, 87–94 (1976).
[21] B. Lalevic, G. Tailor, and W. Slusark, Jr., Thin Solid Films **39**, 143–154 (1976).
[22] R. L. Auble, J. K. Bair, D. M. Galbraith, C. M. Jones, P. H. Stelson, and D. C. Weisser, Nuclear Instruments and Methods **177**, 289–294 (1980).
[23] D. W. Johnson, Jr., Am. Ceram. Soc. Bull. **60** (2), 221–224 (1981).
[24] W. M. Shen and C. F. Chang, Advances in Ceramics, Ceramic Powder Science, Vol. 21, G. L. Messing, K. S. Mazdiyasni, J. W. McCauley, and R. A. Haber, eds., American Ceramic Society, Westerville, Ohio (1987), pp. 193–201.
[25] A. Kato, Advances in Ceramics, Ceramic Powder Science, Vol. 21, G. L. Messing, K. S. Mazdiyasni, J. W. McCauley, and R. A. Haber, eds., American Ceramic Society, Westerville, OH (1987), pp. 181–192.
[26] J. A. Venables, J. Vac. Sci. Technol. **B4** (4), 870–873 (1986).
[27] Y. Pauleau, A. Bouteville, J. J. Hantzpergue, J. C. Remy, and A. Cachard, J. Electrochem. Soc. **129** (5), 1045–1052 (1982).
[28] H. J. Kim, Y. Egashira, and H. Komiyama, Appl. Phys. Lett. **59** (20), 2521–2523 (1991).
[29] W. J. Lackey and T. L. Starr, Fiber Reinforced Ceramic Composites, K. S. Mazdiyasni, ed., Noyes Publications, Park Ridge, NJ (1990), pp. 397–450.
[30] R. R. Melkote and K. F. Jensen, Chemical Vapor Deposition of Refractory Metals and Ceramics, T. M. Besmann and B. M. Gallois, eds., MRS Symposia Proceedings, Vol. 168, Materials Research Society, Pittsburgh, PA (1990), pp. 67–72.
[31] S. M. Gupte and J. A. Tsamopoulos, J. Electrochem. Soc. **136** (2), 555–561 (1989).
[32] A. Lachter, M. Trinquecoste, and P. Delhaes, Carbon **23** (1), 111–116 (1985).
[33] O. Levesque, M. Trinquecoste, and P. Delhaes, Twentieth Biennial Conference on Carbon Extended Abstracts, American Carbon Society, Pennsylvania State University, University Park, PA (1991), pp. 374–375.
[34] J. Chin, A. F. Weinberg, and J. R. Lingren, General Atomic Report GA-7324, 1966.
[35] A. F. Weinberg, J. R. Lindgren, and R. G. Mills, General Atomic Report GA-6473, 1965.
[36] F. J. Huegel and W. R. Holman, Chemical Vapor Deposition, Second International Conference, J. M. Blocher, Jr. and J. C. Withers, eds., Electrochemical Society, New York (1970), pp. 171–191.
[37] L. Yang, R. G. Hudson, T. Tagami, and J. W. R. Creagh, 1968 Thermionic Conversion Specialist Conference, Institute of Electrical and Electronics Engineers (1968), pp. 31–40.
[38] J. Chin and J. Horsley, 1968 Thermionic Conversion Specialist Conference, Institute of Electrical and Electronics Engineers (1968), pp. 51–59.
[39] J. I. Federer, W. C Robinson, and R. M. Steele, 1967 Thermionic Conversion Specialist Conference, Institute of Electrical and Electronics Engineers (1967), pp. 287–295.
[40] R. G. Hudson, T. Tagami, and L. Yang, Second International Conference on Thermionic Electric Power Generation, Stresa, Italy (1968), pp. 565–573.
[41] F. A. Glaski, Chemical Vapor Deposition, Second International Conference, J. M. Blocher, Jr. and J. C. Withers, eds., Electrochemical Society, New York (1970), pp. 839–858.
[42] J. C. Bokros, W. V. Goeddel, J. Chin, and R. J. Price, U.S. Patent, 3,298,921 (1967).
[43] W. V. Goeddel, C. S. Luby, and J. Chin, U.S. Patent, 3,335,063 (1967).
[44] J. Chin, C. S. Luby, and R. G. Mills, U.S. Patent, 3,649,452 (1972).
[45] L. H. Ford, N. S. Hibbert, and D. G. Martin, J. Nucl. Mat. **45**, 139–149 (1972).
[46] T. Koyama, M. Endo, and Y. Onuma, Japan J. Appl. Phys. **11** (4), 445–449 (1972).
[47] A. Oberlin and M. Endo, J. Cryst. Growth **32**, 335–349 (1976).
[48] G. G. Tibbetts, Appl. Phys. Lett. **42** (8), 666–668 (1983).
[49] J. J. Petrovic and G. F. Hurley, Fiber Reinforced Ceramic Composites, K. S. Mazdiyasni, ed., Noyes Publications, Park Ridge, NJ (1990), pp. 93–121.
[50] J. Bloom, Y. S. Oei, H. H. C. de Moor, J. H. L. Hanssen, and L. J. Giling, J. Electrochem. Soc. **132** (8), 1973–1985 (1985).
[51] K. Sugawara, R. Takahashi, H. Tochikubo, and Y. Koga, Chemical Vapor Deposition, Second International Conference, J. M. Blocher, Jr. and J. C. Withers, eds., Electrochemical Society, New York (1970), pp. 713–729.
[52] M. L. Hammond, Solid State Technol. **31** (5), 159–164 (1988).
[53] L. Jastrzebski, J. F. Carboy, J. T. McGinn, and R. Pagliaro, Jr., J. Electrochem. Soc. **130** (7), 1571–1580 (1983).
[54] G. N. Parsons, Appl. Phys. Lett. **59** (20), 2546–2548 (1991).
[55] G. Lucovsky, D. V. Tsu, and R. J. Markunas, Plasma Processing, MRS Symposia Proceedings, Vol. 68, J. W. Coburn, R. A. Gottscho, and D. W. Hess, eds., Materials Research Society, Pittsburgh, PA (1986), pp. 323–334.
[56] G. N. Parsons, D. V. Tsu, and G. Lucovsky, J. Vac. Sci. Technol. **A6** (3), 1912–1916 (1988).
[57] D. Landheer, N. G. Skinner, T. E. Jackman, D. A. Thompson, J. G. Simmons, D. V. Stevanovic, and D. Khatamian, J. Vac. Sci. Technol. **A9** (5), 2594–2601 (1991).
[58] R. P. Gower and J. Hill, Chemical Vapor Deposition, Fifth International Conference, J. M. Blocher, Jr., H. E. Hintermann, and L. H. Hall, eds., Electrochemical Society, Inc., Princeton, NJ (1975), pp. 114–129.
[59] K. E. Spear, Chemical Vapor Deposition, Ninth International Conference, McD. Robinson, C. H. J. van den Brekel, G. W. Cullen, J. M. Blocher, Jr., and P. Rai-Choudhury, eds., Electrochemical Society, Inc., Pennington, NJ (1984), pp. 81–97.

[60] K. Spear and R. R. Dirkx, Chemical Vapor Deposition of Refractory Metals and Ceramics, T. M. Besmann and B. M. Gallois, eds., MRS Symposia Proceedings, Vol. 168, Materials Research Society, Pittsburgh, PA (1990), pp. 19–30.

[61] C. Bernard, Chemical Vapor Deposition, Eighth International Conference, J. M. Blocher, Jr., G. E. Vuillard, and G. Wahl, eds., Electrochemical Society, Inc., Pennington, NJ (1981), pp. 3–16.

[62] K. E. Spear, Chemical Vapor Deposition, Seventh International Conference, T. O. Sedgwick and H. Lydtin, eds., Electrochemical Society, Inc., Pennington, NJ (1979), pp. 1–16.

[63] K. E. Spear and M. S. Wang, Solid State Technology **21** (7), 63–68 (1980).

[64] C. Bernard and R. Madar, Surf. Coat. Technol. **49**, 208–214 (1991).

[65] C. Bernard and R. Madar, Chemical Vapor Deposition of Refractory Metals and Ceramics, T. M. Besmann and B. M. Gallois eds., MRS Symposia Proceedings Vol. 168, Materials Research Society, Pittsburgh, PA (1990), pp. 3–17.

[66] A. I. Kingon, L. J. Lutz, P. Liaw, and R. F. Davis, J. Am. Ceram. Soc **66** (8), 558–566 (1983).

[67] D. E. Rosner and J. Collins, Chemical Vapor Deposition of Refractory Metals and Ceramics, T. M. Besmann and B. M. Gallois, eds., MRS Symposia Proceedings, Vol. 168, Materials Research Society, Pittsburgh, PA (1990), pp. 43–48.

[68] A. I. Kingon, L. J. Lutz, and R. F. Davis, J. Amer. Ceram. Soc. **66** (8), 551–557 (1983).

[69] K. G. Nickel, R. Riedel, and G. Petzow, J. Amer. Ceram. Soc. **72** (10), 1804–1810 (1989).

[70] T. S. Moss, J. A. Hanagofsky, and W. J. Lackey, J. Mater. Res. **7** (3), 754–764 (1992).

[71] T. M. Bessmann, J. Am. Ceram. Soc. **69** (1), 69–74 (1986).

[72] S. Gordon and B. J. McBride, NASA SP-273, 1971.

[73] S. A. Gokoglu, Chemical Vapor Deposition, Eleventh International Conference, K. E. Spear and G. W. Cullen, eds., Electrochemical Society, Inc., Pennington, NJ (1990), pp. 1–9.

[74] C. H. J. van den Brekel, Chemical Vapor Deposition, Eighth International Conference, J. M. Blocher, Jr., G. E. Vuillard, and G. Wahl, eds., Electrochemical Society, Inc., Pennington, NJ (1981), pp. 116–127.

[75] T. S. Cale and G. B. Raupp, J. Vac. Sci. Technol. **B8** 8 (6), 1242–1248 (1990).

[76] A. E. T. Kuiper, C. H. J. van den Brekel, J. de Groot, and G. W. Veitkemp, J. Electrochem. Soc. **129** (10), 2288–2291 (1982).

[77] M. H. J. de Croon and L. J. Giling, J. Electrochem. Soc. **137** (9), 2867–2876 (1990).

[78] M. H. J. de Croon and L. J. Giling, J. Electrochem. Soc. **137** (11), 3606–3612 (1990).

[79] K. Watanabe and H. Komiyama, J. Electrochem. Soc. **137** (4), 1222–1227 (1990).

[80] J. D. Chapple-Sokol, C. J. Giunta, and R. G. Gordon, J. Electrochem. Soc. **136** (10), 2993–3003 (1989).

[81] C. H. J. van den Brekel, R. M. M. Fonville, P. J. M. van der Straten, and G. Verspui, Chemical Vapor Deposition, Eighth International Conference, J. M. Blocher, Jr., G. E. Vuillard, and G. Wahl, eds., Electrochemical Society, Inc., Pennington, NJ (1981), pp. 142–156.

[82] H. Lydtin, Chemical Vapor Deposition, Second International Conference, J. M. Blocher, Jr. and J. C. Withers, eds., Electrochemical Society, New York (1970), pp. 71–88.

[83] H. Lydtin, Presentation at the third International Conference on Chemical Vapor Deposition in Salt Lake City, April, 1972.

[84] A. Yeckel, S. Middleman, and A. K. Hochberg, J. Electrochem. Soc. **136** (7), 2038–2050 (1989).

[85] H. Rebenne and R. Pollard, J. Am. Ceram. Soc., **70** (12), 907–918 (1987).

[86] R. Arora and R. Pollard, J. Electrochem Soc. **138** (5), 1523–1537 (1991).

[87] M. L. Hitchman, Chemical Vapor Deposition, Seventh International Conference, T. O. Sedgwick, and H. Lydtin, eds., Electrochemical Society, Inc., Pennington, NJ (1979), pp. 59–73.

[88] H. Tanji and K. Monden, Chemical Vapor Deposition, Seventh International Conference, T. O. Sedgwick, and H. Lydtin, eds., Electrochemical Society, Inc., Pennington, NJ (1979), pp. 562–569.

[89] W. D. Partlow and L. E. Kline, Plasma Processing, MRS Symposia Proceedings, Vol. 68, J. W. Coburn, R. A. Gottscho, and D. W. Hess, eds., Materials Research Society, Pittsburgh, PA (1986), pp. 309–319.

[90] T. A. Cleland and D. W. Hess, J. Electrochem Soc. **136** (10), 3103–3111 (1989).

[91] J. H. Comfort and R. Reif, J. Electrochem. Soc. **136** (8), 2386–2398 (1989).

[92] J. H. Comfort and R. Reif, J. Electrochem. Soc. **136** (8), 2398–2405 (1989).

[93] R. Takahashi, Y. Koga, and K. Sugawara, J. Electrochem Soc. **119** (10), 1406–1412 (1972).

[94] H. K. Moffat and K. F. Jensen, J. Electrochem. Soc. **135** (2), 459–471 (1988).

[95] W. L. Holstein, J. Electrochem. Soc. **135** (7), 1168–1173 (1988).

[96] M. E. Coltrin, R. J. Kee, and Greg H. Evans, J. Electrochem. Soc. **136** (3), 819–829 (1989).

[97] F. C. Eversteyn, P. J. Severin, C. H. J. v. d. Brekel, and H. L. Peek, J. Electrochem. Soc. **117** (7), 925–931 (1970).

[98] J. H. Scholtz and V. Hlavacek, J. Electrochem. Soc. **137** (11), 3459–3469 (1990).

[99] T. S. Cale, M. K. Jain, and G. B. Raupp, J. Electrochem. Soc. **137** (5), 1526–1533 (1990).

[100] G. Wahl, Thin Solid Films **40**, 13–26 (1977).

[101] G. Wahl and R. Hoffmann, Rev. Int. Hautes Temper. Refract., Fr. **17**, 7–22 (1980).

[102] G. Wahl, Chemical Vapor Deposition, Ninth International Conference, McD. Robinson, C. H. J. van den Brekel, G. W. Cullen, J. M. Blocher, Jr., and P. Rai-Choudhury, eds., Electrochemical Society, Inc., Pennington, NJ (1984), pp. 60–77.

[103] J. Juza and J. Cermak, J. Electrochem. Soc. **126** (7), 1627–1634 (1982).

[104] H. Rebenne and R. Pollard, J. Electrochem. Soc. **132** (8), 1932–1939 (1985).

[105] K. F. Jensen and D. B. Graves, J. Electrochem. Soc. **130** (9), 1950–1957 (1983).

[106] Y. He and Y. Sahai, Chemical Vapor Deposition, Tenth International Conference, G. W. Cullen and J. M. Blocher, Jr., eds., Electrochemical Society, Inc., Pennington, NJ (1987), pp. 193–203.

[107] D. I. Fotiadis and K. F. Jensen, Chemical Vapor Deposition, Eleventh International Conference, K. E. Spear and G. W. Cullen, eds., Electrochemical Society, Inc., Pennington, NJ (1990), pp. 92–98.
[108] P. Duverneuil and Jean-Pierre Couderc, J. Electrochem. Soc. **139** (1), 296–304 (1992).
[109] C. Azzaro, P. Duverneuil, and Jean-Pierre Couderc, J. Electrochem. Soc. **139** (1), 305–312 (1992).
[110] A. Yeckel and S. Middleman, J. Electrochem. Soc. **137** (1), 207–212 (1990).
[111] Kuan-Cheng Chiu and F. Rosenberger, Chemical Vapor Deposition, Tenth International Conference, G. W. Cullen and J. M. Blocher, Jr., eds., Electrochemical Society, Inc., Pennington, NJ (1987), pp. 175–180.
[112] T. Nyce and F. Rosenberger, Chemical Vapor Deposition, Eleventh International Conference, K. E. Spear and G. W. Cullen, eds., Electrochemical Society, Inc., Pennington, NJ (1990), pp. 53–60.
[113] M. E. Coltrin, R. J. Kee, and J. A. Miller, Chemical Vapor Deposition, Ninth International Conference, McD. Robinson, C. H. J. van den Brekel, G. W. Cullen, J. M. Blocher, Jr., and P. Rai-Choudhury, eds., Electrochemical Society, Inc., Pennington, NJ (1984), pp. 31–43.
[114] J. A. Thornton, Deposition Technologies for Films and Coatings, R. F. Bunshah, ed., Noyes Publications, Park Ridge, NJ (1982), pp. 19–62.
[115] M. J. Rand, J. Vac. Sci. Technol. **16** (2), 420–427 (1979).
[116] J. L. Vossen and J. J. Cuomo, Thin Film Processes, J. L. Vossen and W. Kern, eds., Academic Press, Inc., San Diego, CA (1978), pp. 25–31.
[117] S. M. Rossnagel, Thin Film Processes II, J. L. Vossen and W. Kern, eds., Academic Press, Inc., San Diego, CA (1991), pp. 11–77.
[118] K. S. Fancey and A. Matthews, Surface and Coatings Technologies **33**, 17–29 (1987).
[119] M. Moisan, C. Barbeau, R. Claude, C. M. Ferreira, J. Margot, J. Paraszczak, A. B. Sa, G. Sauve, and M. R. Wertheimer, J. Vac. Sci. Technol. **B9** (1), 8–25 (1991).
[120] D. L. Flamm, J. Vac. Sci. Technol. **A4** (3), 729–738 (1986).
[121] P. L. Colestock, J. Vac. Sci. Technol. **A6** (3), 1975–1983 (1988).
[122] C. M. Ferreira and L. Loureiro, J. Phys. D: Appl. Phys. **17**, 1175–1188 (1984).
[123] W. M. Hobler and J. Foster, J. Vac. Sci. Technol. **A6** (5), 3720–3725 (1990).
[124] S. Samukawa, S. Mori, and M. Sasaki, J. Vac. Sci. Technol. **A9** (1), 85–90 (1991).
[125] J. B. O. Caughman II and W. M. Hobler, J. Vac. Sci. Technol. **A9** (6), 3113–3118 (1991).
[126] R. A. Dandl and G. E. Guest, J. Vac. Sci. Technol. **A9** (6), 3119–3125 (1991).
[127] S. Miyake, W. Chen, and Y. Kawai, Appl. Phys. Lett. **59** (18), 2234–2236 (1991).
[128] M. Matsuoka and K. Ono, J. Vac. Sci. Technol. **A6** (1), 25–29 (1988).
[129] M. Dahimene and J. Asmussen, J. Vac. Sci. Technol. **B4** (1), 126–130 (1986).
[130] P. Kidd, J. Vac. Sci Technol. **A9** (3), 466–473 (1991).
[131] S. Pongratz, R. Geshe, K.-H. Kretschmer, G. Lorenz, M. Hafner, and J. Zink, J. Vac. Sci. Technol. **B6** (6), 3493–3497 (1991).
[132] O. M. Kuttel, J. E. Klemberg-Sapieha, L. Martinu, and M. R. Wertheimer, Thin Solid Films **193**, 155–163 (1990).
[133] E. Nasser, Fundamentals of Gaseous Ionization and Plasma Electronics, Wiley-Interscience, New York (1971), pp. 188–423.
[134] D. J. Economou, D. R. Evans, and R. C. Alkire, J. Electrochem. Soc. **135** (3), 756–763 (1988).
[135] M. R. Wertheimer and M. Moisan, J. Vac. Sci. Technol. **A3** (6), 2643–2649 (1985).
[136] S. V. Nguyen and K. Albaugh, J. Electrochem. Soc. **136** (10), 2835–2840 (1989).
[137] W. A. P. Claassen, W. G. J. N. Valkenburg, F. H. P. M. Habraken, and Y. Tamminga, J. Electrochem. Soc. **130** (12), 2419–2423 (1983).
[138] A. Piccirillo and A. L. Gabbi, J. Electrochem. Soc. **137** (12), 3910–3917 (1990).
[139] R. S. Rosler, W. C. Benzing, and J. Baldo, Solid State Technol. **19** (6), 45–50 (1976).
[140] E. P. G. T. van de Ven, Solid State Technol. **25** (4), 167–171 (1981).
[141] M. Surendra and D. B. Graves, Appl. Phys. Lett. **59** (17), 2091–2093 (1991).
[142] J. Wagner, C. H. Wild, A. Bubenzer, and P. Koidl, Plasma Processing, MRS Symposia Proceedings, Vol. 68, J. W. Coburn, R. A. Gottscho, and D. W. Hess, eds., Materials Research Society, Pittsburgh, PA (1986), pp. 205–210.
[143] Y. L. Khait, A. Inspektor, and R. Avni, Thin Solid Films **72**, 249–260 (1980).
[144] S. Veprek, Pure and Appl. Chem. **48** (2), 163–178 (1976).
[145] M. H. Cho, N. Hershkowitz, and T. Intrator, J. Vac. Sci. Technol. **A6** (5), 2978–2986 (1988).
[146] D. B. Graves and K. F. Jensen, Plasma Processing, MRS Symposia Proceedings, Vol. 68, J. W. Coburn, R. A. Gottscho, and D. W. Hess, eds., Materials Research Society, Pittsburgh, PA (1986), pp. 219–230.
[147] D. B. Graves, J. Appl. Phys. **62** (1), 88–94 (1987).
[148] H. Fujiyama, H. Kawasaki, Y. Matsuda, and N. Ohno, Plasma Processing and Synthesis of Materials III, MRS Symposia Proceedings, Vol. 190, D. Apelian and J. Szekely, eds., Materials Research Society, Pittsburgh, PA (1990), pp. 161–166.
[149] E. Hyman, K. Tsang, I. Lottati, A. Drobot, B. Lane, R. Post, and H. Sawin, Surface Coatings and Technol. **49**, 387–393 (1991).
[150] J. C. Bokros, Carbon **3**, 17–29 (1965).
[151] D. V. Tsu, G. N. Parsons, and G. Lucovsky, J. Vac. Sci. Technol. **A6** (3), 1649–1654 (1988).
[152] P. K. Shufflebotham and D. J. Thompson, J. Vac. Sci. Technol. **A8** (5), 3713–3719 (1990).
[153] C. Charles, R. W. Boswell, and R. K. Porteous, J. Vac. Sci. Technol. **A10** (2), 398–403 (1992).
[154] J. E. Heidenreich III, J. R. Parazczak, M. Moisan, and G. Sauve, J. Vac. Sci. Technol. **B5** (10), 347–354 (1987).
[155] B. Anthony, T. Hsu, L. Breauk, R. Qian, S. Banerjee, and A. Tasch, Plasma Processing and Synthesis of Materials III, MRS Symposia Proceedings, Vol. 190, D. Apelian and J. Szekely, eds., Materials Research Society, Pittsburgh, PA (1990), pp. 267–272.
[156] R. W. Clements, J. Vac. Sci. Technol. **15** (2), 193–198 (1978).
[157] J. A. Thornton, J. Vac. Sci. Technol. **15** (2), 188–192 (1978).
[158] B. A. Raby, J. Vac. Sci. Technol. **15** (2), 205–208 (1978).
[159] H. L. Brown, G. B. Bunyard, and K. C. Lin, Solid State Technol. **31** (7), 35–38 (1978).

[160] J. N. Bradley and G. B. Kistiakowsky, J. Chem. Phys. **35** (1), 264–270 (1961).
[161] F. Shinoki and A. Itoh, Japan J. Appl. Phys. Suppl. **2** (1), 505–508 (1974).
[162] J. W. Coburn and E. Kay, Appl. Phys. Lett. **18** (10), 435–438 (1971).
[163] K. R. Evans, C. E. Stuz, P. W. Yu, and C. R. Wie, J. Vac. Sci. Technol. **B6** (2), 271–275 (1990).
[164] C. V. Deshpandey, B. P. O'Brian, H. J. Doerr, R. F. Bunshah, and D. Hofmann, Surf. Coat. Technol. **33**, 1–16 (1987).
[165] S. A. Self, Plasma Processing and Synthesis of Materials III, MRS Symposia Proceedings, Vol. 98, D. Apelian and J. Szekely, eds., Materials Research Society, Pittsburgh, PA (1987), pp. 183–195.
[166] Y. Nakayama, T. Ohtsuchi, and T. Kawamura, J. Appl. Phys. **62** (3), 1022–1028 (1987).
[167] J. E. Greene, J. Vac. Sci. Technol. **15** (5), 1718–1729 (1978).
[168] T. A. Cleland and D. W. Hess, Plasma Chem. Plasma Proc. **7** (4), 379–394 (1987).
[169] W. G. Breiland and P. Ho, Chemical Vapor Deposition, Ninth International Conference, McD. Robinson, C. H. J. van den Brekel, G. W. Cullen, J. M. Blocher, Jr., and P. Rai-Choudhury, eds., Electrochemical Society, Inc., Pennington, NJ (1984), pp. 44–59.
[170] S. G. Hansen, G. Luckman, G. C. Nieman, and S. D. Colson, J. Vac. Sci. Technol. **B8** (2), 128–130 (1990).
[171] V. M. Donnelly, D. L. Flamm, and G. Collins, J. Vac. Sci. Technol. **21** (3), 817–823 (1982).
[172] C. Weissmantel, Thin Solid Films **58**, 101–105 (1979).
[173] P. Pan, L. A. Nesbit, R. W. Douse, and R. T. Gleason, J. Electrochem. Soc. **132** (8), 2012–2019 (1985).
[174] D. V. Tsu and G. Lucovsky, J. Vac. Sci. Technol. **A4** (3), 482–485 (1986).
[175] J. L. Kaae, P. K. Gantzel, J. Chin, and W. P. West, J. Mater. Res. **5** (7), 1480–1489 (1990).
[176] T. Harai, Emergent Process Methods for High-Technology Ceramics, R. F. Davis, H. Palmour III, and R. L. Porter, eds., Plenum Press, New York (1982), pp. 329–345.
[177] J. Chin, P. K. Gantzel, and R. G. Hudson, Thin Solid Films **40**, 57–72 (1977).
[178] S. Yoshida, E. Sakuma, H. Okumura, S. Miswa, and K. Endo, J. Appl. Phys. **62** (1), 303–305 (1987).
[179] P. D. Richard, R. J. Markunas, G. Lucovsky, G. G. Fountain, A. N. Mansour, and D. V. Tsu, J. Vac. Sci. Technol. **A3** (3), 867–872 (1985).
[180] G. Lucovsky, P. D. Richard, D. V. Tsu, S. Y. Lin, and R. J. Markunas, J. Vac. Sci. Technol. **A4** (4), 681–688 (1986).
[181] D. Nir, J. Vac. Sci. Technol. **A4** (6), 2954–2955 (1986).
[182] Y. Z. Hu, M. Li, J. Simko, J. Andrews, and E. A. Irene, Chemical Vapor Deposition, Eleventh International Conference, K. E. Spear and G. W. Cullen, eds., Electrochemical Society, Inc., Pennington, NJ (1990), pp. 166–172.
[183] T. Fujita and O. Matsumoto, J. Electrochem. Soc. **136** (9), 2624–2629 (1989).
[184] J. C. Barbour, H. J. Stein, O. A. Popov, M. Yoder, and C. A. Outten, J. Vac. Sci. Technol. **A9** (3), 480–484 (1991).
[185] C. F. Powell, Vapor Deposition, C. F. Powell, J. H. Oxley, J. M. Blocher, Jr., eds., John Wiley & Sons, Inc. New York (1966), pp. 191–218.
[186] A. J. Perry and L. Chollet, J. Vac. Sci. Technol. **A4** (6), 2801–2808 (1986).
[187] C. T. Wu, Thin Solid Films **64**, 103–110 (1979).
[188] H. Tsai and D. B. Bogy, J. Vac. Sci. Technol. **A5** (6), 3287–3312 (1987).
[189] T. I. Kamins and K. L. Chiang, J. Electrochem. Soc. **129** (10), 2326–2335 (1982).
[190] W. M. Paulson and R. P. Lorigan, J. Vac. Sci. Technol. **14** (1), 210–218 (1977).
[191] P. V. Plunkett, R. M. Johnson, and C. D. Wiseman, Thin Solid Films **64**, 121–128 (1979).
[192] D. W. Hoffman and J. A. Thornton, Thin Solid Films **40**, 355–363 (1977).
[193] J. A. Thornton, J. Tabock, and D. W. Hoffman, Thin Solid Films **64**, 111–119 (1979).
[194] P. Murray and G. F. Carey, J. Electrochem. Soc. **136** (9), 2666–2673 (1989).
[195] K. Kinosita, Thin Solid Films **12**, 17–28 (1972).
[196] F. A. Doljack and R. W. Hoffman, Thin Solid Films **12**, 71–74 (1972).
[197] J. A. Thornton and D. W. Hoffman, Thin Solid Films **171**, 5–31 (1989).
[198] J. A. Thornton and D. W. Hoffman, J. Vac. Sci. Technol. **18** (2), 203–207 (1981).
[199] R. C. Tailor and B. A. Scott, J. Electrochem. Soc. **136** (8), 2382–2386 (1989).
[200] H. Fujiyama, T. Yamashita, T. Takahashi, and H. Matsuo, Chemical Vapor Deposition, Tenth International Conference, G. W. Cullen and J. M. Blocher, Jr., eds., Electrochemical Society, Inc., Pennington, NJ (1987), pp. 857–866.
[201] I. K. Varga, J. Vac. Sci. Technol. **A7** (4), 2639–2645 (1989).
[202] R. R. Burke and C. Pomot, Solid State Technology, **31** (2), 67–71 (1988).
[203] P. Burggraaf, Semiconductor Int. **13** (3), 70–75 (1990).
[204] J. Asmussen, J. Vac. Sci. Technol. **A7** (3), 883–893 (1989).
[205] K. A. Buckle, K. Pastor, C. Constantine, and D. Johnson, J. Vac. Sci. Technol. **B10** (3), 1133–1138 (1992).
[206] J. S. Ma., H. Yagyu, A. Hiraki, H. Kawarada, and T. Yonehara, Thin Solid Films **206**, 192–197 (1991).
[207] J. T. Glass, B. E. Williams, and R. F. Davis, Micro-Optoelectronic Mater., SPIE **877**, 56–63 (1988).
[208] J. Chin, Fiber Reinforced Ceramic Composites, Ed. K. S. Mazdiyasni, Noyes Publications, Park Ridge, NJ, pp. 342–396.
[209] H. O. Pierson, Gorham International data, Handbook of Chemical Vapor Deposition (CVD), Noyes Publications, Park Ridge, NJ (1992).
[210] Cahners Economics data, Semiconductor International Magazines, 1990–1992, Des plaines, IL.

About the author: *Mr. Chin was on the staff of General Atomic from 1962 to 1989, where he was responsible for laboratories engaged in refractory materials research and development. His involvement with vapor deposition processes encompassed fluidized bed CVD coatings, fixed substrate CVD, PECVD, ion plating, evaporation, and sputtering processes. Since 1989 Mr. Chin has been a technical advisor on niobium-aluminide, titanium-silicide, and molybdenum-disilicide*

CVD filament coating programs; carbon, silicon nitride, and boron doped carbon chemical vapor infiltration studies; silicon, boron, yttria, and titanium diboride vapor deposition efforts; and the design of hardware for CVD, PECVD, and sputtering processes.

Technical Challenges of Chemical Vapor Deposited Diamond and Diamondlike Carbon Films

C. H. (George) Wu and M. A. Tamor

Ford Research Laboratory
P.O. Box 2053, MD 3028
Dearborn, MI 48121-2053
(313) 322-0566 or 337-4108
Fax: (313) 594-6863

In addition to its beauty as a gem stone, diamond possesses a unique combination of superb material properties which offer a wide variety of industrial applications. Interest in the synthesis of diamond has been strong for nearly a century. Although high-pressure high-temperature processes are now a major source of industrial diamond, the scope of technical application of diamond is still very limited. Recent advances in low-pressure chemical vapor deposition (CVD) of diamond and diamondlike films will expand greatly the range of diamond applications.

This chapter is a practical overview of the current status of technology of the CVD diamond and diamondlike carbon (DLC). Unifying principles for both diamond and DLC deposition are introduced to guide the design and control of deposition systems. Several proven deposition methods and reactors are described and their features compared to assist in the selection of reactors. Key techniques for the characterization of various properties of diamond and DLC are addressed. A range of diamond and DLC applications are presented. In addition, several economic and technical challenges are discussed, and some general recommendations are offered.

Key words: application; characterization; chemical vapor deposition (CVD); deposition method; diamond; diamondlike carbons (DLC); film; overview; property; Raman spectra; reactor; synthesis.

Contents

1. Introduction

The hardest material known to man, slippery as teflon, an electrical insulator yet an excellent thermal conductor, chemically inert, and transparent from the near ultraviolet to the far infrared, diamond would appear to be ideal for myriad mechanical, optical, and electronic applications [1, 2]. Unfortunately, another extreme property of diamond is its rarity. While industrial grade grit is essentially a commodity, high quality stones large enough for macroscopic fabrication are far too precious for use in any but very high-value applications. Even so, diamond has a long and distinguished history of use in mechanical devices. Very small diamonds have long been used in precision low-friction bearings, for example watch movements and phonograph needles. Larger stones are drilled to form durable wire-drawing dies or shaped into small surgical blades. Very large stones may be sawn into plates for extremely durable windows for high intensity laser light or heat spreaders for high power electronic devices. Over the last decade, amazingly rapid advances in the technology for deposition of diamond in the form of coatings and films have alleviated the need for large stones for many applications, and have opened the way to full exploitation of the combination of extreme characteristics unique to diamond.

1.1 A Brief History of Diamond Synthesis

Diamond is a metastable allotrope of carbon with a cubic crystal structure. This metastability is not apparent under normal circumstances because the energy difference with respect to graphite, the lower-energy carbon phase, is very small (0.5 kcal/mole) while the energy barrier which must be overcome in the transformation is very large (30 kcal/mole). Unless heated above roughly 1500 °C or exposed to an extremely high radiation dose, diamond is indeed forever. (Diamond burns in pure oxygen at 600 °C). The small energy difference between diamond and graphite reverses at elevated pressure. The pressure-temperature dependence of this diamond-graphite transition is illustrated in the carbon phase diagram (fig. 70). When carbon is exposed to appropriate conditions of high pressure and high temperature (HPHT) deep underground, natural diamond may grow at a finite, albeit extremely low rate. With sudden spurts and actual reversals, the average growth rate is equivalent to only microns per year. (This low rate is in part due to the fact that this process involves solid-to-solid transport. Actual liquefaction of carbon can occur at much higher temperature but does not appear to play a role in the formation of most natural diamond.)

Due to the rarity and correspondingly high cost of natural diamond, efforts to produce diamond synthetically have been intense. The first successful synthesis of diamond from graphite by the high-pressure high-temperature (HPHT) process was announced by General Electric (GE) in the United States in 1955 [3]. Researchers at ASEA in Sweden obtained very similar results roughly simultaneously, but chose not to disclose them immediately. This synthetic or man-made diamond grows by liquid-solid transport from a molten metal-carbon solution. Metals such as iron, nickel, cobalt, manganese, chromium, and tantalum are used as solvents and catalysts. Other more advanced catalytic systems are closely held trade secrets. Subsequently, other HPHT methods were developed. In shock wave synthesis, fine grits are formed essentially instantaneously by shock-compression in a carefully controlled explosion. Several major companies are actively engaged in HPHT diamond synthesis. These include GE and Du Pont in United States, De Beers in South Africa, and Sumitomo Electric in Japan. More than 70 tons of HPHT synthetic diamond grit are produced each year [4].

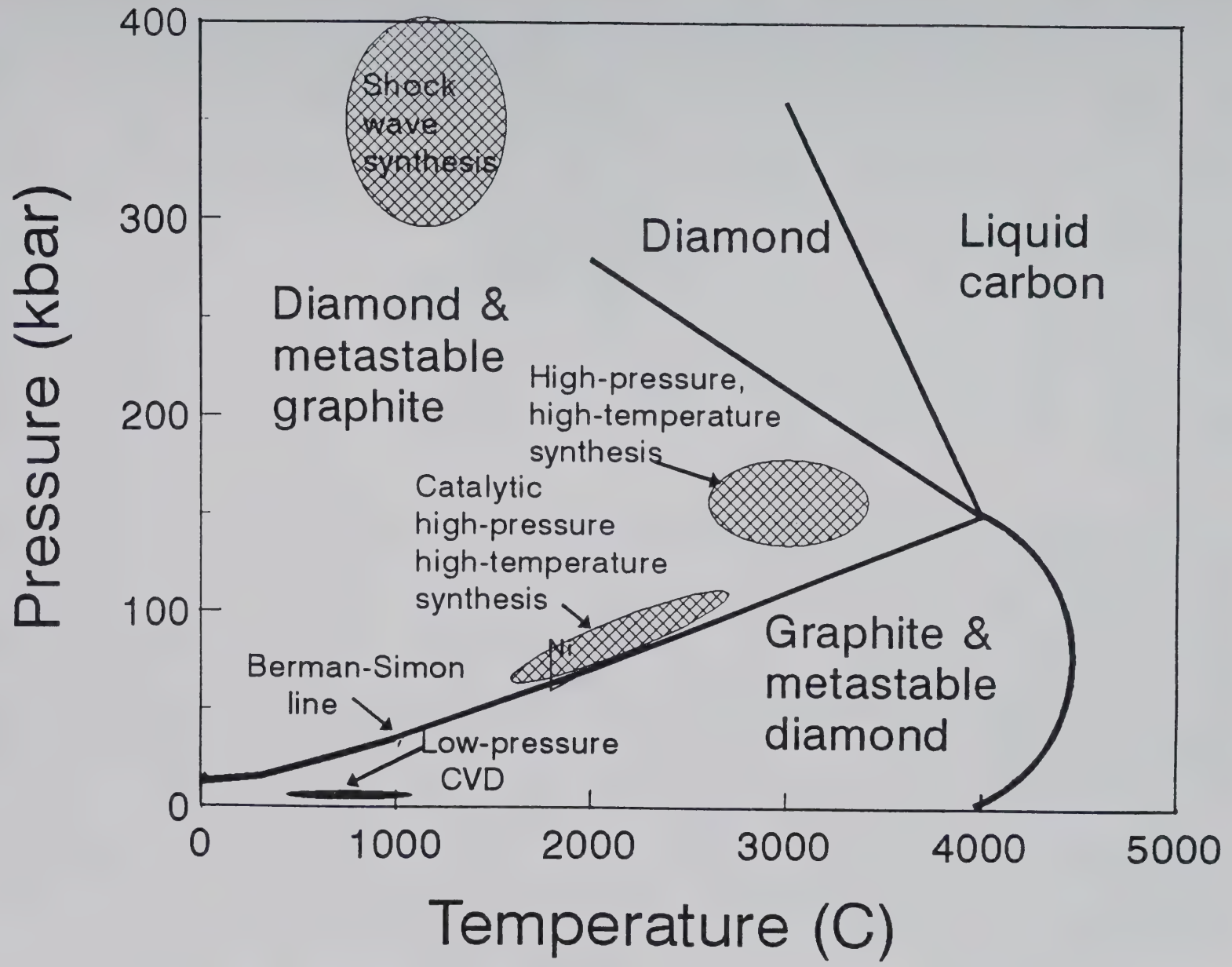

Figure 70. Equilibrium phase diagram for the carbon system. Also shown here are the relative locations for various methods of diamond synthesis.

At present, the dominant industrial application of diamond is in the form of sintered polycrystalline diamond (PCD) compact, mostly for cutting and grinding tools. While they are extremely durable, PCD-enhanced tools are expensive relative to more conventional competitors and are severely restricted in geometry. Although high quality single crystals of diamond (as large as 17 mm) have been produced, HPHT processes have their limitations: the equipment is cumbersome and expensive, and production of large high purity single crystals is difficult and slow. Even the largest HPHT crystals are too small for many proposed diamond applications. It appears that full exploitation of diamond's superior properties requires the ability to form high quality, large area films on a variety of substrate materials.

Recent advances in low-pressure chemical vapor deposition (CVD) of polycrystalline diamond thin films provide this ability and so pave the way for rapid expansion in the technological applications of diamond. A variety of methods can now be used to deposit well faceted single crystals or polycrystalline diamond films on diamond or non-diamond substrates at sub-atmospheric pressures. A poor cousin to diamond in many respects, very smooth films of amorphous diamondlike carbon (DLC) may be deposited on virtually any substrate at room temperature. With similar low friction, and hardness at least one third that of diamond (still comparable to the hardest ceramics), DLC promises a wider range of application than CVD diamond at much lower cost. A large number of excellent review papers have been published and several conferences entirely devoted to the subject of CVD diamond and related materials have been held. A few representative reviews and conference proceedings are listed in References [5] through [15]. A brief account of historical development of CVD diamond and DLC is shown in Table 15.

1.2 Challenges of CVD Diamond and Diamondlike Carbons

The state of understanding and challenges of diamond and DLC are quite different. While crystalline diamond is readily identified, the deposition mechanism of the diamond CVD process is only poorly understood. In contrast to diamond, DLC is easy to make simply by hurling ions or radicals of carbon or hydrocarbon with the appropriate energy at a substrate. The atomic structure of DLC is not well characterized and is occasionally a subject of heated debate. In general, DLC can be classified into two types: (1) hydrogen-free DLC (i-C) and (2) hydrogenated DLC (a-C:H). Some of their properties are quite different. For convenience, a comparison of many key properties of several carbon-based materials is listed in Table 16 [7]. The thrust of development in diamond CVD is to improve understanding of the growth process to guide the design of more efficient and flexible reactors. Other challenges include achievement of better control of nucleation, adhesion, and heteroepitaxy. On the other hand, the major tasks for DLC development are to explore the connections between deposition conditions, atomic structure and macroscopic properties.

Table 15. Historical development of CVD diamond and DLC

1.	Lavoisier (France) 1972 [16]	First established diamond as a crystalline form of carbon.
2.	Eversole (Union Carbide) 1953 [17]	First success in vapor deposition of diamond on diamond seeds.
3.	Derjaguin & Fedoseev (USSR) 1956 [18]	Thermal CVD diamond on diamond powders.
4.	Lander & Morrison (Bell Lab.) 1963 [19]	Stabilization of diamond by H_2 gas.
5.	Angus et al (Case West. Res. U) 1967 [20]	Deposition of diamond from CH_4/H_2 mixture; graphite etching by H-atom.
6.	Aisenberg & Chabor (Whittaker) 1971 [21]	Deposition of diamondlike carbons.
7.	Vickery (Diamond Squared) 1970 [22]	Single step CVD diamond on diamond.
8.	Derjaguin et al (USSR) 1976 [23]	First success in CVD diamond on nondiamond substrates.
9.	Setaka, Sato, Matsumoto, & Kamo (NIRIM, Japan)	Great advances in CVD diamond using various activation 1974–1982 [24–26]techniques, MW, RF, HF, DC arc, torch.
10.	Roy, Badzian, Spear, & Messier (Penn. State Univ.) 1986 [27]	First to repeat Japanese work and to revive diamond research in U.S.

Table 16. Properties of CVD diamond, diamondlike carbons (i-C, a-C:H), natural diamond, and graphite[1]

	CVD diamond	Hydrogen-free DLC (i-C)	Hydrogenated DLC (a-C:H)	Natural diamond	Graphite
Crystal structure	diamond; cubic; a = 3.561; 3.601 Å; (222) reflection	< 5 nm crystallites; mixed sp^3 and sp^2 bonds	amorphous with small crystalline regions; mixed sp^3 and sp^2 bonds	cubic; a = 3.567	hexagonal; a = 2.47; c = 6.79
Form	faceted crystals; < 1 – 100 μm; twins on (111) films; rough	generally as films; smooth to rough	films; smooth	(100), (111), (110); twins on (111)	plates
Hardness					
Mohs	> 9	> 7, > 9	> 7, > 9	10	1–2
Vickers (kg/mm^2)	3000–12,000	1200–3000	900–3000	7000–10,000 +	---
Density (g/cm^3)	3.52	2.0–3.5	0.9–3.0; most 1.8–2.0	3.51	2.26
Optical					
refractive index	2.41	1.5–3.1	1.6–3.1; most 1.8–2.2	2.42	2.15 (‖C); 1.81 (⊥C)
transparency	near UV, visible IR (2.5–5 μm)	--- IR	visible; interference colors IR	near UV, visible IR	opaque ---
optical band gap (eV)	5.5	0.4–3.0	0.7–3.0	5.5	---
Electrical					
resistivity (ohm cm)	10^9 to 10^{16}	10^{14} to 5	10^2–10^{13};	IIa, 10^{16}; IIb, 10–10^3	0.04 (‖C); 0.20 (⊥C)
dielectric constant	5.7	8–14	---	5.7	2.6 (‖C); 3.28 (⊥C)
dielectric strength (V/cm)	---	---	10^6–10^{10}	---	---
Thermal conductivity (W cm^{-1} K^{-1})	18	---	---	20 (IIa, 20 °C)	K‖, 30–40; K⊥, 1–2
expansion coefficient (K^{-1})	1.0×10^{-6}	---	---	1.34×10^{-6} (20–100 °C)	---
graphitization temp. (°C)	1400	> 500	800–900	1500 (vacuum)	---
Chemical stability	inert, inorganic acids	inert, inorganic acids	inert, inorganic solvents; inert inorganic acids	inert, inorganic acids	inert, inorganic acids
composition	H impurity	---	Si, Ge, F, D_2, "alloys"	N, B, H, impurity	---
Mechanical coefficient of friction	0.08–0.15	0.15–0.45	0.2–2.0	(humidity sensitive); 0.153 (steel); 0.093 (Cu)	0.05–0.15
compressive stress (N/m^2)	along < 110 > in films	5×10^8	3×10^7	–0–	–0–
adhesion (erg/cm^2)	---	1–3 × 10^2 (glass)	< 10 μm adheres; > 10 μm cracks	---	---
modulus (GPa)	370–430	41	35–135	900–1050	9–15
Growth rates (μm/hr)	< 0.1 to > 1000	< 0.1 to 18	≤ 0.1 to 54; most, 1–5	$< 10^{-4}$	---

[1] This table is adapted from Ref. [7] with some modifications.

This chapter is intended to provide a practical overview of the emerging technologies of CVD diamond and DLC. In the following sections we (1) propose unifying principles for both diamond and DLC depositions to guide the selection and control of deposition systems, (2) describe key techniques for the characterization of diamond and DLC, (3) describe some examples of applications, and (4) discuss some economic and technical issues related to commercial applications of diamond and DLC.

2. Methods of CVD Diamond Growth

2.1 Unifying Principles of Diamond CVD

Chemical vapor deposition (CVD) of diamond proceeds under conditions radically different from those of HPHT synthesis. Rather than growing under conditions in which diamond is stable (as defined by the Berman-Simon line shown in fig. 70), diamond CVD relies on the large barrier to graphitization of diamond at "moderately" low temperature (rarely exceeding 1000 °C) and low pressure (usually sub-atmospheric) while exploiting the special chemistry of the growth atmosphere which favors deposition of carbon in the form of diamond rather than graphite. Because existing diamond (beneath the growth surface) remains essentially stable while diamond growth is favored by the special gas chemistry, the stability of diamond is effectively reestablished in the reactor.

Although various "methods" of diamond CVD have been developed (see below), all current reactors appear to operate on the same principle and embody the same three generic zones: (1) an "excitation" zone in which atomic hydrogen and other reactive hydrocarbon species are generated, (2) a "transport" zone in which excited gas cools as it flows or diffuses to the vicinity of the substrate, and (3) a boundary layer in which the gas cools to the substrate temperature as it diffuses to the growth surface. One key ingredient in the special atmosphere of diamond CVD is atomic hydrogen or other similar reactive species. Highly reactive H atoms are believed to play a dual role by (1) adding or abstracting bonded hydrogen to maintain nearly full hydrogenation of the diamond surface, thereby stabilizing it against graphitization while simultaneously offering sufficient reactive sites (hydrogen vacancies) for growth, and (2) attacking non-diamond (graphitic or sp^2-bonded) carbon by etching it or converting it to sp^3-bonded diamond configurations [28,29]. Obviously, another essential ingredient of the diamond CVD atmosphere is carbon. Carbon-containing feed gases may enter the reactor at the excitation or transport zone in almost any form, most often as hydrocarbon (e.g., methane, acetylene), CO, or oxygenated organic compounds (e.g., alcohol, acetone, and acid). The carbon borne by the precursor is then converted to the diamond growth species. Unfortunately, the identity of the essential growth species remains unclear. Considerable evidence supports the CH_3 radical [30-34], while acetylene, which is stable at the high gas temperatures associated with diamond CVD, is also a strong candidate [29, 35–38]. Other carbonaceous species are not present in sufficient concentration to account for the observed rates of diamond growth. However, the dominant *growth* species may not be the *rate controlling* species; a rarer species may control the overall deposition rate by mediating initiation of growth steps or nucleation of layers at which another much more populous reactant is incorporated [39(a)].

The construction and behavior of the various reactors can be characterized in terms of the relevant temperatures of the three reactor zones. Three temperatures are considered here: the gas temperature, T_g, and electron temperature, T_e, which refer to the kinetic temperatures of gas molecules and electrons, respectively, and chemical temperature, T_c, which is the temperature at which the instantaneous local gas composition would be in thermodynamic equilibrium. In the excitation zone, the electron temperature, $T_e(E)$, the chemical temperature, $T_c(E)$, and the gas temperature, $T_g(E)$, are all at their maxima. In general, the temperature relationship is $T_e(E) \geq T_c(E) \geq T_g(E)$. In the transport zone, the gas temperature, $T_g(T)$, is falling more rapidly than the chemical temperature, $T_c(T)$, due to fast gas dilution and slowing of chemical reactions with rapid cooling. A typical behavior of these temperatures in a hot filament reactor is shown in figure 71. The chemical temperatures are higher than the gas temperatures by 200–500 °C at 6–10 mm from the filament, the position where the substrate is normally located [39(b)]. In the boundary zone, the gas temperature, $T_g(B)$, falls to the substrate temperature, T_s, while the chemical temperature, $T_c(B)$, remains considerably higher, again due to reduced reaction rates at lower temperatures. Thus, in the boundary zone, the concentrations of reactive species are in a super-saturated state which is essential for the formation of metastable diamond. The actual values of these temperatures, $T_e(E)$, $T_g(E)$, and $T_c(E)$, depend on the method of excitation, and will affect the quality and the growth rate of diamond films. An increase

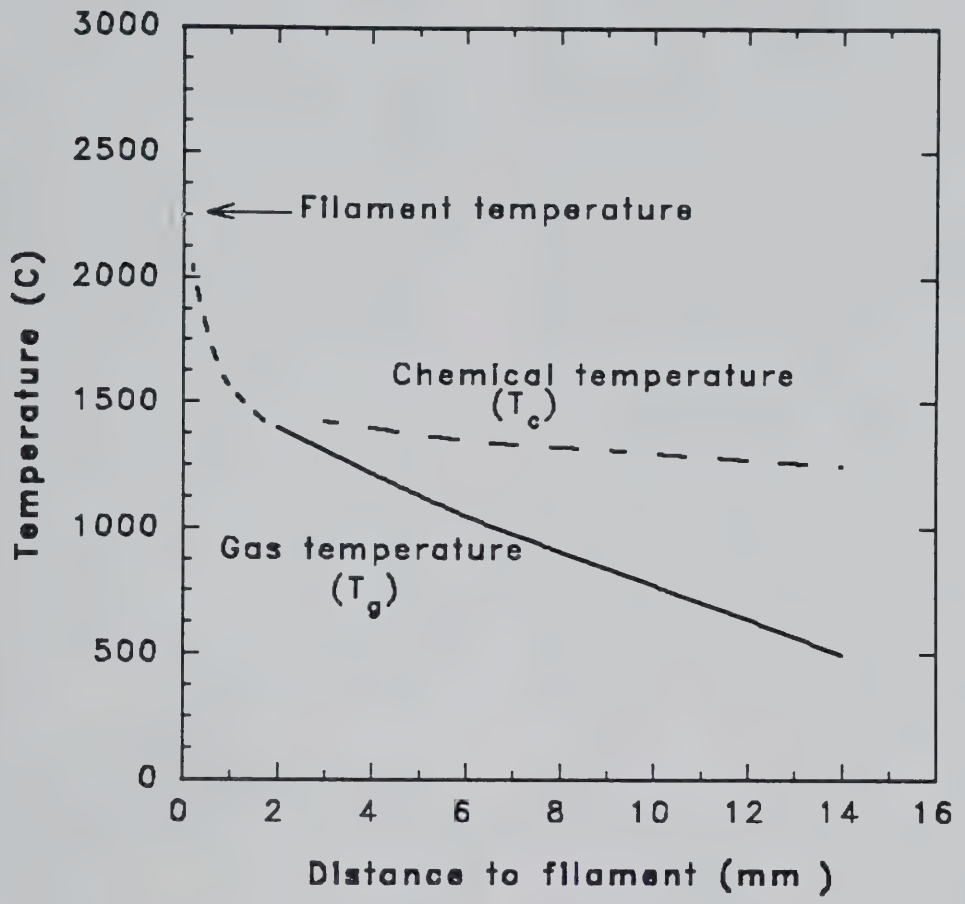

Figure 71. The temperature profiles vs the distance to the filament for measured gas temperature (T_g) and calculated chemical temperature (T_c) in a hot-filament CVD reactor using a feed gas mixture of CH_4(1%) in H_2 at 50 Torr.

in these temperatures translates to an increase in power density and commensurate increase in energy flow through the reactor [40].

In general, the relationship between the lateral sizes of the excitation zone and substrate, and the length of the transport zone can be used to classify reactors as one of two types: (1) immersion, where the transport distance is short and the substrate is actually in or adjacent to the excitation zone (both of which are of the same lateral size), and (2) downstream, where the transport zone is long and excited gas is transported a macroscopic distance (several times the lateral dimension of the excitation zone) before encountering the substrate. For immersion reactors, the growth area is comparable to the size of the excitation zone, transport is usually dominated by diffusion, gas feed rates may be relatively low and the power density is limited by the need to maintain the proper substrate temperature, usually in the range 800 °C to 1050 °C. Supplementary heating or water cooling may be required depending on details of the reactor design. For downstream reactors the power density and gas feed rate may be very high and the fast moving stream of excited gas, often a flame, may be expanded to cover an area much wider than the excitation zone. Again, care must be taken to maintain the desired substrate temperature.

The prevalence of substrate temperatures in the 800 °C to 1050 °C range can be viewed in terms of the "turnover" rate of bonded hydrogen. This rate is determined by the balance between hydrogen desorption which becomes very rapid at higher temperature, and the hydrogen flux from the excited gas. In this temperature range, thermal desorption and hydrogen abstraction by supersaturated atomic H provide sufficient reactive sites for diamond growth at rates of 1 to 10 μm/h. For deposition outside this substrate temperature range, modifications of gas composition are required. The addition of a minute amount of oxygen to the feed gas in a low power density reactor

allows deposition at much lower temperature (albeit at a reduced rate) [41]. It is believed that this is due to the formation of OH radicals which may abstract surface hydrogen and create surface active sites more effectively than H-atoms. Up to the limit where the available carbon is "burned" and deposition stops, oxygen also improves diamond quality by suppressing formation of nondiamond carbon. Using fluorine-based chemistry, diamond deposition at temperatures as low as 300 °C has been reported [42]. However, this method has not been widely used due to the difficulties with reproducibility and problems with corrosion of reactor components and subsequent film contamination [43]. Conversely, the extremely high flux of atomic hydrogen in high power density reactors may be used to overcome a greatly increased desorption rate at higher temperature and stabilize the growing surface at temperatures up to 1200 °C [44]. For high power density excitation with very high $T_g(E)$, a larger fraction of hydrogen is in the form of atoms, permitting a feed mixture much richer in carbon which in turn allows growth rates approaching 1 mm/hour [45].

Up to this point, only deposition from dilute hydrocarbon-in-hydrogen, with some enhancement from oxygen and halogen, has been considered. The full range of compositions in the C-H-O system suitable for diamond CVD has been compiled by Bachmann et al. [46] and mapped in the triangular diagram shown in figure 72. The diagram indicates that diamond may be deposited from any C-H-O mixture within the narrow triangular region abutting the H-CO line. This conclusion is valid only for excitation schemes with excitation power density (or $T_c(E)$) sufficient to dissociate CO. Because the dissociation energy of the C-O bond (257 kcal/mole) is nearly triple that of the C-H (104 kcal/mole) or C-C (88 kcal/mole) bonds [47], CO is stable in a low power density thermal reactor and does not play a significant role in diamond CVD. Higher energy or nonthermal (see below) plasma reactors can maintain significant steady-state dissociation of CO thus allowing continued deposition almost anywhere along the H-CO line of the triangular diagram. The requisite power density does tend to increase as the relative fraction of CO is increased.

2.2 CVD Diamond Reactors

Excitation of gas mixtures may be achieved by a wide variety of means ranging from direct contact with a hot filament, actual chemical combustion within the gas stream, to a glow discharge or electric arc [2, 5–15]. As described earlier, the various excitation schemes may be characterized by their power density and the relevant temperatures of the excitation zone [40]. The equipment cost of current reactor technology is difficult to estimate due to variation in the excitation means, size of the reactor, and different requirements for flow, vacuum, and process controls. Crude cost estimates are included in the description of each reactor.

2.2.1 Thermal Excitation Reactors

Hot-Filament CVD (HFCVD) Reactor The hot-filament CVD (HFCVD) system is the simplest and most common diamond growth reactor [48–52]. A typical schematic of an HFVCD reactor is shown in figure 73. It uses resistively heated refractory metal filaments (filament temperature 2000 °C–2400 °C) to thermally excite a dilute mixture of hydrocarbon in hydrogen. Typical deposition conditions and characteristics of the reactor are shown in Table 17. Hot-filament reactors are extremely flexible; any number and size of filaments may be configured to coat large areas and complex surfaces.

Table 17. Typical deposition conditions and features of hot filament reactors for CVD of diamond

Substrate temp. (°C)	800–1050
Reactor pressure (mbar)	5–200
Total gas flow (sccm)	10–300
Filament temp. (°C)	2000–2400
Deposition rate (μm/hour)	0.2–3
Deposition area (cm^2)	2–100 (depending on filament configuration).
Filament materials	W, Ta, Re (0.2 to 5 mm diameter).
Types of substrates	Si, Mo, Silica, alumina, diamond, etc.
Quality/crystallinity	Excellent quality (except with minor co-deposit of the filament material).
Uniformity/homogeneity	Poor to good (depending on substrate configuration).
Advantages of the method	Simple set up, low cost, large area possible.
Drawbacks of the method	Filament stability problematic, no long term growth process, metal contamination, higher oxygen concentration difficult.
Special remarks	Filament material and applied bias voltage affect quality and rate.

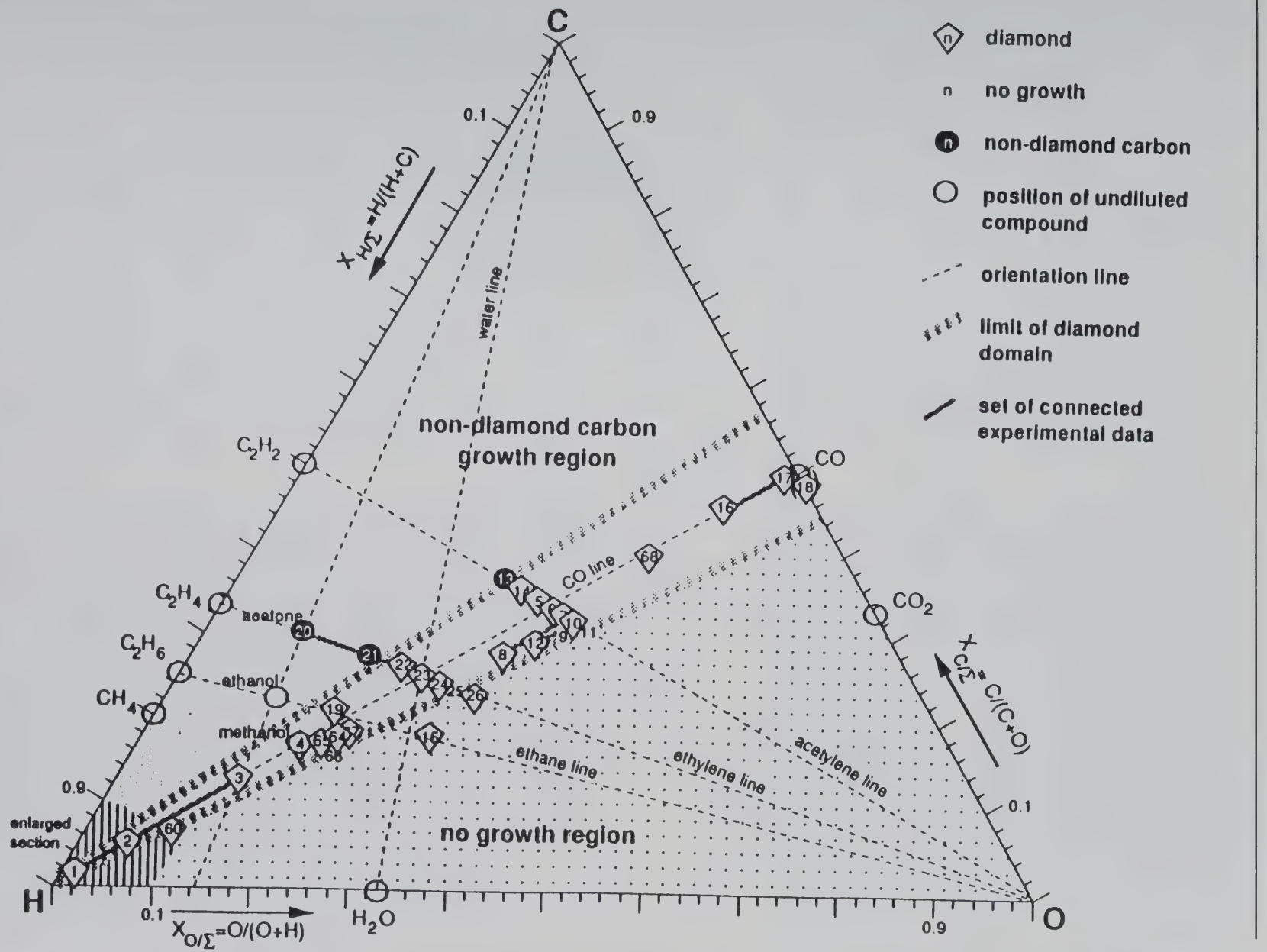

Figure 72. The C-H-O system diamond deposition phase diagram. The "diamond domain" is bounded between two broad dotted lines along with the H-CO line. (Reproduced from Ref. [46]).

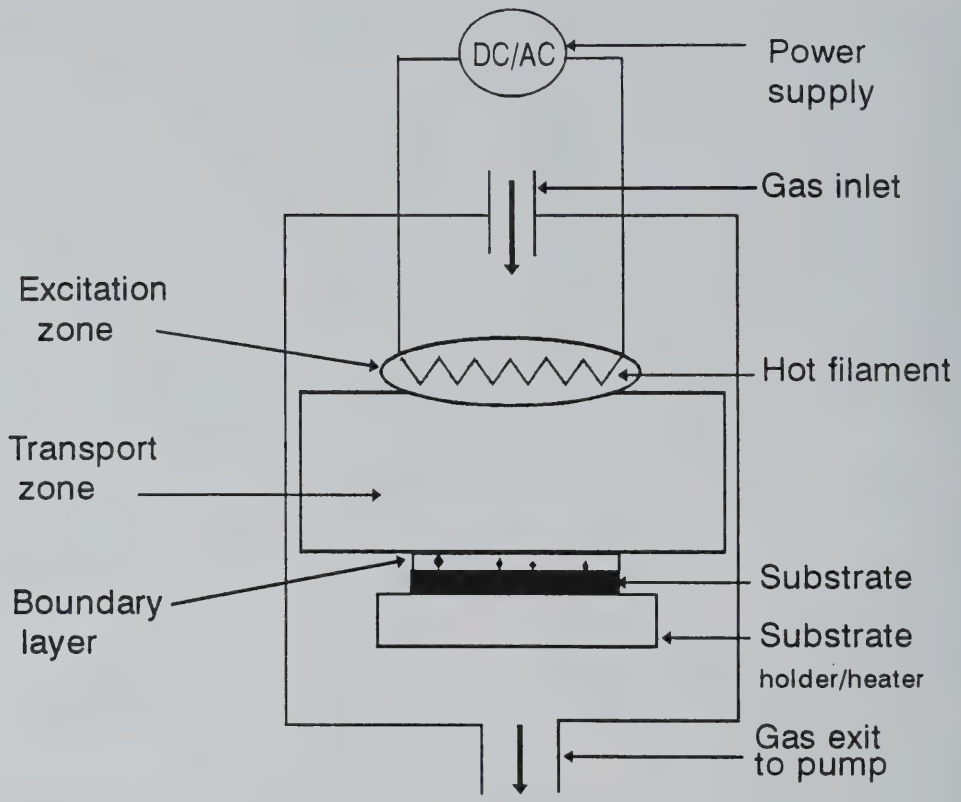

Figure 73. Schematic diagram of a hot-filament CVD reactor, consisting of a hot filament with a DC or AC power supply, a substrate and its holder or heater, and a vacuum chamber with gas inlet and outlet. It also shows the locations of excitation, transport, and boundary zones.

However, they are limited in the power density which can be achieved by direct contact of hot metal with gas and so are capable of growth rates of only a few microns per hour at best. Also, because the hot filaments are readily oxidized, the HFCVD technique precludes the use of feed gases rich in oxygen. Because the gas chemical temperature, $T_c(E)$ never exceeds the filament temperature, CO is not significantly dissociated in this system. Interestingly, although nitrogen degrades and ultimately suppresses diamond growth in reactors with higher excitation energy, the hot filament reactor cannot significantly dissociate N_2 (240 kcal/mole). Thus, the HFCVD system is insensitive to minor air leaks which would jeopardize the diamond-growing ability of most other reactor types. So long as the filaments are not damaged, the small amount of oxygen may actually be of some benefit!

Hot filament reactors are generally home built, and do not require any expensive or specialized components. Because the operating pressure is usually a fraction of an atmosphere (5 to 200 Torr), gas flow rates are generally low (10–300 sccm), and the HFCVD process is largely unaffected by small air leaks, the vacuum chamber needs not meet ultra high vacuum (UHV) specifications for cleanliness and integrity. The deposition zone and substrate are also hot and so are self-cleansing. Conventional mechanical vacuum pumps are generally adequate, but a Roots blower may be desirable for a higher flow rate system. For low-flow systems, even a large chamber with appropriate pumps costs only a few thousand dollars. In addition, gas handling and pressure/temperature control equipment are needed. This equipment, again costing only a few thousand dollars, will serve any size reactor. An optical pyrometer is useful for monitoring filament temperature. Simple to build and easy to operate, HFCVD reactors are the most common type of diamond reactor in current use. A hot-filament system is an excellent "first reactor" for those new to the field. The total material cost of a basic HFCVD reactor, even one capable of coating fairly large areas, is unlikely to exceed $20,000. Of course, elaborate diagnostic systems (interferometry, ellipsometry, spectroscopy, gas analysis) can increase the cost substantially.

Combustion Flame Reactors

The simplest and cheapest high energy density reactor is a conventional atmospheric-pressure oxy-acetylene torch which derives its excitation energy from combustion within the gas stream [44, 53–55]. A typical torch arrangement is shown in figure 74a. With careful control of the gas mixture (slightly carbon-rich) and position of the substrate in the flame, high quality diamond can be grown over a small area (1 cm diameter) at rates up to 200 microns/hour. The substrate for torch-growth must be vigorously cooled. The combustion torch is difficult to scale to larger areas for two reasons: (1) extremely high and nonuniform heat flux to the substrate, and (2) limited ability to expand the flame. A partially successfully attempt to expand the deposit area by using a multiple-torch arrangement has been reported [56]. To increase the deposition area and permit better control, other more benign combustion methods at low pressure, such as the flat flame burner (fig. 74b), have been explored [57,58]. However, these are characterized by lower flame temperature and cannot reproduce the high local deposition rates of the oxy-acetylene flame. Typical deposition conditions and characteristics of the reactors are shown in Table 18.

The initial cost of an oxy-acetylene torch system is very low and all components are available at a good hardware store. Because of the special vacuum system and high speed pumping requirements, low pressure flame systems are substantially more expensive. Good control of the flame shape and composition, and substrate temperature is essential but not easy. In addition, large gas flow rates of several liters/min. for reactants, with deposition over such a small area corresponds to a very low yield of diamond growth for the carbon consumed.

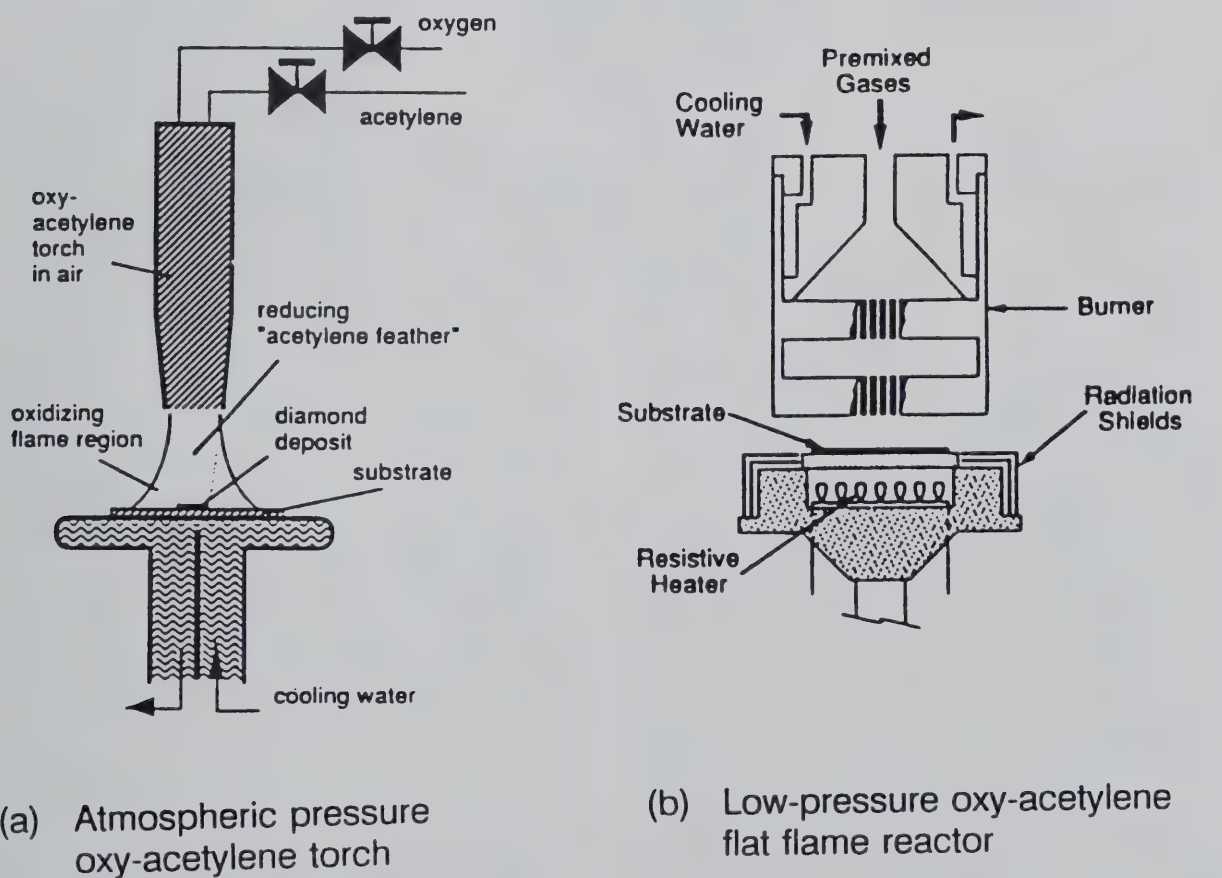

Figure 74. Schematic diagram of combustion flame CVD reactors. (a) atmospheric pressure oxy-acetylene torch, (b) low-pressure flat flame burner.

Table 18. Typical conditions and features of atmospheric oxy-acetylene torch and low-pressure combustion flame reactors for CVD of diamond

	Atmospheric oxy-acetylene torch	Low pressure combustion flame
Substrate temp. (°C)	600–1300 (cooling required)	800–1250 (heating required)
Reactor pressure (mbar)	1000	25–50
Total gas flow (sccm)	2000–9000	3000–8000
Flame temp. (°C)	3000–3300	2000–2400
Deposition rate (μm/hour)	50 (high quality) 200 (poor quality)	0.5–1
Deposition area (cm^2)	Approx. 1	20–30
Types of substrates	Si, Mo, alumina, TiN, diamond	Same
Quality/crystallinity	Good to excellent	Poor to good
Uniformity/homogeneity	Poor	Good
Advantages of the method	Simple set up, high growth rates, no vacuum chamber needed	Large area possible
Drawbacks of the method	Control of substrate temperature difficult, inhomogenous deposition, contaminations, small deposition area, substrate cooling required, poor reproducibility, low yield	Low growth rate, low film quality, Low yield, vacuum chamber and high-speed pumping
Special remarks	Rates and quality depend on nozzle and oxygen-acetylene ratio used, nozzle-substrate distance critical.	Flame control difficult in low pressures

2.2.2 Discharge Excitation Reactors

Microwave Plasma CVD (MWCVD) Reactors After hot-filament systems, the most common diamond reactor is the microwave plasma (MWCVD) reactor [25, 59]. At present, several types of MWCVD reactors are available commercially (fig. 75). A low pressure (0.1 to 100 Torr) MWCVD reactor uses a resonant microwave cavity to generate a plasma "fireball" in a hydrocarbon-hydrogen mixture similar to that used for HFCVD. The substrate is placed adjacent to, or in contact with the plasma. Among diamond CVD reactors, the low pressure microwave reactor is unique in that the microwave plasma is nonthermal. Because microwave energy is coupled to the plasma via the free electrons, their temperature is far higher than the background of ions and neutral gas. The chemistry of a very "hot" gas is created by the high electron temperature without the associated gas kinetic energy ($T_e(E) \approx T_c(E) > > T_g(E)$). Even though $T_g(E)$ is comparable to that of a hot-filament reactor, stable molecules such as CO and N_2 are dissociated in the microwave plasma. This in turn allows the use of gas mixtures almost anywhere in the H-CO system (fig. 72). However, it appears that increasing power density is required as the CO fraction is increased. For a 1 kW microwave reactor, deposition rates of 1 μm/h over a 5 cm diameter area are typical. Substitution of a larger power supply, with appropriate precautions for cooling both the substrate and the reactor walls allows deposition at rates exceeding 10 μm/h.

As most commonly operated, with the plasma in near-contact with the substrate, these MWCVD reactors are in "immersion" mode. Operated in this mode, they suffer two serious drawbacks: (1) they are difficult to scale to coat large surfaces, and (2) due to microwave coupling to the substrate, it is difficult to coat complex objects, especially those with sharp edges and corners.

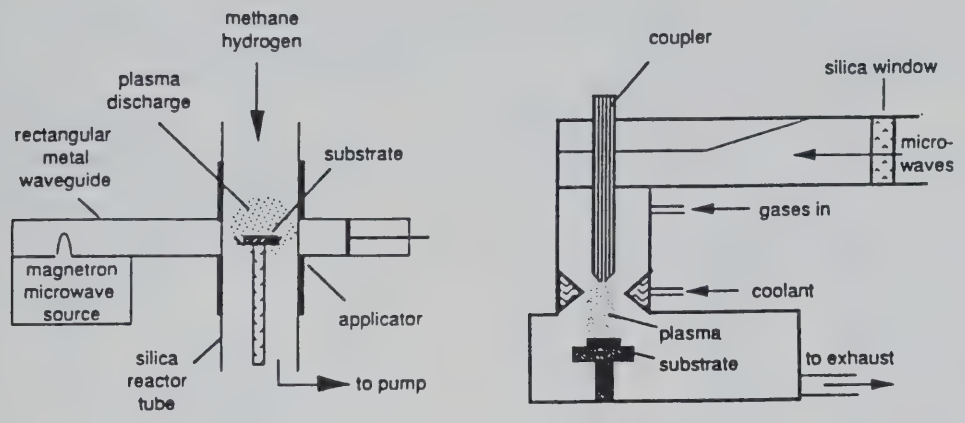

(a) Low-pressure MW plasma reactor

(b) Atmospheric pressure MW plasma torch

Figure 75. Schematic diagrams of microwave (MW) CVD reactors: (a) low-pressure MW plasma reactor, (b) atmospheric pressure MW plasma torch.

Microwave reactors have been built to operate in the "downstream" mode. A promising design is one in which gas flows rapidly through a compact, very high power plasma, and then is allowed to expand rapidly and coat a much larger surface [60]. In a sense, this might be called a microwave-jet Although the average deposition rate is reduced relative to "immersion," both drawbacks of immersion microwave deposition are overcome. Another type of reactor is called a "microwave plasma torch," which is operated at atmospheric pressure and high power, developed by Mitsuda et al. [61]. At this pressure, the plasma is closer to thermal equilibrium and allows for high gas temperature ($T_e(E) \approx T_c(E) \approx T_g(E)$). Growth rates up to 30 μm/h are achieved, but the deposition area is reduced. Another type of microwave reactor is equipped with a proper arrangement of magnets and operated at low pressure ($10^{-4} - 10^{-1}$ Torr) in the electron cyclotron resonance (ECR) mode. This ECR operation greatly increases the degree of ionization and excitation efficiency and may be used for large area diamond deposition [62,63]. However, both the film quality and growth rate are reduced. Typical operation conditions and features for MWCVD reactors are listed in Table 19.

Moderately sized microwave power supplies are relatively inexpensive due to the mass production of microwave sources for ovens. A reactor with a cavity and 1 kW power supply might be purchased for less than $60,000, while basic turnkey systems are available from the $150,000 range. For high rate deposition at higher power or for larger diameters, costs increase rapidly. A commercial version of the expanded microwave-jet reactor, or large area deposition system is available [60]. This machine is capable of coating nominally flat surfaces up to 10 cm in diameter, and larger versions should be available soon. The absence of physical contact between the substrates and the excitation zone has two advantages: (1) reduced possibility for contamination, and (2) increased deposition area. Representatives of the manufacturers of MW apparatus in the United States include Applied Science and Technology, (Astex, Woburn, MA), Wavemat (Plymouth, MI), and Conversion Technology (Livermore, CA).

Radio Frequency Plasma CVD (RFCVD) Reactors

Radio-frequency (RF) reactors operated in the megahertz range (typically 4 to 13.6 MHz) have been used for low pressure plasma deposition of various films and have been successfully applied to synthesize polycrystalline diamond films [26, 64–66]. Both inductive and capacitive coupling are

Table 19. Typical conditions and features of microwave plasmas and low-pressure and atmospheric pressure torch reactors for CVD of diamond

	Low-pressure MWCVD reactor	MW atmospheric pressure torch
Substrate temp. (°C)	350–1100	800–110 (cooling required)
Reactor pressure (mbar)	0.1–100	1000
Total gas flow (sccm)	100–1000	50,000
Input power data	300–2000 W	5 kW
Deposition rate (μm/hour)	1–5	10–30
Deposition area (cm^2)	20–100	5
Types of substrates	Si, silica, alumina, graphite, Ni, soft glass, Ti, Ta, Si-nitride, SiC, SiAlON, WC, Pt, Cu, and others.	Same
Quality/crystallinity	Excellent quality	Good
Uniformity/homogeneity	Excellent quality	Poor
Advantages of the method	Very stable (continuous operation possible), high quality; uniform rates	Torch control difficult
Drawbacks of the method	Rate and area need further improvement	Plasma instability, vigorous cooling required, contamination by electrode materials
Special remarks	Magnetized plasmas (ECR) at low pressures of <0.1 mbar yield diamond at lower rates and reduced quality.	

available, but inductively-coupled reactors are most commonly used (fig. 76). Diamond growth in the immersion mode is possible, but is very inefficient due to the low ionization and low chemical activity of the nonthermal RF plasma. However, an inductively coupled RF-jet can generate a thermal plasma ($T_e(E) = T_c(E) = T_g(E)$) with very high temperature (3000 °C). This produces correspondingly more atomic H and higher deposition rates. Operated at a low pressure (0.01–10 Torr) where heat transfer to the substrate is reduced, RFCVD reactors have been used to deposit diamond from selected precursors at low, but nevertheless potentially useful rates (0.2 μm/h) at temperatures less than 400 °C [65,66]. An inductively coupled RF torch reactor operated at atmospheric pressure (fig. 76b) which deposits diamond at a rate up to 180 μm/h over 2 cm^2 has been demonstrated [67]. However, reactors with extremely high power (60 kW) and high gas flow rates (approaching 100 l/m) are difficult to control and costly to operate. Typical deposition conditions and reactor characteristics are listed in Table 20.

The RFCVD reactors seem to combine the advantages of high temperature chemistry with the scalability and convenience of low energy excitation modes. Although the laboratory built reactors are nominally capable of coating areas only 1 to 2 cm in diameter, spreading the gas stream over much larger areas is possible. Some commercial coating operations have used the expanded RF-Jet method [68(a)]. Since RF reactors are sold for other industrial applications, RF power supplies and components are readily available [68(b)]. Because these must be configured by the user to build a useful reactor, costs are nearly impossible to estimate. The high gas flow rates of jet reactors require much larger pumping capacity, usually with the assistance of a roots blower.

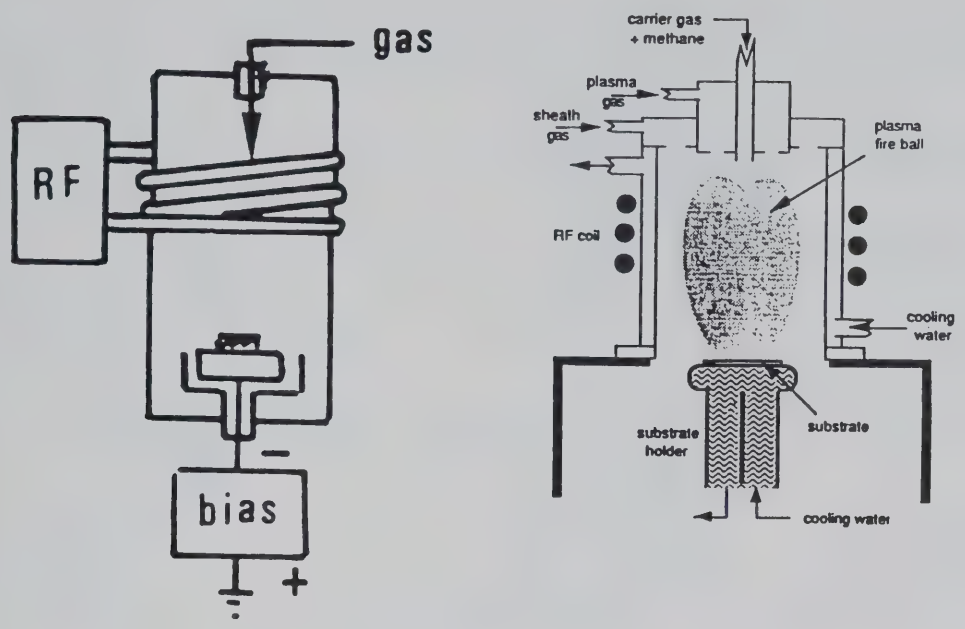

(a) Low-pressure RF plasma reactor

(b) Atmospheric pressure RF plasma torch

Figure 76. Schematic diagrams of radio frequency (RF) plasma CVD reactors. (a) low-pressure RF plasma reactor, (b) atmospheric pressure RF torch.

DC-Plasma Reactors

For convenience, DC-plasma reactors are roughly divided into two types: the low pressure (LP, 2-200 Torr) DC discharge and high pressure plasma jet (PJ, >200 Torr). Because of the relative simplicity of low-pressure DC discharge systems, several versions of LP-DC discharge reactors have been constructed for diamond CVD [69–73]. Figure 77a depicts a schematic of a typical LP DC discharge reactor, which consists of a vacuum chamber (not shown), a gas inlet, and two electrodes with a DC power supply. The substrate is usually placed on the anode to avoid deposition of graphitic materials. When the reactor pressure is below 20 Torr, large area deposition (~10 cm diameter) can be obtained, but the growth rate is low (<0.1 μm/h) and film quality is fair [69–70]. Higher rate diamond growth (1–3 μm/h) was reported using a hollow cathode discharge at high current (8 A) and low voltage (75–115 V) [71]. By increasing the reactor pressure up to 200 Torr and the discharge current up to 10 A at 1 kV, both growth rate (up to 250 μm/h) and quality are improved substantially at relatively low total gas flow rate (20–100 sccm) [72, 73]. However, the deposition area is greatly reduced.

The high pressure plasma DC-jet (PJ) reactor was introduced by Matsumoto and others [45, 74-78]. These reactors (fig. 77b) use concentric nozzle electrodes with a high power DC discharge to generate an extremely hot (4000–6000 °C) thermal plasma at very high gas flow (3–70 l/m). The plasma is blown out of the nozzle to form a flame with the tip touching the substrate. The substrate needs to be carefully cooled during deposition. The highest diamond deposition rates, reaching 1 mm/hour, have been demonstrated with the DC-Jet reactors [45, 78]. However, the operation of these reactors is complex, and rapid erosion of the nozzles is a hazard. In addition, the power and feed gas consumptions are extremely high while the deposition area is small and homogeneity of the films is poor.

Typical conditions for DC plasma reactors are listed in Table 21. Some commercial DC plasma jets manufacturers are listed as follows: Onoda Cement (Japan) and Hercules, AeroChem Research Labs. (Princeton NJ), and Technion, Inc. (Irvine, CA).

Table 20. Typical conditions and features of RF plasmas at low pressure and atmospheric pressure reactors for CVD of diamond

	Low-pressure reactor	Atmospheric pressure torch
Substrate temp. (°C)	500–900	900–1200 (cooling required for)
Reactor pressure (mbar)	0.1–50	1000
Total gas flow (sccm)	100–200	80,000
Input power data	300–3000 W	20–60 kW at 4 MHz
Deposition rate (μm/hour)	<0.5	120–180
Deposition area (cm^2)	large area	<3
Types of substrates	Si, silica, BN, alumina, Ni,	Mo
Quality/crystallinity	Poor to good	Excellent
Uniformity/homogeneity	Poor to good	Poor to good
Advantages of the method	Easy scale-up option, complex substrate shape option	High deposition rate
Drawbacks of the method	Low rates, poor crystalline quality, contaminations	Small deposition area; stability and temperature; contamination control problematic; thickness and quality variations; poor adhesion
Special remarks	Discharges are less stable than MW, thus Ar is added; higher pressures, power, and frequency work better	Very hot plasma fire ball, high power consumption and flow rates, low yield; RF power sources are more expensive than thos of MW

3. Diamondlike Carbon

3.1 Just what is DLC?

Diamondlike carbon (DLC) is not a well-defined material. Rather, it is a broad class of amorphous carbon-based materials exhibiting properties (most importantly high hardness) suggestive of diamond. By a controlled combination of diamond, graphitic and polymeric local atomic configurations in an amorphous structure, a wide range of material properties can be obtained. This range of properties can be extended by incorporation of a small fraction of a second carbide forming element (e.g., Si, W, Ti). Unlike CVD diamond, which is usually grown at quite high substrate temperature, diamondlike carbon can be produced at or even below room temperature. Although DLC is inferior to diamond in many respects, the ability to deposit a very smooth film of diamondlike carbon on virtually any solid substrate opens a much broader range of application.

A unifying concept for all forms of amorphous carbon is the "hydrocarbon phase diagram" (fig. 78) first proposed by Angus et al. [79]. This diagram maps the degree of fourfold or sp^3 carbon coordination as a function of hydrogen content. The solid line is derived from the theory of random covalent networks (RCN). Along this curve lie materials with barely sufficient constraint (defined by the degree of carbon-carbon bonding) to be rigid (there are no remaining zero-frequency oscillators, i.e., there are restoring forces to displacement of every atom in all three dimensions). Materials to the left of this line are overconstrained and so may be macroscopically hard. The dashed curve represents a modification of the random networks which admits large graphitic clusters; the C-RCN model.

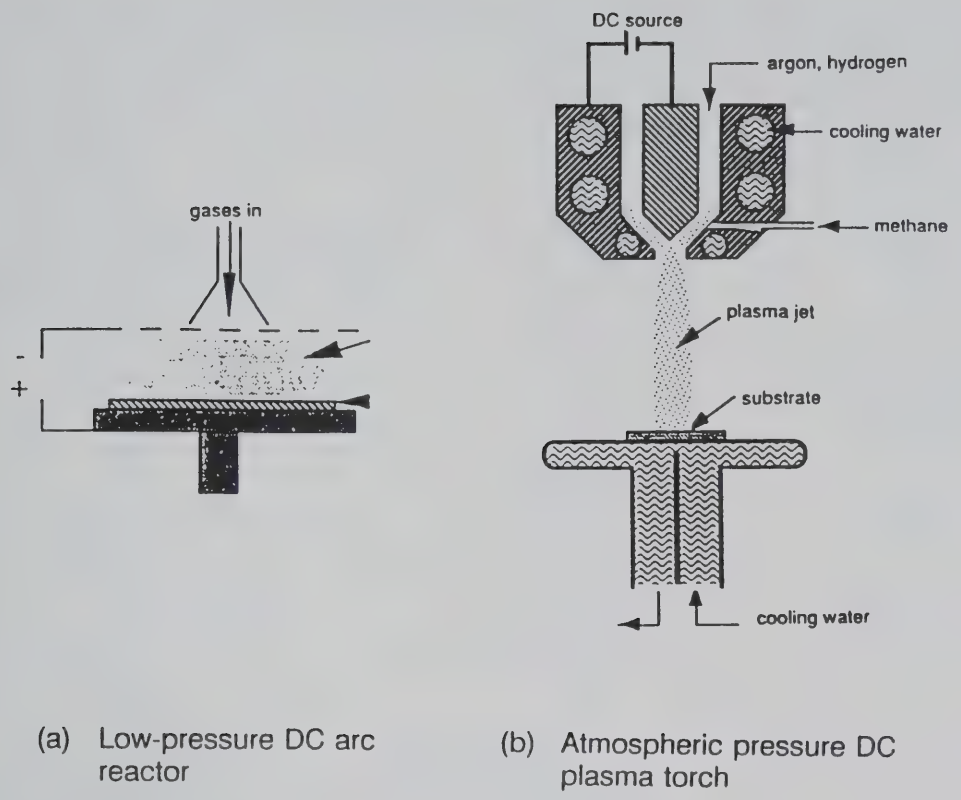

Figure 77. Schematic diagrams of DC plasma reactors. (a) low-pressure DC arc reactor, (b) atmospheric pressure thermal plasma jet.

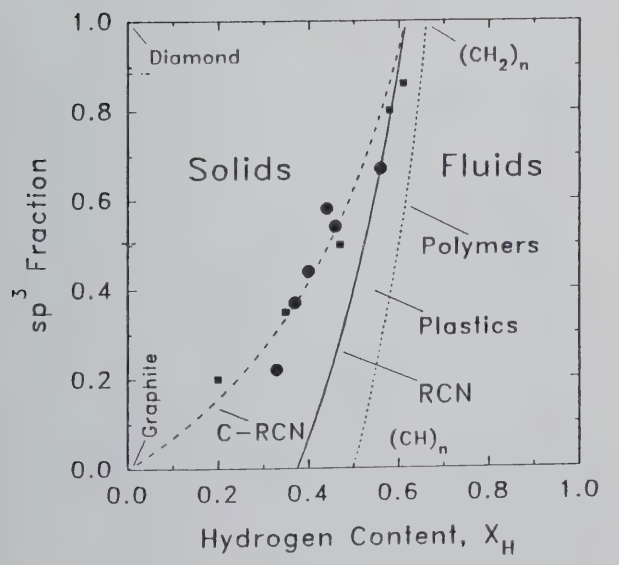

Figure 78. Phase diagram of hydrocarbons with respect to the sp^3 fraction and hydrogen content. Data points (■) are from Ref. [79] and (●) from Ref. [80].

The dotted curve (polymer line) denotes simple long-chain polymers varying continuously from polyacetylene to polyethylene. Materials to the right of the polymer line must be disconnected and so are fluids. Materials between the solid and polymer lines are connected (atoms or clumps of atoms cannot be pulled out) but are not rigid covalent solids (some atoms may be displaced with only weak restoring force). This may be used as a new definition of plastic. Graphite and amorphous carbons with threefold (sp^2) coordination lie at the origin, while diamond and "amorphous diamond" (analogous to amorphous silicon) lie at the top left. Measured sp^3 fractions for hydrogen-free amorphous carbons range from as low 10% to nearly 100%. The measured sp^3 fractions and compositions of a-C:H films (the solid symbols) are in good agreement with the C-RCN model [79, 80].

Table 21. Typical conditions and features of low pressure DC arc and plasma jet reactors for CVD of diamond

	Low-pressure reactor	DC arc & plasma jet
Substrate temp. (°C)	600–1000	800–1100 (cooling required)
Reactor pressure (mbar)	20–200	200–1000
Total gas flow (sccm)	100–200	3,000–70,000
Input power data	300–3000 W	>10 A/cm², 3,000–18,000 V
Plasma temperature (°C)	1000–1200	4000–6000
Deposition rate (μm/hour)	0.1–25	500–930
Deposition area (cm²)	approx. 70	<2
Types of substrates	Si, Mo, silica, alumina, diamond	Same
Quality/crystallinity	Fair to good	Excellent at center; poor at periphery
Uniformity/homogeneity	Excellent	Poor
Advantages of the method	Simple set up, large area	Extremely high deposition rates of up to 930 μm/h
Drawbacks of the method	Low linear deposition rate; medium quality substrate preferably on anode to avoid graphitic material	High heat flux; possible thermal shock shock destruction of substrates; possible severe deformation of substrates; impurity contamination; instability of flame and temperature

3.2 DLC Deposition

Several comprehensive reviews of the formation and properties of diamondlike carbon (DLC) are available [2,3,79–81]. The essential ingredient in the formation of hard amorphous carbon, hydrogenated or not, is control of the kinetic energy with which the carbon or hydrocarbon species impinge on the growing surface. In general, for any deposition scheme and any precursor, the hardest material is obtained when the kinetic energy *per carbon atom* of the precursor is in the range 50 to 200 eV.

3.2.1 Hydrogenated DLC (a-C:H) Hydrogenated DLC (a-C:H, HDLC) films can be produced by virtually any means which can direct a flux of hydrocarbon ions with kinetic energy in the optimal 50 to 200 eV onto a substrate. The substrate temperature may be varied from slightly above to well below room temperature with only small effect on film properties. Holland and Ojha [82] first reported the chemical vapor deposition (CVD) of a-C:H from a hydrocarbon plasma in a parallel plate reactor in which the substrate was fixed to an electrode to which RF-power was applied through a series capacitor (fig. 79). In this configuration, the powered electrode acquires a negative bias determined by the reactor geometry, the applied power and the type and pressures of the gas. We note that this voltage is the rms average of the oscillating substrate-plasma potential difference and is not simply related to the ion kinetic energy. For the most common conditions of DLC growth, the ion energy is estimated to be roughly one-third the average self-bias voltage (i.e., the optimal bias voltage is in the range 150 to 600 V_{rms}). Because virtually any sputtering reactor can be adapted for a-C:H deposition, this self-biased CVD technique is widely used. Alternatively, a hydrocarbon plasma may be generated by DC, RF or microwave discharges and the substrate biased independently, or an accelerated ion source, such as a Kaufman gun, may be used [83–86].

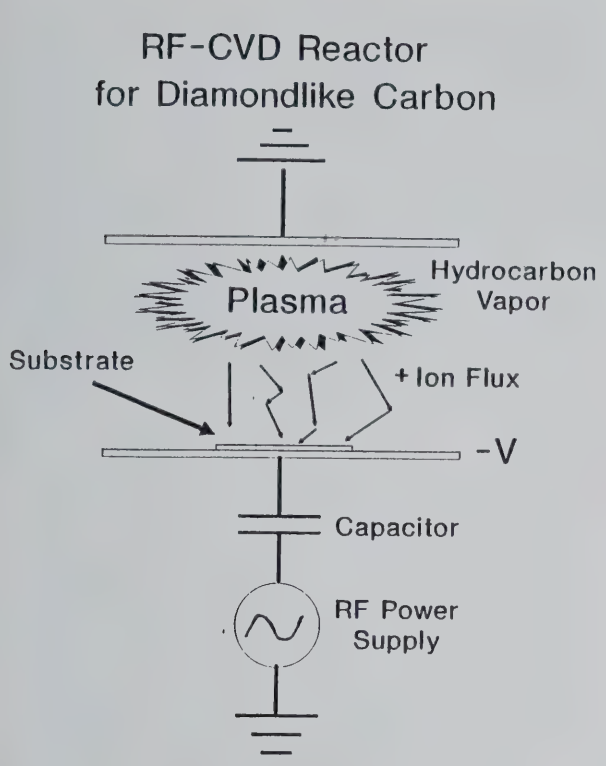

Figure 79. Parallel-plate RF-plasma CVD reactor for diamondlike carbon.

As noted above, the properties of a-C:H films are determined in large part by the energy with which hydrocarbon ions arrive at the growing surface. With increasing ion energy a-C:H evolves from transparent, hydrogen-rich, polymer-like material to a brittle, nearly opaque, conducting material resembling carbon glass. The most diamondlike properties, maximum hardness and density, are obtained at intermediate energy. Several key properties of a-C:H deposited by RF plasma CVD from several precursors are compared as a function of rms self-bias voltage, V_b, in figure 80 [87].

Gas pressure, choice of precursor and substrate temperature play secondary roles in determining film properties. With increasing gas pressure, collisions with the background of neutral species reduce the effective bombardment energy. The pressure at which this effect is significant depends upon the reactor geometry. At very low energy, precursors may not entirely decompose and some may incorporate nearly intact in the film. Films deposited from benzene may contain pendant benzene (phenyl) groups, while those formed from butane can be highly polymeric [84]. At higher energy densities film properties are similar for all precursors, but heavier hydrocarbons generally provide proportionately higher deposition rates. Rates up to several microns per hour can be achieved from butane or benzene vapor. The effect of increased substrate temperature during deposition is approximately the same as that of higher ion energy.

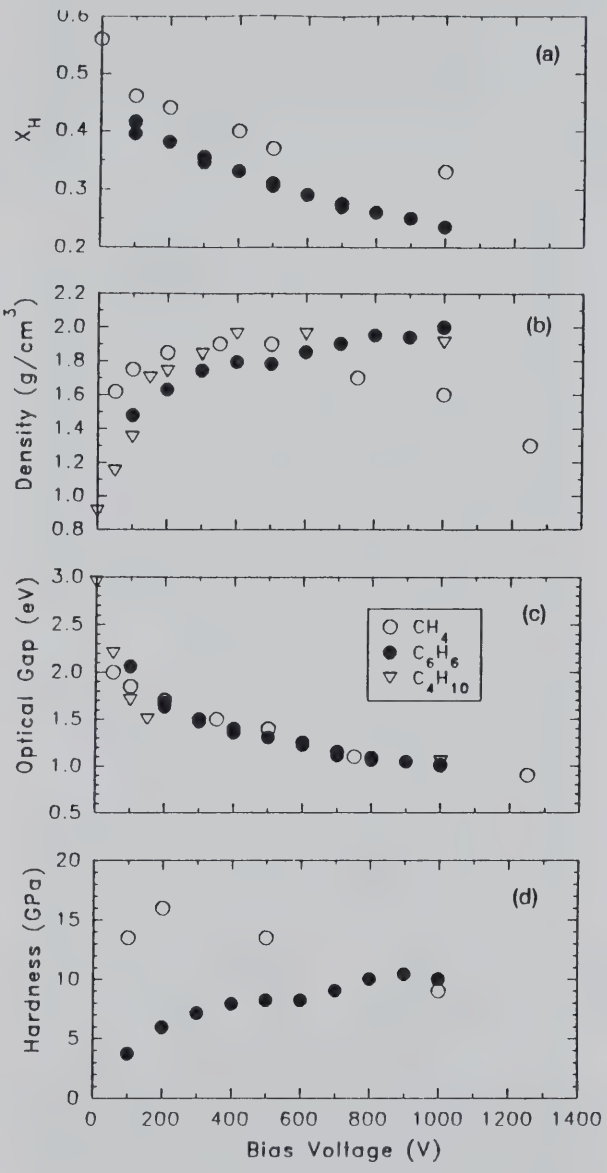

Figure 80. Properties of a-C:H deposited by RF plasma CVD from several precursors are compared as a function of rms self-bias voltage.

A critical parameter of a prospective optical coating material is its optical gap, E_g. A gap of 3 eV is required for optical transparency. Figure 80 shows that hard a-C:H does not meet this requirement; thin films (less than roughly 0.2 μm) are

red-brown in transmission, while thicker films are opaque. Fortunately, this connection between ion energy and optical gap is not rigid. Controlled bombardment by high energy noble gas ions (e.g., 1000 eV Ar ions) during growth can increase the optical gap to meet this transparency requirement without sacrifice of other key film properties [88]. a-C:H is quite transparent in the near infrared with the exception of a strong absorption band near 3.4 μm due to C-H bond stretching vibrational modes. Thus a-C:H films which are quite opaque in the visible are well suited for protection of optics for the 4–6 μm atmospheric infrared transmission band.

The density of a-C:H correlates well with the hydrocarbon ion energy. Densities as low as 0.9 g/cm^3 for films formed at low energy are consistent with the other polymerlike characteristics (softness, transparency). Such films are similar to another form of hydrocarbon film, called plasma-polymer, which forms when little or no potential appears between the plasma and substrate. The film density reaches a maximum of 2.0 g/cm^3 for bias in the 200 to 400 V range, at which the hardness can be as high as 30 GPa, comparable to the hardest ceramics, but far lower than that of diamond (105 GPa). Far less hard, dense and transparent than diamond, hydrogenated DLC is inferior to actual diamond but is certainly the hardest of hydrocarbon materials. With further increase in bombardment energy, the density decreases to only 1.7 g/cm^3, typical of glassy carbon.

3.2.2 Hydrogen-free DLC (i-C) Hydrogen free DLC (i-C) represents a subset of the possible carbon structures quite different from those found in a-C:H. In the "phase diagram" of Figure 9, i-C lies high on the left axis. As it contains no hydrogen, i-C cannot include a polymeric component and must be composed of some combination of networks of sp^3 and sp^2 carbon and possibly graphitic clusters. The first and second dominate the mechanical properties while the last determines the optical properties. Again, the degree of fourfold coordination is controlled by the energy with which carbon atoms or ions arrive at the substrate.

Hydrogen-free DLC (i-C) is usually deposited from a carbon ion beam with mass selection [89-94]. Hardness and density are maximized for ion energies in the range 30 to 80 eV [95]. Just as for a-C:H, the substrate may be at or below room temperature. In fact, the substrate must be actively cooled during high rate deposition. The major challenge in production of i-C lies in finding a source of carbon prolific enough to enable coating large areas at reasonable rates. Conventional C-ion sources depend upon ion sputtering of graphite or decomposition of CO gas and ion extraction followed by mass filtering to produce a pure carbon ion beam. An alternative approach which embodies the essential elements of a an ion-beam system employs a cathodic arc discharge on a graphite electrode as an ion source. The pure carbon plasma is extremely hot and so provides ions in the desired energy range. If desired, an external substrate bias may be included to further increase this energy. Magnetic mass filtering must be added to remove the multi-atom clusters (including the now-famous Buckyballs) produced in high-rate erosion of graphite.

Thermal evaporation and sputtering of carbon cannot be used to form i-C because the atom kinetic energy is too low. Under these marginal conditions, the ability of the substrate to dissipate the kinetic energy of incoming carbon atoms, through low initial temperature and high thermal conductivity, appears to play an important role in determining the film properties. Carbon films sputtered onto diamond at 77 K exhibit densities as high as 2.8 g/cm^3 and up to 60% sp^3 coordination [96]. Pulsed laser evaporation can impart energies of a few eV and so is an intermediate case between sputtering and ion-beam deposition [97]. Carbon films laser-deposited on low temperature substrates (77 K) show a systematic increase in density and estimated sp^3 content with increasing thermal conductivity of the substrate. At low laser fluency (10^8 W/cm^2 in a 10 ns pulse), the carbon kinetic energy increases as the laser wavelength decreases, and the sp^3 content and density of the resulting carbon films are found to increase accordingly. For UV-laser (248 nm) evaporation the ion kinetic energy can exceed 20 eV, approaching the optimal value determined for ion-beam deposition. Indeed, carbon films UV-laser deposited on high quality diamond substrates at room temperature have a density 3.2 g/cm^3 and an estimated sp^3 fraction exceeding 85% [98]

Carbon films produced by laser ablation of carbon at very high laser fluence (10^{12} W/cm^2) appear to be quite different from those formed by evaporation at lower fluence. Above a critical energy density, an extremely hot carbon vapor plume rich in small clusters (C_3, C_4 etc.) is produced [99]. This carbon stream may be similar to that produced by the cathodic arc. Films deposited from the most energetic portion of the plume are highly insulating and exhibit both density (up to 3.1 g/cm^3) and hardness (typically 40 GPa, but up to 77 GPa)

approaching that of diamond, all suggestive of a very high sp^3 content. Microscopic examination of these films shows a nodular structure. The developers of this material have named it "amorphic diamond" and conclude that it is composed of small (100 nm) nodules of quaternary carbon (partially or entirely amorphous) captured in a more graphitic, but nevertheless very strong, matrix. This composite structure permits very high hardness to coexist with relatively low compressive stress, but seriously compromises the optical and electronic properties of the film.

4. Characterization

Film characterization is critical to the preparation, development, and application of CVD diamond and DLC. From even a cursory review of the literature, it would appear that every conceivable analytic tool has been brought to bear in the course of innumerable basic studies of formation and structure of diamond and related materials. Many general purpose tools have been well described [100, 101]. For the purpose of this review, we will focus only on methods of characterization which are particularly powerful for diamond and DLC or relate to applications. One important consideration is that despite frequent use of the phrase "high quality diamond film," there is no single measure of "quality": quality is measured by the customer, and must always be defined by the application. An adherent, tough film which makes a superior tool coating may have relatively poor thermal conductivity and downright dismal optical properties.

4.1 Film Purity

Laser Raman spectroscopy, an inelastic light scattering spectroscopy which detects optically active vibrational modes of a material, is widely used in characterization of diamond and DLC [102–105]. Crystalline diamond has a single Raman mode at 1332 cm^{-1} (fig. 81a). The appearance of the 1332 cm^{-1} line positively confirms the presence of diamond in a film. The width of the peak is also an indication of crystallite size and internal structure; a wider peak corresponding to smaller crystallite size or more internal disorder such as dislocations and grain boundaries. As a diagnostic, the width of the Raman peak correlates well with other more specific properties such as thermal conductivity, carrier mobility and optical transparency. Macroscopic stress, whether due to differential thermal expansion or intrinsic to the film, will shift the peak considerably. Correspondingly, widely varying local stresses will also broaden the peak.

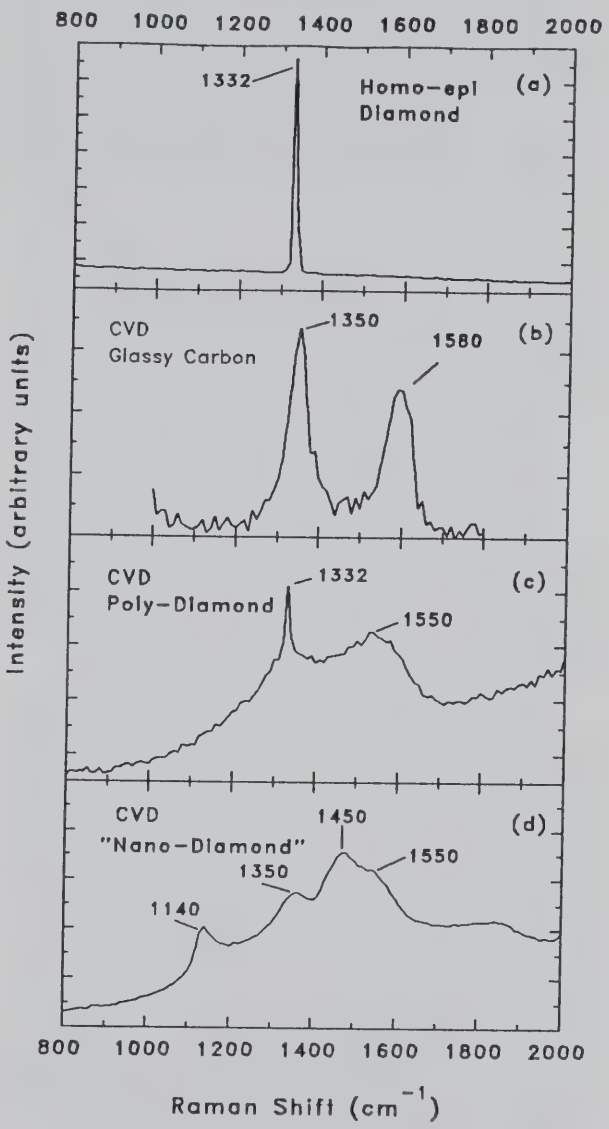

Figure 81. Raman spectra of various forms of carbon. (a) homo-epitaxial diamond, (b) CVD glassy carbon, (c) CVD polycrystalline diamond, and (d) nonocrystalline diamond.

Because Raman spectroscopy is much more sensitive to nondiamond carbon than to diamond itself, it can be used as a sensitive but nonquantitative measure of the "purity" of CVD diamond. Highly ordered graphite has a single Raman mode at 1580 cm^{-1} (the so-called G-peak), while disordered graphite also exhibits a symmetry forbidden mode at 1350 cm^{-1} (the D-peak) (fig. 81b). As the

crystallinity of CVD diamond is degraded (e.g., by increasing the hydrocarbon gas mixture or lowering the substrate temperature) a broad peak centered at approximately 1550 cm^{-1} first appears (fig. 82c). As the material degrades further, this feature grows in intensity and a second feature near 1350 cm^{-1} appears. A third set of related features at 1140 cm^{-1} and 1450 cm^{-1} appear in films with fine particles (nanocrystalline diamond, (fig. 81d) [9(a)]. All these features are derived from sp^2-bonded nondiamond carbon. Direct measurements by NMR spectroscopy show that only a very small fraction (less than 1%) non-diamond carbon is required to submerge the diamond signal in the Raman spectrum [106]. This relative sensitivity is highly variable with the choice of excitation wavelength; a hidden diamond signal may be revealed by using deep blue laser light, while a small residual non-diamond component is brought out with near-infrared excitation. Other features unrelated to Raman scattering also appear in the spectrum and so provide useful information. By scanning to very large downshifts, the photoluminescence spectrum is also obtained. A variety of defects in CVD diamond may be identified by comparison with the literature on natural and synthetic diamond [102,103,107].

Although Raman spectroscopy cannot be used as a rough measure of "quality" of DLC as it can for diamond, the spectrum of DLC does correlate very well with numerous other properties that are less accessible. Figure 82 shows the Raman spectra of several DLC films compared to that of microcrystalline graphite. As the energy of hydrocarbon impact during deposition (the bias voltage) increases, the Raman spectrum evolves toward that of graphite. This is consistent with the description of DLC as a composite of small graphitic clusters embedded in a more transparent matrix (the C-RCN model described earlier). The optical gap of such a cluster varies as $E_g = 6.0/N^{1/2}$ (eV) where N is the number of rings in the cluster. As the bias voltage increases clusters grow larger and more "graphite-like" and their optical gap decreases [108]. The resemblance between the Raman spectra of DLC and that of the non-diamond component in CVD diamond further supports interpretation of the latter in terms of a growing fraction of sp^2 bonded carbon which is amorphous (no D-peak, an indicator of order) in low quantities but also evolves toward graphitic carbon at high concentration.

X-ray diffraction can be used to characterize the internal structure, texture and orientation of the crystallites in CVD diamond [1,103,105]. While these may be of incidental importance for mechanical applications, they are critical to optical and electronic applications where properties approaching single-crystal diamond are desired.

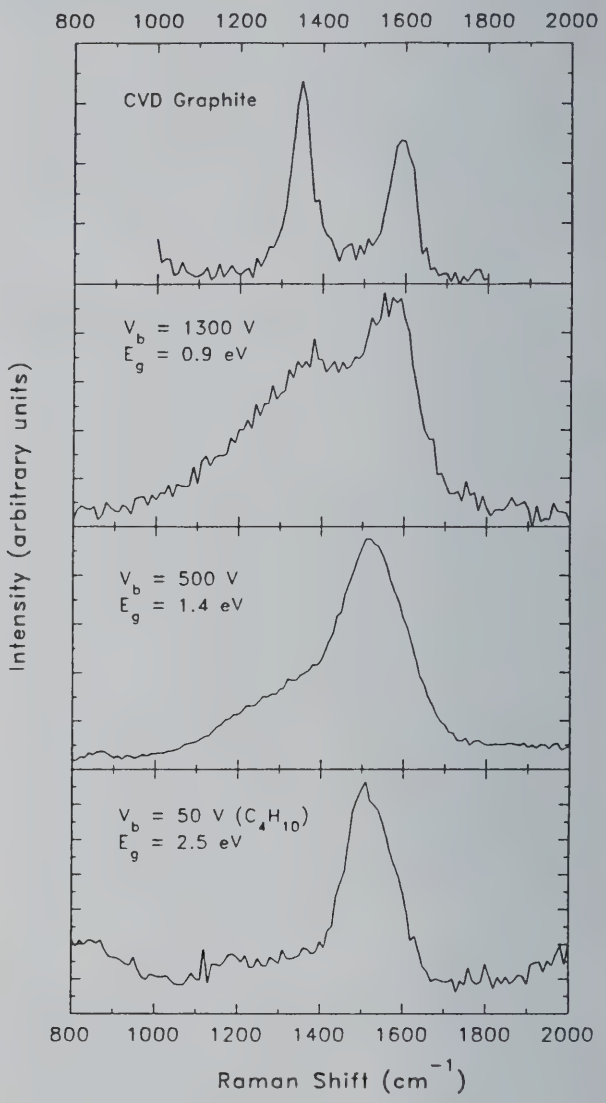

Figure 82. Raman spectra of CVD graphite and diamondlike carbon formed under different impct energies of hydrocarbons.

4.2 Hardness and Adhesion

Conventional indentation hardness measurements, which require creation of an indent large enough to find and measure with an electron microscope, are problematic when the film is as hard as the indenter or thinner than the depth of the smallest detectable indent. (As a rule, the indent depth must be less than one-tenth the film thickness.) Reliable measurement of the hardness of

CVD diamond films have been obtained, but the risk of damage to the indenter diamond is always present. The hardness of thick, high quality CVD diamond films does indeed approach that of single crystal diamond. Nanoindentation methods rely on analysis of the load-unload response to a very shallow indentation rather than examination of the indent itself [109–113]. Such systems are less prone to loss of the indenter tip but are not suitable to the industrial environment due to their cost and complexity. However, a crucial advantage of the nanoindentation method is its ability to measure hardness of films as thin as 100 nm. To date, nanoindentation has been the only reliable measure of hardness of DLC which is not available in thickness greater than several microns due to its high intrinsic stress.

Adhesion measurement is problematic for both diamond and DLC. One common method is the scratch test in which a stylus (usually diamond) is drawn across the film with increasing force until the film fails. Failure may be observed visually or detected by a sound transducer. For CVD diamond, scratch testing is usually destructive to the stylus and so is quite unreliable and costly. DLC can be made so hard and adherent that "deadhesion" is often due to subsurface failure of the substrate (spalling). Although pull-tests have proven effective in some cases, these usually provide only a lower limit. A common method for comparing adhesion to metals and composites measures the radius of film deadhesion surrounding the deep indent into the substrate produced by a hardness test such as the Rockwell test. In general, adhesion strength must be evaluated by performance under the stresses of actual application.

4.3 Electronic, Optical and Thermal Properties

Electronic, optical and thermal properties of diamond and DLC are generally measured by well established means. Electronic properties have been examined using the full array of tools developed for other semiconductor systems [114-116]. Two important considerations which are occasionally overlooked are electrical isolation from the substrate (which is most often a semiconductor as well) and ohmic contacts. Free standing diamond films have been examined by optical transmission spectroscopy from the near ultraviolet (200 nm) to the mid-infrared (5000 nm) [117]. Properly prepared CVD diamond films exhibit transmission spectra essentially the same as that of good natural diamond.

One area where specialized techniques have been applied is measurement of thermal conductivity. Measurement of the thermal conductivity of thin films is complicated by the substrate or prone to large errors due to the very small specimen size if the substrate is removed. Fast transient measurements of the heat flow following focussed pulsed laser heating overcome this difficulty [118–121]. Polycrystalline films with heat conduction approaching the best single crystal diamond have been demonstrated.

4.4 Friction and Wear

The methods for tribological evaluation of thin films are well established [122]. The most common method is the pin-on-disk apparatus which measures the lateral force on a loaded ball in contact with the spinning disk. One important consideration in evaluating the wear of CVD diamond is the effect of transferred films. It is extremely difficult to grow a very smooth diamond film. Even a small degree of surface roughness will transfer ball material to the disk. The wear measurement is then no longer that for the ball material on diamond, but the ball material on itself. The much touted low friction of diamond is obscured and coefficients of friction (COF) on the order of unity are observed. Very smooth, polished CVD films exhibit very low friction coefficients (0.05) and extremely low wear rates. If both ball and disk are coated with unpolished CVD diamond, they will wear one another to form a smooth track and the low friction of diamond will be recovered after a wear-in period. It should be kept in mind that the low friction of diamond depends on surface bonded hydrogen. Prolonged sliding in vacuum or inert atmosphere will remove the hydrogen and the COF increase to values greater than unity [123]. High temperature (>800 °C) will also desorb the hydrogen.

Because diamondlike carbon films are very hard and extremely smooth, they are well suited for use as low wear coatings. For dry sliding against steel, COF's of 0.1 are readily obtained with a wear rate at least an order of magnitude less than that of competing coatings such as Si_3N_4 and TiN (which give much higher friction) [124]. The COF of DLC is sensitive to humidity and rises to above 0.3 in saturated air, but falls to less than 0.03 in very dry atmosphere. This is diametrically opposed to the behavior of graphite lubricants and so contradicts the popular belief that the low friction of DLC derives from conversion to graphite under the heat and stress of sliding. It is more likely that the

origins of the low friction of DLC are the same as those of diamond: the combination of extreme hardness and a stable hydrogen terminated surface. In contrast to diamond, hydrogenated DLC contains plentiful hydrogen throughout the film and so retains its low friction under conditions where diamond does not. The addition of metals or other additives stabilizes the humidity dependence of DLC friction [125]. The proper choice of additive can result in low friction over a wide range of conditions [126].

5. Example Applications

5.1 Diamond

5.1.1 Cutting and Grinding Tools In the near term, the primary application of CVD diamond is in cutting and grinding tools. Some advantages of diamond tools include longer tool life, higher cutting speeds, better surface finish, reduced machine down time and material scrap, and ultimately higher product quality at lower unit cost. Diamond tools are particularly suited for machining of extremely abrasive lightweight metal-matrix and polymer-matrix composite materials. These include hypereutectic silicon-aluminum alloys which contain macroscopic silicon grains, metal matrix composites including grains of SiC or TiC, and graphite reinforced composites. At present, polycrystalline diamond (PCD) compact tools are used when necessary. In the PCD process, diamond grit is sintered with a suitable binder to form an extremely tough compact from which small plates are cut. These platelets are then brazed to conventional tool substrates and finally ground (dressed) to the desired shape. Even though PCD tools are extremely durable and may be resharpened several times, this elaborate fabrication process makes them too expensive for many applications. Furthermore, the composite construction from brazed platelets places severe restrictions on tool geometry.

CVD diamond coating promises both lower cost and much greater flexibility in tool design. While the shape of PCD tools is generally limited to planar surfaces, CVD coatings may be applied over complex surfaces such as chip-breakers. Substantial increase in tool life, improved surface finishing, and improved product quality have already been demonstrated [127-129]. At present several manufacturers [130] are producing CVD diamond tool inserts for machining of metal-matrix composites. Diamond coated twist drills are under development. One interesting property of both diamond and DLC is their low adhesion to organic materials. Diamond surgical knives permit more precise incisions with less scarring than metal tools. For the same reason, diamond coated industrial knives for thin cutting of wood for plywood and veneers are vastly superior to their metal predecessors.

One issue in the introduction of CVD diamond coated tools is the choice of substrate. A significant fraction of the current tool investment is in machinery designed for very tough cemented carbide tools (most often cobalt-cemented WC). However, reliable adhesion of CVD diamond to WC/Co has proven difficult because Co poisons diamond growth, but may not be removed because it holds the tool together. While there has been some success in this area using interlayers and special chemical treatments, the alternative of a ceramic substrate is also very attractive. Diamond adhesion to these Si_3N_4-based materials is readily achieved and they are a closer thermal expansion match which reduces interfacial stress. However, ceramic tools are not as widely accepted because they require more advanced tooling (with much more rigid fixturing) and more careful handling on the shop floor. Recent announcements of mastery of the WC/Co adhesion problem may herald the end of this impasse [130].

5.1.2 Dies and Nozzles Hardness, toughness, low friction, chemical inertness, high thermal conductivity, and smoothness make diamond an ideal material for die and nozzle applications. Polycrystalline diamond wire-drawing dies have been demonstrated [131]. These may be cheaper and more flexible in terms of geometry than those made by drilling of single crystal diamond. The problems of anisotropic wear due to different hardness on different surfaces of diamond and weakness due to cleavage of single crystals can be eliminated. In one interesting variation of the method for die making, a fuel injector nozzle for highly abrasive coal-water slurry (used as diesel fuel in some railroad locomotives) exhibits a working life many times that of its conventional predecessors. Long-lived diamond nozzles for controlled high velocity spraying of abrasive powder-liquid and powder-gas mixtures are realizable with CVD technology.

5.1.3 Friction/Wear Coatings The ubiquitous diamond bearing, the jeweled watch movement, is now obsolete. Although diamond does indeed exhibit low friction (at least against itself) and wear, it may not be as attractive for bearings as is widely believed. As noted earlier, the diamond coating must be highly polished to achieve low

friction unless both surfaces are coated (in which case they polish each other). Either way, the cost will be high. For surfaces subject to distortion, such as heavily loaded ball bearings, adhesion of extremely brittle diamond to the constantly flexing bearing surface may be problematic. The wide smooth surfaces of journal bearings might appear suitable to diamond coating. However, in most cases, "quality" must be measured in a comparison to a properly lubricated system. Dynamically lubricated journals have COF as low as 0.005, much lower than that of dry diamond. Because there is no actual solid-to-solid contact in a properly lubricated bearing, the low (apparently not all that low) friction and wear of diamond are relevant only during aberrant no-oil conditions. In such conditions, a diamond film may indeed reduce friction and significantly postpone catastrophic failure, but must be compared to the soft bronze-based surfaces designed for just such a contingency. In critical applications such as helicopter rotor hubs and aircraft turbines, even a small improvement may be life-saving [132].

Where lubrication is a viable option, the dry sliding friction of diamond is unlikely to be competitive. Worse, diamond does not appear to be compatible with conventional lubrication systems; wetting with conventional oils often results in higher friction! In fact, the greases used to separate diamond grit at the mine must be carefully designed to adhere to diamond, and their formulations are closely held trade secrets. Diamond may not even serve where lubrication is not an option, such as in vacuum (space or vacuum machinery) or at high temperature. In both conditions, loss of surface-bonded hydrogen (which also stabilizes against graphitization) is fatal; both low friction and low wear are irretrievably lost.

5.1.4 Optical Components and Coatings Because of the combined properties of hardness, chemical inertness, high thermal conductivity and low thermal expansion (which translates to thermal shock resistance), and wide range of spectral transparency, diamond is an ideal material for optical components and coatings for use in harsh environments [133-136]. Windows, lenses, and mirrors made of diamond are suitable for IR, visible, and UV optics and can endure abrasion, corrosion, high temperature, intense photon flux and ionizing radiation. Such properties are particularly important for aerospace, defense, space and communication industries where optics must endure high velocity dust and water droplet impact both in air and the harsh environment of space. For example, some conventional IR seeker objectives must be refurbished after only 4 hours of near-sonic flight, and objectives for tank gun sights are damaged by corrosive vapor from the projectile propellant. Diamond lenses, windows, and mirrors can handle extremely high light flux, and so may be used in high-power excimer and free-electron lasers. Thin diamond membranes are used for x-ray windows and are under consideration for use in synchrotron radiation lithographic masks (for integrated circuits) because of their low x-ray absorption, high strength, resistance to radiation damage, and low thermal expansion coefficient.

5.1.5 Protective Coatings Impermeability and chemical stability in corrosive environments, at high temperature, and in the presence of ionizing radiation make diamond an excellent corrosion preventive coating for vessels containing reactive chemicals or nuclear fusion and nuclear particle accelerators. The high surface energy and hydrophobicity of diamond resist the bacterial and viral attachment, thus allow it to be the coating material for medical implants and instruments.

Diamond is also a candidate material for a protective cladding on turbine compressor blades, which are rapidly eroded in dusty conditions. [Witness the concern about air cleaning and engine reliability for low-flying helicopters and turbine-powered tanks during Operation Desert Storm.] Diamond is certainly very light, hard and abrasion resistant, but may prove too brittle and temperature sensitive for this application.

5.1.6 Thermal Management With the highest thermal conductivity of any solid at room temperature and still a good electrical insulator, diamond is the ultimate thermal management material [137-138]. Single crystal diamond heat-spreaders are already in use for high power microwave devices and lasers for long-distance fiber optic cables. Replacement of conventional copper or BeO heat spreaders improves heat rejection to such an extent that power output may be increased as much as tenfold. Polycrystalline diamond with thermal conductivity equivalent to that of single crystal diamond has been demonstrated, and it is hoped that CVD diamond will be a low cost replacement for rather expensive single crystal spreaders. At present all applications involve small and widely separated heat sources and are served by small diamond plates. These may be single crystals or similarly sized high thermal conductivity polycrystalline plates. Currently in development is a much more dramatic application where large area high thermal conductivity CVD diamond plates are used as

circuit boards in an extremely dense supercomputer. Even when constructed with the same electronic devices, such a computer could be far faster than its conventional predecessor simply due to the large reduction in the distances over which signals must travel. As an intermediate case of area heat management, even a few microns of diamond on a more conventional AlN board significantly improves heat extraction from electronics. Large diamond plates might also be used for extremely high performance, albeit commensurately expensive, heat exchangers. The market for diamond in these and related applications is predicted to be $1 billion in 5 years [138].

5.1.7 Electronics Endowed with good mobility for both electrons and holes, high saturation velocity for electrons, high dielectric strength and high thermal conductivity, diamond appears to be the ultimate semiconductor for both analog and digital devices [139]. Figures of merit (FOM) derived from material limitations to device speed, power, and density greatly exceed those of any other semiconductor [140]. Promising as they are, such estimates must be treated with extreme caution. For example, one simplistic estimate of the limiting device frequency as a function of operating voltage presumes carriers travelling at the saturation velocity through a distance defined by the operating voltage divided by the breakdown strength of diamond. Terahertz switching of 10 V is predicted. However, closer examination of such an estimate reveals that the gate length of such a device is only a few angstroms, well within the quantum regime where macroscopic concepts such as mobility lose their meaning. When high speed switching of the highest possible voltage is considered, such objections disappear. One promising application of diamond is for improved power electronics [141]. In the case of digital circuitry, diamond's advantage derives mainly from its superior thermal conductivity. Some of this advantage might be captured by laminating conventional Si-based or faster GaAs-based circuitry on a very thin substrate to a diamond heat spreader.

The large band gap of diamond translates to functionality at temperatures much higher than those where Si becomes intrinsic (thermally generated charge carriers outnumber those deliberately introduced by doping) and device operation ceases. In principle, diamond electronics should operate up to the point of graphitization near 1000 °C. Even poor functionality at such high temperature would be so valuable as to outweigh relatively poor room-temperature performance. The low neutron scattering cross section, radiation hardness, high breakdown voltage, and the chemical stability of diamond also promise durable electronics for space-based applications, nuclear reactor control, and sensing chemically harsh environments.

Diamond-based electronics is in its infancy. Only simple Schottky diodes, p-n junctions and a crude field-effect transistor have been demonstrated [142–144]. One handicap diamond faces is the lack of a shallow acceptor and the lack of any reliable donor. Boron is a reliable acceptor, but has an activation energy of 0.38 eV; only 1% of the boron impurity is activated at room temperature. This translates to large changes in device characteristics with temperature and consequent design difficulties. For single crystal diamond, carefully controlled carbon ion implantation can produce light n-type doping with an apparently low activation energy [145]. Although some researchers report n-type doping of polycrystalline diamond by phosphorous, positive results are intermittent and reported activation energies range from 0.1 to 0.6 eV [146].

5.1.8 Sensors Semiconducting diamond is well suited for use as a sensor material, possibly with rudimentary signal conditioning, for hot, corrosive or high radiation environments. Diamond thermistors with reproducible behavior from 77 to 1200 K have been demonstrated in several laboratories [147, 148]. Single crystal diamond has been shown to have a very large piezoresistive gauge factor, at least five times that of silicon at room temperature [147]. Furthermore, polycrystalline diamond films were found to have a usable piezoresistive response that actually increased with temperature [149]. The large piezoresistive response of diamond suggests that pressure transducers, strain gauges, and accelerometers with very high sensitivity may be made compatible with very harsh operating environments. It has also been suggested that gas flow sensors (hot-wire anemometers) with fast response and high spatial resolution might be fabricated by taking advantage of diamond's low heat capacity and high thermal conductivity [150]. Because of the simplicity of such devices and the less stringent electronic property requirements (relative to active devices) low cost diamond-based sensors suited to harsh environments seem to be a real possibility in the near term.

In one fascinating very large scale application, diamond may be the material of choice for a large particle detector to surround a collision zone in the superconducting supercollider (SSC). Because it is so resistant to radiation damage, the diamond

the diamond detector may be placed much closer to the reaction zone than could silicon, and therefore would be proportionately smaller. This one-time application will require millions of carats of high quality diamond.

5.1.9 Electro-optics Diamond can be made to emit light via electroluminescence (EL), photoluminescence (PL), and cathodoluminescence (CL). The emission spectrum depends on both the method of excitation and impurities in the diamond. Blue EL devices have been constructed which show an emission band peaked around 430–440 nm [151, 152]. Other blue emitter EL devices based on DLC films have also been fabricated [153]. Picosecond high-voltage electro-optic switches which exploit the high breakdown strength and high carrier mobilities of diamond have been proposed [154].

Another important feature of diamond is its negative electron affinity which enables it to emit electrons in vacuum at room temperature and low bias potential. Devices based on cold diamond cathodes (CDC) could be used in small gas discharge lamps, flat-panel computer or television displays, and, submicron vacuum triodes. Stable room temperature CDC operation at high current density (10 Amp/cm^2) has been demonstrated [141]. In principle, CDC devices should be very stable and reliable.

5.2 Diamondlike Carbon (DLC)

Most applications described above for CVD diamond are pertinent to DLC, often with some compromise in performance. However, because DLC can be deposited over large areas at low temperature, it offers a range of applications vastly greater than that for diamond, and at much lower cost. With less publicity than is devoted to even the most doubtful diamond product, a-C:H coatings are in production in a variety of applications. All are related to protective coatings. DLC coated infrared optics in various military systems are already in the field [155, 156]. These include missile domes, submarine periscopes, and night-sights for aircraft. All are subject to various forms of attack: dust abrasion, corrosion, water droplet impacts, chemical attack from propellant gas and even barnacles. DLC modified for greater visible transparency is available on premium sunglasses and ski-goggles [157]. These may be conveniently cleaned with fine steel wool! It is used on solar photovoltaic cells to increase their efficiency and windows for supermarket bar code scanners for scratch resistance. Very thin DLC coatings are used for protection of magnetic media on hard disks (which virtually eliminates damage from head crashes) and metal thin-film recording tape (where an protective anti-oxidation layer is necessary) [158]. DLC coating of tape-drive guide components in small video cameras reduces tape and camera wear, and promotes smoother tape motion. Because of its bio-compatibility and smoothness, it is good for prostheses, biomedical implant, and surgical instruments. DLC coating of scalpels, dental instruments, surgical implants, artificial heart valves, and blood handling hardware have also been demonstrated. DLC coating is also used to stiffen thin-metal high fidelity loudspeakers to raise their resonant frequency and so flatten their response in the audio frequency range. The superior tribological properties of DLC allow its use on various moving parts: copy machine drums, thermal printers, recorders, and printer heads. It may serve as a vapor barrier for various electronic packaging, sensors, and optical fibers. Given the ease with which DLC may be applied to metals, ceramic and plastics, the possibilities are uncountable.

6. Technical Challenges

The superior chemical and physical properties of diamond and DLC certainly promise innumerable new business opportunities. Interestingly, the capital investment for entry into the CVD diamond arena is very small. The field is already congested with competitors large and small, conflicting and sometimes overly optimistic economic forecasts, and barely credible claims of technical breakthroughs. Newcomers might be well advised to carefully target their effort to address specific applications or well defined research challenges. For the purpose of discussion only, we classify these into two broad categories. The first of these might be loosely defined as "technical issues" which relate to development of a coating system to serve a specific purpose using processes derived from existing technology. This may include process development, control and stabilization. Because so many diamond applications are nearing commercialization, this type of work will generally be funded by and serve an industrial customer. The second area might be termed "economic" and relates to the fundamental cost structure and *breadth* of application of diamond materials. These include improving the economics of diamond CVD relative to current practice (extremely inefficient and too hot for many substrates of interest) and the suitability of diamond relative to DLC or another material.

As it addresses the essentials of the chemistry of diamond CVD, research in this area is relatively basic, and so might also garner government support. With no claim of completeness, some specific examples of each type of issue are described below.

6.1 Diamond

6.1.1 Controls of Film Quality, Morphology, and Purity The ability to obtain reproducibly the desired structure, morphology, adhesion and chemical composition of the deposited films is a prerequisite for serious application of CVD diamond [13]. Film properties are strongly dependent on the growth parameters and deposition methods and must be optimized and controlled for each application. On occasion, properties unobtainable in as-grown films may be imparted by post deposition treatments.

Nucleation and Growth Parameters

It is well known that the properties of diamond and DLC films are complex functions of many deposition parameters, such as nucleation treatment, gas composition, substrate temperature and material, gas flow and reactor pressure [5–15, 159]. In general, some nucleation pre-treatment is necessary to obtain a complete (pinhole-free) film of reasonably low thickness. Most, but not all, of these involve scratching or bombardment with diamond powder. While a residue of submicroscopic diamond grit is the prime suspect, the mechanism of such pretreatment is not entirely clear; although diamond is most effective, other abrasive powders (e.g., SiC) do work, while the presence of an appropriate fluid (for example, vacuum pump oil) strongly affects the efficacy of the treatment. It is reasonable to expect that adhesion would be enhanced if diamond were nucleated directly on the substrate, rather than on loosely attached diamond residues. Methods for promoting nucleation directly on Si have been demonstrated, and such direct nucleation has proven essential for good adhesion to carbide tools [160]. A variety of interlayer systems have also been evaluated for their ability to nucleate diamond (or compatibility with diamond powder treatment) and enhance adhesion [161]. Clearly, as the first link in the diamond chain, control of nucleation is the essential first step in the control of film performance.

Control of diamond texture and morphology is the second essential to diamond film applications. The systematics of the relationship between growth conditions, crystal morphology, phase purity (non-diamond carbon) and optical properties have been studied [162–165]. In general, the <110> directions are the direction of fastest growth, resulting in <110> texture, with mixtures of triangular (111) and square (100) faces on the surface. The relative area of triangular and square facets itself varies systematically. Furthermore, with careful control of growth conditions, other textures closely approaching <100> have been obtained [117]. This permits growth of very smooth films which do not require polishing before use as optical coatings. Growth from carbon-rich gas mixtures or at low temperature often results in a great deal of secondary nucleation and therefore a smoother surface. However, the complex internal structure may result in a mechanically weak coating and compromised optical properties due to the formation of non-diamond carbon in the increased intragranular surfaces. The latter effect may be at least partially offset by inclusion of oxygen in the growth gas, resulting in what have been termed transparent "nanocyrstalline" diamond films. Heavy doping is also accompanied by an increase in secondary nucleation.

Post Deposition Treatment

Smoothness is critical to many key applications of diamond films. Unless prepared under the narrow range of conditions mentioned in the previous section, as-grown films usually have rough, facetted surfaces. Several methods have been used for surface smoothing [166, 167]. Polishing of the diamond against hot cast iron (300 °C) takes as long as 6 weeks to attain a smooth surface. Recently, a smoothing method involving gradual dissolution into a compressed iron film was reported [168]. Heat-treating the diamond at 1000 °C in a flowing gas of 0.01% O_2 of Ar will smooth it in 4 hours. Soaking in KNO_3 solution, surface of diamond is oxidized at a fast rate, but it may be damaged if not done with care. Other methods of modification of properties include exposure to high vacuum or different gases at high temperatures, electron bombardment, and ion implantation.

6.1.2. Growth Rate Improvement Although growth rates approaching 1 mm/h have been reported, the area of film deposition at such rates is small (<2 cm^2). Furthermore, the high energy density associated with such high rate growth may be difficult or impossible to deliver over a larger area because the excess heat cannot be extracted fast enough. In other words, these are essentially 1-dimensional "point" reactors, not true coating

machines. In fact, it has been estimated that all types of diamond CVD reactors consume roughly the same amount of energy for each carat of diamond produced. Even the low range of these estimates translates to 10 kWhr/ct. This uniformity in energy cost for all reactors may be a reflection of the fact that they all work on essentially the same principle. At \$0.10/kWhr, this is \$1.00/ct, approximately the same as industrial grade grit. Of course, this cost must be seen in terms of the amount of diamond actually required, often very little, and the value added to the product. Nonetheless, CVD diamond is not cheap. The essentials of the growth chemistry are still not known and the preponderance of the energy investment is almost certainly going to waste; we have burned the house down just to bake a cake. Thus, growth of diamond at a moderately high rate (at least 20 μm/h) over large areas with low energy consumption remains the paramount "economic" challenge.

Several minor variations on current reactor concepts have been reported. By the addition of substrate biasing and increased carbon concentration (up to 3% CH_4 made permissible by the "quality" improvements from the bias current) the growth rate was increased to 5–10 μm/h at temperatures as low as 400 °C [50, 167]. Addition of O_2, H_2O, halogen, or oxygenated organic compounds have also been shown to increase the growth rate [41,42,49]. Also, some enhancement was obtained by alternating the carbon deposition and etching by rapid switching of the feed gas flows [169].

The next generation of reactors must invest energy only in necessary reactions to sustain diamond growth at higher rate (significantly greater than 20 ηm/h) without sacrificing other desirable properties ("quality"). Recent advances in laser-driven chemistry seem to point the way. Subramanian and coworkers recently reported excimer-laser driven diamond CVD in a CO/H_2 mixture (0.7%) with no other energy input and no substrate heating [170]. The laser was tuned to selectively dissociate the CO molecule by multiphoton absorption. This demonstrates that it is possible to generate the essential diamond growth species by a nearly direct process without resort to brute force thermal or quasithermal techniques.

6.1.3 Low Temperature Deposition To be applicable to a large number of substrates which may be thermally sensitive, to reduce stress due to expansion mismatch and to reduce cost, low temperature deposition is essential. Addition of oxygen, water, and halogen to the feed gases results in some improvement of the growth rate at reduced temperature [41,42,66,171,172]. Substrate temperatures as low as 250 °C and diamond growth rate as high as 1 μm/hr have been demonstrated recently using an RF-plasma reactor at relatively low power [66]. Again, reactors operating on non-thermal principles would be a great improvement.

6.1.4 Film Adhesion Adhesion is one of the most important criteria which determine the useful life of hard coatings. Several factors which affect the film adhesion include surface treatment, nucleation density, interlayer, and film stress [173]. Pretreatment of the substrate surface by cleaning and etching is required to remove undesirable matter which may weaken film adhesion. Pre-decarburization of substrates has been reported to increase film-surface contact area, thus improving the adhesion [174]. On the other hand, pre-carburization to form carbides on substrates has been shown to increase nucleation density to as high as 8×10^{10} /cm^2, therefore, adhesion is improved [175]. Introduction of an interlayer between the substrate and the coating may serve as a diffusion barrier and nucleation promoter to improve adhesion. It may also reduce stress due to thermal mismatching. The stress between the coating and the substrate can cause delamination. It can be minimized by annealing, deposition of an interlayer, proper selection of substrate material, and reduction of the deposition temperature.

6.1.5 Heteroepitaxy As noted earlier, some simple electronic applications are adequately served by polycrystalline CVD diamond films. However, it is a virtual certainty that full exploitation of diamond as a semiconductor will require single crystals of unprecedented size (diamond boules) or large area single crystal films at reasonable cost. At present, most serious device work depends on natural or synthetic diamond substrates. These are expensive and small (a 3×3 mm substrate is approximately \$200).

The "diamond substrate" problem has been attacked from two directions. First, many researchers have attempted heteroepitaxy on a variety of substrates. True heteroepitaxy has been achieved only over very small areas on cubic boron nitride (c-BN) and copper [176, 177]. While c-BN is a good lattice match with diamond, large c-BN crystals are essentially nonexistent. The latter is still a polycrystalline film. In an alternative approach, oriented mosaic polycrystalline films, where crystallites are of uniform size and close orientation, have been grown by several methods which control the nucleation. Such films exhibit some electronic properties equivalent to those of single crystal diamond.

Mosaic films have been formed by three methods: (1) "racking" of diamond powder in an array of pits micromachined in Si [178], (2) nucleation by hydrocarbon ion bombardment of SiC [160], and (3) a textured growth of diamond on Si by carburization and biasing [179]. It is entirely possible that these mosaic films will be in all respects an adequate substitute for true single crystal films. A third approach which has yet to be demonstrated is to produce a large single crystal diamond plate by successively thickening (by CVD) and "shaving" (by oxygen ion implantation) a flat seed diamond [180]. The thin shavings are arrayed to make a progressively wider seed plate which can be thickened and shaved to produce large single crystal sheets.

6.1.6 Cost Reduction For CVD diamond and DLC technology to be widely used, reduction of cost is a must. To accomplish this, the yield and growth rate of films must be improved. At the same time, energy and feed gas consumption should be reduced. Recirculation of feed gas appears to cut down the gas consumption. Substitution of expensive feed gases, e.g., hydrogen and hydrocarbons, with low cost gases, e.g., water and CO_2 has been demonstrated [181]. Once again, non-thermal reactors may be the critical technology for broad commercialization of CVD diamond. Even for more conventional reactors, optimizing for stability and controllability could significantly enhance productivity.

6.1.7 Scale-up For mass commercialization and various applications, the capability of coating large surface areas and large articles is critical. Large scale reactors could potentially improve the efficiency and increase productivity. Some reactors with certain excitation methods are readily scalable while others are not. Currently, a hot-filament reactor capable of depositing on substrates of 30 cm diameter is available. Large reactors for 45 cm diameter substrates are being planned [157]. For microwave reactors, coating of 15 cm diameter substrates is available. Coating of larger substrates (20 cm diameter) will be possible soon [60]. As noted earlier, the high energy density reactors are suitable for "jet expansion" to cover large areas, but with a proportionate reduction in deposition rate.

6.2 Diamondlike Carbon

DLC can be deposited using commercial large-area RF coating machinery. For small-scale development purposes, any commercial sputter-etch reactor which can produce a self-bias of the substrate relative to a plasma can be used. Several technical issues must be addressed in applying DLC. First, the very large compressive stress intrinsic to the growth process places limits on film thickness. For the thickest possible films, careful substrate preparation is a must and interlayers are often required. The interfacial stress in a 2 μm film is sufficient to rupture single-crystal silicon. Means of reducing this stress must be found. Some approaches to stress reduction involve cobombardment with high energy ions (usually Ar), modifications of the growth chemistry (by microwave excitation) and inclusion of impurities (usually metals). These modifications may reduce the stress considerably, but total elimination remains elusive. The second issue is optical transparency, if needed. As shown in figure 80, large optical gap and hardness appear to be mutually exclusive. The conditions which produce the greatest hardness seem to encourage formation of graphitic clusters opaque to most visible light. Unless the film is to be very thin, these clusters must be reduced in size or made transparent. Ion co-bombardment appears to do the former, while addition of appropriate impurities may achieve the latter.

7. Summary and Recommendations

The previous sections attempt to provide a general overview of the state of diamond CVD and DLC technologies. While the authors have included some explicit remarks, most suggestions for directions for future work derive implicitly from the current state of affairs. The following guidelines are essentially editorial. They reflect the authors' (possibly myopic) view of the economic and technical situation, and are not meant to be quantitative, objective or reflective of any industrial consensus. More complete, systematic surveys are commercially available, albeit at considerable expense (cf., Gorham Advanced Materials Reports).

7.1 Think Big—Diamond CVD is an "Enabling" Technology

It has been argued that the status of diamond film technology today is analogous to that of silicon some twenty five years ago. Even though diamond does seem to promise some electronic devices vastly superior to Si-based predecessors, this analogy should be taken more broadly. Diamond embodies a unique combination of superb mechanical, optical, thermal, and chemical properties. One

should not limit oneself to the view that CVD diamond is a "niche occupier" which exploits only one or two properties at a time to do established jobs a little better. Diamond CVD is an enabling technology which will open new technological opportunities by allowing use of new material and functional systems. An immediate example is the availability of reduced-cost CVD coated tool inserts which might in turn make new metal-matrix composites cost effective in automobiles, which in turn improves fuel efficiency and reduces emissions. To extend the automotive analogy beyond the point of hyperbole, in 1913, few could have imagined the breadth and depth of changes to be wrought by the availability of low cost individual motor transportation (the Ford Model-T).

7.2 Economics May be Everything—Know Your Customer

The drive toward CVD diamond applications proceeds on two fronts. At present, most effort is expended on identifying and developing products which are compatible with the current state-of-the-art of diamond growth. Substrate choices are limited by the high deposition temperatures, and applications are constrained by the very high cost of CVD diamond. While "dreaming up" new diamond applications, it must be kept clearly in mind that the value is in the form of the diamond, not the diamond itself. [Many proposed diamond applications appear to be solutions without a problem.] Current applications are limited to those wherein the value lies in the "enabling" characteristic of diamond. Reliably identifying such applications requires a very good understanding of the needs of the customer and the economics of his or her business. Nearly all current CVD diamond products fall into a very high value added, "price is no object" category. (The decline in government subsidized military aerospace research has considerably reduced the customer base for this type of product.) While there may be enough such applications to support several small entrepreneurial companies (or entrepreneurial divisions of large corporations), they may not be the basis for a volume industry.

As noted earlier, the major cost of vapor-deposited diamond is the electricity, not the precursor materials. The second front for attack is in breaking this cost-value logjam by dramatically reducing the cost of CVD diamond and thereby increasing the range of "cost effective" applications. This will be achieved by development of more "specific" reactors which generate the requisite diamond growth precursors (once they are positively identified) without the tremendous waste of energy endemic to current practice. It is entirely possible that this breakthrough will also lower the growth temperature and so expand the range of substrate materials correspondingly.

7.3 More Research is Required—We Still Don't Know What We're Doing

As described earlier, the utility of diamond and DLC coatings for a given application may be determined as much by subtleties of adhesion, morphology and chemistry, as by the grosser properties (hardness, transparency) of the film. A great deal of research remains in gaining a fundamental understanding of the connections between deposition conditions, chemical properties and atomic structure, and film morphology. This may be basic research addressing fundamental mechanisms, or applied parametric studies for process optimization. As noted in the previous section, the preeminent research challenge is the development of a high-rate, low energy density next generation diamond CVD system.

7.4 Be Aware of Other Superhard Materials—Diamond Isn't Sacred

In the rush to embrace diamond as the wonder coating of the century, other important material systems have been neglected. One of the most important of these is cubic boron nitride (c-BN). Slightly less hard than diamond, c-BN is suitable for machining of ferrous materials, while diamond is not, is more resistant to oxidation, and in some ways is a better candidate for semiconductor electronics. The bad news is that vapor-phase deposition of macrocrystalline, high purity c-BN has yet to be demonstrated. As of this writing, CVD of c-BN has produced only very fine grained ("nanocrystalline") films with a considerable content of hexagonal BN (h-BN, analogous to graphite). Success in CVD of c-BN is potentially more important than the much celebrated developments in diamond CVD. A properly coordinated and supported multi-disciplinary effort on c-BN, at least comparable to that devoted to the basics of diamond CVD, would be most timely.

The flexibility offered by CVD, PVD and hybrid deposition processes enables deposition of innumerable metastable materials with tailored atomic structure and chemical properties. Other super-

hard materials include amorphous and nanocrystalline ceramics formed by vapor deposition, and layered nanophase materials [182]. The latter consist of very thin alternating layers of vapor deposited ceramic. With proper selection of layer thickness, these "polycrystalline superlattice" films are significantly harder than a thick film of either constituent. For example, NbN/TiN nanolayered films exhibit hardness in excess of 5000 kg/mm^2, rivalling that of c-BN!

8. References

[1] The Properties of Diamond, J. E. Field, ed., Academic Press, New York (1979).

[2] Status and Applications of Diamond and Diamondlike Materials: An Emerging Technology, National Materials Advisory Board, National Academic, Washington, DC (1990).

[3] F. P. Bundy, H. T. Hall, H. M. Strong, and R. H. Wentorf, Jr., Nature **176**, 51-54 (1955).

[4] J. Martin, Industrial Diamond Rev. **6/90**, 291 (1990).

[5] (a) D. V. Fedoseev, V. P. Varmin, and B. V. Derjaguin, Synthesis of diamond in its thermodynamic metastability region, Uspekhi Khimii, **53**, 753 (1984), English translation, Russian Chem. Rev., **53**, 435 (1984); (b) B. V. Spitsyn, L. L. Bouilov, and B. V. Derjaguin, Diamond and diamond-like films: deposition from the vapor phase, structure and properties, Prog. Cryst. Growth and Charact. **17**, 79 (1988).

[6] (a) J. C. Angus and C. C. Hayman, Low pressure, metastable growth of diamond and "diamond-like" phases, Science, **241**, 913 (1988); (b) J. C. Angus, Y. Wang, and M. Sunkara, Annu. Rev. Meter. Sci. **21**, 221 (1991); (c) J. A. Angus, F. A. Buck, M. Sunkara, T. F. Groth, C. C. Hayman, and R. Gat, Diamond growth at low pressure, MRS Bull. Oct. 38, (1989); (d) J. C. Angus, P. Koidl, and S. Domitz, Carbon thin films, in Plasma Deposited Thin Films, J. Mort and F. Jansen, eds., CRC Press, Boca Raton, FL, (1987) p. 89.

[7] R. C. DeVries, Synthesis of diamond under metastable conditions, Annu. Rev. Mater. Sci., **150**, 161 (1987).

[8] K. E. Spear, Diamond-ceramic coating of the future, J. Am. Ceram. Soc. **72**, 171 (1989).

[9] (a) W. A. Yarbrough and R. Messier, Current issues and problems in the chemical vapor deposition of diamond, Science, **247**, 688 (1990); (b) P. K. Bachmann and R. Messier, Emerging technology of diamond thin films, Chem. Eng. News, May 15, 24 (1989).

[10] M. Kamo and Y. Sato, Diamond synthesis from the gas phase, Prog. Cryst. Growth and Charact. **23**, 1 (1991).

[11] A. Grill and B. S. Meyerson, in Synthetic Diamond: Emerging CVD Science and Technology, K. E. Spear and J. P. Dismukes, eds., John Wiley & Son, New York, (1991).

[12] International Conference on New Diamond Science and Technology (ICNDST) (a) Proceedings of the First ICNDST, New Japan Diamond Forum, Tokyo, (1988); (b) Proceedings of the Second ICNDST, R. Messier, J. T. Glass, and J. E. Butler, and R. Roy, eds, Materials Research Society, Pittsburgh (1990); (c) The Third ICNDST and 3rd European Conference on Diamond, Diamondlike and Related Coatings, August, 1992, Heidelberg, Germany.

[13] (a) Technology Update on Diamond Films, R. P. H. Chang, D. Nelson, and A. Hiraki, eds., Materials Research Society, Pittsburgh (1989); (b) Diamond, Silicon Carbide and Related Wide Bandgap Semiconductors, J. T. Glass, R. Messier, and N. Fujimori, eds., Materials Research Society, Pittsburgh (1990); (c) Diamond and Diamondlike Materials Synthesis, G. H. Johnson, A.R. Badzian, and M.W. Geis, eds., Materials Research Society, Pittsburgh (1988).

[14] Diamond and Diamondlike Films and Coatings, R. E. Clausing, L. L. Horton, J. C. Angus, and P. Koidl, eds., Plenum Press, New York (1990).

[15] Proceedings of the First International Conference on the Applications of Diamond Films and Related Materials-ADC '91, Y. Tzeng, M. Yoshikawa, M. Murakawa, and A. Feldman, Elsevier, New York (1991).

[16] A. L. Lavoisier, Memoire Academie des Sciences, p. 564 (1882).

[17] W. G. Eversole, U.S. Patent No. 3,030,187; 3,030,188, (1962).

[18] B. V. Derjaguin and D. V. Fedoseev, Russ. Chem. Rev., **39**, 783 (1970).

[19] J. J. Lander and J. Morrison, Surf. Sci. **2**, 553 (1964); J. Chem. Phys. **34**, 1403 (1963).

[20] J. C. Angus, H. A. Will, and W. S. Stanko, J. Appl. Phys. **39**, 2915 (1968).

[21] S. Aisenberg and R. Chabot, J. Appl. Phys. **42**, 2953 (1971).

[22] E. C. Vichery, U.S. Patent No. 3,714,334 (1970).

[23] B. V. Spitsyn, L. L. Bouilov, and B. V. Derjaguin, Vapor growth of diamond on diamond and other surfaces, J. Cryst. Growth **52**, 219 (1981).

[24] S. Matsumoto, Y. Sato, M. Kamo, and N. Setaka, Vapor deposition of diamond particles from methane, Jpn. J. Appl. Phys. **21**, L183 (1982).

[25] M. Kamo, Y. Sato, S. Matsumoto, and N. Setaka, J. Crystal Growth, **62**, 642 (1983).

[26] S. Matsumoto, J. Mater. Sci. Lett., **4**, 600 (1985).

[27] A. R. Badzian, B. Simonton, T. Badzian, R. Messier, K. E. Spear, and R. Roy, in Infrared and Optical Transmitting Materials, R. W. Schwartz, ed., Soc. of Photo-optical and Instrum. Eng., Bellingham, WA, SPIE Conf. Vol. **683**. (1986), p. 127.

[28] J. C. Angus, Y. Wang, and M. Sunkara, Metastable growth of diamond and diamond-like phase, Annu. Rev. Mater. Sci., **21**, 221 (1991).

[29] M. Frenklach, The role hydrogen in vapor deposition of diamond, J. Phys. Chem. **65**, 5142 (1989).

[30] M. Tsuda, M. Nakajima, and S. Oikawa, J. Am. Chem. Soc. **108**, 5780 (1986); Jpn. J. Appl. Phys. **26**, L527 (1987).

[31] S. J. Harris and L. R. Martin, Methyl vs acetylene as diamond growth species, J. Mater. Res. **5**, 2313 (1990).

[32] C. Judith Chu, M. P. D'evelyn, R. H. Hauge, and J. L. Margrave, Mechanism of diamond homoepitaxy by hot-filament CVD: carbon-13 studies, in Ref. [12(b)], p. 307.

[33] S. J. Harris, A mechanism for diamond growth from methyl radicals, Appl. Phys. Lett. **56**, 2298 (1990).

[34] D. G. Goodwin, Simulation of high-rate diamond synthesis: methyl as growth species, Appl. Phys. Lett., **59**, 277 (1991).

[35] M. Frenklach and K. E. Spear, Growth mechanism of vapor-deposited diamond, J. Mater. Res., **3**, 133 (1988).
[36] (a) D. Huang, M. Frenklach, and M. Maroncelli, J. Phys. Chem. **92**, 6379 (1988); (b) M. Frenklach, Monte CArlo simulation of diamond growth by methyl and acetylene reactions, J. Chem. Phys. **97**, 5794 (1992).
[37] M. Frenklach and Hai Wang, Detailed surface and gas-phase chemical kinetics of diamond deposition, Phys. Rev. B, **43**, 1520 (1991).
[38] D. N. Belton and S. J. Harris, Growth from acetylene from on a diamond (111) surface, J. Chem. Phys., **76**, 2371 (1992).
[39] (a) C. H. Wu, T. J. Potter, and M. A. Tamor, The role of heavy hydrocarbons in CVD diamond growth, in Novel Forms of Carbon, C. L. Renschler, J. J. Pouch, amd D. M. Cox, eds., MRS Symp. Proc. Vol. **270**. Materials Research Society, Pittsburgh, PA (1992) p. 371; (b) C. H. Wu, M. A. Tamor, T. J. Potter, and E. W. Kaiser, A study of gas chemistry during hot-filament vapor deposition of diamond using methane/hydrogen and acetylene/hydrogen gas mixtures, J. Appl. Phys. **68**, 4825 (1990).
[40] P. K. Backmann and H. Lydtin, High rate versus low rate diamond CVD methods, in Ref. [14], p. 829.
[41] Y. Liou, R. Weimer, D. Knight, and R. Messier, Appl. Phys. Lett. **56**, 437 (1990).
[42] D. E. Patterson, B. J. Bai, C. J. Chu, R. H. Hauge, and J. L. Margrave, in Ref. [12(b)], p. 433.
[43] M. S. Wong and C. H. Wu, Complications of halogen-assisted chemical vapor deposition of diamond, Diam. and Rel. Mater. **1**, 369 (1992).
[44] L. M. Hanssen, W. A. Carrington, J. E. Butler, and K. A. Snail, Diamond synthesis using an oxygen-acetylene torch, Mater. Lett. **7**, 289 (1988).
[45] N. Ohtake and M. Yoshikawa, J. Electrochem. Soc. **137**, 717 (1990).
[46] P. K. Bachmann, D. Leers, and H. Lydtin, Towards a general concept of diamond chemical vapor deposition, Diamond and Rel. Mater. **1**, 1 (1991).
[47] S. W. Benson, Thermochemical Kinetics, John Wiley & Sons, New York (1968).
[48] S. Matsumoto, Y. Sato, M. Kamo, and N. Setaka, Vapor deposition of diamond particles from methane, Jpn. J. Appl. Phys. **21**, L183 (1982).
[49] Y. Hirose and Y. Terasawa, Synthesis of diamond thin films by thermal CVD using organic compounds, Jpn. J. Appl. Phys. **Part 2, 25**, L519 (1986).
[50] A. Sawabe and T. Inuzuka, Growth of diamond thin films by electron-assisted CVD and their characterization, Appl. Phys. Lett. **46**, 146 (1985).
[51] M. Sommer and F.W. Smith, Importance of filament reactivity for CVD diamond growth, in Ref. [13(b)], p. 139.
[52] S. Okoli, R. Haubner, B. Lux, Influence of the material on low-pressure hot-filament CVD diamond deposition, J. De Physique II, **1**, C2-923, (1991).
[53] Y. Hirose and N. Kondo, in Extended abstracts of 35th Spring Meeting, Jpn. Appl. Phys. Soc. March 29, 1988, p. 434.
[54] Y. Hirose, S. Ananuma, N. Okada, and K. Komaki, in Proceedings of the First International Symposium on Diamond and Diamondlike Films, The Electrochemical Society, Pennington, NJ, Proceedings Vol. **89-12** (1989) p. 80.
[55] Y. Matsui, A. Yuuki, M. Sahara, and Y. Hirose, Jpn. J. Appl. Phys. **28**, 1718 (1989).
[56] Y. Tzeng, P. Phillips, C. Cutshaw, and T. Srivinyunon, Characterization and scaling-up of diamond films deposited from oxy-acetylene flames, in Ref. [12(b)], p. 523.
[57] J. A. Cooper and W. A. Yarbrough, Diamond Optics **III**, SPIE Proc. **1325**, 41 (1990).
[58] N. G. Glumac and D. G. Goodwin, Diamond synthesis in low-pressure flat flame, Thin Solid Films **212**, 122 (1992).
[59] For more examples, please see cited references in Ref. [5-15].
[60] The LADS (Large Area Deposition System) manufactured by Astex$_{TM}$, Woburn, MA.
[61] Y. Mitsuda, T. Yoshida, and K. Akashi, Rev. Sci. Instrum. **60**, 249 (1989).
[62] H. Kawarada, K. S. Mar, and A. Hiraki, Jpn. J. Appl. Phys. **26**, 6, L1032 (1987).
[63] J. Suzuki, Jpn. J. Appl. Phys. **28**, 2, L 281 (1989).
[64] D. E. Meyer, R. O. Dillon, and J. A. Woolham, J. Vac. Sci. Tech. **7**, 2325 (1989).
[65] I. Watanabe, T. Matsushida, and K. Sasahara, Low-temperature synthesis of diamond films in thermaoassisted rf plasma chemical vapor deposition, Jpn. J. Appl. Phys. **31**, 1428 (1992).
[66] (a) R. A. Rudder, G. C. Hudson, J. B. Posthill, R. E. Thomas, R. C. Hendry, D. P. Malta, and R. J. Markunas, T. P. Humpherys and R. J. Nemanich, Chemical vapor deposition of diamond films from water vapor rf-plasma discharges, Appl. Phys. Lett., **60**, 329 (1992); (b) R. A. Rudder, G. C. Hudson, R. C. Hendry, R. E. Thomas, J. B. Posthill, and R. J. Markunas, Formation of diamond films from low pressure radio frequency induction discahrges, Surf. Coat. Technol. **54/55** 397 (1992).
[67] S. Matsumoto, M. Hino, and T. Kobayashi, Appl. Phys. Lett. **51**, 737 (1987).
[68] (a) Norton Industrial Ceramics (Northboro, MA). (b) See for examples: Advanced Energy Industries (Fort Collins, CO); CVC Products (Rochester,NY); ENI, (Div. of Astec America, Rochester, NY); and RF Plasma Products (Mariton, NJ).
[69] B. V. Derjaguin, L. L. Bouilov, and B. V. Spitsyn, Arch. Nauki Mater. **7**, 111 (1986).
[70] J. M. Pinneo, 1st Diamond Technology Inititive Workshop, MIT Lincoln Labs., Boston, MA, Feb. 2, (1987), Paper 4.
[71] B. Singh, O. R. Mesker, A. W. Levine, and Y. Arie, Appl. Phys, Lett. **52**, 1658 (1988).
[72] K. Suzuki, A. Sawabe, H. Yasuda, and T. Inuzuka, Growth of diamond films by dc plasma chemical vapor deposition, Appl. Phys. Lett. **50**, 728 (1987).
[73] K. Suzuki, A. Sawabe, and T. Inuzuka, Growth of diamond films by dc plasma chemical vapor deposition and characterization of the plasma, Jpn. J. Appl. Phys. **29**, 153 (1990).
[74] S. Matsumoto, M. Hino, Y. Moriyoshi, T. Nagashima, and M. Tsutsmui, U.S. Patent No. 4 767 608, August 30, 1988 (filed Oct. 19, 1987).
[75] S. Matsumoto, in Ref. [13(c)], p. 119.
[76] F. Akatsuka, Y. Hirose, and K. Komaki, Rapid growth of diamond films by arc discharge plasma CVD, Jpn. J. Appl. Phys. **27**, L1600 (1988).
[77] K. Kurihara, K. Sasaki, M. Kawarada, and N. Koshino, High rate synthesis of diamond by dc plasma jet chemical vapor deposition, Appl. Phys. Lett. **52**, 437 (1988).

[78] N. Ohtake, H. Tokura, Y. Kuriyama, Y. Mashimo, and M. Yoshikawa, in Proceedings of First International Symposium on Diamond and Diamondlike Films, The Electrochemical Society, Pennington, NJ, Proceedings Vol. **89-12**, (1989) p. 93.

[79] (a) J. C. Angus and F. Jansen, J. Vac. Sci. Technol. **A6**, 1778 (1988); (b) J. C. Angus and Y. Wang, Diamondlike hydrocarbon and carbon films, in Ref. [14], p. 173.

[80] M. A. Tamor, W. C. Vassell, and K. R. Carduner, Atomic constraint in hydrogenated "diamond-like" carbon, Appl. Phys. Lett. **58**, 592 (1991).

[81] Y. Catherine, Preparation techniques for diamond-like carbons, in Ref. [14], p. 193.

[82] L. Holland and S. M. Ojha, Deposition of hard carbonaceous films on an RF target in a butane plasm, Thin Solid Films, **38**, L17 (1976)

[83] A. Bubenzer, B. Dischler, G. Brandt, and P. Koidl, RF plasma deposited amorphous hydrogenated hard carbon thin films: preparation, properties, and applications, J. Appl. Phys. **54**, 4590 (1963).

[84] M. A. Tamor, C. H. Wu, R. O. Carter, III, and N. E. Lindsay, Pendant benzene in hydrogenated diamond-like carbon, Appl. Phys. Lett. **55**, 1388, (1988).

[85] D. Nir, R. Kalish, and G. Lewin, Diamondlike carbon films of low hydrogen contents made with a mixture of hydrocarbon and reactive gas, Thin Solid Films, **117**, 125 (1984).

[86] O. Matsumoto, T. Fujita, and M. Uyama, Application of ECR plasma apparatus to the deposition of carbonaceous films, ISPC9, Pugnochiuso, 1989, Symp. Proc. **3**, R. d'Agostino, ed., (1989) p. 1804.

[87] M. A. Tamor, private communication.

[88] S. Aisenberg and F. M. Kimock, Mat. Sci. Forum **52-53**, 1 (1988).

[89] S. F. Pellicori, C. M. Peterson, and T. P. Henson, Transparent carbon films: Comparison of properties between ion and plasma deposition processes, J. Vac. Sci. Technol., **A4**, 2350 (1986).

[90] J. H. Freeman, W. Temple, D. Beanland, and G. A. Gard, Ion beam studies. I. The retardation of ion beam to very low energies in an implantation accelerator, Nucl. Instrum. Methods **135**, 1 (1976).

[91] J. Ishikawa, Y. Takeiri, K. Ogawa, and T. Takagi, Transparent carbon films prepared by mass-separated negative-carbon-ion-beam deposition, Jpn. J. Appl. Phys. **61**, 2509 (1987).

[92] S. Kasi, H. Kang, and J. W. Rabalais, Chemically bonded diamondlike carbon films from ion-beam deposition, Phys. Rev. Lett. **59**, 1 (1987).

[93] M. J. Mirtich, Ion-beam deposited protective films, NASA Technical Memorandum 81722, NASA Lewis Research Center (1981).

[94] D. Nir and M. Mirtich, Thin film growth rate effects for primary ion beam deposited diamondlike carbon films, J. Vac. Sci. Technol. **A4**, (1986).

[95] D. R. McKenzie, D. Muller, B. A. Pailthorpe, Z. H. Wang, E. Kravtchinskaia, D. Segal, P. B. Lukins, P. D. Swift, P. J. Martin, G. Amaratunga, P. H. Gaskell, and A. Saeed, Properties of tetrahedral amorphous carbon prepared by vacuum arc deposition, Diamond Relat. Mater. **1**, 51 (1991).

[96] J. J. Cuomo, J. P. Doyle, J. Bruley and J. C. Liu, Appl. Phys. Lett. **58**, 466 (1991).

[97] S. Fujimori, T. Kasai, and T. Inamura, Carbon film formation by laser evaporation and ion beam sputtering, Thin Solid Films, **92**, 71 (1982).

[98] D. L. Pappas, K. L. Saenger, J. Bruley, W. Krakow, and J. J. Cuomo, T. Gu and R. W. Collins, J. Appl. Phys. **71**, 5675 (1992).

[99] C. B. Collins, F. Davanloo, D. R. Jander, T. J. Lee, H. Park, and J. H. You, J. Appl. Phys. **69**, 7862 (1991).

[100] D. P. Woodruff and T. A. Delchar, Modern techniques of surface analysis, Cambridge University Press, Cambridge, (1986).

[101] L. C. Feldman and J. W. Mayer, Fundamentals of surface and thin film analysis, North-Holland, New York, (1986).

[102] D. S. Knight and W. B. White, Characterization of diamond films by Raman spectroscopy, J. Mater. Res. **4**, 385 (1989).

[103] P. Backmann and D. U. Wiechert, Characterization and properties of artificially grown diamond, Ref. [14], p. 677.

[104] A. M. Bonnot, Overview of the characterization method of the growth mechanism of low pressure diamond, Surf. & Coating Technol. **45**, 343 (1991).

[105] C. P. Sung and H. C. Shih, The interfacial structure and composition of diamond films grown on various substrates, J. Mater. Res. **7**, 105 (1992).

[106] K. M. McNamra and K. K. Gleason, J. Appl. Phys. **71**, 2884 (1992).

[107] Y. Tzeng, C. K. Teh, R. Phillips, A. Joseph, T. Srivimyunon, C. Culshaw, C. C. Tin, R. Miller, T. H. Hartnett, C. Willingham, A. Ibrahim, and B. H. Loo, Electrical and optical properties of diamond films deposited from an oxy-acetylene flame, in Ref [14], p. 805.

[108] M. A. Tamor, J. A. Haire, C. H. Wu, and K. C. Hass, Correlation of the optical gaps and Raman spectra of hydrogenated amorphous carbon films, Appl. Phys. Lett. **54**,123 (1989).

[109] C. J. McHargue, Mechanical properties of diamond and diamond-like films, in Ref. [15], p. 113.

[110] B. Lux and R. Haubner, in Proc. 12th Int Plasma-Seminar, (1989) p. 615.

[111] R. C. McCune, D. W. Hoffman, T. J. Whalen, and C. O. McHugh, MRS Symp. Proc. Vol. 130, 261 (1989).

[112] N. Kiuch and H. Yoshimura, in Ref. [12(a)], p. 42.

[113] M. E. O'Harn and C. J. McHargue, Mechanical properties testings of diamond and diamond-like films by ultra-low load indentation, in Ref. [14], p. 715.

[114] G. S. Gildenblat, S. A. Grot, and A. Badzian, The electrical properties and device applications of honoepitaxial and polycrystalline diamond films, Proc. IEEE, **79**, 647, (1991).

[115] M. W. Geis, N. N. Efremow, and D. D. Rathman, J. Vac. Sci. Technol. **A6**, 1953 (1988).

[116] K. Das, V. Venkatesan, K. Miyata, J. T. Glass, and D. L. Dreifus, A review of the electrical characteristics of metal contacts on diamond, Thin Solid Films, **212**, 19, (1992).

[117] W. Mueller-Sebert, Ch. Wild, P. Koidl, N. Herres, J. Wagner, and T. Eckermann, Polycrystalline diamond for optical thin films, Mat. Sci. & Eng., **B11**, 173, (1992).

[118] G. Lu, Thermal conductivity measurement using the converging thermal wave technique, in Ref. [15], p. 273.

[119] H. P. R. Frederikse and X. T. Ting, Heat conductivity of oxide coating by photothermal radiometry between 293 and 1173 K, Appl. Opt. **27**, 4672 (1988).
[120] J. E. Graebner, S. Jin, G. W. Kammlott, J. A. Herb, and C. F. Gardiner, Unusually high thermal conductivity in diamond films, Appl. Phys. L. **60**, 1576 (1992).
[121] R. W. Pryor, L. Wei, P. K. Kuo, and R. L. Thomas, Thermal wave and Raman measurement of polycrystalline diamond film quality, in Ref. [14], p. 723.
[122] B. Bhushan and B. K. Gupta, Handbook of Tribology, McGraw-Hill, New York, (1991).
[123] M. N. Gardos and B. L. Soriano, J. Mater. Res. **5**, 2599 (1990).
[124] A. K. Gangopadhyay, W. C. Vassell, M. A. Tamor P. A. Willermet, private communication.
[125] H. Dimigen and H. Hübsch, Phillips Tech. Rev. **41**, 186 (1983/1984).
[126] K. Oguri and T. Arai, J. Mater. Res. **5**, 2567 (1990).
[127] R. A. Hay and C. D. Dean, Cutting tool performance of CVD thick film diamond, in Ref. [15], p. 53.
[128] N. Kikuchi, H. Eto, T. Okamura, and H. Yoshimura, Diamond coated inserts: characteristics and Performance, in Ref. [15], p. 61.
[129] P. Craig, Thin film-diamond derby, Cutting Tool Eng. **44**, 23 (1992).
[130] For examples, U.S. companies; (a) Norton Industrial Ceramics (Northboro, MA), (b) Crystallume (Menlo Park, CA), and (c) Kennametal (Latrobe, PA), and Japanese companies; (d) Mitsubishi Materials, (e) Toshiba Tungaloy, (f) Nichi Fujikoshi, (g) Sumimoto Electric, and (h) Idemitzu Petrochemical.
[131] T. R. Anthony, private communication.
[132] R. Messier and T. C. Ovaert, Diamond and related materials coatings for advanced heat engine, Proc. 1990 Coatings for Advanced Heat Engines Workshop, Castine, Maine, Aug., 1990.
[133] L. Connor & M. Pinneo, CVD diamond films open new vista, Photonic Spectra, Jan., 1989.
[134] G. Davies, The optical properties of diamond, in Chemistry and Physics of Carbon, P. L. Walker, ed., Maecel Dekker, New York, (1977), p. 13.
[135] C. Willingham, T. Hartnett, C. Robindon, and C. Klain, Polycrystalline diamond for infrared optical applications prepared by the microwave plasma and hot filament chemical vapor deposition techniques, in Ref. [15], p. 157.
[136] J. A. Willingham, Infrared optional windows and thin anti-reflective coating, Academy Helgu, Boston (1985).
[137] R. C. Eden, Application of synthetic diamond substrates for thermal management of high performance electronic multi-chip modules, in Ref. [15], p. 259.
[138] S. Holly, Critical properties of CVD diamond films for heat sink and thermal radiator applications, in Ref. [15], p. 267.
[139] M. N. Yoder, Novel electron devices based on the unique properties of diamond, in Ref. [15], p. 287; Nav. Res. Rev. **39**, 27 (1987).
[140] M. N. Yoder, Diamond: potential and status, in Ref. [14], p. 1.
[141] M. W. Geis and J. C. Angus, Diamond film semiconductors, Scientific American, October, 84 (1992).
[142] M. W. Geis, D. D. Rathman, D. J. Ehrlich, R. A. Murphy, and W. T. Lindley, High-temperature point-contact transistors and Schottky diodes formed on synthetic boron-doped diamond, IEEE Electron Device Lett. **EDL-8**, 341 (1987).
[143] G. Sh. Gildenblat, S. A. Grot, C. W. Hasfield, and A. R. Badzian, High temperature thin film diamond field effect transistor fabricated using a selective growth method, IEEE, Electron. Dev. Lett. **12**, 37 (1991).
[144] G. Sh. Gildenblat, S. A. Grot, C. W. Hatfield, C. R. Wronski, A. R. Bodzian, T. Bodzian, and R. Messier, High temperature Schottky diodes with boron-doped homoepetaxial diamond base, Mat. Res. Bull. **25**, 129 (1990).
[145] J. F. Prins, Appl. Phys. Lett. **41**, 950 (1982).
[146] K. Okano, T. Iwasaki, H. Kiyota, T. Kurosu, and M. Iida, Thin Solid Films **201**, 183 (1991).
[147] M. Aslam, A. Masood, R. J. Fredricks, and M. A. Tamor, Thin film diamond temperature sensor array for harsh aerospace environment, SPIE- Int. Soc. Opt. Eng., Orlando, FL, April, 1992.
[148] D. R. Kania, M. A. Plano, M. Landstrass, Y. Sugimoto, S. Schnetzer, S. K. Kim, R. Stone, G. B. Thomson, and F. Sannes, Diamond Radiation Detectors, Paper abstracts in Diamond 92, August, 1992, Heidelberg, paper 16.1.
[149] M. Aslam, I. Taher, A. Masood, M. A. Tamor, and T. J. Potter, Piezoresistivity in vapor-deposited diamond films, Appl. Phys. Lett. **60**, 2923 (1992).
[150] M. Marchywk, J. F. Hochedez, M. W. Geis D. G. Socker, D. Moses, and R. T. Goldberg, Appl. Optics **30**, 5011 (1991).
[151] Y. Taniguchi, K. Horabayashi, K. Ikoma, N. Iwasaki, K. Kurihara, and M. Matsushima, Jpn. J. Appl. Phys. **28**, L1848 (1989).
[152] N. Fujimori, Y. Nishibaya, and H. Shiomi, Electroluminescient devices made of diamond, Jpn. J. Appl. Phys. **30**, 1728 (1991).
[153] H. Shimizu, M. Yoshimi, K. Hattori, H. Okamoto, and Y. Hamakawa, Improvement of blue-light emission in amorphous carbon based electroluminescent device, J. Non-cryst. Solid **137 & 138**, 1275 (1991).
[154] J. Glinski, X. J. Gu, R. F. Code, and H. M. Van Driel, Appl. Phys. Lett., **45**, 260 (1984); P. S. Panchii and H. M. Van Driel, IEEE J. Quant. Elec. **QE-22**, 101 (1986).
[155] A. H. Lettington, Application of DLC films to optical windows and tools, in Ref. [15], p. 703.
[156] A. H. Lettington, J. C. Lewis, C. J. H. Wort, B. C. Monachan, and A. J. N. Hope, Development of GeC as a durable IR coating material, E-MRS Meeting, **17**, 469 (1987).
[157] See for example: Diamonex (Allentown, PA).
[158] A. Grill, V. Patel, and B. S. Meyerson, Applications of diamondlike carbon in computer technology, in Ref. [15], p. 683.
[159] B. Lux and R. Haubner, Nucleation and growth of low-pressure diamond, in Ref. [14], p. 579.
[160] B. R. Stoner and J. T. Glass, Textured diamond growth on (100) βSiC via microwave plasma chemical vapor deposition, Appl. Phys. Lett. **60**, 698 (1992).
[161] T. P. Ong, F. Xiong, R. P. H. Chang, and C. W. White, Mechanism for diamond nucleation and growth on single crystal copper surface implanted with carbon, Appl. Phys. Lett. **60**, 2083 (1992).
[162] K. Kobashi, K. Nishimura, Y. Kawate, and T. Horiuchi, Synthesis of diamonds by use of microwave plasma chemical-vapor deposition: Morphology and growth of diamond films, Phys. Rev. B, **38**, 4067 (1988).

[163] Ch. Wild, N. Herres, and P. Koidl, Texture formation in polycrystalline diamond films, J. Appl. Phys. **68**, 973 (1990).
[164] R. E. Clasusing, L. Heatherly, and E. D. Specht, Control of texture and defect structure for hot-filament assisted CVD diamond films, in Ref. [14], p. 611.
[165] P. Joeris, C. Benndort, and S. Bohr, Diamond deposition by hot filament and microwave CVD: Influence of deposition parameters on phase purity, surface roughness, and film quality, in Ref. [15], p. 561.
[166] A. Hirata, H. Tokura, and M Yoshikawa, Smoothing of diamond films by ion beam irradiation, in Ref. [15], p. 227.
[167] H. Li, M. Mecray, W. Yarbrough, and X. H. Wang, The growth of diamond films using DC biased hot-filament technique, in Ref. [12(b)], p. 461.
[168] S. Jin, J. E. Graebner, G. W. Kammlott, T. H. Tiefel, S. G. Kosinski, L. H. Chen, and R. A. Fastnacht, Massive thinning of diamond films by diffusion process, Appl. Phys. Lett. **60**, 1948 (1992).
[169] J. Wei, J. M Chang, and Y. Tzeng, Deposition of diamond films with controlled nucleation and growth using hot-filament CVD, Thin Solid Films **212**, 91 (1992).
[170] V. Subramanian, private communication.
[171] D. E. Patterson, C. J. Chu, B. J. Bai, N. J. Komplin, R. H. Hauge, and J. L. Margrave, Thermochemical vapor deposition of diamond in a carbon-halogen-oxygen and/or sulfur atmospheric hot wall reactor, in Ref. [15], p. 569.
[172] Y. Liou, A. Inspector, R. Weimer, and R. Messier, Appl. Phys. Lett. **55**, 631 (1989).
[173] S. Hesomi and I. Yoshida, Diamond research as patent applied, in Ref. [15], p. 15.
[174] V. A. Mernagh, T. C. Kelly, M. Ahern, A. D. Kennedy, A. P. Adriaans, P. P. Ramaker., L. McDonnel, and R. Koekoek, Adhesion improvement in silicon carbide deposited by plasma enhanced CVD, Surf. Coating **49**, 462 (1991).
[175] K. Saijo, M. Yagi, K. Shibuki, and S. Takatsu, Surf. Coat. Technol. **43**, 30 (1990).
[176] S. Koizumi, T. Murakami, K. Suzuki, and T. Inuzuka, Epitaxial growth of diamond film on c-BN, Appl. Phys. Lett. **57**, 563 (1990).
[177] J. Narajan, V. P. Godbole, and C. W. White, Science, **252**, 416 (1991).
[178] M. W. Geis, H. I. Smith, A. Argoitia, J. Angus, G. H. M. Ma, T. J. Glass, J. Butler, C. J. Robinson, R. Pryor, Appl. Phys. Lett. **58**, 2485 (1991).
[179] (a) S. D. Walter, B. R. Stoner, J. T. Glass, P. J. Ellis, D. S. Buhaenko, C. E. Jenkins, and P. Southworth, Appl. Phys. Lett. **62**, 1215 (1993); (b) X. Jiang and C.-P. Klages, Heteroepitaxial diamond growth on (100) silicon, in **Diamond 1992**, Ed. P. K. Backmann, A. T. Collins, and M. Seal, Elsevier, Lausanne, p. 1112 (1993).
[180] K. Snail, private communication.
[181] C. F. Chen, C. L. Lin, T. M. Hong, Growth of diamond from CO_2-(C_2H_2, CH_4) gas systems, without supplying additional hydrogen gas, Surf. Coat. Technol., **52**, 205 (1992).
[182] X. Chu, M. S. Wong, W. D. Sproul, S. L. Rohde, and S. A. Barnett, J. Vac. Sci. Technol., **A 10**, 1604 (1992).

About the Authors: *Dr. Ching-Hsong (George) Wu, a principal research specialist with Ford Research Laboratory, received a Ph.D in Chemistry from the University of California at Berkeley. He has worked on various areas including laser-induced photochemistry, free radical formation and reactions, atmospheric chemistry, mechanisms of photochemical smog formation, catalytic convertors, gas-phase and gas-surface reaction kinetics, and CVD of silicon nitride. Dr. Wu has been engaged in research on the science and applications of CVD diamond films and DLC since 1988. Dr. Michael. A. Tamor, a staff scientist with Ford Research Laboratory, received his M.S. and Ph.D. in Physics from the University of Illinois at Urbana-Champaign. He has worked for six years in the areas of optical and electronic properties, semiconductor alloys, transport in highly disordered materials, and electronics for high temperature operation. He is currently the project leader for research on the formation, structure, properties and applications of diamond and diamondlike carbon materials.*

Ion Nitriding

Gary Sharp

President, Advanced Heat Treat Corp.,
2839 Burton Avenue
Waterloo, IA 50703
(319) 232-5221
Fax: (319) 232-4952

While used for many years in a laboratory environment, Ion Nitriding has over the last ten years emerged as an excellent method of case hardening for industrial components. In addition to its technical advantages, the process is environmentally friendly. Almost every industry has applications which could benefit from the Ion Nitriding treatment.

Key words: arcing; case hardening; ion nitriding; duplex treatments; glow discharge; ionization; ion nitriding; masking; plasma nitriding; sputtering.

Contents

1. The Ion/Plasma Process

Ion Nitriding and Plasma Nitriding are often used interchangeably to describe a method of heat treatment utilizing energy provided by a dense collection of ions and neutral atoms. While frequently confused with such processes as ion implantation or plasma coating, Ion Nitriding is a case hardening process—not a coating.

1.1 Description of Process

Ion nitriding is a vacuum case hardening process developed for engineered steel and cast iron parts. The hardening takes place in the plasma of a current intensive glow discharge. By varying the type of gas a wide variety of properties can be provided to improve the abrasive wear resistance, gliding resistance, and corrosion resistance of treated parts. For many parts fatigue strength is also improved.

Ion nitriding has many advantages over salt or gas nitriding. The most prominent advantages are:

- single phase compound zone for greater ductility;
- better case uniformity;
- shorter cycle times;
- lower process temperatures;
- ease of masking;
- the process does not pollute the environment.

In addition ion nitriding often replaces shallow case carburizing, carbonitriding, and various plating processes.

A glow discharge reaction or plasma reaction is set up by introducing a specific nitrogen/hydrogen gas mixture into a vacuum chamber, in which the work pieces forms a cathode with respect to the walls of the vacuum vessel. The nitrogen and hydrogen ions and neutral atoms accelerate towards the work piece and heat it via the transfer of their kinetic energy. The hydrogen and nitrogen ions bombard the cathode surface providing a depassivated effect, removing oxides and other contaminants. After this sputtering (or super cleaning) takes place the parts are elevated to an operating temperature generally between 800 °F–1050 °F and a negative potential between 400 and 1000 V. Parts are held for a period of time allowing the nitrogen to react with the alloy constituents of the steel. The thermochemical reaction between the alloy elements and the nitrogen causes the hardening to take place.

The parameters which determine the case depth, and type of metallurgical structure obtained are material chemistry, gas composition, time, and temperature. With ion nitriding these variables can be controlled to custom tailor the surface layer to meet almost any requirement. The various materials which can be treated are noted in Table 22. Typical cyucles can vary from 1 h to 48 h at temperature depending on the customer specifications and application demands.

1.2 History

From a technical standpoint ion nitriding has had a long history. In 1920 Franz Skaupy of Germany invented a heat treating furnace which utilized the heat of an ion discharge in an inert gas. As for nitriding, Egan of America proposed an ion nitriding method which used a corona discharge in ammonia gas (NH_3) or (N_2) gas at atmospheric pressure, but did not succeed with this method. In 1932 Bernhardt Berghaus of Germany invented the ion nitriding method, utilizing a glow discharge. However, for both technical and proprietary reasons the process was not advanced commercially around the world until well after World War II.

1.3 Growth of Technology

With the introduction of the high speed breaker systems which control the unstable arc discharge, ion nitriding has prospered and grown. The superior properties provided by ion nitriding along with the fact that it is pollution-free and offers considerable energy and labor savings, further enhance the demand for the process.

The earliest ion nitriding units in the United States were located at a captive user in the southeast and at a commercial heat treater in the midwest. Worldwide there are estimated to be 1200–1400 ion nitriding units in operation. However, only a small portion (70–100) are operating in the United States. The remainder are in use in Europe, Russia, China, Japan, and other far eastern countries. As one might surmise from the numbers, the opportunity for growth in the United States utilizing this technology is significant.

2. Overview of Equipment

There are numerous ion nitriding equipment manufacturers throughout the world. The more prominent ones are Nippon Denshi Kogyo of Japan, Surface Combustion of Maumee, OH, Abar Ipsen of Festerville, PA, and Klockner Ionon GmbH of West Germany. All offer various sizes and options based on user requirements.

The ion nitriding system is composed of a vacuum chamber, DC power supply, vacuum pump, and a gas supply system (see fig. 83). The vacuum chamber is pumped down to a vacuum level of approximately 10^{-2} or 10^{-3} Torr with a vacuum pump, then filled with the mixture of nitrogen and hydrogen, and adjusted to an operating pressure

Table 22. Ion nitrided materials

Steel group	Hardness RC or tensile strength Ksi	Nitriding temperature °F	Surface hardness R15N	Total case depth inches	Compound zone thickness inches	Compound zone type
1. *Carbon Steels*						
1008	--	950–1050	FILE HARD	--	.0002–.0006	E
1045	--	950–1050	FILE HARD	.012–.030	.00015–.0006	E or G′
2. *Free Cutting Steels*						
1118	--	950–1050	FILE HARD	--	.00015–.0006	E
1144	28–32 RC	900–1000	85–90	.012–.030	.00015–.0006	E or G′
3. *Gray-Cast Iron*						
G2500	25 ksi	950–1000	77–82	.004–.008	.0002–.0004	E
G3500	25 ksi	950–1000	77–82	.004–.008	.0002–.0004	E
4. *Nodular-Cast Iron*						
D5506	80 ksi	950–1025	82–88	.004–.012	.0002–.0004	E
D7003	100 ksi	950–1025	83–89	.004–.012	.0002–.0004	E
5. *Malleable-Cast Iron*						
M5003	75 ksi	950–1000	71–81	.004	.0002–.0004	E
6. *Case Hardening Steels*						
8620	--	950–1025	77–85	--	.00015–.004	E or G′
9310	--	950–1025	77–92	--	.00015–.004	E or G′
7. *Heat Treatable Steels*						
41401	28–32 RC	900–1000	84–90	.012–.030	.00015–.0006	E or G′
4340	28–32 RC	900–1000	84–90	.012–.030	.00015–.0006	E or G′
52100	36–45 RC	900–1000	84–90	.012–.030	.00015–.0006	E or G
8. *Nitriding Steels*						
Nitralloy 135	26–30 RC	900–1000	90–95	.010–.030	.00005–.0004	E or G′
9. *Hot Work Tool Steels*						
H 13	48–55 RC	900–1000	90–94	.004–.013	.0001–.0002	E or G′
H 19	52–56 RC	900–1000	90–94	.005–.020	.0001–.0002	E or G′
P 20	28–30 RC	900–1000	87–91	.010–.020	.00015–.0006	E or G
10. *Cold Work Tool Steels*						
A-2	54–60 RD	850–1000	90–94	.008–.012	.0001–.0003	E or G′
O-2	38–47 RC	850–1000	81–88	.008–.020	.00005–.0002	E or G
D-2	55–60 RC	850–1000	90–94	.005–.010	--	--
11. *High Speed Tool Steels*						
M-2	63–66	900–950	92–95	.001–.004	--	--
T-15	63–66 RD	900–950	92–95	.001–.004	--	--
12. *Shock-Resisting Tool Steels*						
S-7	45–55 RC	950–1025	91–94	.008–.020	.00015–.0003	E or G′
13. *Maraging Steel*						
250	250 Ksi	850–875	91–93	.002–.006	.00005–.0002	G′
350	350 Ksi	850–875	91–94	.002–.006	.00005–.0002	G′
14. *Stainless Steels*						
303	--	1000–1050	90–95	.002–.005	--	--
410	--	1000–1050	90–95	.004–.008	--	--
420	--	1000–1050	90–95	.004–.008	--	--
422	--	950–1000	90–95	.004–.008	--	--
17-4	--	1000–1050	90–95	.002–.006	--	--
A286	--	1000–1050	90–95	.002–.006	--	--
316	--	1000–1050	90–95	.002–.005	--	--
15. *Powdered Metal Tool Steels*						
CPM-9V	48–55 RC	900–1000	90–94	.005–.010	--	--
CPM-10V	49–56 RC	900–1000	90–94	.004–.010	--	--
16. *Sintered Powered Metal*						
B-484	--	950–1050	FILE HARD	.010–.040	--	--
17. *Titanium—All Grades—Contact AHT for Process Specifications*						

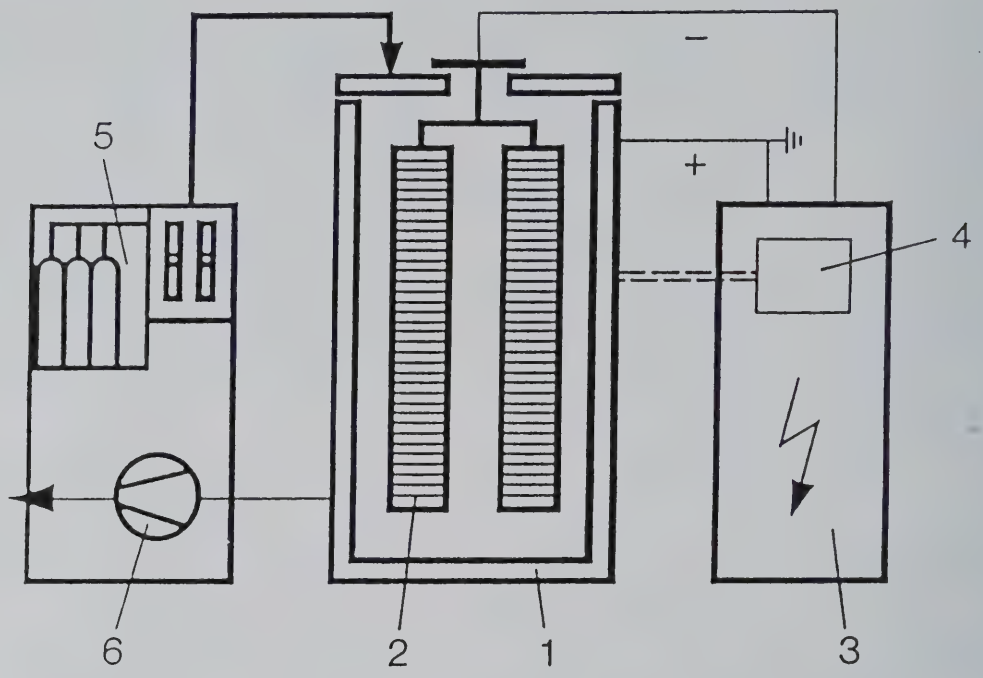

Figure 83. Schematic of a typical ion nitriding system.

of approximately 1–10 Torr. The vacuum chamber is water cooled and the glow discharge is caused by applying the DC voltage between the cathode hearth plate (or fixture ring) and the anode (vessel wall). The ratio of process gases as well as the treatment temperature is adjusted as required, depending on the material being processed and the required surface layer. Temperature is controlled with a shielded type K thermocouple or an optical pyrometer. Most industrial units are microprocessor controlled, thus simplifying the operation to a large degree.

2.1 Vacuum Chamber

The vacuum chamber for an ion nitriding system generally comes in two configurations, horizontal and vertical. The horizontal ion nitriding chambers are similar to conventional vacuum chambers. Within the vessel a hearth plate is constructed on electrical supports/splitters to isolate it from the vessel walls.

The hearth plate is negatively charged and becomes the cathode in a DC circuit. The parts to be treated are placed on the support plate and also become negatively charged.

Vertical chambers are configured as bottom loaders (base plate) top loaders (hanging ring) or combination units (both the above). Vessel extensions can be added as required to handle long parts. O-ring seals between the extensions maintain the vacuum seal. Most chambers have water cooled jackets. However, several manufacturers utilize hot wall construction.

2.2 Power Supplies

There have been lengthy discussions and considerable controversy surrounding the best design or type of power supplies, often to the detriment of the process itself. In any case, it should suffice to say that the choice of the power source is one of personal preference. This preference is often based on user experience as well as the type and configuration of parts to be ion nitrided.

2.2.1 DC Power Sources A DC power supply provides continuous ionization of the gas and relies on an electrical system with appropriate controls, and a choke transformer to interrupt an arc if one is formed. With the DC power source some, or in many cases all, of the heating requirements are derived from the created plasma.

2.2.2 Pulse Power Source With a pulse type ion nitriding power supply the ionization process is discontinuous. Special conditions are engineered into a pulse power supply with the objective of actually preventing the formation of sustained arcs, and at the same time separating the glow formation from the heating process. These units usually use some form of auxiliary heating.

2.3 Heating Methods

As previously mentioned, for many ion nitriding units the heating is created strictly by the bombardment of ions and neutral atoms which transfer their kinetic energy as they hit the work piece. However, there is equipment on the market today that utilizes auxiliary heat. Auxiliary heat comes in several forms.

2.3.1 The Cathode Heater The cathode heating systems require the addition of internal shields or cathodes which are electrically isolated from the wall of the vacuum chamber. At the start of each ion nitriding cycle the cathode "preheater" is turned on and heats up. The heat is then radiated to the work load to help heat the work pieces. At some point during the cycle, typically around 400 °F, the cathode heater is turned off and the heating is continued by the use of the plasma.

2.3.2 Resistance Heating Resistance heating generally requires the use of a low voltage AC power supply which is connected to graphite or alloy heating elements. As with the cathode heater these elements heat up and radiate to the work pieces, thus shortening the work piece heat-up time. Auxiliary heat, while having its place, does limit the size of the work load that can be placed in a chamber. In addition, the graphite or alloy heating elements also restrict the design and flexibility of the ion nitriding chamber.

2.4 Operating Costs

The successful commercialization of any surface treating process requires that the operating costs be identifiable and controllable. The primary operating costs are electricity, process gas, cooling water, consumables and preventive maintenance.

2.4.1 Electricity Electricity is the largest cost item in the operation of the ion nitriding system. Electricity is used to provide ionization of the gases and, in one form or another, provide heat to the work piece. Electricity is also used to run the vacuum pump, cooling fan, and the microprocessor controllers.

2.4.2 Process Gases Process gases are composed of nitrogen, hydrogen, methane, and argon. These gases, while used in relatively low volumes compared to other heat treatments, are an important element for ion nitriding systems. It is necessary that the gases are of high purity and free from contaminants. When volumes warrant, a central mixing system can be used as well as the bulk gas systems to help reduce unit costs.

2.4.3 Cooling Water Cooling water is used to cool the vacuum chamber to help prevent equipment overheating and to prevent damage to the O-ring seals between the chamber segments. It also provides a heat sink which helps the power supply maintain a constant current density. Cooling water is also used to cool the vacuum pump, as well as the circulation fan. The water cooling system can be a single pass-through system or it can utilize a chiller or cooling tower set-up. The most cost-effective method will vary with each individual customer.

2.4.4 Consumables and Maintenance There are additional items which contribute to the cost of the total ion nitriding cycle. Thermocouples are buried in the work pieces to control the power output as well as monitor the work piece temperature. These thermocouples, while reusable, do break after repeated usage and must be replaced. Thermocouple splitters are required to maintain electrical neutrality at the point of insertion into the work piece. These too can be reused and cleaned; however, they do breakdown after repeated use. Base plate splitters and feedthroughs need to be rebuilt from time to time to insure that the cathode is isolated from the vessel wall (the anode).

Preventive maintenance is as important to an ion nitriding operation as it is to other forms of heat treatment. Vacuum pump oils need to be changed on a frequent basis. It is also necessary to provide regular cleaning to the cathode rings or hearth plate as well as the internal surfaces of the vacuum chamber and heat shield. Leak detection and electrical system calibration are also required.

2.5 Capital Costs

Ion nitriding costs will vary based on the options required by the end user. For a captive user the process equipment and fixturing can be specifically tailored to meet a customer's part or family of

parts. This equipment, however, may vary considerably from a commercial ion nitriding service center. In a commercial ion nitriding setting, the equipment must have the versatility to process a wide variety of applications and configurations. Ion nitriding system costs range from $150,000–$750,000. The capital costs are broken down into three segments; first the power supply, second the vacuum system and microprocessor controls, and third the gas mixing system.

2.5.1 Power Supplies Power supplies comprise approximately 45% of the total system capital costs. These power supplies will vary in design as well as size. The power supplies are matched by the equipment manufacturer to a given vessel. The design of the power supply takes into consideration the customer's expected work load.

2.5.2 Vacuum System & Microprocessor Controls Vacuum systems and microprocessor controls comprise another 45% of total system costs. The mechanical pumping equipment is sized to the vessel to provide for a minimum pump-down cycle. The microprocessor controls the functions of the ion nitriding cycle and is programmable by the customer.

2.5.3 Gas Mixing System The gas mixing system comprises the final 10% of the total system costs. The gas can be provided in bottle or bulk, depending on the total volume requirements of the heat treater. The gas mixing system combines the various gases used in a mixing chamber prior to their being disbursed into the vacuum chamber. The mix ratios can be easily changed to meet the application demands.

3. Equipment Sizing and Work Load Considerations

Ion nitriding equipment comes in all sizes. Some are top loading (hanging fixture), some bottom loading, and some a combination. In addition to the type and size of chamber there are various methods of opening and closing the vacuum system. Some utilize bridge cranes, some lift control arms, and some are manually loaded.

Technically speaking there is no limit to the size of parts that can be treated with the ion nitriding process. However, there are some considerations that need to be addressed before equipment requirements can be determined. Two primary factors for consideration are vessel size and power supply capacity.

First the ion nitriding chamber needs to be of such size as to meet production schedules and/or revenue targets. Since parts need to be spaced in a suitable manner, to allow the plasma to surround all areas of the part, preliminary loadings should be estimated. Typical spacing between parts are one to two inches. The total number of parts that can fit in the load are determined by the vessel dimensions, fixturing arrangement, and by temperature uniformity considerations. Based on the expected work load, the equipment supplier will size the power source to meet expected load demands. At this time it will also be determined if auxiliary heat is needed.

3.1 Temperature Uniformity

Temperature uniformity within a load is a critical factor for parts with tight specifications or tolerances. For those parts with non-stringent requirements a 30 °F–40 °F variance is acceptable. The target range for most loads is ± 15 °F.

In mixed loads of parts, the part with the greatest temperature sensitivity becomes the control item. Monitor thermocouples are also placed within the load to record the temperature of other parts. Experience dictates what parts can and cannot be run together. The results of the temperature measurements, as well as other key parameters, are displayed on a CRT screen and printed periodically to a chart.

3.2 Part Spacing

As mentioned briefly before, parts require a minimum spacing to allow the plasma to uniformly surround the work piece. This part spacing and placement within the load can affect temperature uniformity. This is particularly true in systems that utilize only the DC power source for heating. While part placement varies with size and configuration, usually parts are loaded more densely on the outer circumference of the plate, gradually decreasing to a point where no parts are on the center of the plate. This prevents excess heat build-up in the middle of the plate.

3.2.1 Heat Shielding Because most ion nitriding chambers are water cooled, the parts on the outer perimeter receive radiation from the inner parts on one side, while receiving a cooling effect from the cold wall water jacket on the other. To eliminate this situation heat shields are often made to surround the work loads thus "blinding" the part to the cold wall and providing similar radiant surfaces. This method of heat shielding has been found to aid in temperature uniformity.

3.2.2 Fixturing and Masking One of the unique features of the ion nitriding process is the ability to mask off areas which must remain soft, or un-nitrided. By simply interrupting the plasma from making contact with the surface the work piece area will not be ion nitrided.

Mechanical masking, such as sheet metal, bolts, pins, and plugs is regularly used to prevent the plasma from making contact with the surface and thus keeping the parts soft. The OD's of round parts can be wrapped with shim stock as another means of masking. Other forms of masking are copper paints or copper plating, which generally adds more cost to the part. The removal of paint and plating products often has pollution consequences.

Fixturing for ion nitriding is as varied as the parts themselves. As mentioned previously parts need to be spaced to allow for proper ion nitriding.

This is often achieved through the design of fixtures, whether they are in the form of base plates or hanging fixtures. Properly designed fixtures can be used to process a wide variety of parts. Because high temperature quenching is not required with the ion nitriding process, fixtures can be made of mild steel and be reused almost indefinitely. Fixtures remain free from distortion and degradation. Periodic cleaning of the fixtures is recommended, and can be done by media blasting, or with a grinding wheel and wire brushes.

4. Typical Materials

A wide variety of materials can be ion nitrided. The type of treatment for each varies with the end use. (see Table 22 for ion nitrided materials). This chart shows the general effect ion nitriding has on each type of material. By varying the control parameters a wide range of results can be achieved.

5. Typical Applications

With the growing recognition of the superior properties provided by the ion nitriding treatment the number of various applications is growing rapidly. Some of these are listed in Table 23.

6. Process Limitations

While ion nitriding offers significant benefits, there are some process limitations. First, the ion nitriding equipment is quite expensive compared to other types of heat treat equipment. In addition the parts have to be handled and fixtured separately to insure proper treatment. A second consideration is that the ion nitriding process requires trained or skilled technicians and operators. It is a relatively new process and important techniques and procedures are not universally known. There is a considerable learning curve. The third consideration is that parts need to be clean and free of contaminants prior to ion nitriding. This is usually accomplished by using vapor degreasers or alkaline washers.

Table 23. Reasons for nitriding

Tooling All	*Reasons for Nitriding*
Tooling for mfg. of plastic components	eliminate sticking, improve part release
Sheet metal from tooling	eliminate galling, improve lubricity
Die casting dies	eliminate sticking & soldering
Forging & extrusion	reduce abrasive wear, eliminate scale & sticking
Engineered Components	*Reasons For Nitriding*
Aerospace (engine pins, bushings)	eliminate post heat treat machining abrasion resistance
(ball screws)	reduce abrasion & improve
(gears)	improve fatigue strength & eliminate scuffing
	eliminate post heat operations noise reduction
Oil field (plungers, subs)	corrosion resistance, improved lubricity
Automotive/Truck (gears) (steering components)	reduce scuffing improve fatigue strength & abrasion resistance
(engine components)	improve fatigue strength
(fuel systems)	reduce erosive wear
Machine Tools (various components)	abrasion resistance improved lubricity
Biomedical (hip & knee implants)	improve abrasion resistance of titanium components
Pumps	reduce erosive wear from solutions
Valves	reduce erosion & abrasion
Agricultural (combine components)	eliminate distortion improve abrasion resistance

7. Growth Opportunities

Ion nitriding technology is relatively new and is in its infancy, particularly here in the United States. Because of this it is very important that the supplier of the services or the equipment manufacturer carefully educates the potential end user, and ensures that the process is properly applied and the right materials are being used. There are potential applications for ion nitriding in nearly all industries.

7.1 Changes From Other Treatments

Ion nitriding readily replaces gas nitriding and salt bath nitriding, as well as shallow case carburizing, and carbonitriding for many applications. Advantages are less distortion, improved surface lubricity, and high surface hardness. Ion nitriding also replaces many plating applications, particularly for wear and abrasion resistance. In addition to the excellent properties provided, ion nitriding does not pose a threat to our environment. With the problems and costs associated with the disposal of toxic plating chemicals and stack emissions, ion nitriding offers a favorable alternative.

7.2 Commercialization of Ion Nitriding for Titanium and Aluminum Components

Recent advances in the technology have allowed the successful processing of titanium and aluminum materials. Both of these materials, while having some excellent physical properties, lack the ability to resist surface wear and galling. Ion nitriding can help in this area. With the increased use of titanium and aluminum base materials in manufacturing, new marketing opportunities will be made available to the commercial ion nitriding specialist.

7.3 Duplex Treatments

Designers are continually stretching the limits of the existing materials. To extend the use of available materials beyond their conventional limits they now perform what we call duplex treatments. These duplex treatments provide improved properties beyond those provided by either single treatment alone. Some duplex treatments are ion nitriding combined with carburizing, ion nitriding combined with induction hardening, ion nitriding combined with laser hardening, and ion nitriding combined with selective coatings such as TiN. It is in these areas that market niches can be established, providing commercial ion nitriders with new opportunities.

7.4 Needed Improvements

The ion nitriding process has proved to be a very successful industrial process. However, improvements could be made in temperature control and uniformity of large multi-layer loads. Incorporation of optical temperature sensing and controlling devices may help in achieving temperature uniformity. An objective determination of the advantages of each type of power source would be helpful. New environmentally acceptable, yet effective, cleaning materials and methods are needed. Methods for straightforward calculation of load and load mixing options would ease operations for new users.

8. Summary

Nitriding is an established and effective method of improving wear and abrasion resistance. The ion nitriding method offers numerous process and environmental advantages over gas and salt bath nitriding. With the emphasis on cost reduction, ion nitriding can eliminate post heat treat machining requirements and thus reduce costs. The process has excellent growth potential, which will continue to evolve as potential users become more aware of its possible uses.

9. References

[1] S. Dressler, "Metals/Materials Technology Series," American Society for Metals, Metals Park, OH (1986).

[2] J. O'Brein and D. Goodman, "Plasma (Ion) Nitriding," ASM International, Materials Park, OH (1990).

[3] B. Edenhofer, "Physical and Metallurgical Aspects of Ionitriding," Heat Treatment of Metals (1974).

[4] J. Erler, "Source Book of Nitriding," American Society for Metals, Metals Park, OH (1977).

About the author: Gary Sharp obtained his BA Degree in Science/Chemistry from the University of Northern Iowa. He is the Founder and President of Advanced Heat Treat Corp., a plasma nitriding service center established in 1981. He is a member of ASM, a certified manufacturing engineer, and a regular conference speaker.

Ion Implantation

James R. Treglio

ISM Technologies, Inc.
9965 Carrol Canyon Road
San Diego, CA 92131
Tel: (619) 530-2332
Fax: (619) 530-2048

Ion implantation is a process to improve the surface characteristics of manufactured components by bombarding the surface with ions having sufficient energy to penetrate 0.1 microns or more into the surface. The combination of the new surface materials and the energy deposition results in significant surface changes, including reduced friction, increased fracture toughness, increased fatigue life, increased hardness, and increased resistance to wear, oxidation and corrosion.

Key words: arc source; corrosion; fatigue; friction; gas ions; hardness; ion beam; ion implantation; ion source; metal ions; MEVVA; surface modification; vacuum arc; wear.

1. Overview

Ion implantation is a difficult concept to understand, particularly for those who are familiar with electrochemical and other deposition processes. Many of the same terms are used, but they have different meanings when applied to ion implantation. In this section, we will provide a general description of the ion implantation process and compare it to coating technologies.

1.1 General Description of the Ion Implantation Process

Ion implantation is a physical method of changing surface properties by high energy ion bombardment. It involves removing electrons from atoms of the element in a vacuum. These atoms now become positively charged ions, and together with the electrons, form a plasma. Ion implantation is accomplished by accelerating the ions in a electric field to high energy, and arranging for the accelerated ions to bombard the surface of the component to be treated. If the energy of the ions is high enough, they will go into the surface, not onto the surface, changing the surface composition. As the added material is in the surface, not on the surface, there are no adhesion problems. No heating of the treated part is required. Alloy solubility does not affect the ability of the process to change the composition of the treated surface.

At high doses the effect of the beam bombardment extends well beyond the introduction of new materials into the surface. Extensive changes in the chemical and mechanical behavior of the surface are observed, as summarized in Table 24.

The result of these changes is a new surface with properties that are often very different from the bulk material. The proper selection of ion species and other implantation parameters determines the suitability of the process for a given application. But since every element of the periodic table, alone or in combinations, can be used, and since the process does not require any heating, ion implantation has the widest range of applications of all surface modification technologies. Table 25 lists some of the surface properties that can be affected with ion implantation [1–5].

Table 24. Surface effects of high dose ion bombardment

Effect	Description
Chemical	Formation of compounds and alloys of the implanted material and the elements of the substrate, not restricted by solubility or other factors. This includes the formation of ceramics-embedded layers by double implantation. Significant changes in the chemical reactivity of the surface can result.
Structural	Change in the structure of the surface, including reduced grain sizes and even amorphicity, such as to inhibit crack formation or propagation. Structural changes depend on dose and ion mass. For heavy ions, the changes extend 50 microns or more into the surface.

Table 25. Surface properties affected by ion implantation

Surface property	Substrate materials	Typical implant elements
Wear resistance	Steels, ceramics, carbides, plastics	Ti, Ti & C, N, Y & N, Ti & Ni, Zr, Y, Y & C, O, C, B
Corrosion resistance	Most metals, ceramics, glasses	Cr, Mo, Ta, Y, Ce
Oxidation resistance	Titanium, superalloys	Y, Ce
Hardness	Most metals, plastics, ceramics	Cr, Mo, Ti, Y, Zr, Nb, Ta
Optical properties	Glasses, plastics	Nb, Ti, Mo, Zr, Y
Resistance to hydrogen embrittlement	Steels	Pt, Pd
Catalysis	Ceramics, metals	Pt, Mo, Pa
Nitride formation	Aluminum, steels	Ti, Mo
Fracture toughness	Ceramics, carbides	Zr, Cr, Ti
Friction	Ceramics, steels, plastics	Ti, Ti & Ni, Co, Cr
Fatigue life	Metals	Ta, W, Re

1.2 Comparison With Coatings

Ion implantation is *not* a coating process. In ion implantation, the existing surface of the material is altered by adding material into the surface, not onto the surface, as is the case with physical vapor deposition (PVD), chemical vapor deposition (CVD), and other coating processes. In this respect, ion implantation bears a greater resemblance to nitriding and shot peening than to coatings.

This is shown in figure 84, where the substrate is on the left. As depicted, the ion implanted surface consists of two distinct regions. The region nearest the surface is very narrow, often less than 0.1 μm thick. In this region, all of the implanted ions reside.

The second region is much thicker, extending over 50 μm into the surface. It is characterized by a significantly altered structure, including an extensive dislocation network and even phase transformations. There is currently no agreement on how this region is formed by the implantation process. One possible explanation is that compressive stresses formed by the material added to the thin, outer layer are sufficient to cause the dislocations. A second explanation is that the dislocations are

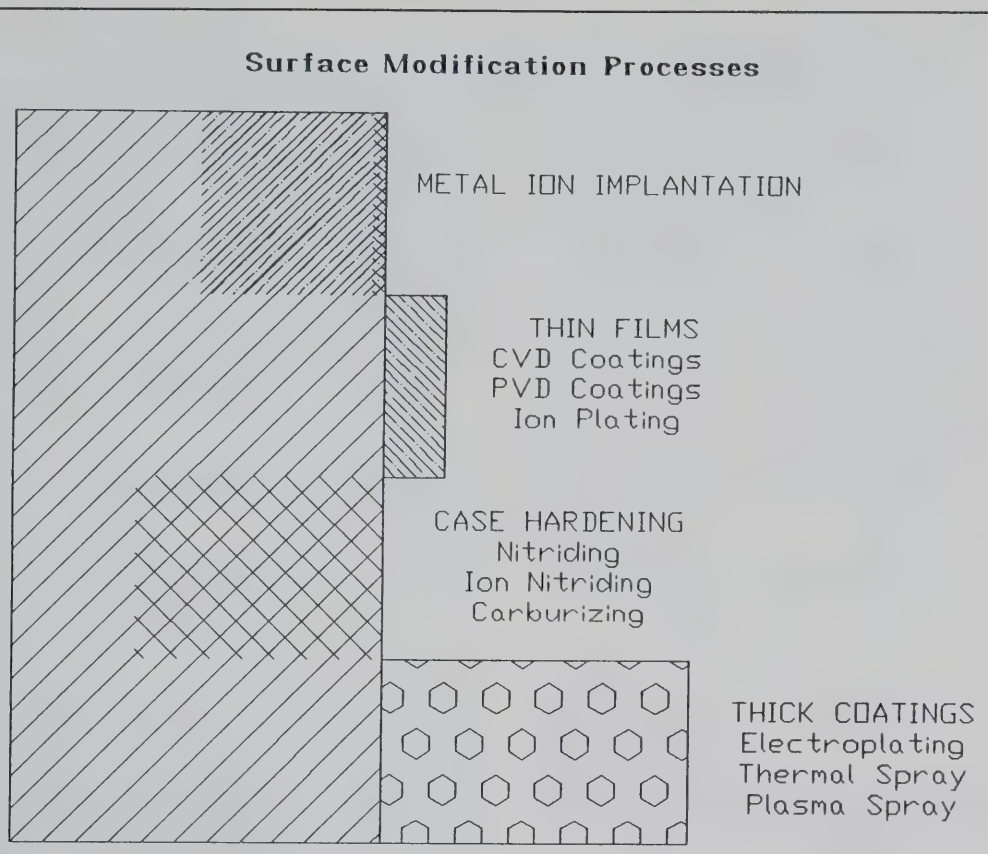

Figure 84. Surface modification process.

formed by the ion bombardment in the outer layer, then propagated inward by subsequent ion bombardment [6–8]. However this region is formed, it is extremely important.

Table 26 summarizes some of the differences between ion implantation, case hardening processes (nitriding, et al.), and hard coatings (CVD or PVD titanium nitride, aluminum oxide, et al.). Note that primary differences include the range of materials treated and the temperatures involved in the processes.

2. Typical Commercial Equipment and Treatment Methods

In this section, we review the three methods of ion implantation: beamline ion implantation, direct ion implantation, and plasma source ion implantation. We then provide an overview of the ion implantation process, and conclude with descriptions of some of the commercially available equipment.

2.1 Ion Implantation Methods

Ion implantation is a relatively simple process. By removing electrons from atoms in a vacuum, a combination of positively charged ions and negatively charged electrons, called a plasma, is formed. Electric fields affect the plasma constituents. Positive electrodes attract the electrons and repel the ions; negative electrodes attract the ions and repel the electrons. If the electric field is strong enough—over 50000 V—the ions will bombard the negative electrode with enough energy to penetrate the surface—and hence ion implant that surface. Of course, the negative electrode can be a screen, in which case many of the ions attracted to the screen will pass through—ion implanting anything behind the screen. In effect, then, ion implantation consists of two steps: form a plasma of the desired material, and find a means of making the surface to be implanted the negative electrode of a high voltage system. The system to form the plasma is called the plasma source; the system to move the ions to the target is called the accelerator. We refer to the combination as the ion source.

Table 26. Comparative features of ion implementation, case hardening, and hard coatings

	Metal ion implantation	Case hardening (nitriding, ion nitriding, carburizing)	Hard coatings (CVD and PVD)
Process temperature	<300 °F	900–1000 °F	CVD 1750–1950 °F PVD 400–950 °F
Thermal distortion	No	Sometimes	Sometimes
Bulk property changes	No	Sometimes	Sometimes
Treatable materials	Metals, ceramics, plastics, glass	Ferrous alloys only	Metals, ceramics
Surface property changes	Wear, hardness, corrosion, friction, etc.	Mostly wear and hardness	Wear, hardness, corrosion, friction, etc.

There are three methods commonly used for ion implantation. They differ in the way in which they accomplish the two steps listed above. The three methods are beamline ion implantation, direct ion implantation, and plasma source ion implantation (also referred to as plasma ion immersion).

2.1.1 Beamline Ion Implantation In the case of beamline ion implantation, the plasma that is formed is not pure—it contains materials that one does not wish to implant, such as chlorine—so these must be separated from the plasma. To facilitate this separation, the plasma source is placed at high voltage and the target at ground—thus the target is at a negative potential with respect to the plasma source. An electrode structure, with holes for ion escape, lies between the two. The ions pass through the holes in the electrode structure, accelerating to high energies, and travel to the target.

Between the electrode structure and the target is a large magnet, with magnetic field perpendicular to the direction of the ion motion. Ions passing through this magnetic field are bent by the field. The amount of bending depends on the ion material and charge. Heavy ions bend less than light ions. By proper selection of the magnetic field, the desired ions can be steered to the target, while the undesirables are expelled from the system.

A sketch of a typical beamline ion implantation system is shown in figure 85. A plasma is formed in the Ion Source and the ions extracted at high energies in a tight beam, passing through the Ion Source Isolation Valve into the beamline. The beamline consists of the Analyzing Magnet, Quadrupole Magnet, and Beam Scanning Magnets. The Analyzing Magnet bends the "good" ions into the opening of the Quadrupole Magnet; the "bad" ions are discarded against the beamline walls. The Quadrupole Magnet focuses the ions and directs them into the Beam Scanning Magnets, which sweep the ions across the surface of the targets located in the Target Area of the End Station. The End Station Isolation Valve separates the End Station from the beamline.

The need for the magnet to separate the good ions from the bad ions makes beamline ion implantation both very expensive and limited in throughput. The magnet is costly to build and consumes a very large amount of energy. In addition, the spread of the ions, or the ion beam, must be small in order to be properly bent to the target, but the number of ions cannot be very high or self-repulsion (remember that all of the ions have a positive charge) will cause the beam to blow up.

For the formation of metal ions, beamline ion implantation can present a toxicity problem. To obtain high currents of metal ions, a plasma source is usually used that forms the plasma by initiating an electric discharge in chlorine or other toxic gas.

The great advantage of beamline ion implantation systems is that they can be used to generate an ion beam of every element in the periodic table. Moreover, the ion beams that are generated, because of the bending magnet, are extremely pure. Beamline ion implantation is used extensively in the electronics industry to dope semiconductors because such purity is very important. For other

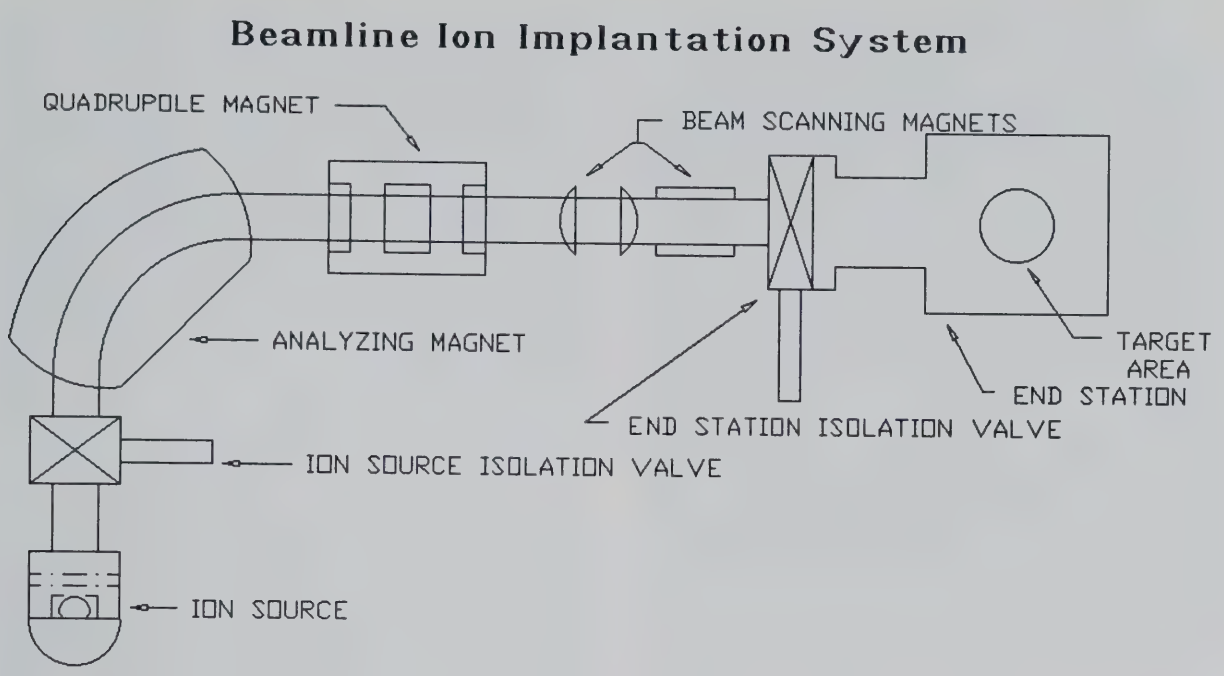

Figure 85. Beamline ion implantation system.

ion implantation applications, beamline systems are less useful because of their high costs and limited throughput. A high current from such a system is 10 mA nitrogen, which corresponds to a throughput of around 200 m^2 per year.

2.1.2 Direct Ion Implantation If the ion source can produce a plasma of just the desired material, then the very costly, beam current limiting, analyzing magnet can be eliminated. In such a case, the beam current is unlimited, costs are greatly reduced, and high-throughput processing is a reality.

We refer to such a system as a direct ion implantation system, depicted in figure 86. A plasma is formed in the Ion Source and the ions extracted at high energies in a wide beam, passing through the Ion Source Isolation Valve directly into the End Station, where they ion implant targets within the Target Area.

It is relatively easy to generate a pure plasma of a gas, such as nitrogen. Indeed, in the fusion research programs around the world gas ion sources are in operation with beam currents in the 100 A range—10000 times the highest achieved with beamline systems. Thus, the first direct ion implantation systems were designed for gas ion implantation only. Recently developed nitrogen direct ion implantation systems have beam currents in the 50 mA range [9].

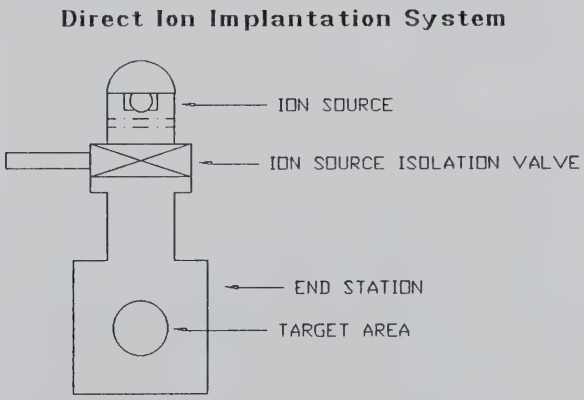

Figure 86. Direct ion implantation system.

Using the cathodic arc phenomenon, pure plasmas of metals can be generated. This process is used in an ion source for direct metal ion implantation systems [10]. To date, beam currents in the 50 mA range have been formed. As in the direct nitrogen ion implantation case, much higher currents and throughputs are in development. Many-ampere systems, with throughputs more than one hundred times that of beamline ion implantation systems, and costs less than one tenth that of beamline ion implantation systems, should be available in 2 to 3 years.

2.1.3 Plasma Source Ion Implantation A final variation of the ion implantation process is the simplest in concept: make the target the negative electrode. In plasma source ion implantation (sometimes referred to as plasma ion immersion), the vacuum chamber holding the part is flooded with plasma. Ions are extracted from the plasma and directed to the surface of the part by biasing the part to very high negative voltages. Because of the bias, the ions impinge virtually at nearly 90 ° to all of the external surfaces, the optimum ion implantation angle [11].

Figure 87 is sketch of a plasma source ion implantation system. The Plasma Source floods the chamber of the End Station with plasma. The targets are placed into the Target Area and attached by the High Voltage Bias Connection to a pulsed, negative high voltage power supply. When the high voltage is on, ions are pulled from the plasma into the surfaces of the targets.

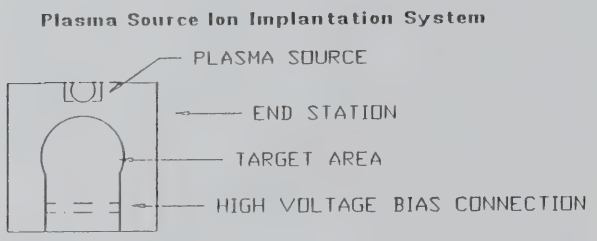

Figure 87. Plasma source ion implantation system.

Plasma source ion implantation is listed last because, while it is the simplest in concept, it is perhaps the most difficult in practice of the three ion implantation methods. To make this process work, the bias voltage must be pulsed, with a very short pulse length. Otherwise, an arc will form between the part to be implanted and the chamber walls or other grounded electrodes, damaging the part. A second problem is knowing how much plasma hits the surfaces of the part, and where it goes. Ion beams are easy to measure and direct; plasmas are not.

Plasma source ion implantation lacks the versatility of beamline and direct ion implantation. It cannot treat insulators without the addition of a biased screen, adding to the system complexity. It is virtually limited to gas ions. Metal ions coat at low voltages. During the dead time between pulses, the metal will coat the target, and ion implantation alone will not occur.

There are safety problems that must be dealt with in plasma source ion implantation as well. As the target must be biased to deadly voltages, steps must be taken to ensure that the targets are not charged up when the chamber is opened for target removal. In addition, the target will emit electrons when it is hit by the high energy ions. In beamline and direct ion implantation, the emitting electrons have very little energy, and do not cause a problem. In plasma source ion implantation, these electrons are given a significant energy from the negative bias. They have enough energy to produce x rays when they strike the chamber walls. Care must be taken to shield the chamber walls.

2.2 The Ion Implantation Process

The ion implantation process is much less sophisticated than other surface treatment processes. Indeed, it is perhaps the most brute-force technique in the vacuum processing arena. Very little needs to be done to the components before treatment; seldom is any post-treatment processing required at all. The process itself is very controllable, and very forgiving in that a precise exposure is not needed. We review the step-by-step procedure for ion implantation.

2.2.1 Pre-Treatment The pre-treatment for ion implantation consists of cleaning the parts to remove surface contaminants, such as hydrocarbons. Even though the high energy ions sputter clean the component surface while ion implanting it, cleaning is still needed for two reasons: to prevent contamination of the vacuum system; and to maintain consistency. Note, however, that a failure to properly clean the surface seldom causes implanted parts to perform at below expected levels, and often actually improves performance. Thus, cleaning is far less critical than for coatings, where surface contaminants can greatly reduce coating adhesion.

A typical cleaning sequence would entail degreasing in a standard detergent, such as Alconox, an acetone or deionized water rinse, and a final methyl alcohol rinse, usually in an ultrasonic cleaner, to remove the acetone or water from the first rinse and any grease that was not removed in the detergent wash. Vacuum outgassing—heating the part in a vacuum furnace to drive out all of the contaminants—works well, if the parts can take the temperature.

2.2.2 Ion Implantation After the parts are cleaned, they are placed in the vacuum chamber for ion implantation. In most beamline systems, the beam is horizontal, and the components must be

mounted against a vertical surface for ion implantation. In direct ion implantation systems, the ion beam is often vertical, so components to be treated can be mounted, or simply placed on a horizontal table. In plasma source ion implantation, components have to be mounted to a high voltage fixture.

As the ion implantation process is performed at a temperature as close to room temperature as is possible, beamline and direct ion implantation vacuum chambers do not contain heating elements, nor is there any need to cool the chamber walls, although the walls of a plasma source ion implantation system are often cooled to remove heat from electron bombardment. The ion bombardment does heat the components, and thus most of the fixtures are cooled.

The processing time depends on the temperature that the component being treated can withstand, and the required dose. For a fixed dose, the shorter the processing time, the hotter the component will become. To maintain temperatures below 150 °C, the processing time is on the order of 1 hour for commonly used doses.

In beamline ion implantation systems, the beam and the parts are moved to obtain coverage over the desired surfaces. In direct ion implantation systems, the ion beam is much wider and harder to sweep, so only the parts are moved. In plasma source ion implantation, no movement is needed.

In all cases, process control is quite easy. Ion beams and plasmas can be measured and monitored with simple electrical equipment, so underprocessing can be prevented. Over-processing is seldom a problem. The ion implantation process is more or less a threshold process in that once a minimum dose is attained there is little sensitivity of the surface properties to the implanted dose.

2.2.3 Post-Treatment There is none.

2.2.4 Quality Control The actual distribution of the ion implanted material in the surface can be determined by Rutherford backscattering (RBS) and Auger electron spectroscopy (AES). AES is destructive. While RBS is not destructive, the sample sizes that can be put in the measurement chamber are generally so small that the part must be cut.

When metal ions are implanted, the dose relative to an implanted standard can be measured non-destructively by x-ray fluorescence (XRF). Unlike AES and RBS, XRF does not require a vacuum. Simple, commercially available equipment, ranging in price from $20,000 to $50,000, can be used. Such equipment can examine a part in seconds, making the process ideal for post-treatment quality control [12].

2.3 Commercially Available Equipment

The choice of type of system is more complicated than choosing one of the three listed above. A second issue is the type of ions desired. Boron, phosphorus, and arsenic are very important ions for doping silicon, and beamline systems are used extensively in the semiconductor industry for this purpose. Gas ions,such as nitrogen, are very effective in many wear applications. Metal ion implantation is far more versatile; in addition to wear applications, metal ion implantation can be used to reduce corrosion, form catalytic surfaces, increase fatigue life, increase fracture toughness, change conductivity, etc. Even in the wear resistance area, metal ion implantation can be used with more materials and more applications.

Until the development of cathodic arc metal ion sources, metal ions could only be obtained from beamline ion implantation systems, and at levels well below those of nitrogen, so metal ion implantation was much more expensive than nitrogen ion implantation. Cathodic arc metal ion sources produce high current beams of pure metals, and thus can be incorporated into high throughput direct ion implantation systems. Metal ion implantation with such systems is cost competitive with nitrogen ion implantation.

Direct, beamline, and plasma source ion implantation systems are available for both research and production ion implantation, both domestically and from foreign suppliers. As mentioned previously, beamline systems are the most versatile, but typically cost two to three times direct or plasma source systems. They are also far more expensive to operate, and require more space.

The primary measure of the throughput of an ion implantation system is the beam current. The higher the beam current, the higher the throughput. It is difficult to compare systems where the applications are different, however, as the total beam current needed (the ion implantation dose) varies with the ion species. As an example, the implantation dose for nitrogen is usually $3 \times 10^{17}/cm^2$, whereas for titanium it is usually one-third of that amount. However, the applications are generally not the same.

Beamline systems are manufactured by Whickham Ion Beam Systems Ltd.[1] (Darlington, England) and Danfysik A/S (Jyllinge, Denmark). Both

[1] Certain commercial equipment, instruments, or materials are identified in this paper to specify adequately the experimental procedure. Such identification does not imply recommendation or endorsement by the National Institute of Standards and Technology, nor does it imply that the materials or equipment identified are necessarily the best available for the purpose.

companies produce systems that can generate up to ten milliamperes of nitrogen, six milliamperes of chromium, and lesser amounts of other metals. The Danfysik 1090 ion implantation system is shown in figure 88.

Tecvac (Stow cum Quy, Cambridge, England) manufactures direct nitrogen ion implantation systems. They currently offer two systems for sale. Their standard system is the Tecvac 221, with an output of three milliamperes. They also manufacture one with an output of 45 mA, based on a magnetic "bucket" design. An interesting aspect of Tecvac systems is that their rectangular vacuum chambers are equipped to hold the ion source on any wall, thus allowing ion implantation from any orientation, or the use of multiple ion sources. The Tecvac 221 is depicted in figure 89.

Only one company manufactures direct metal ion implantation systems, ISM Technologies, Inc., located in San Diego, California. Based on cathodic arc technology, the MEVVA® (standing for MEtal Vapor Vacuum Arc) ion source produces a high current beam of ions of almost any metal—including platinum and other heavy ions that are extremely difficult to obtain from other ion sources. In addition, the MEVVA ions are largely multiply charged. This gives them higher energy for the same applied voltage. Figures 90 and 91 are photographs of MEVVA metal ion implantation systems built by ISM Technologies [13,14].

Table 27 summarizes the cost and performance of systems manufactured by Danfysik, Tecvac, and ISM Technologies, as regards performance and cost. A number of assumptions went into the preparation of this table:

1) We assume two shift operation at 80% duty cycle. The down time includes time for batch change-out, including pump down time. Doses are $3 \times 10^{17}/cm^2$ for nitrogen ion implantation (Tecvac specifications for chromium-plated tools), and $1 \times 10^{17}/cm^2$ for metal ion implantation (ISM specifications for tool inserts).
2) Labor costs are assumed to be $120,000 per year.
3) Power consumption is assumed to be $225 m^2/yr implanted for beamline systems, and $45 m^2/yr for direct systems. The higher value for the beamline systems is to power the bending magnet.

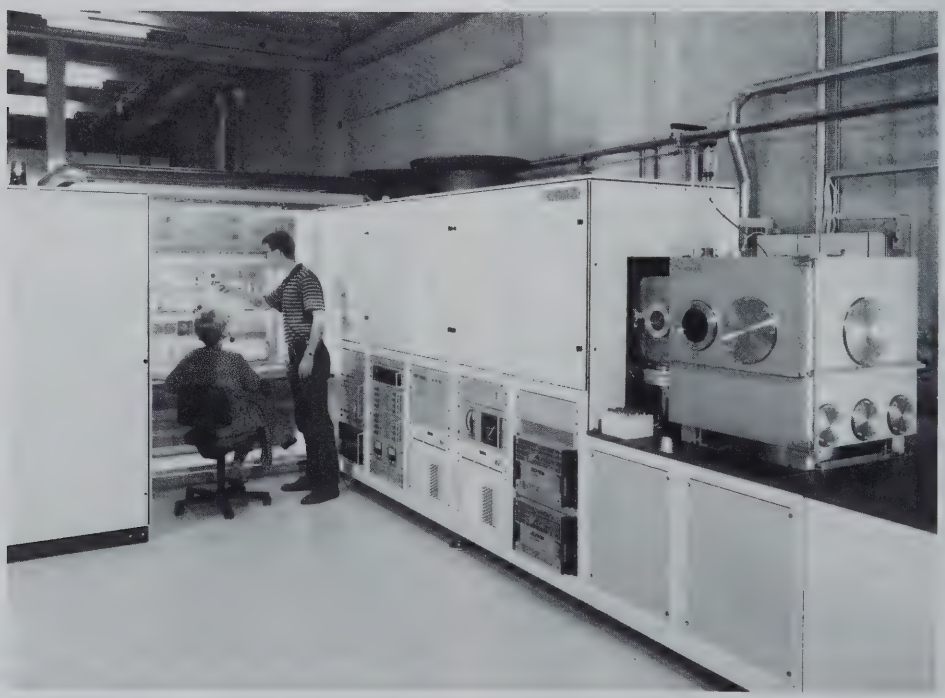

Figure 88. Danfysik 1090 ion implantation system, manufactured by Danfysik A/S, Jyllinge, Denmark. (Courtesy of Danfysik.)

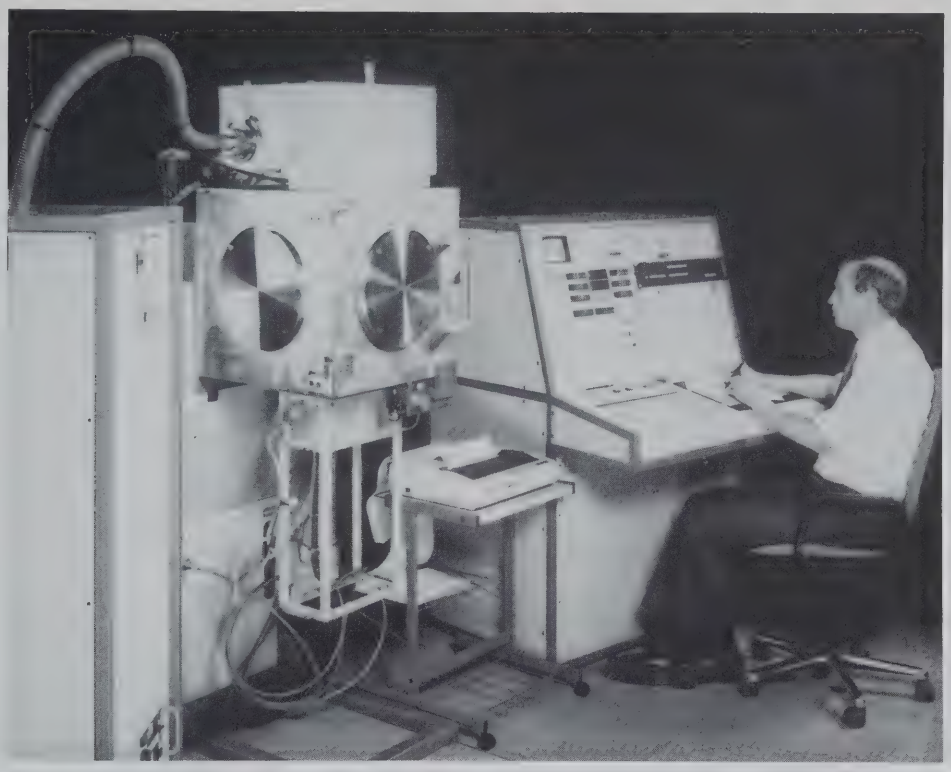

Figure 89. Tecvac 221 gas ion implantation system, manufactured by Tecvac Ltd., Stow cum Quy, Cambridge, England. (Courtesy of Tecvac, Ltd.)

Figure 90. MEVVA IV 80-10 metal ion implantation system manufactured by ISM Technologies, Inc., San Diego, CA. (Courtesy of ISM Technologies, Inc.)

Figure 91. MEVVA IV 100-50 metal ion implantation system manufactured by ISM Technologies, Inc., San Diego, CA. (Courtesy of Nippon Steel Corp.)

Table 27. Ion implantation cost comparisons

System	Throughput (m^2/year)	Capital cost ($\times 10^3$)	Operating cost ($\times 10^3$/yr)	Implant cost ($/cm^2)
Danfysik 1090 (metal)	200	$1,000	$182	$0.16
MEVVA IV 80-10 (metal)	200	$450	$146	$0.11
MEVVA IV 100-50 (metal)	1000	$1,000	$250	$0.04
Danfysik 1090 (gas)	110	$1,000	$148	$0.26
Tecvac 221 (gas)	70	$400	$125	$0.28
Tecvac bucket (gas)	1000	$1,400	$190	$0.04

4) Metal consumed in metal ion systems is assumed to cost \$60 m^2/yr. The cost of nitrogen consumption is assumed negligible. Other consumables (back fill gas, etc.) are assumed to cost \$25 m^2/yr for all systems.
5) We assume that the capital cost of the systems is amortized over a 7 year time period.

It is important to note that the cost of the implantation systems scales approximately as the square root of the throughput. Thus, the TecVac system with a throughput of 1000 m^2/yr costs 3.5 times that of the 70 square meter per year system; the square root of the throughput ratio, 15, is 3.87. Similarly, the MEVVA IV 100-50 costs 2.2 times the MEVVA IV 80-10, and has five times the throughput. The square root of five is 2.2. At the same time, labor costs dominate the annual operating costs. As only one man is needed per shift, regardless of system size (within this size range), ion implantation with the larger systems is much cheaper than with the smaller units.

As can be seen, ion implantation with beamline systems is more expensive than with direct systems. This is particularly reflected in the relative costs of metal ion implantation, where two systems with the same throughput are compared. It is also reflected in the costs to implant with the larger direct ion implantation systems, where costs are in the \$0.04 per square centimeter range, a value well below that achievable with beamline systems. Plasma source ion implantation systems should have costs similar to those of direct systems.

3. Uses

At the time that ion implantation was introduced as a means of improving surface properties such as wear and corrosion resistance, only expensive beamline ion implantation equipment, designed for research or semiconductor implantation, was available. In addition, the process was thought to be useful only in mild wear situations, because it was thought by non-experts in the field that the implanted zone represented the extent of the protection. As a result, ion implantation was thought to be a specialized process suitable only for high cost, small items.

3.1 Biomedical

The largest use of ion implantation is in the biomedical field. It has been found that titanium alloys have excellent mechanical and chemical properties for use in medical prostheses—artificial hips, knees, etc. However, the wear resistance of titanium is not very good, as it is subject to galling. It has been found that ion implantation of nitrogen and/or carbon into titanium alloys makes them very resistant to galling. Today, ion implantation is used extensively to treat the wear surfaces of medical prostheses made from titanium alloys.

3.2 Tools

Molds and dies used to form plastic components, mint coinage, and generally fabricate components

are regularly implanted to increase life. Two approaches are applied: direct treatment of the mold or die, and treatment of the mold or die after electrodeposition of chromium. In this latter case, it has been found that dies and molds coated with chromium can be reused after the chromium wears down by stripping off the chromium and re-coating. However, this can be accomplished only a limited number of times before the die or mold is damaged to a degree that reuse is impossible. As some of these components cost over $250,000 to manufacture, any increase in life of the chromium coating is of considerable interest. Ion implantation, typically with nitrogen, increases by around a factor of two the life of the chromium coating without reducing the number of times it can be stripped and replaced.

Punches are being implanted with great success. The outer circumference of the punch is implanted. As a result, not only does one increase the life of the punch, but the punch can be reground, retaining extended life without ion implanting a second time. In fact, in some cases the punch lasts longer after the regrinding. Similarly, knives need be implanted on one side only to allow resharpening. Tests have been conducted comparing V-shaped knives implanted with carbon or nitrogen on one side with unimplanted and titanium nitride coated. In all of the tests, the implantation increased the life by a factor 3.5 to 4, even after resharpening. The coating increased the life 1 (no change) to 2.5 times the first time around; after resharpening, the coated knives lasted only half that of uncoated, unimplanted [15].

Cutting tools have been implanted for some time with varying degrees of success. Generally speaking, if the material being cut is very hard, the implant will have little effect on the life of the tool, probably because the failure mechanism for the tool has little relation to the tool surface. If, on the other hand, the material being cut is not particularly hard, ion implantation will increase the tool life by a factor of two to five.

Tool inserts are a subset of the cutting tool market, and latest to be treated by ion implantation. Generally, the harsh conditions associated with the cutting applications where tool inserts are used—turning, grooving, drilling, threading, and milling of metals—were considered too severe for the surface effects of ion implantation to produce any improvement. A group of machinists at Corpus Christi Army Depot, with support from the Army Materials Laboratory, proved otherwise, demonstrating that nitrogen ion implantation of both uncoated tungsten carbide and titanium nitride coated tungsten carbide tool inserts will more than double tool insert life and increase the life consistency for cutting stainless steel. Subsequently, it has been found that metal ion implantation can provide similar increases in tool life for cutting other steels, titanium alloys, cast iron, fiberglass, phenolics, and a wide variety of other metals. In addition to increased life, use of implanted inserts results in faster cutting, more consistent insert performance, and better surface finish.

Tool inserts give a good idea of the effect of ion implantation when used in wear applications. Figure 92 is a scanning electron microscope (SEM) photograph of the surface of a corner of coated tool insert after cutting four parts. Figure 93 is a similar photograph of a corner of a coated tool insert that was ion implanted with nickel and titanium prior to use, after cutting seven of the same parts. The unimplanted tool insert surface is significantly rougher, even though it cut fewer parts. In addition, the surface is damaged beyond the edge area that was in contact with the material being cut, while the same surface on the insert that had been implanted appears untouched.

3.3 Aerospace

Several years ago, the U.S. Navy explored the use of ion implantation to improve the corrosion resistance of ball bearings for their jet engines. This work culminated in a Manufacturing Technology program that proved that chromium ion implantation could increase the life of the bearings by a factor of 2.5; that the cost to implant the bearings was less than the cost of a new set of bearings; and that the savings from reduced overhauls, combined with reduced bearing costs, would provide a benefit to cost ratio of around 20:1 [16]. Despite these exceptional results, the Navy has taken no steps to equip its jets with ion implanted bearings.

Recently, the U.S. Army has taken up where the Navy left off, exploring the use of ion implantation to improve the performance of a number of Army helicopter components. These include bearings, gears, and pillow blocks subject to wear and/or corrosion. To date, ground tests have been conducted with great success, demonstrating significant increases in component lifetimes. Additional tests have been conducted on the effect of ion implantation on the fatigue life of implanted components, to determine if there is a possibility that ion implantation of components can lead to reduced

Figure 92. Coated tungsten carbide tool insert after use. SEM photograph. Insert cut four parts before machinist decided it could no longer be used. (Courtesy of ISM Technologies, Inc.)

fatigue life and potential catastrophic failure. These tests have not shown any evidence of reduced fatigue life. As a result, the Army will conduct flight tests of ion implanted components, with the intent of introducing ion implantation as a standard treatment method for its components. The Navy is actively involved and supporting the Army program [17].

4. Future Advances

Ion implantation has been recognized in Japan as a technology of the future, worthy of priority consideration. At least four Japanese companies have invested heavily in the field—Nippon Steel Corporation, Nissin Electric, Mitsubishi, and Kobe Steel, Ltd. As a result, it is safe to say that the future of ion implantation is quite bright. In this section, we relate areas where future advances are likely to open up business opportunities for both small and large companies: the treatment of non-metallic materials, such as ceramics, plastics and glasses; applications in the automotive field; and, last, the potential for combining ion implantation with other treatment processes. Before discussing these opportunities, we review some of the areas where further work is needed to fully commercialize ion implantation, and the development of new equipment with lower cost and higher throughput that will be needed to meet the needs of this emerging industrial process.

4.1 Problem Areas

As we discussed early in this chapter, there is a great deal of disagreement as to the mechanism by which ion implantation increases the wear resistance of materials. This is partly due to the fact that the mechanism is not the same for all wear systems, as might be expected. It is also due to the fact that tribological testing is extremely difficult, particularly in mild wear applications. Improvements in this area could lead to more information

Figure 93. SEM micrograph of titanium/nickel implanted, coated tungsten carbide tool insert after use. Insert cut seven parts before machinist decided it could no longer be used. (Courtesy of ISM Technologies, Inc.)

on the mechanisms, and extend applications much further.

The problem in tribological testing of wear components is duplicating in the laboratory the conditions that the actual components see in use. It is extremely hard to even determine the conditions. Even if a particular wear environment can be duplicated, if the wear is extremely mild, realistic tests can take years to run. Techniques that accelerate the wear rate, mostly by increasing the applied load, may work for changes in bulk materials, but for surfaces modified by ion implantation usually yield inaccurate information. For example, such increases in load can change the system from one of mild wear, where the oxidation rate equals the wear rate, to one of severe wear, where the oxidation rate is less that the wear rate. If ion implantation affects the oxidation rate, the effect will be obscured by the change in wear regime. Thus, improvements in tribological testing are needed before the ion implantation process can be accepted for many applications.

Treating interior surfaces of tubes and pipes is virtually impossible for ion implantation. Even with plasma source ion implantation, it is difficult to treat interior surfaces where the depth to diameter ratio is greater than one. There are many areas where this is inadequate, such as the nozzles for water jet cutters.

Finally, there is still a large area to be explored in regard to optimum ion implantation parameters, including ion species, ion energy, implantation dose, and ion current density. Most research on ion implantation has been done at parameters that reflect the available equipment, not the optimum parameter range. For instance, a significant amount of work has involved ion implantation with beam energies in the million electron volt range. While the results have been quite good, the energy is too high for production work. New equipment is now available, such as the MEVVA metal ion implantation systems, and new processes, such as plasma source ion implantation, that open new areas for exploration with excellent prospects for

production. Analysis needs to done of their applicability, and appropriate specifications written such that a designer needs only to call out a process, rather than spelling out the details of the implantation.

4.2 Equipment

Before entering into an extensive discussion of future advances in applications of ion implantation, it is useful to remember that cost plays an important role in determining the utility of any technology. The acceptance of the ion implantation process by industry has been hampered by the lack of high throughput, low cost ion implantation equipment. The most dramatic advances in this area have been in the development of high throughput direct metal ion implantation systems.

Large scale systems to directly extract gas ions have been developed for the fusion program and for ion thrusters. Thus, in the area of gas ion implantation, little additional development is actually needed.

As metal ion implantation has many more applications than gas ion implantation, which is largely limited to wear reduction in metals, developments in the metal ion implantation field are very important. As has been previously noted, beamline ion implantation systems have reached close to their maximum throughput capability for metal ions. Fortunately, direct metal ion implantation systems, most based on cathodic arc technology, have already exceeded beamline throughput levels by a factor of five, and much larger systems are under development. It is anticipated that systems with throughputs in excess of 5000 m^2 per year will be commercially available within 2 years.

4.3 Non-metallic Materials

As described in the last section, ion implantation greatly increases the wear resistance of tool inserts. Since most tool inserts are made out of cobalt-cemented tungsten carbide, a cermet material, and coated with ceramics, such as titanium nitride, it would be natural to assume that ion implantation could be used to improve the surface properties of monolithic ceramic materials. This is indeed the case.

While ceramic systems are simpler than metals, the highly-ordered ceramic structure yields some very interesting results. For example, ion implantation of metals almost always results in an increase in surface hardness. In the case of ceramic materials, if the ceramic remains crystalline, the surface hardness will be increased by ion implantation. However, it is possible for implantation to make the surface amorphous, in which case the surface will become softer. In either case, the implantation results in reduced crack formation and propagation, and accordingly reduced wear. There is also data indicating that the fracture toughness of ceramic materials is increased by ion implantation [18].

The most exciting results of ion implantation of ceramic materials were obtained in experiments conducted by the Southwest Research Laboratory in San Antonio, Texas. The project was to find materials suitable for high temperature, adiabatic internal combustion engines—engines operating at temperatures too high for steel or normal lubrication systems. Ceramic materials such as silicon nitride were selected for potential cylinder liners, with titanium carbide chosen for the piston rings. Without any surface treatment, sliding tests at elevated temperatures yielded coefficient of friction values in the range of 0.6—far too high for engine use.

Lubricating metals were deposited onto the surface of the cylinder liner, but these wore off in a very short time. It was only when the researchers turned to ion implantation that they were able to achieve satisfactory results. It was found that ion implantation of a titanium and nickel metallic coating on silicon nitride resulted in enormous, and lasting, decreases in the coefficient of sliding friction—down to below 0.1—in a diesel engine environment [19]. Clearly, ion implantation offers an excellent means of improving the properties of ceramic materials, including ceramic coatings, for engine and other applications.

Of course, care must be taken in ion implanting ceramics. Unlike metals, ceramics are not as easily modified by gas ions. Indeed, there is ample evidence that ion implantation with gas ions into ceramic materials can lead to blistering and actual softening of the surface. This is because the gas ions can agglomerate into voids, eventually accumulating to a degree that they destroy the ceramic surface. Therefore, it is far safer to ion implant ceramic materials with metals.

Plastics are another material subject to surface modification by ion beams. As one might expect, the surface conductivity of plastics has been shown to be easily increased by ion implantation [20]. Perhaps of greater importance, tests have shown that ion implantation increases the hardness of a number of plastics by more than an order of magnitude.

Moreover, the peak of the hardness is not at the peak of the distribution of the implanted material, but nearly ten times that depth. In order to cut the plastic at all after hardening by ion implantation of gold, the force on the cutting blade had to be increased six-fold [21].

The coefficient of friction of hard plastics can also be affected by ion implantation. Experiments indicate that the friction coefficient of hard plastics can readily be reduced by a factor of three in rolling contact by chromium ion implantation. Chromium and titanium ion implantation both increase the hardness of a variety of plastics three to six times. Applications of these results are wanting, and the field offers an excellent opportunity for future development.

Of course, ion implantation of plastics is not without its drawbacks. The most serious is the energy carried by the beam. As most plastics are poor conductors of heat, and melt at relatively low temperatures, it is easy to overheat plastics during the implantation process. Thus, systems designed for implantation of metals may not be suitable for implanting plastics.

Optical properties are probably the most important feature to be improved by ion implantation of glass. The general idea is to find an implantation process that limits infrared and ultraviolet transmission without reducing visibility. Infrared radiation causes the interior temperature of closed automobiles to climb to unbearable levels. Ultraviolet radiation fades car and house fabrics and cracks leather and vinyl. The potential gains from ion implantation of glass for improving optical properties are thus quite significant, and studies are under way in both of these areas.

Another interesting area of exploration is the use of ion implantation to reduce the corrosion of glass. Generally, we think of glass as being oblivious to environmental conditions. However, acidic pollutants in the air or water will attack additives in glass, resulting in structural or optical problems. It has been found that ion implantation of molybdenum will protect glass from sulfuric acid attack. It needs to be determined if such is a viable application of the technology.

4.4 Automotive

The largest market for ion implantation will be the automotive market. The conservative nature of this market is not conducive to introduction of new technologies; however, competitive pressures from Japan and regulatory pressures should combine to make ion implantation an acceptable process for future automobiles. We have identified a few areas where ion implantation could play a role.

Cylinder liners and piston rings are subject to wear, as one might expect. As they wear, they allow more oil into the engine's combustion chamber. Oil in the combustion chamber results in particulate emissions. Ion implantation of both cylinder liners and piston rings, alone or in combination with other surface treatments, could be used to increase wear resistance of these components, and in turn reduce emissions of particulates.

In a similar vein, cams and cam followers wear with time, reducing engine performance efficiency. A combination of ion implantation and other surface technologies could reduce wear of these components, maintaining engine performance over the lifetime of the automobile. Higher efficiency operation of the engine through better timing might be accomplished as well.

In Southern California, methanol-burning engines may be needed to reduce air pollution. Methanol is more corrosive than gasoline, so while engines can burn this fuel, their internal components will not last as long. Ion implantation has been demonstrated to improve corrosion resistance of cast iron, steel and aluminum, common engine materials, and can thus be used to allow methanol-burning without design changes that would be needed to introduce new base materials, such as stainless steel.

Reducing the weight of automobile components is an easy way to increase gas mileage and reduce pollution. Wherever possible, automobile manufacturers are looking to substitute aluminum or magnesium for steel and cast iron. This substitution is often prevented by the fact that they do not have as good wear and/or corrosion resistance as the heavier metals that they are to replace. Ion implantation could modify the surface properties of these materials to allow them to be used.

4.5 Combination Processes

As has been already described, very good results have been obtained by combining ion implantation with other processes. The need for electroplating of chrome can be greatly reduced by ion implantation of the plated surface. The life of hard coatings deposited by chemical and physical vapor processes are extended by ion implantation.

Other combinations also offer large potential gains. Ion implantation after ion nitriding (or plasma nitriding) has been found to produce a

surface that has greater wear resistance than can be produced by either ion nitriding or ion implantation alone. Preliminary tests combining ion implantation before plasma nitriding have been conducted. In these tests, aluminum samples were ion implanted with a variety of materials prior to plasma nitriding. Plasma nitriding was found to have no effect on unimplanted aluminum. But the nitrided layer in aluminum implanted first with molybdenum was found to be 1 mm thick [22].

Heat treating after ion implantation has been shown to cause formation of buried ceramic layers in metal surfaces, especially when carbon or nitrogen is implanted along with a metal. Post-implantation heat treating may also be useful for implantations into glass and ceramic materials.

5. References

[1] C. J. McHargue, "Ion Implantation in Metals and Ceramics," International Metals Reviews **31**, 49–76 (1986).

[2] A. Galerie, M. Caillet, and M. Pons, "Oxidation of Ion-Implanted Metals," Materials Science and Engineering **69**, 329–340 (1985).

[3] M. Saqib, J. M. Hampikian, and D. I. Potter, "Improving Tantalum's Oxidation Resistance by Al+ Ion Implantation," Metallurgical Transactions A **20A**, 2101–2108 (1989).

[4] J. G. Cowie, L. J. Lowder, R. J. Culbertson, W. E. Kosik, and R. Brown, "Reduced Hydrogen Embrittlement Susceptibility in Platinum Implanted High Strength Steel," Nuclear Instruments and Methods in Physics Research **B59/60**, 871–874 (1991).

[5] R. G. Musket, "Applications of Ion Implantation for Modifying the Interactions between Metals and Hydrogen Gas," Nuclear Instruments and Methods in Physics Research **B40/41**, 591–594 (1989).

[6] A. N. Didenko, A. I. Ruabchikov, G. P. Isaev, N. M. Arzubov, Yu. P. Sharkeev, E. V. Kozlov, G. V. Pushkareva, I. V. Nikonova, and A. E. Ligachev, "Dislocation Structures in Near-surface Layers of Pure Metals Formed by Ion Implantation," Materials Science and Engineering **A115**, 337–341 (1989).

[7] N. Nishimiya, K. Ueno, M. Noshiro, and M. Satou, "Chemical Processes and Surface Hardening in Ion-implanted Polyester Films," Nuclear Instruments and Methods in Physics Research **B59/60**, 1276–1280 (1991).

[8] Yu. E. Kreindel and V. V. Ovchinnikov, "Structural Transformations and Long-range Effects in Alloys Caused by Gas Ion Bombardment," Vacuum **42**, 81–83 (1991).

[9] G. Dearnaley, "Developments in Ion Implantation for Industrial Applications," Ion Implantation and Plasma Assisted Processes, edited by R. F. Hochman, H. Solnick-Legg, and K. O. Legg, (ASM International, Metals Park, OH, 1988) 63–68.

[10] I. G. Brown, J. E. Galvin, B. F. Gavin, and R. A. MacGill, "Metal Vapor Vacuum Arc Ion Source," Rev. Sci. Instrum. **57**, 1069–1084 (1986).

[11] J. R. Conrad, R. A. Dodd, F. J. Worzala, X. Qiu, and R. S. Post, "Plasma Source Ion Implantation – A New, Cost-Effective, Non-Line-of-Sight Technique for Ion Implantation," Ion Implantation and Plasma Assisted Processes, edited by R. F. Hochman, H. Solnick-Legg, and K. O. Legg, (ASM International, Metals Park, OH, 1988) 185–191.

[12] M-L. Jarvinen, H. Katajamaki, J. Kosinen, J. Ojanpera, and S. Piorek, "On Site Analysis of Steels," Presented at the Pittsburgh Conference, Chicago, March 4–8, 1991.

[13] J. R. Treglio, G. D. Magnuson, and R. J. Stinner, "Performance of the Advanced MEVVA IV 80-10 Metal Ion Implantation System," Surface and Coatings Technology **51**, 546–550 (1992).

[14] B. L. Gehman, G. D. Magnuson, J. F. Tooker, J. R. Treglio, and J. P. Williams, "High Throughput Metal Ion Implantation System," Surface and Coatings Technology **41**, 389–398 (1990).

[15] Chr. A. Straede, "Ion Implantation as an Efficient Surface Treatment," Nuclear Instruments and Methods in Physics Research **B68**, 380–388 (1992).

[16] F. A. Smidt, B. D. Sartwell, and S. N. Bunker, "U. S. Navy Manufacturing Technology Program on Ion Implantation," Materials Science and Engineering **90**, 385–397 (1987).

[17] R. J. Culbertson, and A. Gonzales, "Application of Ion Implantation to U. S. Army Helicopter Maintenance," presented at the Seventh International Conference on Surface Modification of Metals by Ion Beams, July 15–19, 1991, Washington, DC.

[18] C. J. McHargue, "Structure and mechanical properties of ion implanted ceramics," Nuclear Instruments and Methods in Physics Research **B19/20**, 797–804 (1987).

[19] W. Wei, J. Lankford, I. Singer, and R. Kossowsky, "High temperature lubrication of ceramics by surface modification," Surface and Coatings Technology **37**, 179–192 (1989).

[20] S. Liu, Z. Liu, B. Zhai, and Z. Wang, "Modification of polyvinyl chloride surface electrostatic properties by an ion beam," Vacuum **39**, 271–272 (1989).

[21] N. Nishimiya, K. Ueno, M. Noshiro, and M. Satou, "Chemical processes and surface hardening in ion-implanted polyester films," Nuclear Instruments and Methods in Physics Research **B59/60**, 1276–1280 (1991).

[22] M. Nunogaki, H. Suezawa, Y. Kuratomi, and K. Miyazaki, "Effects of Ion Implantation on Nitriding Metal by the Plasma Source Nitriding," Vacuum **39**, 281–284 (1989).

About the author: Jim Treglio has an Sc.B. in physics from Brown University (1968), an M.S. in physics from Rutgers University (1975), and a Ph.D. in plasma physics from Stevens Institute of Technology (1977). In 1986, he founded ISM Technologies, Inc., to apply technology developed for the fusion program to ion implantation and the development of the high-throughput MEVVA series of metal ion implantation systems. He has authored several papers on metal ion implantation equipment and on uses of metal ion implantation, and holds three patents in the field of surface modification.

Thermal Spray Coatings

Robert C. Tucker, Jr.

Praxair Surface Technology, Inc.
1500 Polco Street
Indianapolis, IN 46224
Tel: (317) 240-2539
Fax: (317) 240-2426

Thermal spray coatings are produced by heating material, usually in the form of fine powder, to near its melting point, accelerating it to a high velocity, and projecting the droplets against the surface to be coated. The advantages and disadvantages of thermal spray coatings, the general process steps, and the specific major thermal spray techniques (flame, plasma, high velocity oxy-fuel, and detonation gun spraying) are briefly described in this paper. The structure and properties of some of the major families of coatings are characterized and their uses and markets partially catalogued. Finally, the status of development of thermal spray coatings and the needs of the industry are discussed.

Key words: detonation gun; flame spray; high velocity oxy-fuel; HVOF; plasma spray; thermal spray.

1. Introduction

In thermal spray coating, material, usually in the form of powder, is heated to near or above its melting point, accelerated, and projected against the surface to be coated. On impact, the fluid or highly plastic droplets flow into thin lamellar particles (called splats) that constitute the coating (fig. 94). Virtually any material that melts without decomposing can be used to produce a coating by one or more of the thermal spray processes. Moreover, even though the coating material is usually molten on impact, the temperature of the substrate can be kept close to ambient. Thus the mechanical and dimensional properties of a metallic substrate remain unchanged and even some polymeric materials can be coated.

While coating material flexibility and the maintenance of a low substrate temperature are major advantages of thermal spray, it is not without disadvantages. The major disadvantage is its inherent "line-of-sight" deposition characteristic. Only surfaces that can be "seen" can be coated. Moreover, the structure and properties of the coating may change with angle of deposition.

The major thermal spray processes are flame, electric arc, plasma, high velocity oxy-fuel, and detonation gun. Historically, the first commercial thermal spray process was probably that patented by M. U. Schoop in Switzerland in 1911, a combustion wire spray process. This was followed by the introduction of various combustion or flame spray processes using powder and by electric arc wire spray. Most of the more advanced thermal spray processes were first developed in the laboratories of Union Carbide Corporation in the United States; detonation gun deposition by R. M. Poorman, H. B. Sargent, and H. Lamprey (patented in 1955), plasma spray by R. M. Gage, O. H. Nestor, and D. M. Yenni (patented in 1958), and high velocity oxy-fuel (HVOF) by G. H. Smith, J. F. Pelton, and R. C. Eschenbach (patented in 1958).

2. General Characteristics of Thermal Spray Processes

A general thermal spray process consists of the following elements: substrate preparation, masking

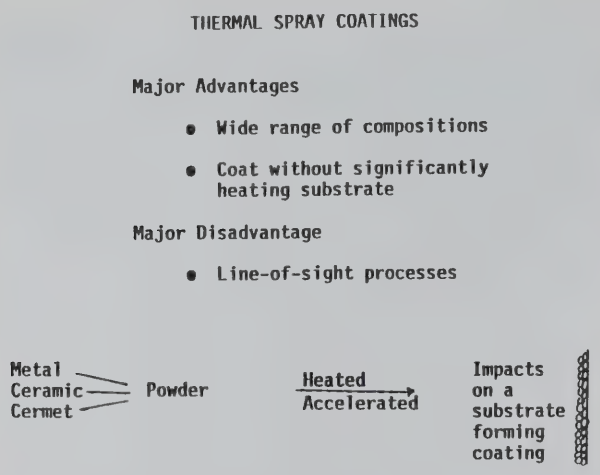

Figure 94. Schematic of the thermal spray process.

and fixturing, coating, finishing, inspection, and stripping (when necessary). Substrate preparation usually involves scale and oil/grease removal as well as surface roughening. Roughening is necessary for most of the thermal spray processes to insure adequate bonding of the coating to the substrate. (Bond strength is usually attributed to a "mechanical interlocking" mechanism.) While very coarse machining may be adequate for some flame or electric arc wire spray coatings, the most common method is grit blasting, usually with alumina, to a surface roughness in excess of 200 microinch (5.8 μm) Ra. With very high velocity processes, e.g., detonation gun deposition, surface roughening may not be necessary with some relatively softer substrates such as aluminum, titanium, or annealed steel alloys.

Masking and fixturing are important elements of thermal spray technology. The coating is usually to be applied to only particular, precisely delineated, areas on a part, and it is generally much better to limit the area of coating deposition to those areas by masking and/or fixturing than to have to remove overspray by grinding, etc., after deposition. Suitable masking may vary from paint-like ceramic slurries for low velocity processes like flame spraying, to various types of tape for intermediate velocity processes like plasma spraying, to precision metallic masking for high velocity processes like detonation gun deposition.

The individual types of coating processes will be described shortly, but with any of them the quality of the coating is strongly a function of the control of the process gases, electrical power, powder morphology and size, powder or wire feed rate, traverse rate, stand-off (distance from the part to the torch or gun), angle of deposition (angle between the axis of the torch or gun and the surface of the part), precision of the deposition pattern, as well as the thermal characteristics of the coating and substrate. All of these parameters have a bearing on the final coating microstructure, mechanical properties (including residual stress and bond strength), wear resistance, corrosion resistance, and other characteristics. Thus the best coating quality can only be achieved through substantial automation of the process.

In general, the most important parameters in thermal spray deposition, regardless of the particular process, are the particle's temperature, velocity, angle of impact, and extent of reaction with gases during the deposition process. (The optimum temperature and velocity may be interrelated and a function of particle size and composition, of course.) Extraordinary gas temperatures and velocities are of no value unless they can be used to effectively heat and accelerate the particles. Therefore, the specific design details and operating parameters of a thermal spray device are very important.

Since the structure and properties of a thermal spray coating are a function of stand-off and angle of deposition, it is important to realize that the coating on a part may vary from point-to-point as these parameters vary because of the geometry of the part. Moreover, the properties may be different from those on a test sample for the same reason. Usually, the sensitivity of coating properties to angle of deposition decreases with increasing particle velocity; thus useful coatings can be made at lower angles of deposition with high velocity processes than with low velocity processes. What is of most importance is that the properties are invariant from piece to piece when coating many pieces of the same part in a given plant or in many plants world wide.

The roughness of as-deposited thermal spray coatings varies widely, but is seldom less than 50 microinches (1.3 μm) Ra. Thus for many applications they must be finished. Few can be single point machined, so grinding, often with diamond, is most often used. With grinding followed by lapping, a finish in the 0.02 to 0.08 μm (1 to 3 microinch) Ra range can be achieved with some of the denser oxide and carbide based materials.

The final inspection of thermal spray coatings is usually limited to verification of dimensions and visual examination for pits, cracks, etc. Nondestructive testing using ultrasonic, x-ray, thermography,

magnetics, or eddy current techniques to find areas with poor bonding, excessive porosity, or cracks has largely been unsuccessful to-date. Magnetic and eddy current techniques can be used with some coating/substrate combinations to measure coating thickness, however. The absence of meaningful NDT techniques forces one to insure that the coating is as it should be by verifying the coating's characteristics before coating the actual part by coating a dummy metallographic sample and relying on the reproducibility of the process. Occasionally dummy samples can be coated with a part or both before and after a part, but this practice adds cost and should not be necessary.

Stripping of residual coating is an essential part of the refurbishment of service worn coatings, and the ability to do so is a major attribute of thermal spray coatings. A practical manufacturing process also usually requires a means to strip misprocessed coatings, since many of the parts coated are far too expensive to scrap. Stripping can frequently be done, depending on the coating and substrate compositions, chemically in acids or bases, electrolytically, or in fused salts. If none of these techniques is possible, mechanical removal by grinding or grit blasting is necessary.

3. Processes

3.1 Flame Spray

A combustion flame spray torch is shown schematically in figure 95. In this process, a fuel gas and oxygen are fed through a torch and burned with the coating material in the form of powder or wire being fed into the flame. The material is heated to near or above its melting point and accelerated. The molten droplets impinge on the surface where they flow into lamellar "splats" forming the coating. Flame spray systems vary in complexity from simple hand-held torches to fully automated systems incorporating robotics and computer control. The materials that can be used to produce flame spray coatings include metals, ceramics, and cermets. Particle velocities range from about 65 to 300 m/s, among the slowest of the thermal spray processes.

There are three basic types of flame spray processes; cold spray, spray + fuse, and spray − fuse. All normally use acetylene as a fuel. In cold spray, the coating is used as-deposited. Metallic, ceramic, or blends (carbides + metal alloys) of powders, solid wire, or composite rod or cord are used. In spray + fuse, a metallic alloy or a blend of a metallic alloy and carbide in powder form is first deposited using a flame spray torch, and then the metallic component is subsequently fused in a second step. The second step can be done with a torch, in a furnace, or inductively. In a spray − fuse process, the deposition and fusion on the surface occur simultaneously using the torch to effect the fusion on the surface. In the spray + fuse or spray − fuse processes, the substrate temperature may be substantially elevated, and its properties significantly changed.

Flame spray coatings are characterized by relatively high as-deposited porosity, significant oxidation of the metallic components, low resistance to impact or point loading, and limited thickness (typically 0.5 to 3.5 mm). Major attributes of flame spraying include the low capital cost of the equipment, its simplicity, and the relative ease of training operators. The result is often low initial cost of the coatings. Typical flame spray materials and their uses are shown in Table 28.

Table 28. Typical flame spray materials and their uses

Material	Use
Self bonding nickel alloy Ni-9Cr-9A1-5Mo-7Fe	Repair of machine bearing surfaces
Bronze alloy Cu-10A1-1Fe	Piston and shaft bearing or seal areas
Blend of carbide + metal WC + (Ni-14Cr-3B-4Si-3Fe)	Wear resistance
Nickel alloy Ni-14Cr-4Si-3B-3Fe	Corrosion and wear resistance
Nickel alloy Ni-20Mo-20Fe-10Ti-4.5W-1.5Si	Corrosion resistance on boiler tubes
Zinc	Corrosion resistance on structures (bridges, etc.)

Wire spray, while not a combustion process, is frequently grouped with the flame spray processes. In wire spray, an electric arc between the ends of two wires continuously melts the ends while a jet of gas (air, nitrogen, etc.) blows the molten droplets toward the substrate. The wires must be conductive, of course, so the process is usually used for simple metallic coatings. Particle velocities may be substantially higher than in the flame spray coatings, but nonetheless much lower than in plasma spray. Extensive oxidation of the metallic coatings is common, and contributes to the low bond strength and high porosity typical of these coatings.

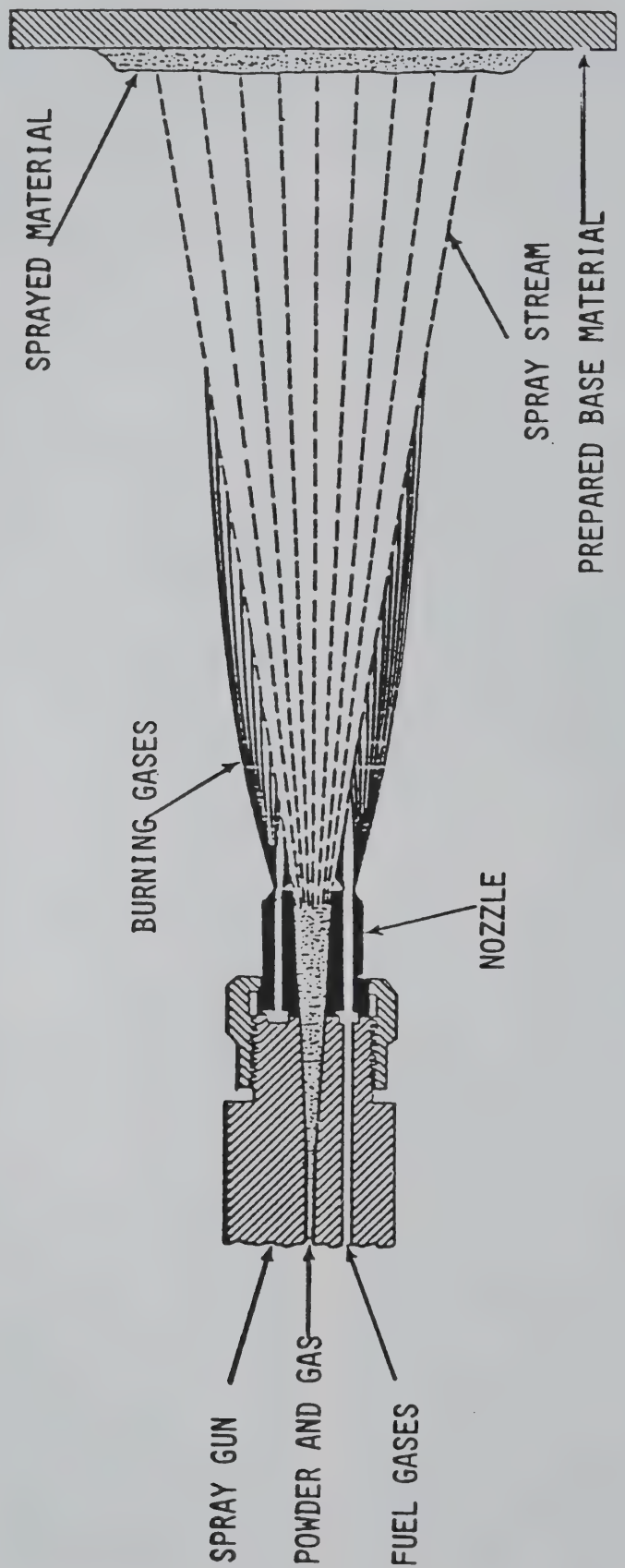

Figure 95. Schematic of a flame spray torch.

3.2 High Velocity Oxy-Fuel

In high velocity oxy-fuel thermal spraying, the material to be deposited, usually in powder form, is heated to near, or above, its melting point and accelerated in a high velocity combustion gas stream. It is similar in principle to flame spraying, but higher gas velocities are achieved, usually by allowing combustion to occur in a confined chamber with expansion through a nozzle. Higher particle velocities are achieved, in part, by introducing the powder into the gas stream within the nozzle. A schematic of a typical HVOF device is shown in figure 96. The fuel is usually propane, propylene, MAPP, or hydrogen, but acetylene can be used in at least one device and liquid kerosene in another. Without the use of acetylene many oxides cannot be melted. Particle velocities achieved vary widely with the type of HVOF device used and operating parameters, but may exceed 550 m/s.

Metallic, ceramic, and cermet coatings can be produced via HVOF deposition, given adequate gas temperatures, etc. Since the particles are heated and accelerated in a combustion gas stream, they may be exposed to either an oxidizing or reducing environment. Thus some oxidation of metallics or carbides may occur or carburization of some metallics or reduction of some oxides, with concomitant changes in the coating's properties. The density of as-deposited HVOF coatings is usually in the range of 85% to 95% of theoretical. Bond strengths frequently exceed the limits of the adhesive used in the standard ASTM test—i.e., they are greater than 69 MPa (10000 psi). Coatings are usually used in the thickness range of about 0.05 to 0.5 mm, a range typical of most applications of plasma and detonation gun coatings as well. The thickness range is a function of economics, service requirements, and residual stress considerations.

The noise level generated by HVOF equipment may exceed 100 dB and requires very effective ear protection, if it is not operated by remote control in sound reducing cubicles.

3.3 Plasma Spray

A schematic of a nontransferred-arc plasma spray torch is shown in figure 97. In a typical plasma spray torch, a flow of gas, usually based on argon, is introduced between a water-cooled copper anode and a tungsten cathode. A DC arc, initiated with a high frequency discharge, ionizes a portion of the gas. The temperature can exceed 30000 °C in the core of the plasma. This high temperature causes, of course, a rapid expansion of the gas through the nozzle of the torch. With proper design, extremely high, even supersonic, gas velocities can be achieved. A flow of powder, carried by a secondary gas stream, is injected into this high temperature, high velocity plasma effluent where the powder particles are heated to near or above their melting point and accelerated to velocities that may exceed 550 m/s, though with most plasma spray systems velocities in the range of 300 to 500 m/s are expected.

The gas used to produce the plasma is usually chosen to be inert relative to the material being deposited. Argon is most commonly used, but helium, hydrogen, or nitrogen may be added. The diatomic gases can significantly increase the enthalpy of the gas at a given temperature and enhance heating of the powder particles. The electrical power consumed is usually in the range of 30 to 80 kW, but can be as high as 120 kW. Unfortunately,

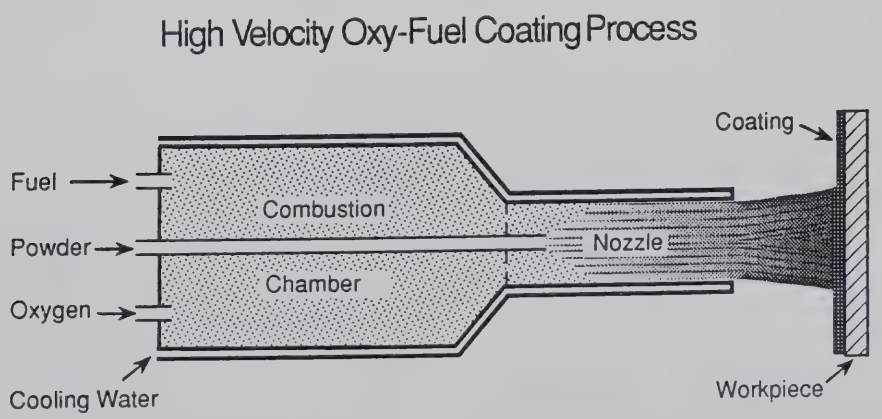

Figure 96. Schematic of a HVOF device.

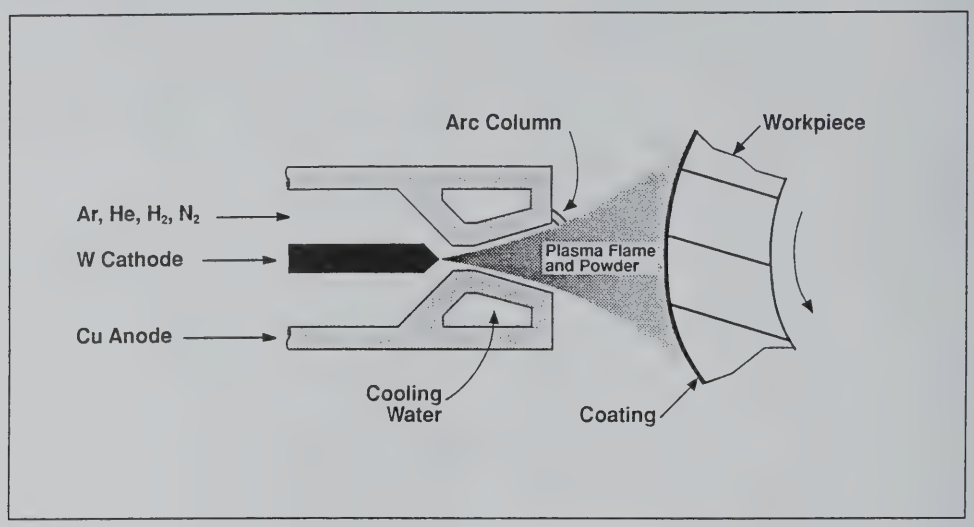

Figure 97. Schematic of a plasma spray torch.

only a small fraction is actually converted to either thermal or kinetic energy of the powder.

The powder size used in plasma spraying is a function of the torch design. Powders that are −60 mesh are most common. Some of the densest coatings are made with substantially finer powder.

Plasma spray coating densities are usually in the range of 80% to 90% of theoretical, although metallographically measured porosity may imply higher densities. Densities are a function of many parameters including torch design, power level, gas flow, powder size, stand-off, and angle of deposition.

Although the gases used in plasma spraying are usually chosen to be inert to the material being sprayed, a substantial amount of air can be drawn into the plasma effluent as a result of turbulence. This may lead to oxidation of metallics and carbides with significant changes in coating properties. The amount of such oxidation is strongly a function of torch design and operating parameters. Such oxidation can be virtually eliminated by using an inert gas shield around the plasma effluent or by spraying in a low pressure inert gas chamber. Using the latter, long stand-offs and higher particle velocities may be obtained as well, but at higher cost.

3.4 Detonation Gun

A schematic of a detonation gun is shown in figure 98. A mixture of oxygen and acetylene along with a pulse of powder is introduced into a water-cooled barrel about a meter long and 25 mm in diameter. A spark initiates a detonation, and the resulting hot, expanding gas heats and accelerates the powder particles. The powder has a velocity of about 750 m/s and is at or near its melting point as it strikes the substrate. This process is cyclic with each detonation followed by a flow of nitrogen to purge the barrel. The process is repeated up to about 10 times per second. Each detonation results in the deposition of a circle of coating about 25 mm in diameter and 0.01 mm thick. The total coating is produced by overlapping the circles of coating in a precise pattern by traversing the gun relative to the substrate. This requires very accurate, highly automated equipment. The high sound level, approximately 150 decibels, requires operation in sound reducing cubicles via remote control.

The detonation gun process produces some of the densest of the thermal spray coatings, with typical metallographic porosities less than two percent. Almost any metallic, ceramic, or cermet material that melts without decomposing can be used to produce a coating. Typical coating thicknesses range from 0.05 to 0.5 mm, but both thicker and thinner coatings are used. Because of the very high velocity of the powder particles, the properties of the coating are much less sensitive to angle of deposition than most other thermal spray coatings, little change being observed between 90° and 45°.

Recently a new Super D-Gun™ [1] coating process has been introduced. It uses a mixture of fuel gases rather than just acetylene and generates particle

[1] Super D-Gun is a trademark of Praxair ST Technologies, Inc.

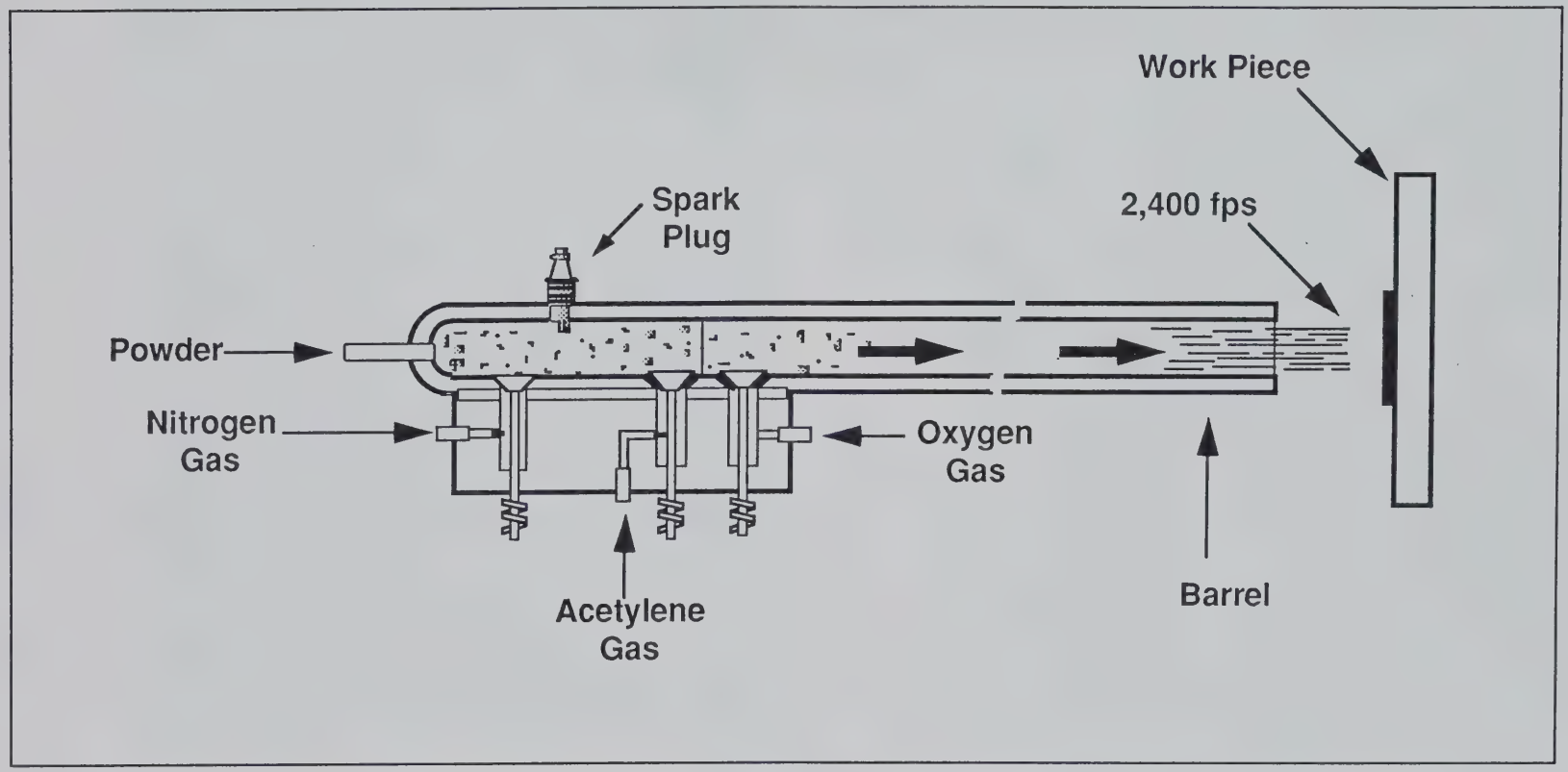

Figure 98. Schematic of a detonation gun.

velocities of about 1000 m/s. This results in higher bond strength, greater density, and improved wear and other characteristics. Of particular note is the significant compressive residual stress that can be generated in the coatings with concomitant improvement in the fatigue properties of the coated component.

Detonation gun coatings can be purchased from a world-wide network of Praxair Surface Technologies plants. Detonation gun equipment can be purchased from Russia or from Russian licensees in Japan or Europe.

3.5 Comparison of Processes

Table 29 contains a comparison of a few of the characteristics of the various processes. The values shown should be considered typical and not absolute limits.

4. Coating Structure and Properties

The as-deposited structure of thermal spray coatings consists of thin, overlapping, lamellar particles, frequently called splats (fig. 99). Of importance are the intrasplat, intersplat, and coating/substrate interface structures. The intrasplat structure may be crystalline, with very fine columnar crystals oriented perpendicular to the substrate surface, amorphous, or a mixture of the two. The crystalline structure may be thermodynamically stable or metastable. This structure is due to the extremely rapid quench rates usually associated with thermal spray, estimated to be in the range of 10^4 to 10^6 °C/s for ceramics and 10^6 to 10^8 °C/s for metallics.

The intersplat structure of coatings can be substantially affected by the amount of oxidation that occurs during deposition. This may be of particular concern with flame spray coatings and with plasma or HVOF coatings requiring a long stand-off, due to air inspirated into the flame or plasma effluent. Generally, oxide films on the splats weaken the splat boundaries, inhibit flow of the material during deposition (thus increasing "turbulence" and porosity), and consume reactive components (modifying the chemistry of the coating). Such oxidation can be virtually eliminated, as noted earlier, when plasma spraying by using an inert gas shroud or by spraying in an inert atmosphere. Proper selection of operating parameters can substantially inhibit oxidation during deposition with detonation gun or HVOF coatings. With any of the combustion processes, the oxygen-to-carbon ratio can be adjusted such that carburization occurs rather than oxidation, but usually parameters are chosen that cause minimal chemical changes.

Table 29. Relative process comparisons

Process	Coating material	Powder size	Powder velocity	Bond strength
Flame spray	Metals,		m/s	psi
Cold	cermets,	Coarse	65–130	1000–5000
Wire	some	N/A	230–295	low
Sp + fuse	ceramics	Coarse	65–130	> 10000
Sp − fuse		Coarse	65–130	> 10000
Plasma	Metals, cermets, ceramics	Medium-fine	300–550	3000– > 10000
HVOF	Metals, cermets, some ceramics	Fine	550	> 10000
Detonation Gun	Metals, cermets, ceramics	Fine	750	> 10000
Super D-Gun	Metals, cermets, ceramics	Fine	1000	> > 10000

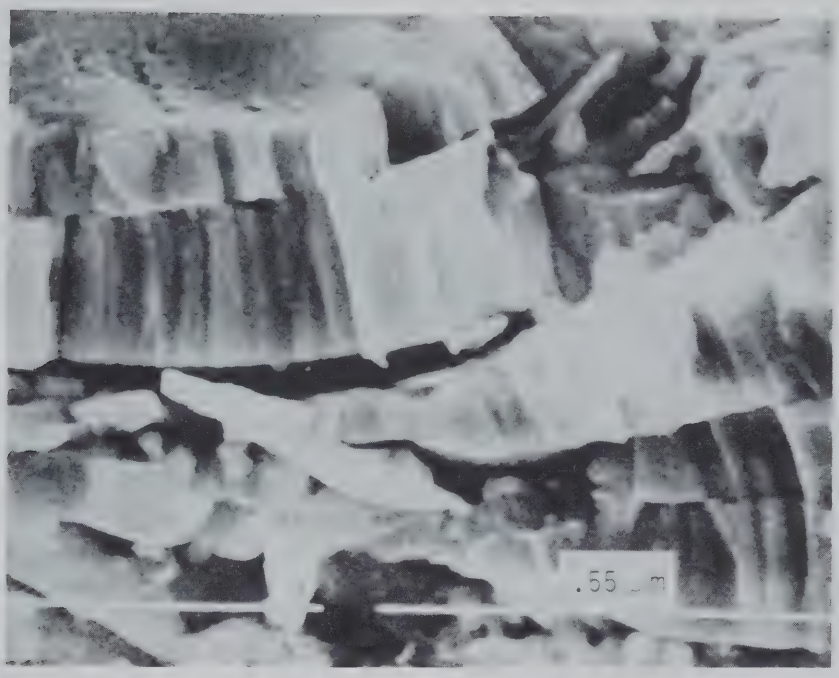

Figure 99a. Scanning electron micrograph of a fractured plasma sprayed tungsten coating illustrating the "splats" typical of thermal sprayed coatings. Note the fine grains within the splats.

Figure 99b. Polished cross section of the coating in figure 6a.

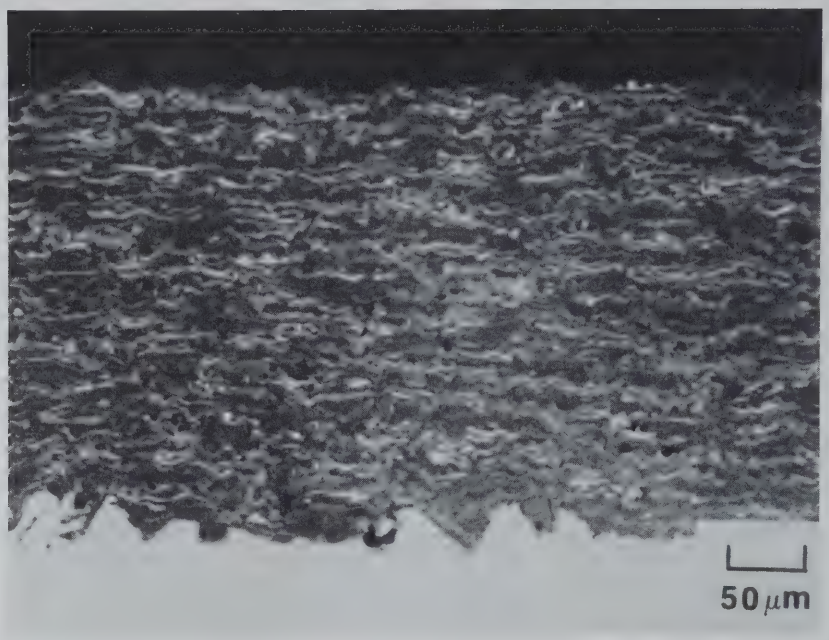

Figure 99c. Micrograph of a cross section of plasma sprayed $Al_2O_3 + TiO_2$ coating illustrating the lamellar nature of thermal spray coatings.

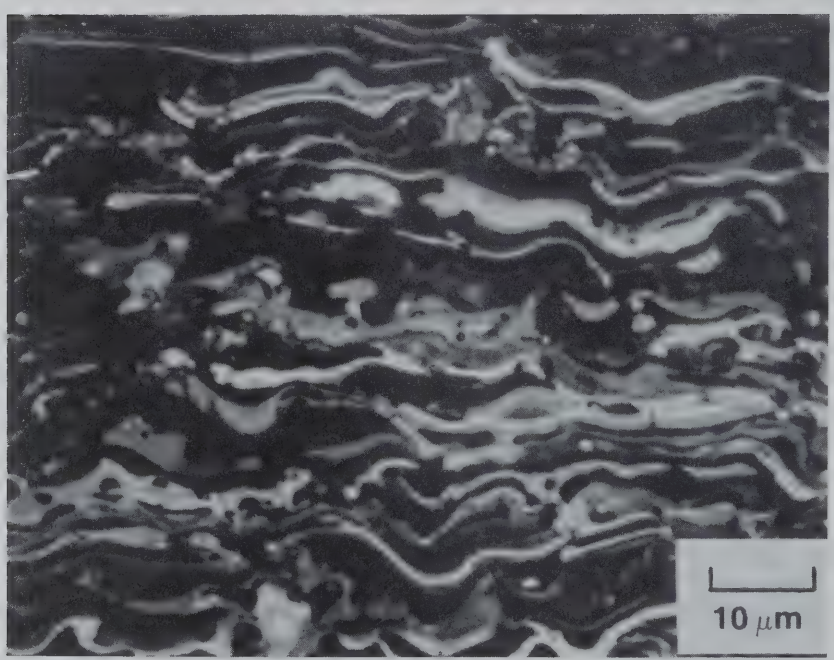

Figure 99d. A higher magnification of the same coating as in figure 6c.

As-deposited thermal spray coatings invariably contain some porosity, the amount usually decreasing with increasing particle velocity. Unfortunately, for most coatings, some of this porosity is interconnected. This can have serious implications when considering the corrosion characteristics of the coating or the coating/substrate combination. Sealants such as epoxies can reduce the impact of interconnected porosity, but they have limited temperature capability and wear or finishing may open new channels through the coating. Heat treatment of the coating at a temperature high enough to effect sealing via sintering has been used in some situations (e.g., metallic coatings on superalloys). Such heat treatment is limited to those substrates that can withstand the high temperatures required, both structurally and dimensionally, and to those situations where there is only a small mismatch in coefficients of thermal expansion between the coating and the substrate. The spray + fuse and spray-fuse processes generally effect sealing of the coating even if all of the porosity is not eliminated.

Examination of the as-deposited coating/substrate microstructure seldom reveals any interdiffusion or other chemical reaction between the coating and the substrate (with the exception of the spray-fuse process). Bond strength is most frequently attributed to a mechanical interlocking mechanism. For most of the thermal spray coatings, a roughening of the substrate is necessary, as previously discussed. On occasion, the microstructure of the coating immediately adjacent to the substrate may have more amorphous material or a finer grain size than the bulk of the coating because of a higher quench rate.

Having described in fairly general terms some of the more important considerations relative to the microstructure of thermal spray coatings, it may be well to illustrate the microstructures of several of the more commonly used thermal spray materials. Coatings based on tungsten carbide may well be the most important type of thermal spray coating. They are primarily used for wear resistance. The basic tungsten carbide—cobalt compositions can be modified with chromium and/or nickel to increase their corrosion resistance. The microstructure, and hence mechanical properties, of a specific composition is a function of the starting powder morphology and the deposition parameters. Coatings made under conditions such that the powder becomes completely molten may appear quite different from those where the powder becomes only partially molten. This is particularly true for powders that contain relatively large WC or W_2C grains. This is illustrated in figure 100, where coatings made with such grains, deposited under different thermal conditions, are compared with coatings made with more homogeneous powder containing very fine-grained WC. It should be kept in mind that none of the microstructures is particularly bad or good, but that each has its uses.

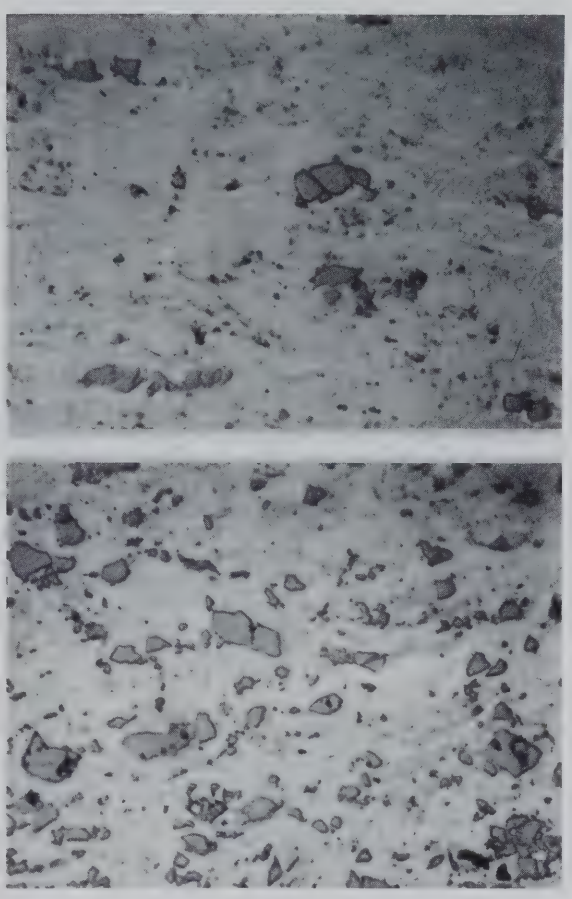

Figure 100. Micrographs of two tungsten carbide-cobalt coatings made with similar powders, but using different thermal energies, illustrating different degrees of melting of the "primary" carbides in the powder.

Another group of widely-used coatings is the chromium carbide cermets, usually made with mechanical mixtures of the carbide and nickel-chromium alloys. Since there is virtually no interaction between powder particles during flight, the coating consists of a mixture of the lamellae of the two constituents, as illustrated in figure 101. Mixed oxides and other materials are also often used.

Figure 101. Micrographs of a detonation gun coating using a powder consisting of a mixture of chromium carbide and a nickel-chromium alloy.

A variety of metallic coatings are used, particularly for build-up and corrosion resistance. Several are listed in Table 28. As mentioned earlier, some applications require virtually oxide-free deposition. That this can be accomplished with even very reactive metals using plasma spray deposition with inert gas shrouding or low pressure inert gas chambers has already been discussed. The significant influence on the type of equipment used when these protective techniques are not employed is illustrated in figure 102.

5. Mechanical Properties

The mechanical properties of thermal spray coatings reflects their microstructure. They are highly anisotropic because of the lamellar splat structure and columnar grains. They also tend to be quite brittle—even the pure metallics—with limited strain-to-fracture.

The most commonly measured mechanical properties are bond strength and hardness. Bond strength is usually measured using a test that involves bonding the coated end of a bar to a mating bar with an epoxy adhesive and pulling the couple apart in tension. Typical values for various flame spray and most plasma spray types of coatings range from about 20 MPa to 60 MPa. With many of the more advanced thermal spray coatings, the strength of the bond of the coating to the substrate exceeds the strength of the epoxy used in the test (about 70 MPa). Thus the test becomes only a "proof" test, and the actual bond strength can only be said to be greater than the epoxy strength.

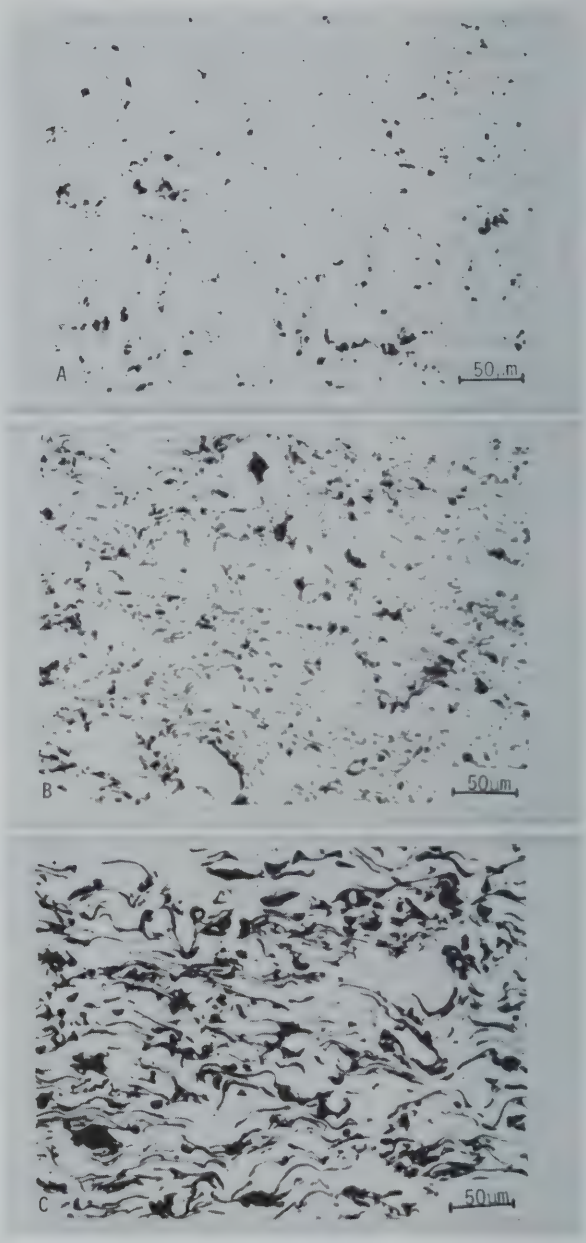

Figure 102. Micrographs of three plasma sprayed aluminum bronze coatings using the same powder, but different torches, illustrating the drastic difference in oxidation during deposition largely due to torch design.

Other tensile tests are being developed, but the results have yet to be published. Tests to measure the shear strength of thermal spray coatings have been developed, but most have serious limitations.

The hardness of thermal spray coatings is usually measured using microhardness techniques (diamond pyramid or Knoop) on metallographically prepared cross sections. Typical values range from about 200 to 300 HV.3 for some of the softer

metallic coatings to over 1400 HV.3 for some of the carbide based coatings. Hardness values are frequently misused in selecting coatings for a given application; they can be a poor indicator of wear resistance in some situations, and do not take into account other factors, such as toughness, that may be critical.

A wide variety of other mechanical properties have been measured and used quite successfully, but they are too numerous (and in some cases too specialized) to be included here. More standardized tests would be of value to the development and wider use of thermal spray coatings, however.

6. Uses

The widest use of thermal spray coatings is probably to combat wear—abrasive, adhesive, and erosive. Only a brief illustration will be given here of each of these major types, but it should be recognized that there are many other variants where coatings are or could be used. It should also be kept in mind that thermal spray coatings are used in virtually every industry on equipment ranging from submarines to the space shuttle, on components whose size ranges from that of a pin head to rolls weighing over 50 tons, and operating from cryogenic temperatures to over 1500 °C. Some examples of laboratory wear data are shown in Table 30. Examples of wear resistant applications are shown in Table 31.

Thermal spray coatings are used for corrosion resistance or for wear resistance in a corrosive environment in a variety of situations, but to be successful the interconnected porosity inherent in most of these coatings must be dealt with. The major corrosion mechanisms in liquid corrosive media are: a) general corrosion of the coating or a coating constituent, b) general or crevice corrosion of the substrate as a result of penetration of the corrosive media through the interconnected porosity in the coating, and c) galvanic corrosion of the coating or the substrate. Appropriate selection of the coating and the substrate compositions can eliminate these concerns in some cases, but economically viable choices are not always available. Thus a means to seal the porosity in the coating

Table 30. Examples of laboratory wear data

Test	Material	Type	Wear rate
Abrasive	Carballoy 883 WC-Co	Sintered	1.2 mm^3/1000rev
	WC-Co	Detonation gun	0.9
	WC-Co	Plasma spray	16.0
	WC-Co	Super D-Gun	0.7
	WC-Co	HVOF	0.9
Dry sand/rubber wheel test, 50/70 mesh Ottawa silica, 200 rpm, 30 lb load, 3000 revolution test duration, ASTM			
Erosive	Carballoy 883	Sintered	0.04 micrometers/g
	WC-Co	Detonation gun	1.3
	WC-Co	Plasma spray	4.6
	WC-Co	Super D-Gun	
	WC-Co	HVOF	
	AISI 1018 steel	Wrought	21.
Silica-based erosion test, 15 μm, 139m/s, 5.5g/m, ASTM			

Table 31. Examples of wear applications

Adhesive	Primary metals process rolls Piston rings Gyroscope components Hydraulic pump components Machine shaft bearing surfaces
Abrasive	Textile mill fiber guides Paper mill rolls Computer tape heads
Abrasive and adhesive	Extruder screws and barrels Pump pistons Compressor rods Ball and gate valves Mechanical seals
Erosive	Gas turbine compressor blades Power recovery blades Valve stems

must be found to prevent internal corrosion of the coating, attack of the substrate, and galvanic effects.

A variety of sealants have been developed, some of the most common being based on epoxies. All are limited, however, in that they can only fill channels or pores that are interconnected to the external surface of the coating. Channels that extend to the substrate, but not the exterior surface, will not be filled. These may be opened during finishing or as a result of wear during service. A further limitation of most sealants is their instability at elevated temperatures. Epoxy sealants, for example, are currently limited to about 250 °C. There exists a significant need for sealants that are effective at higher service temperatures, but do not require high temperature curing or sintering (which, in many cases, would cause spalling of the coating or undesirable changes in the coating or substrate).

For some applications, for example MCrAlY coatings on superalloys, the coated parts can be heat treated (usually in vacuum) at a temperature high enough to seal the coatings by sintering. This is possible, in this example, because the mismatch in coefficients of thermal expansion between the coating and the substrate are small, and the substrate can be heat treated without damage at a temperature high enough to effect sealing of the coating. Even in most of these cases, however, an additional mechanical working of the surface, for example by peening, is necessary to complete the sealing.

The sintering approach to sealing in the above refers to solid state sintering. In the spray – fuse or spray + fuse types of coatings, densification occurs largely via fusion or liquid diffusion. Significant dilution or interdiffusion with the substrate usually occurs.

7. Markets

Thermal spray coatings are used in virtually every industrial segment, both on original equipment and for repair and refurbishment. A few examples are given in Table 32. With the exception of a few industries, such as aircraft gas turbines, most thermal spray coatings were used as a repair, or to fix a design problem, until fairly recently. There is a growing trend, however, to incorporate these coatings in original equipment design and manufacture in high volume applications such as automobiles.

Table 32. Examples of market segments and applications

Aircraft	Landing gear Tracks for flaps and slats
Gas turbines	Blades and vanes Shrouds Seals
Paper	Rolls Hydrofoils
Primary metals	Hearth rolls Process rolls
Petrochemical and oil/gas production	Pump and compressor seals Mechanical seals Valves
Transportation	Ship decks Auto exhaust systems Bridge structures

Coatings are applied both in-house and by vendors. Most of the companies that apply the coatings in-house are fairly large and technically sophisticated, such as the aircraft engine manufacturers and airline repair shops. The level of expertise of vendors of coating services varies widely, not only in their understanding of the processes, but in the level of quality control they employ. Most vendors serve only local or regional markets; only one or two could be considered international in scope.

8. Status of Development and Industry Needs

Thermal spray process development is becoming quite mature. Recent years have seen the introduction of Super D-Gun coatings and the reintroduction of high velocity oxy-fuel systems by several equipment manufacturers. While only a few thermal spray systems seem to have fully implemented adequate process control, the technology is readily available. Automation and computer control are becoming commonplace.

While new coating compositions are constantly being introduced, the most widely used thermal spray materials have been in existence for a long time. There has been, however, a renewed interest in the "quality" of thermal spray powders which has been reflected in coatings with better, more uniform, microstructures. Newer methods of manufacture, e.g., sol-gel, improved spray drying, and higher purity reactive metal atomization, have been introduced. These and new material compositions will undoubtedly yield coatings with even more uniform properties, as well as better properties.

Although reasonably effective epoxy sealants exist for use at temperatures up to about 250 °C, sealants for use at higher temperatures that do not require even higher temperature curing or sintering are needed. While fully dense thermal spray coatings that would not require sealants have been claimed in sales literature from time to time, none exist in the as-deposited condition. A few coatings have been developed, however, that appear to be functionally sealed so long as the thickness of the coating exceeds about 200 μm. More development along these lines would be useful.

Effective nondestructive testing of thermal spray coatings remains virtually nonexistent, except for thickness measurements that are possible with some combinations of coatings and substrates. Attempts to develop methods to detect excessive porosity, microcracks, or delamination have led only to extremely expensive instruments with very limited levels of detectable flaw size. Measurement of residual stress on most parts is impossible, but such stresses can play a key role in the success or failure of the coating.

About the author: *Dr. Tucker received his BS in chemistry/mathematics from North Dakota State University and his MS and PhD from Iowa State University in metallurgy, with minors in ceramics and nuclear science. He is a Corporate Fellow and Associate Director-Technology at Praxair Surface Technologies (formerly Union Carbide Coatings Service Corporation). He has been responsible for programs to develop thermal barriers and composite materials, materials resistant to high- and low-temperature wear and corrosion, and materials resistant to high-temperature oxidation and sulfidation. This work utilizes plasma, detonation gun, physical vapor, and chemical vapor deposition coatings. He is a member of ACerS, AIME, ASTM, AVS, NACE, WRC, and Sigma Xi, is a Fellow of ASM International, and Adjunct Professor, University of Illinois, Urbana-Champaigne. He has presented and/or published over 80 papers and has been granted 16 U.S. patents with many foreign derivatives.*

Developments in Laser Surface Modification and Coating

Dr. J. A. Folkes

Center for Advanced Materials
(ZFW)
Clausthal
Agricolastraße 6
38678 Clausthal-Zellerfeld,
Germany
Phone: 011 49 53 23 72 3125
Fax: 011 49 53 23 72 3148

The use of lasers to modify the characteristics of a surface for improved properties is increasing in various industrial applications. Laser cladding, hardening, patterning and alloying have proved to be viable industrial processes for improving the surface performance. Modern ultra violet lasers have further increased the range and flexibility of surface modification possibilities. Surface texturing, sensitization, adhesion, smoothing, and deposition of coatings has opened up a whole new area of potential process applications. This paper discusses the process technology, potential application areas, end uses and some economics of the process.

Key words: alloying; excimer; hardening; infrared; laser; laser cladding; laser coating; LCVD; LPVD.

1. Introduction

Over the last decade the use of lasers in industry for surface modification applications has grown substantially. The development of reliable and economical systems has promoted the acceptance of this technology in a range of application areas. Developments in laser technology have also led to a new generation of ultra violet lasers with the potential to open up the field of surface treatment in the future.

Surface modification using a laser can take a variety of forms, depending on the laser type, the way it is used, and the material or materials on which it is used.

The three main types of laser used in surface modification are:

- The Carbon Dioxide (CO_2) laser (continuous wave—CW—or pulsed)
- The Neodymium Yttrium Aluminum Garnet (Nd:YAG) laser (usually pulsed)
- The Excimer laser (pulsed)

Other lasers such as the copper vapor, ruby or argon ion lasers, can also be used in a limited way for some industrial applications. With the two common industrially used infrared lasers, the carbon dioxide laser (wavelength of 10.6 μm) and the Neodymium:YAG laser (wavelength 1.06 μm) the substrate is usually modified by a heat-related process. The excimer laser, which produces ultraviolet light, is usually used to promote photochemical processes.

2. Surface Modification Techniques

Typical surface alteration processes using lasers include

- Surface Cladding
- Surface Alloying
- Transformation Hardening
- Surface Melting
- Laser Engraving
- Surface Smoothing
- Surface Texturing
- Micromachining

Some of the general surface interactions used in these processes are illustrated in figure 103. Figure 104 shows several of the basic laser surface treatment processes.

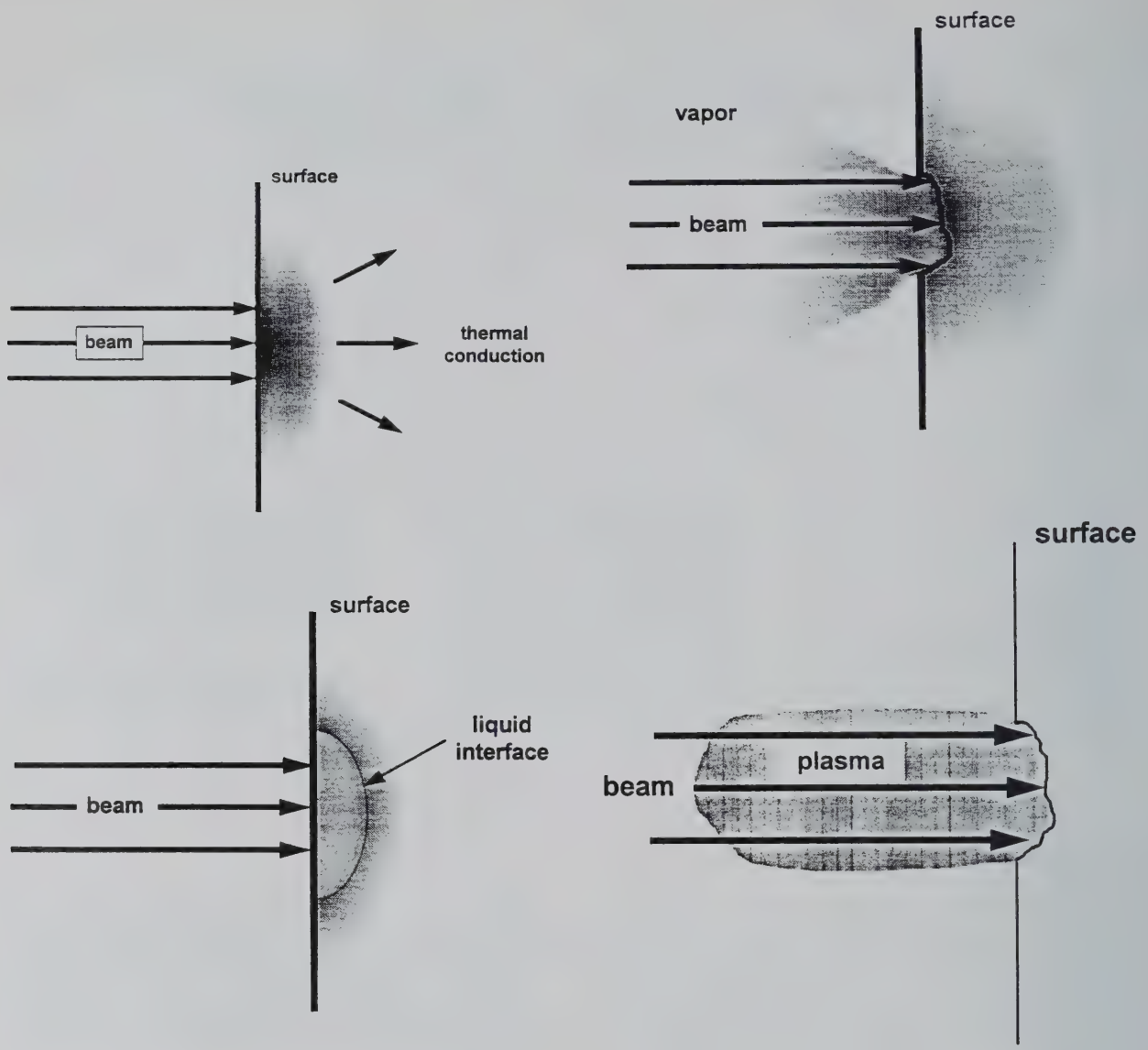

Figure 103. Schematic diagram of the general interactions between a laser beam and a surface.

In surface modification, the length of time the laser illuminates the surface (or stays at one point on the surface) primarily controls what process will occur. For example, long interaction times at high laser energy density (as with a scanned CW laser) will cause melting, while long interaction times at low energy density are used for heat treatment. Each process has its own particular characteristics.

2.1 Transformation Hardening

The aim of laser hardening is to use the laser to produce a quench hardened case, without melting, on selected areas of the substrate surface subject to wear. It is effective for steels with an appropriate carbon content, or pearlitic cast irons. The exact structure depends on the cooling rate and T.T.T. diagram, but generally improves hardness and wear.

For example, General Motors has used lasers to harden a cast iron automotive steering component. The process had significant advantages over other conventional processes since the engineering requirements could be achieved with less distortion, and no post treatment machining. Fiat uses the technology to heat treat cylinder blocks, while Nissan uses it in the heat treatment of engine and transmission components [1,2,3]. The method is expected to become used more widely in new advanced materials.

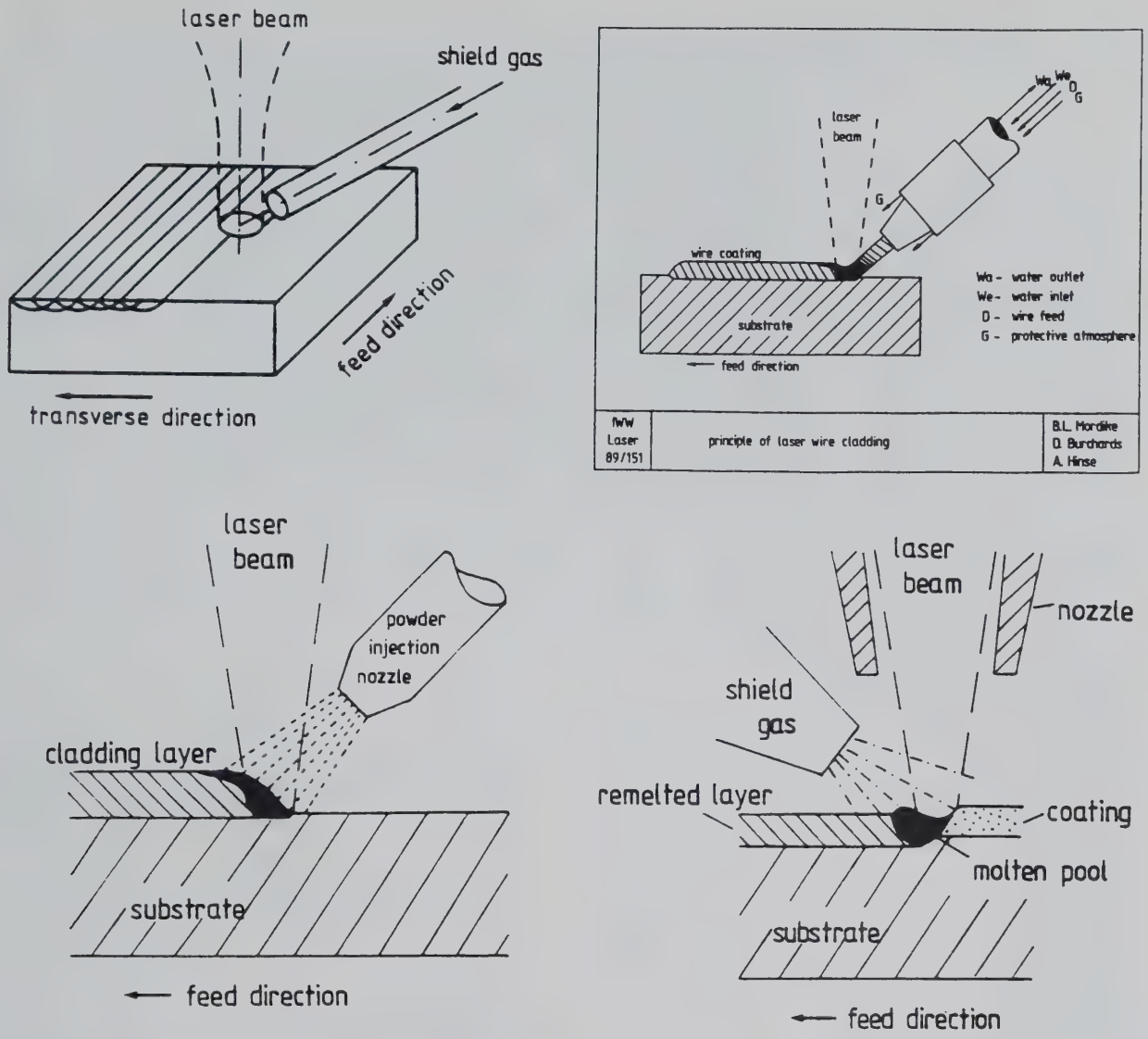

Figure 104. Different laser surface modification techniques: (a) surface melting, (b) surface cladding, (c) wire feeding, and (d) surface alloying with preplaced coatings.

2.2 Laser Surface Melting

With a high enough heat input, the surface can be melted without affecting the underlying material to modify the grain structure and finish. The microstructure depends on the temperature gradient (determined by power density and thermal properties), and the solidification rate (controlled by interaction time—a function of the scanning speed of the beam or the work piece). Typical melt depths vary from a few microns to more than 1 mm, and structure refinement varies from coarse to extremely fine textures, from dendrites to martensites to metastable (or in some cases with specific compositions, amorphous) structures. The microstructure varies as a function of depth, and in some systems the hardness is greatest in the surface melt region, underlying which is a softer tempered region.

Laser surface melting has recently been applied to cam shafts [4]. The majority of engines use lamellar grey cast iron as the cam shaft material. The camshaft is typically treated by conventional techniques such as TIG remelting or directly chill cast to produce a wear resistant ledeburite surface. Although the same transformation can be achieved by using a laser, laser spot scanning (fig. 104a) is too slow for production. The development of reliable high power lasers and optics to produce a line focus has made the laser process economically

viable [4]. It is now replacing the previous TIG process in production in companies such as Volkswagen.

2.3 Other Uses

The laser may be used to induce stresses in a surface. This process can be made more effective by the use of a coating. A Nd:YAG laser has been used in this way to refine the magnetic domain size of transformer steels to reduce eddy current losses. The laser treatment causes slip plane dislocations to form, forming a new subdomain structure, and by adjusting the spacing of the laser lines, the domain sizes can be controlled [5,6].

Laser engraving is now frequently used for etching control numbers or part numbers on components, such as drills, medical instruments, and automobile components.

Laser removal of coatings, such as paint, is being used more and more widely because of its avoidance of environmentally unacceptable or unhealthy solvents (especially volatile organics).

Lasers have also been used to smooth brake pads [7], and (in the form of a chopped laser beam) to make a regular pattern on the surface of sheet metal. This patterning of the surface creates an almost perfectly flat surface for painting [8,9], on which the paint adheres better. Nissan uses this method for car panels.

Excimer lasers have extended the potential range of applications to surface sensitization, improved bonding/adhesion, laser engraving, and micromachining. New applications are constantly being developed.

2.4 Surface Alloying

In common with surface melting, surface alloying involves substantial heating of the surface, but alloying is promoted by injecting another material into the melt pool, so that the new material alloys into the melt layer. The alloying material can be added in many ways:

- Wire feed (fig. 104c)
- Pre-deposited coatings (fig. 104d)
- Electroplating
- Reactive gas shroud
- Vacuum evaporation
- Thin foils application
- Blown powder
- Ion implantation
- Diffusion (e.g., boronising)

There are as yet few commercial applications of this technology, but its use is growing [10]. For example, if nitrogen is used in a gas shroud on melting titanium, titanium nitride forms. The depth, smoothness and hardness of the nitride layer can be controlled. A typical depth is 0.3 μm, and the hardness ranges from 400 Hv to 1600 Hv. Titanium carbide can be formed by laser melting carbon into the surface of titanium, while carbonitrides can be formed by combining this process with a nitrogen shroud. Although nitriding of steel cannot be easily done in this manner, cladding with titanium nitride may be possible. Alloying of cast iron and low alloy steels with Cr, Si, or C may be used to make inexpensive bulk materials with exotic surfaces [11]. Some alloys are being accepted for specific applications, such as Ti with nickel for corrosion applications, surface hardening of aluminum, etc. [12]. The flexibility of surface alloying allows the designer to choose what material is required for the surface and what is required for the bulk.

3. Laser Coating Methods

Lasers are being used more and more widely for surface coating, using such techniques as:

- Laser Physical and Chemical Vapor Deposition (LPVD and LCVD)
- Surface Sensitization and Enhancement (for adhesion and bonding)
- Ablation for coating (e.g., paint) removal.

3.1 Laser Cladding

The aim of laser cladding is to selectively coat a defined area. A cladding powder is fed into the laser beam, so that the powder melts within the beam and clads the surface (fig. 104b). Interdiffusion between the layer and the substrate is controlled by the heat input. Depending on the powder and substrate metallurgy, the microstructure of the surface layer can be controlled, using the interaction time and laser parameters.

Figure 105 shows a cross section of a single pass clad on titanium. Note the large thickness of clad material and the depth of the diffusion bonding layer.

Laser cladding (hard facing) of turbine blades by Rolls Royce was one of the first industrial applications of laser cladding. The process was flexible, easily controlled, and did not require a vacuum—significant advantages over electron beam treat-

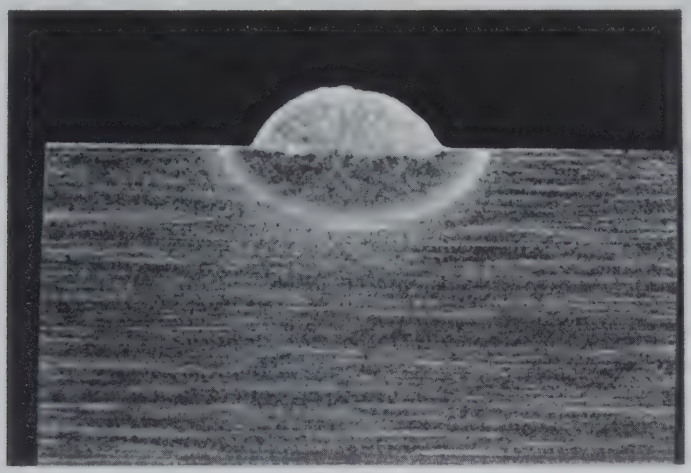

Figure 105. Single pass clad on titanium using a 2.5 kW CO_2 laser (beam diameter 3 mm, traverse speed 5 mm/s).

ments. Other industries have now begun to use laser cladding. For example, Nissan clads aluminum engine components with a copper bronze alloy.

3.2 Laser Physical and Chemical Vapor Deposition

Surface coating with a laser can take place in many ways. However, for Laser Physical Vapor Deposition (LPVD) or Laser Chemical Vapor Deposition (LCVD) the laser is used purely as a source to induce a given material to be deposited. The process is usually undertaken in a partial vacuum, and the material to be deposited is derived from either a solid target (PVD) or pyrolysis or photolysis of a vapor (CVD). The laser is particularly useful as it is a powerful, controllable, directed source of energy that can produce high quality, epitaxially grown thin films. Some of the materials deposited by LPVD or LCVD are summarized in Table 33.

The laser used as the energy source to deposit these materials can be either a CO_2 or a Nd:YAG laser. Both provide high pulse energies in the infrared. More recent advances, however, have seen the development and use of the excimer laser, particularly for the production of thin films. This laser emits in the ultraviolet and can cause not only vaporization or pyrolysis, but can also directly photodissociate molecules. This has had significant impact on the growth of superconducting and mixed semiconductor films.

Table 33. Summary of films deposited by laser deposition techniques[1]

Application	Substance	Layer structure
Optics	C	Amorphous
	CdTe, Bi_2Te_3	Polycrystalline
X-ray	W-C, Ni-C	Multilayer
Microelectronics	C	Polycrystalline
	Si, Ge, Si_xGe_{1-x}	Amorphous
	GaAs	Polycrystalline
	SnO, Cd_3As_2	Monocrystalline
Optoelectronics	As_xP_{1-x}, InSb	Polycrystalline
	$Hg_{1-x}Cd_xTe$	Polycrystalline
	InSb-GaAs, -CdTe	Superlattice
HT-Superconductors	$YBa_2Cu_3O_x$	Monocrystalline
	Bi-Ca-Sr-Cu-O	Polycrystalline
Thermoelectric	PbS, Sn	Polycrystalline
	PbSe, PbTe	Monocrystalline
	$Pb_{1-x}Cd_xSe$	Monocrystalline
Wear protection	BC, WC, BN	Polycrystalline
	Polymers	Amorphous

A schematic diagram of the laser PVD process is shown in figure 106. The high powered laser beam is focused onto a solid target. A plasma is readily produced and material is ablated from the focal spot. The ejected material, in the form of small particles and vapor, then deposits as a uniform film on surfaces nearby. The target stoichiometry can be

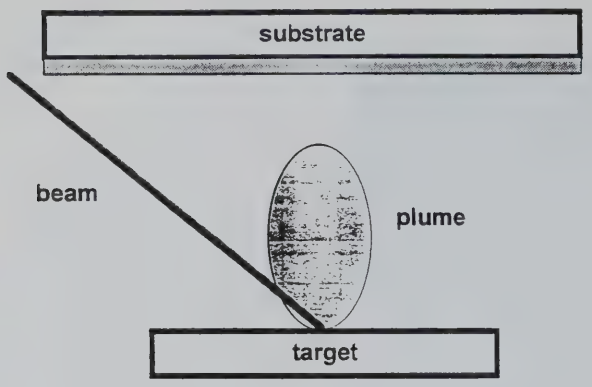

Figure 106. Schematic diagram of the LPVD process.

replicated in the film, particularly if an excimer laser is used. Deposition rates tend to be of the order of 1 to 10 μm per hour. Attempts to increase this value are currently under development using a combined laser and vacuum arc technique [13].

The target may or may not be heated depending on the film growth regime required, and a processing gas may be used to realize any desired chemical reactions during film growth. The growth of high quality, polycrystalline, epitaxial high temperature ($T_c > 90$ K) superconducting ceramic materials or mixed semiconductors such as CdS is possible [14]. The superconducting films tend to be extremely robust, retaining the target stoichiometry, and do not have to be post annealed in oxygen to make them superconducting. Laser deposition therefore has advantages over other methods for depositing these films, such as electron beam evaporation, ion beam sputtering, or rf sputtering. Laser deposition is also cheaper and faster than other techniques such as molecular beam epitaxy (MBE).

Films are deposited by laser CVD by using the focused beam to pyrolyse a thermally sensitive vapor (see fig. 107), or, with the excimer laser, the high energy UV photons can also be used to directly photodissociate gases. If pyrolysis occurs, the rate of deposition is controlled by chemical reaction rates up to certain deposition rates dependent on surface temperature. Above these temperatures, the process is controlled by mass transport, and the quality of the deposit falls from a smooth to a rough film, and ultimately to a powder. If photodissociation occurs, the deposition rate does not depend on the substrate temperature. Excimer lasers come in several wavelengths, so to optimize the photodissociation process, the incident wavelength should be within the absorption limit of the molecule to be photodissociated. For example an Argon Fluoride (193 nm) or Krypton Fluoride (248 nm) laser can be used to photodissociate the molecule $Al_2(CH_3)_6$ so that a thin film of aluminum can be deposited onto a wafer. Many metals (e.g., Au, Cd, Cr, Cu, Fe, Ga, In, Mo, Ni, Pt, Sn, W, and Zn) have been deposited in this way. Deposition rates are an order of magnitude faster in the beam area than those achieved using plasma or electron beam techniques. Excimer LCVD is a low temperature process, so it can be used with temperature-sensitive substrate materials and components. The substrate is also not bombarded with energetic ions, so the technique is less invasive the other methods.

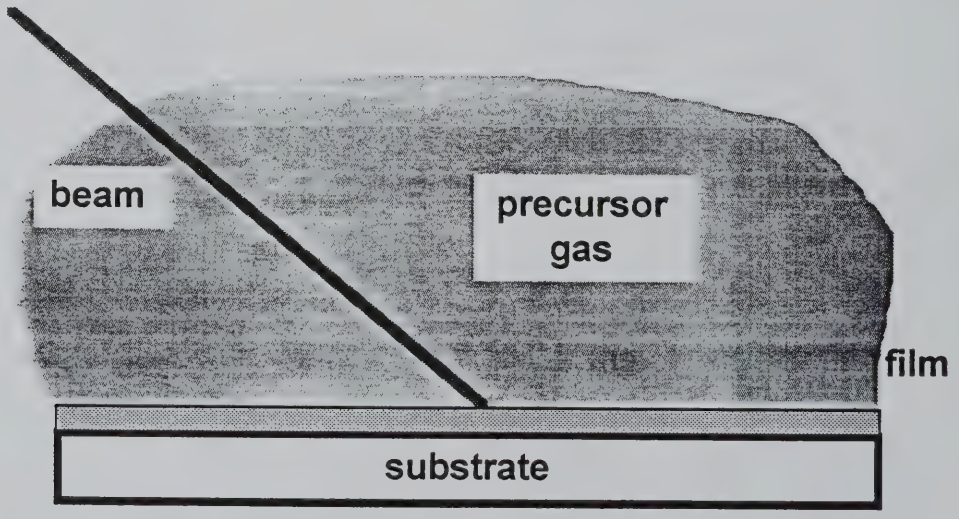

Figure 107. Schematic diagram of the LCVD process.

Companies such as Toyota [15] have been evaluating LCVD of W films on silica using $W(CO)_6$ and H_2. The deposition process takes 10 minutes, compared with 60 minutes for thermal CVD. The difference in apparent activation energies (E_a) is 18.0 kcal/mole for thermal CVD and 0.1 kcal/mole for ArF (193 nm) CVD. Higher deposition rates could also be achieved if an excimer laser (XeCl at 308 nm) outside the absorption limit of $W(CO)_6$ (300 nm) was used ($E_a = 1.8$ kcal/mole). The deposition rate in this case increases as the substrate temperature increases.

Other materials, such as Si, Ge, GaAs, InP and HgCdTe semiconductors, can be grown by excimer dissociation of precursor gases, such as silane (SiH_4), germane (GeH_4) or appropriate mixtures of organometallics such as $Ga(CH_3)_3$, $HgCdTe(CH_3)_2$. Thin insulating crystalline layers of alumina (sapphire), silicon nitride ceramics and diamond like carbon can all be laser deposited by low temperature reactions using a UV laser, for example:

$$Al(CH_3)_6 + N_2O + h\nu\ (193\ nm) > Al_2O_3 + Products$$
$$SiH_4 + NH_3 + h\nu\ (193\ nm) > Si_3N_4 + Products$$
$$C_2H_2 + H_2 + h\nu\ (193\ nm) > C_x\ (Diamond) + Products$$

These films all have a range of applications, from integrated circuits or detector fabrication to coatings for wear resistance. Laser PVD and CVD are therefore exciting subject areas, and cannot be ignored as a significant potential industrial coating technology in the future.

4. Examples of Industrial Use

Although laser processing technology has been researched and used commercially on a limited scale for many years, the increase in commercial use is tied to the development of reliable commercial high-power lasers. The availability of commercial laser systems is leading to the adoption of laser treatment technologies on a broader industrial scale, and the uses of the technology are expected to increase as high power lasers become increasingly cheaper and more reliable.

Many companies have already realized significant production and cost benefits from implementation of laser systems for a variety of uses. Laser cladding and smoothing are illustrative of the industrial use of laser methods.

4.1 CO_2 Laser Cladding

Before deciding on the use of laser cladding, the aims of the process have to properly defined. For example, one might want to change the surface composition to produce a required structure for better wear or high temperature performance, or one might wish to build up a worn part or provide better corrosion resistance.

In order to achieve the desired properties, the material parameters must be considered. If the item to be coated is made of Ti6Al4V aircraft alloy, for example, one must prevent oxidation as well as optimizing the composition and microstructure of the cladding. A β-Ti + TiC layer at the interface will provide good wear resistance, but to achieve this the cladding powder must be properly chosen. The proper layer may be formed by adding a transition metal or other carbide:

$$Ti6Al4V + XC \rightarrow \beta\text{-}Ti + TiC$$

where X is Mn, Fe, Cr, Co, W, Ni, Mo, V, Cb, or Ta. WC, Cr_3C_2 or Mo_2C powders should give the required structure.

Having established the surface coating material, one must

- Optimize the laser cladding parameters to create the best surface shape, coating thickness, etc.
- Evaluate the microstructure and wear properties of the coating.

It has been found that a satisfactory coating of Ti6Al4V can be made using a powder of 10–20 wt% Cr_3C_2, and 20 wt% Mo_2C. The material gave β-Ti + TiC, and had excellent hot hardness.

4.2 Excimer Smoothing

Two main factors influence the interaction of the laser with the surface—the laser energy density and the number of laser pulses. Together with the presence of different gases [16] these factors affect the surface roughness, allowing smoothing or roughening can be achieved for a given material. Figure 108 shows the removal of grinding lines from a surface. The surface finish could be controlled by naturally roughening the surface to produce surface textures, or by using a mask to produce patterns. The surface could also be alloyed to form surfaces such as TiN, or TiO_2.

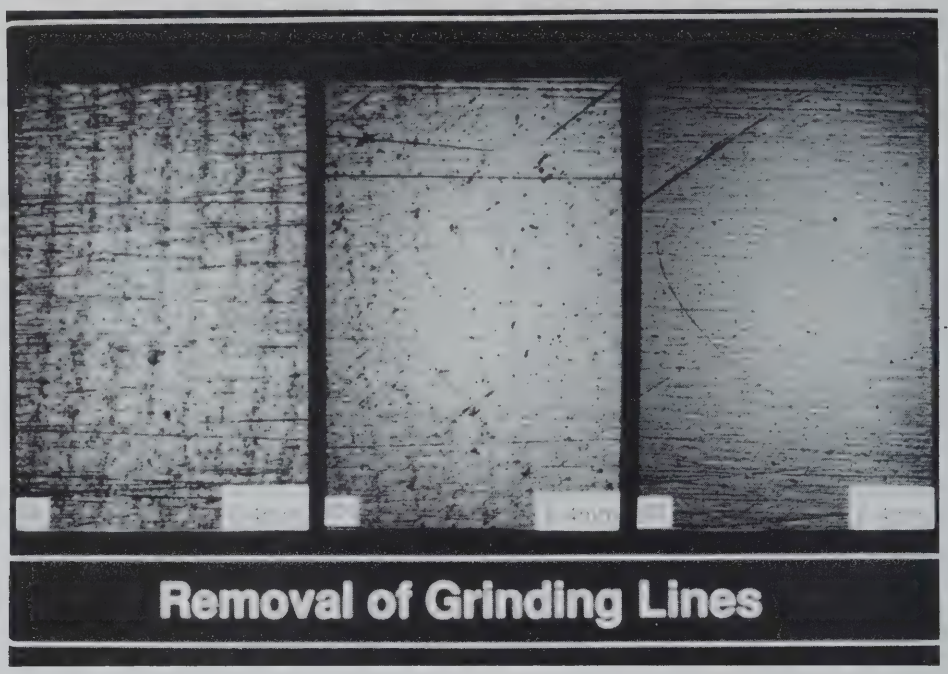

Figure 108. Removal of grinding lines from a surface using an excimer laser (2, 6, and 16 pulses respectively).

5. Economics of Laser Processes

In putting any process into production one must consider both its technical and economic advantages and limitations.

While research and development usually shows the technological limits and advantages, the calculation of economic advantage is industry-dependent. The calculation of economics requires consideration of competing processes and of production needs, as well as a detailed knowledge of current manufacturing methods and accounting practices for the industry. Production costs must be properly calculated, including personnel, maintenance, capital cost, cost of space, etc. Finally, the potential user must be willing and able to adapt the production system to accommodate the new laser equipment and procedures.

For the cam shaft application, for example, it could be demonstrated that the process had both technological and economic advantages [4]. For instance, the processing time was about 3 seconds per cam compared with 21 seconds for TIG remelting. For actual workstations the production rates were 29 seconds for the laser and 35 seconds for the TIG station (4 rows, each with 2 TIG torches) for each cam shaft.

The operating costs for this process are reported in detail elsewhere (4). A cost of $350 per hour is reasonable for assessing the feasibility of a process. Remelting costs per camshaft were calculated at just under $1.75 per camshaft—a 54% reduction in cost [17].

6. Future Development of Laser Processes

Laser treatment technology is continuing to grow in importance with the commercial availability of high power lasers. Some of the future uses of the technology (separated by type of laser used) are likely to be:

Carbon Dioxide Laser:

- Transformation hardening (cylinder blocks, couplings)
- Melting (cam shafts)
- Alloying (laser nitriding)
- Cladding (engine exhaust valves and parts, turbine blades, molds)

Neodymium YAG Laser:

- Texturing (steel substrates)
- Smoothing (brakes)
- Adhesion and bonding
- Coating removal, or depainting (paints, etc.)

Excimer Laser:

- Surface texturing and smoothing (metals)
- Surface patterning (metal films)
- Micromachining
- Laser PVD and CVD coating deposition
- Bonding
- Coating removal (depainting)
- Surface sensitizing

7. Technology Requirements

Laser technology has gained a significant foothold in industry to date and is being used more and more widely. However, one of the main factors limiting its industrial development is the high initial capital cost of equipment. The excimer laser, especially, suffers from high cost and complexity with low reliability. Reliable, inexpensive production excimer lasers will be needed to bring excimer laser surface treatment to widespread industrial use.

While there is always a need for higher power lasers, this must be traded off against other considerations, such as optics limitations, scanning speed limits, and overheating of the surface. When material is ablated by the laser beam, fouling of optical components and sensing of such things as the laser position are serious concerns. When using high power excimer lasers, for example, maintaining focus can be a serious problem since the plasma produced at the surface interferes with measurement.

In industrial applications at the present time, the process is usually run according to a "recipe" rather than with feedback control. As more sophisticated processes become industrially viable, the need for better on-line quality control will become greater. For example, although they are seldom used in industry at present, precision treatments will require simple, robust, inexpensive beam diagnostics for on-line beam shape profiling and analysis.

The large size of CO_2 lasers and their associated power supplies is a serious problem when they are used in expensive manufacturing space. A reduction in their size and complexity will be important if they are to broadly compete industrially with Nd:YAG lasers.

As the demand for laser systems grows, more effective, lower power, lower cost portable systems are beginning to be developed that are compatible with user-friendly CNC work handling systems. There is a general need for user-friendly software to integrate these laser systems with CNC work handling systems.

With the newer laser techniques there are still some significant technological barriers to be addressed before the technology can be successfully implemented. Lack of effective technology transfer between research and practical industrial applications (and of course the natural public conception of lasers, such as the James Bond or Star Wars image) also hinders its effective use in industry. Proper understanding of the technology and development of industrial systems should lead to a more application-oriented development of the technology in the future.

8. References

[1] D. M. Roessler, Industrial Laser Annual Handbook (1990) ed., D. Belforte & Morris Levitt, Penn Well Publishing Co., Tulsa, OK, pp. 109–127.

[2] D. Belforte, Industrial Laser Review, Penn Well Publishing Co., Tulsa, OK (Dec. 1988).

[3] F. D. Seaman, Industrial Laser Handbook (1990), ed. D. Belforte & Morris Levitt, Penn Well Publishing Co., Tulsa, OK, pp. 68–73.

[4] S. Mordike, Lasers in Engineering, Vol. 2(1) (1993). To be published.

[5] G. L. Neiheisel, LIA Vol. 44 ICALEO'84 Boston Nov. (1984) pp. 102–111.

[6] A. Gillner, et. al., Proc. 5th Int. Conf. Lasers in Manufacturing (LIM5) ed. H. Hugel, Stuttgart, (Sept. 1988), publ. IFS (publ.) Ltd. UK pp. 137–144.

[7] Anon., American Machinist & Automated Manufacturing 130, 4, pp. 33–37 (Apr. 1986).

[8] B. Kellock, Machinery and Production Engineering 146, 3729, pp. 26–27 (Jan. 1988).

[9] K. Shibata, Proc. Conf. Lasers in Automobile Industry, The Weld. Inst., Cambridge, (Dec. 1987).

[10] A. M. Walker, J. Folkes, W. M. Steen, D. R. F. West, Surface Engineering 1 (1985) 1.

[11] W. M. Steen, Z. D. Chen, D. R. F. West, Industrial Laser Annual Handbook (1987), ed. D. Belforte & Morris Levitt pp. 80–96.

[12] W. M. Steen, Laser Materials Processing, Springer-Verlag London (1991).

[13] Pompe, et. al., Thin Solid Films 208 (1992) pp. 11–14.

[14] T. Verkatesan, T. Solid State Techn., 39 (Dec. 1987).

[15] S. Takagi, et. al., Industrial Laser Handbook 106–108.

[16] J. A. Folkes, Internal Report, Nissan Motor Company Ltd. (1991).

[17] F. Bachmann, Chemtronics, (4 Sept. 1989) pp. 149.

About the author: *The author gained her PhD in Laser Surface Treatment from Imperial College, London, in 1986. This work was in collaboration with Rolls Royce Aero Ltd. She then worked with industrially related applications of laser technology, including laser safety, before moving in 1989 to work on automotive applications of lasers for Nissan Motor Co. Ltd. in Japan. On returning to the U.K. she undertook a short-term project on laser etching of satellite antennae at Spectrum Technologies, a subsidiary of British Aerospace, and is currently working in Germany at the Center for Advanced Materials in Clausthal Zellerfeld.*

U.S. Department of Commerce
Technology Administration
National Institute of Standards and Technology
Gaithersburg, Maryland 20899

NIST